

**NON-DESTRUCTIVE TESTING OF COLUMNS UNDER AXIAL
COMPRESSION USING TRANVERSE VIBRATION TECHNIQUE, AND
ULTRASONIC APPROACHES**

MEHMET KAYNAK

JANUARY 2004

NON-DESTRUCTIVE TESTING OF COLUMNS UNDER AXIAL
COMPRESSION USING TRANVERSE VIBRATION TECHNIQUE, AND
ULTRASONIC APPROACHES

A THESIS SUBMITTED
TO
THE GRADUATE SCHOOL OF NATURAL AND APPLIED SCIENCES
OF
MIDDLE EAST TECHNICAL UNIVERSITY

BY
MEHMET KAYNAK

IN PARTIAL FULFILLMENT OF THE REQUIREMENTS FOR THE DEGREE
OF
MASTER OF SCIENCE
IN
THE DEPARTMENT OF CIVIL ENGINEERING

JANUARY 2004

Approval of the Graduate School of Natural and Applied Sciences

Prof. Dr. Canan ÖZGEN
Director

I certify that this thesis satisfies all the requirements as a thesis for the degree of Master of Science.

Prof. Dr. Erdal ÇOKÇA
Head of the Department

This is to certify that we have read this thesis and that in our opinion it is fully adequate, in scope and quality as a thesis for the degree of Master of Science.

Asst. Prof. Dr. Ahmet TÜNER
Supervisor

Examining Committee Members

Prof. Dr. Tanvir WASTI (Chairman)

Asst. Prof. Dr. Ahmet TÜNER (Supervisor)

Prof. Dr. A. Bülent DOYUM

Inst. Dr. Engin KARAESMEN

Dr. M. Altuğ ERBERİK

ABSTRACT

NON-DESTRUCTIVE TESTING OF COLUMNS UNDER AXIAL COMPRESSION USING TRANVERSE VIBRATION TECHNIQUE, AND ULTRASONIC APPROACHES

Kaynak, Mehmet

M.Sc., Department of Civil Engineering

Supervisor : Asst. Prof. Ahmet Türer

January 2004, 229 pages

The level of axial compressive load on an existing column is one of the most important parameters to be known. This thesis aims to investigate current state of the art of NDT techniques, their application, and investigate alternative ways of using current technology to estimate the axial compressive load on columns. For this purpose, transverse vibration technique, ultrasonic pulse velocity method, and waveform and frequency content evaluation of ultrasound are investigated and implemented.

Analytical and experimental studies on column transverse vibration frequency and axial load relationship are conducted and presented. The measured experimental lateral vibration frequency of the first bending mode decreased under increased axial compressive load as expected from analytical studies.

Relationships between axial load and vibration frequency are derived and defined for different boundary conditions. Relationship charts are prepared for complicated solution sets. Numerical calculations, laboratory and field tests revealed that natural frequencies of slender columns are more sensitive to axial load changes.

The available ultrasonic methods are investigated and described. Stress wave propagation in anisotropic solids is studied. Previous works have shown that the propagation velocity of stress waves depends on the density, Poisson's ratio, modulus of elasticity of the medium, and the state of stress. The orientation of the loading direction to the wave propagation direction, the couplant (ultrasonic transmission gel) uniformity, variability in the pressure applied to hold the transducers, alignment of the transmitting and receiving transducers, accuracy and modelling of Poisson's ratio make the ultrasonic testing more complicated.

Keywords: Columns, Compression, Non-Destructive Testing, Transverse Vibration Technique, Vibration, Ultrasonic Pulse Velocity Method, Waveform Evaluation, Ultrasound.

ÖZ

KOLONLARIN SADECE EKSENEL BASINÇ ALTINDAYKEN SERBEST TİTREŞİM YÖNTEMİ VE ÜLTRASONİK YÖNTEMLERLE HASARSIZ ÖLÇÜLEREK DEĞERLENDİRİLMESİ

Kaynak, Mehmet

Yüksek Lisans, İnşaat Mühendisliği Bölümü

Tez Yöneticisi: Yrd. Doç. Dr. Ahmet Türer

Ocak 2004, 229 sayfa

Kolonlar üzerinde var olan aksenal basınç seviyesi, o kolonla ilgili bilinmek istenen değişkenlerin başında gelmektedir. Bu çalışmada, kolonlar üzerindeki aksenal basıncın hasarsız yöntemlerle hesaplanması amaçlanmıştır. Bu amaç için çapraz titreşim yöntemi, ultrasonik hız, dalga biçimi ve titreşim sayısı değerlendirmesi yöntemleri araştırılmış ve kullanılmıştır.

İlk olarak serbest titreşim yöntemi uygulanmıştır. Aksenal basınç altında serbest titreşim sıklığı beklenildiği gibi azalmaktadır. Farklı sınır şartları için yük ve serbest ilk titreşim sıklığı arasında bağıntılar çıkarılmaya çalışılmıştır. Bu çalışmada ayrıca serbest titreşim yönteminin neden sadece ince (narin) yapıları ögelerinde uygulanabilir olduğu ve ilk (ana) salınım biçiminin neden daha çok azalma gösterdiği yanıtlanmaya çalışılmıştır.

İkinci ve son olarak ¼ltrasonik yntemler anlatılmıřtır. Bir mekanik titreřimin, farklı ynlerde lm yapıldıęında farklı zellikler gsteren katılarda yayılma kuralları incelenmiřtir. Dalganın yayılma hızının, ortamın yoęunluęuna, Poisson oranına, elastik indeksine ve y¼kleme kořullarına baęlı olduęu tekrarlanmıřtır. Y¼kleme yn¼n¼n dalga yayılma yn¼ne gre konumunun ve aısının, numuneye dalga iletimini saęlayan sıvının zelliklerinin, aygıtları yerinde tutmak iin uygulanan basıncın, verici ve alıcı aygıtların karřılıklı denk getirilme zorunluluęunun, hata payının, Poisson oranının tanımlanmasının ¼ltrasonik ynteme olan etkileri ve karřılařılan genel problemler aıklanmıřtır.

Anahtar Kelimeler: Kolonlar, Eksenel Basınc, Hasarsız lm, Serbest Titreřim Yntemi, ¼ltrasonik Hız Yntemi, Dalga Biimi Deęerlendirmesi.

This thesis is dedicated to
my father and mother,
Zeki & Nazlı Kaynak.

ACKNOWLEDGMENTS

I express sincere appreciation to my supervisor Asst. Prof. Dr. Ahmet Türer for his guidance, insight and patience throughout the research.

Thanks go to Assistant Chairman, Civil Engineering Department, Dr. İsmail Özgür Yaman, for his suggestions and comments.

The technical assistance of the structural mechanics laboratory personnel; Mr. Burhan Avcı, Mr. Hasan Hüseyin Gürer, Mr. Hasan Metin, Mr. Murat Pehlivan, Mr. Ömer Metin, and Mr. Osman Keskin, is gratefully acknowledged.

I thank Mrs. Birnur Doyum from Non-Destructive Testing Center at METU, and Mr. Melekzat Öktem from Yüksel Construction Company for their valuable contributions.

To my family; my father, Zeki Kaynak, my mother, Nazlı Kaynak, my sister, Havva Kaynak, and my brother, Ramazan Kaynak, I offer sincere thanks for their patience throughout my research. To my friends, I thank them for understanding my frequent absence.

TABLE OF CONTENTS

ABSTRACT	iii
ÖZ	v
DEDICATION	vii
ACKNOWLEDGEMENTS	viii
TABLE OF CONTENTS	ix
LIST OF TABLES	xi
LIST OF FIGURES	xviii
LIST OF ABBREVIATIONS	xxiv
LIST OF SYMBOLS	xxv
CHAPTER	
1. INTRODUCTION	1
1.1. Objectives and Scope of the Thesis	1
1.2. General	2
1.3. Commonly Used Non-Destructive Testing Methods	3
1.4. Development of Non-Destructive Testing Methods in Turkey	6
2. FREE TRANSVERSE VIBRATION OF PRISMATIC COLUMNS UNDER AXIAL COMPRESSION	8
2.1. General	8
2.2. Derivations of Formulas and Different Boundary Conditions	9
2.2.1. Equilibrium Equations	11
2.2.2. Equation of Motion	12
2.2.3. Pinned Ends on Both Supports	21
2.2.4. Fixed Ends on Both Supports	29
2.2.5. Transverse Springs with Rollers on Both Ends	39
2.2.6. Fixed End and Springs with Roller on Other End	45

3. ULTRASONIC TESTING	51
3.1. General	51
3.2. Historical Perspective of the Use of Ultrasonic Testing	52
3.3. Theory of Ultrasonic Testing	55
3.4. Factors Influencing the Ultrasonic Testing	58
3.5. Related Standards	84
3.6. Advantages and Drawbacks of the Ultrasonic Testing	86
4. THE EXPERIMENTS AND RESULTS	88
4.1. Transverse Vibration Measurement Tests	88
4.1.1. Concrete Shear Wall Test	88
4.1.2. Simply Supported I120 Steel Beam-Column Test	110
4.1.3. Full Size 24-Storey High Building Test	121
4.2. Ultrasonic Pulse Velocity Measurement during a Standard Cylinder Compression Test	129
4.3. Waveform and Frequency Evaluation of Transmitted Ultrasound Wave During an Axial Compression Test of a Concrete Cylinder .	139
5. DISCUSSION OF RESULTS AND CONCLUSION	155
5.1. Transverse Vibration Measurement Tests	156
5.2. Ultrasonic Pulse Velocity Measurement	159
5.3. Waveform and Frequency Content Evaluation of Transmitted Ultrasound Waves	161
5.4. Future Studies	162
REFERENCES	163
APPENDICES	
A. FUNDAMENTAL FREQUENCY CHANGE IN PERCENTAGE VERSUS AXIAL LOAD LEVEL FOR I SECTION STEEL COLUMNS FOR DIFFERENT LENGTHS	165
B. TICO ULTRASONIC INSTRUMENT	226

LIST OF TABLES

Table

2.1	The effects of support conditions on mode shapes	19
2.2	The fundamental frequency ratio of the concrete member of 25x25 cm	27
2.3	Fundamental frequency change in <u>percentage</u> versus axial load level for I120 steel column for different lengths	35
2.4	Fundamental frequency versus axial load level for I120 steel column for different lengths	36
3.1	Pulse velocity vs. concrete quality	53
3.2	Typical propagation velocities for various materials	56
3.3	Path length error in typical transducer arrangements	63
3.4	Effect of specimen dimensions on pulse transmission	72
3.5	Effect of temperature on pulse transmission	75
4.1	The properties of the concrete shear wall	89
4.2	Measured fundamental frequencies of the concrete shear wall	99
4.3	Expected fundamental frequencies of the concrete shear wall from the model with pinned ends on both supports	101
4.4	Expected fundamental frequencies of the concrete shear wall from the model with fixed ends on both supports	101
4.5	Analytical fundamental frequencies of the concrete shear wall with fixed and spring with roller supports	102
4.6	Analytical modal periods and frequencies of SAP2000 concrete shear wall model	108
4.7	Analytical modal participating mass ratios of SAP2000	

	concrete shear wall model	108
4.8	Comparison of experimental modal frequencies versus analytical results for different boundary conditions	109
4.9	Measured first bending frequencies during I120 steel column compression test	114
4.10	The expected (analytical) fundamental frequencies steel I120 column (simply supported, L= 160 cm, transverse springs at the two ends)	115
4.11	The expected (analytical) fundamental frequencies of steel I120 column (simply supported, L= 160 cm, no springs)	116
4.12	Analytical modal periods and frequencies of SAP2000 steel I120 beam-column model	119
4.13	Analytical modal participating mass ratios of SAP2000 steel I120 beam-column model	119
4.14	Comparison of I120 steel column test and analytical results	120
4.15	Correlation between the results of I120 steel column test	121
4.16	Member properties and axial load on the members of the full size 24-storey high building	126
4.17	Measured fundamental frequencies and expected analytical frequencies of the full size 24-storey high building members ...	127
4.18	Required braced lengths for fixed-ended boundary condition in order to match the test results for the <u>interior column</u>	128
4.19	Required braced lengths for fixed-ended boundary condition in order to match the test results for the <u>exterior column</u>	128
4.20	Required braced lengths for fixed-ended boundary condition in order to match the test results for the <u>interior shear wall</u>	129
4.21	Properties of the standard cylinders for ultrasonic tests	129
4.22	Properties of cylinder for ultrasonic test no 1	132
4.23	Constants of the logarithmic relationship between strain and ultrasonic pulse velocity	138
4.24	Analytical modal periods and frequencies of SAP2000 model of the standard cylinder	150

4.25	Correlation factor (R) of the vibration frequencies of the cylinder for different load levels in measurement across 15 cm	150
4.26	Correlation factor (R) of the vibration frequencies of the cylinder for different load levels in direct measurement across 30 cm	152
4.27	Correlation factor (R) of the vibration frequencies of the cylinder for different load levels in indirect measurement across 30 cm	153
A.1	Fundamental frequency change in percentage versus axial load level for <u>I80</u> steel column for different lengths <u>for load level</u>	165
A.2	Fundamental frequency change in percentage versus axial load level for <u>I80</u> steel column for different lengths <u>for frequency change</u>	166
A.3	Fundamental frequency change in percentage versus axial load level for <u>I100</u> steel column for different lengths <u>for load level</u>	168
A.4	Fundamental frequency change in percentage versus axial load level for <u>I100</u> steel column for different lengths <u>for frequency change</u>	169
A.5	Fundamental frequency change in percentage versus axial load level for <u>I120</u> steel column for different lengths <u>for load level</u>	171
A.6	Fundamental frequency change in percentage versus axial load level for <u>I120</u> steel column for different lengths <u>for frequency change</u>	172
A.7	Fundamental frequency change in percentage versus axial load level for <u>I140</u> steel column for different lengths <u>for load level</u>	174
A.8	Fundamental frequency change in percentage versus axial load level for <u>I140</u> steel column for different lengths <u>for frequency change</u>	175

A.9	Fundamental frequency change in percentage versus axial load level for <u>I160</u> steel column for different lengths <u>for load level</u>	177
A.10	Fundamental frequency change in percentage versus axial load level for <u>I160</u> steel column for different lengths <u>for frequency change</u>	178
A.11	Fundamental frequency change in percentage versus axial load level for <u>I180</u> steel column for different lengths <u>for load level</u>	180
A.12	Fundamental frequency change in percentage versus axial load level for <u>I180</u> steel column for different lengths <u>for frequency change</u>	181
A.13	Fundamental frequency change in percentage versus axial load level for <u>I200</u> steel column for different lengths <u>for load level</u>	183
A.14	Fundamental frequency change in percentage versus axial load level for <u>I200</u> steel column for different lengths <u>for frequency change</u>	184
A.15	Fundamental frequency change in percentage versus axial load level for <u>I220</u> steel column for different lengths <u>for load level</u>	186
A.16	Fundamental frequency change in percentage versus axial load level for <u>I220</u> steel column for different lengths <u>for frequency change</u>	187
A.17	Fundamental frequency change in percentage versus axial load level for <u>I240</u> steel column for different lengths <u>for load level</u>	189
A.18	Fundamental frequency change in percentage versus axial load level for <u>I240</u> steel column for different lengths <u>for frequency change</u>	190
A.19	Fundamental frequency change in percentage versus axial load level for <u>I260</u> steel column for different lengths <u>for load</u>	

	<u>level</u>	192
A.20	Fundamental frequency change in percentage versus axial load level for <u>I260</u> steel column for different lengths <u>for frequency change</u>	193
A.21	Fundamental frequency change in percentage versus axial load level for <u>I280</u> steel column for different lengths <u>for load level</u>	195
A.22	Fundamental frequency change in percentage versus axial load level for <u>I280</u> steel column for different lengths <u>for frequency change</u>	196
A.23	Fundamental frequency change in percentage versus axial load level for <u>I300</u> steel column for different lengths <u>for load level</u>	198
A.24	Fundamental frequency change in percentage versus axial load level for <u>I300</u> steel column for different lengths <u>for frequency change</u>	199
A.25	Fundamental frequency change in percentage versus axial load level for <u>I320</u> steel column for different lengths <u>for load level</u>	201
A.26	Fundamental frequency change in percentage versus axial load level for <u>I320</u> steel column for different lengths <u>for frequency change</u>	202
A.27	Fundamental frequency change in percentage versus axial load level for <u>I340</u> steel column for different lengths <u>for load level</u>	204
A.28	Fundamental frequency change in percentage versus axial load level for <u>I340</u> steel column for different lengths <u>for frequency change</u>	205
A.29	Fundamental frequency change in percentage versus axial load level for <u>I360</u> steel column for different lengths <u>for load level</u>	207
A.30	Fundamental frequency change in percentage versus axial	

	load level for <u>I360</u> steel column for different lengths <u>for</u> <u>frequency change</u>	208
A.31	Fundamental frequency change in percentage versus axial load level for <u>I380</u> steel column for different lengths <u>for load</u> <u>level</u>	210
A.32	Fundamental frequency change in percentage versus axial load level for <u>I380</u> steel column for different lengths <u>for</u> <u>frequency change</u>	211
A.33	Fundamental frequency change in percentage versus axial load level for <u>I400</u> steel column for different lengths <u>for load</u> <u>level</u>	212
A.34	Fundamental frequency change in percentage versus axial load level for <u>I400</u> steel column for different lengths <u>for</u> <u>frequency change</u>	213
A.35	Fundamental frequency change in percentage versus axial load level for <u>I425</u> steel column for different lengths <u>for load</u> <u>level</u>	214
A.36	Fundamental frequency change in percentage versus axial load level for <u>I425</u> steel column for different lengths <u>for</u> <u>frequency change</u>	215
A.37	Fundamental frequency change in percentage versus axial load level for <u>I450</u> steel column for different lengths <u>for load</u> <u>level</u>	216
A.38	Fundamental frequency change in percentage versus axial load level for <u>I450</u> steel column for different lengths <u>for</u> <u>frequency change</u>	217
A.39	Fundamental frequency change in percentage versus axial load level for <u>I475</u> steel column for different lengths <u>for load</u> <u>level</u>	218
A.40	Fundamental frequency change in percentage versus axial load level for <u>I475</u> steel column for different lengths <u>for</u> <u>frequency change</u>	219

A.41	Fundamental frequency change in percentage versus axial load level for <u>I500</u> steel column for different lengths <u>for load level</u>	220
A.42	Fundamental frequency change in percentage versus axial load level for <u>I500</u> steel column for different lengths <u>for frequency change</u>	221
A.43	Fundamental frequency change in percentage versus axial load level for <u>I550</u> steel column for different lengths <u>for load level</u>	222
A.44	Fundamental frequency change in percentage versus axial load level for <u>I550</u> steel column for different lengths <u>for frequency change</u>	223
A.45	Fundamental frequency change in percentage versus axial load level for <u>I600</u> steel column for different lengths <u>for load level</u>	224
A.46	Fundamental frequency change in percentage versus axial load level for <u>I600</u> steel column for different lengths <u>for frequency change</u>	225

LIST OF FIGURES

Figure

2.1	2-D view of the beam	9
2.2	A section of the beam	10
2.3	The sketch of a simply supported beam	21
2.4	The sketch of a fixed ended column	29
2.5	3-D surface chart of the first vibration frequency ratios of the steel I120 beam-column for certain lengths	33
2.6	Contour chart of the first vibration frequency ratios of the steel I120 beam-column for certain lengths	34
2.7	The ratio of load to buckling load versus the ratio of vibration frequency to unstressed frequency for I120 for various lengths	37
2.8	Relation between the ratio of the vibration frequency to the unstressed frequency and the ratio of the load to the buckling load for various I sections in 5 m	37
2.9	The sketch of the beam with springs at the ends	40
2.10	The sketch of the beam with fix support at one end and spring at the other end	46
3.1	Planes of isotropy P_{\perp} and anisotropy $P_{//}$	57
3.2	Transducer arrangement alternatives	61
3.3	Typical schemes of ultrasonic testing	62
3.4	Indirect measurement method	64
3.5	Mean pulse velocity at the surface	64
3.6	Inferior quality surface concrete	65
3.7	Ultrasonic pulse velocity at inferior quality surface concrete	65

3.8	Transducer diameter effect on indirect UPV measurement	66
3.9	Indirect UPV evaluation procedure using different wave path lengths	63
3.10	Sound fields of a transducer	67
3.11	Correction factor for pulse velocity in case of directly lying reinforcing bars	73
3.12	Reinforcing steel bar that do not directly lie under the path	74
3.13	Velocity correction factor for far lying steel bars	74
3.14	Velocity of the compressional wave versus age of the concrete	77
3.15	Pulse velocity versus age of concrete for different temperature values	77
3.16	Velocity of the compressional wave as function of age and water/cement ratio	78
3.17	Velocity of the compressional wave as function of age and dosage of retarder	79
3.18	Velocity of the compressional wave as function of age and dosage of super retarder	80
3.19	Velocity of compressional wave in concrete with CEM III and CEM I as function of age	80
3.20	Force, velocity and transmitted energy as function of deflection	81
3.21	Ultrasonic pulse velocity as a function of temperature and quenching	83
3.22	Ultrasonic pulse velocity as a function of cylinder crushing strength and fire damage	83
4.1	The reinforcement of the concrete shear wall	89
4.2	The fresh concrete of the shear wall	90
4.3	Front view of the concrete shear wall test setup	90
4.4	Front-top view of the concrete shear wall test setup	91
4.5	Back-top view of the concrete shear wall test setup	91
4.6	Back view of the concrete shear wall test setup	92

4.7	Back-bottom view of the concrete shear wall test setup	92
4.8	General view of the test equipments	93
4.9	Accelerometer readings and coherence	94
4.10	Two accelerometer readings	94
4.11	Evaluating damping from frequency-response curve of concrete shear wall	96
4.12	Vibration frequencies of the concrete shear wall and the test setup under different axial load levels	98
4.13	Closer view of the vibration frequencies of the concrete shear wall under different axial load levels	99
4.14	The ultrasonic pulse velocity ratio versus stress in parallel direction on C12 concrete shear wall	100
4.15	SAP2000 model of the concrete shear wall	103
4.16	Stress distribution on the concrete shear wall at 470.9 kN	104
4.17	Model for computing I-beam stiffness	104
4.18	First vibration mode of the concrete shear wall	105
4.19	Second vibration mode of the concrete shear wall	106
4.20	Third vibration mode of the concrete shear wall	106
4.21	Fourth vibration mode of the concrete shear wall	107
4.22	Fifth vibration mode of the concrete shear wall	107
4.23	Comparison of concrete shear wall test and analytical solution results	110
4.24	Evaluating damping from frequency-response curve of steel I120 beam-column	112
4.25	Change in the transverse vibration frequency of steel I120 column in the first mode under monotonic axial compression ..	114
4.26	The SAP2000 model of steel I120 beam-column	117
4.27	First vibration mode of the steel I120 beam-column	117
4.28	Second vibration mode of the steel I120 beam-column	118
4.29	Third vibration mode of the steel I120 beam-column	118
4.30	Comparison of I120 beam-column test and analytical solution results	120

4.31	Interior column of the 24-storey high building	121
4.32	Exterior column of the 24-storey high building	122
4.33	Shear wall (interior) of the 24-storey high building	122
4.34	Typical reinforcement plan of the 24-storey high building	123
4.35	Typical beam plan of the 24-storey high building	124
4.36	Typical floor plan of the 24-storey high building	125
4.37	Cylinder tests setup	130
4.38	Closer view of the cylinder test setup	131
4.39	Ultrasonic pulse velocity reduction measured perpendicular to the load under axial compression	133
4.40	Time versus ultrasonic pulse velocity ratio in unstressed case	133
4.41	The ultrasonic pulse velocity ratio versus stress in perpendicular direction on C16 standard cylinder	134
4.42	The ultrasonic pulse velocity ratio versus stress in perpendicular direction on C16 standard cylinder	135
4.43	The ultrasonic pulse velocity ratio versus stress in parallel direction on C16 standard cylinder	136
4.44	The relation between stress on the cylinders and ultrasonic pulse velocity ratio	137
4.45	The relation between strain and ultrasonic pulse velocity ratio	138
4.46	The loading setup of the C12 standard cylinder for waveform evaluation	140
4.47	The frequency content of the ultrasonic waves measured directly across 15 cm	140
4.48	The frequency content of the ultrasonic waves measured directly across 30 cm	141
4.49	The frequency content of the ultrasonic waves measured indirectly across 30 cm	141
4.50	The relation between the number of turns and the strain	142
4.51	Frequency versus load levels in direct measurement across 15 cm between 0-42 kHz	143
4.52	Frequency versus load levels in direct measurement across	

	15 cm between 42-84 kHz	143
4.53	Frequency versus load levels in direct measurement across 15 cm between 84-125 kHz	144
4.54	Frequency versus load levels in direct measurement across 30 cm between 0-42 kHz	145
4.55	Frequency versus load levels in direct measurement across 30 cm between 42-84 kHz	145
4.56	Frequency versus load levels in direct measurement across 30 cm between 84-125 kHz	146
4.57	3D surface plot of the two times of frequencies measured directly across 15 cm	147
4.58	3D surface plot of the two times of frequencies measured directly across 30 cm	147
4.59	Closer view to the 3D surface plot of the two times of frequencies measured across 15 cm	148
4.60	SAP2000 model of the standard cylinder	149
4.61	Fourty third vibration mode of the standard cylinder	149
4.62	3D surface plot of the correlation factor (R) of the cylinder vibration frequencies for different load levels across 15 cm	151
4.63	3D surface plot of the correlation factor (R) of the cylinder vibration frequencies for different load levels directly measured across 30 cm	152
4.64	3D surface plot of the correlation factor (R) of the cylinder vibration frequencies for different load levels indirectly measured across 30 cm	153
4.65	Number of turns versus load level	154
A.1	Contour lines of the first vibration frequency ratios of the <u>I80</u> steel column (in percentage) for certain lengths and loads	167
A.2	Contour lines of the first vibration frequency ratios of the <u>I100</u> steel column (in percentage) for certain lengths and loads	170
A.3	Contour lines of the first vibration frequency ratios of the <u>I120</u> steel column (in percentage) for certain lengths and loads	173

A.4	Contour lines of the first vibration frequency ratios of the <u>I140</u> steel column (in percentage) for certain lengths and loads	176
A.5	Contour lines of the first vibration frequency ratios of the <u>I160</u> steel column (in percentage) for certain lengths and loads	179
A.6	Contour lines of the first vibration frequency ratios of the <u>I180</u> steel column (in percentage) for certain lengths and loads	182
A.7	Contour lines of the first vibration frequency ratios of the <u>I200</u> steel column (in percentage) for certain lengths and loads	185
A.8	Contour lines of the first vibration frequency ratios of the <u>I220</u> steel column (in percentage) for certain lengths and loads	188
A.9	Contour lines of the first vibration frequency ratios of the <u>I240</u> steel column (in percentage) for certain lengths and loads	191
A.10	Contour lines of the first vibration frequency ratios of the <u>I260</u> steel column (in percentage) for certain lengths and loads	194
A.11	Contour lines of the first vibration frequency ratios of the <u>I280</u> steel column (in percentage) for certain lengths and loads	197
A.12	Contour lines of the first vibration frequency ratios of the <u>I300</u> steel column (in percentage) for certain lengths and loads	200
A.13	Contour lines of the first vibration frequency ratios of the <u>I320</u> steel column (in percentage) for certain lengths and loads	203
A.14	Contour lines of the first vibration frequency ratios of the <u>I340</u> steel column (in percentage) for certain lengths and loads	206
A.15	Contour lines of the first vibration frequency ratios of the <u>I360</u> steel column (in percentage) for certain lengths and loads	209
B.1	TICO ultrasonic instrument	226
B.2	TICO display unit	227
B.3	Application of TICO	227
B.4	Another application of TICO	228
B.5	The package of TICO	228

LIST OF ABBREVIATIONS

BS12	Beton Sınıfı (12 MPa) (Concrete Class 12 MPa)
C12	Concrete class (12 MPa)
cm	Centimeter
FFT	Fast Fourier Transformation
m	Meters
METU	Middle East Technical University
MPa	Mega Pascal(s)
NDE	Non-Destructive Evaluation
NDT	Non-Destructive Testing
POD	Probability of Detection
QNDE	Quantitative Non-Destructive Evaluation
R/C	Reinforced Concrete
UPV	Ultrasonic Pulse Velocity

LIST OF SYMBOLS

a:	acceleration
A:	area of cross-section
c:	viscous damping coefficient
d:	represents the change
D:	diameter of the transducer plate
E:	modulus of elasticity
f_{ck} :	characteristic ultimate strength
f_n :	fundamental frequency in n-th mode
G:	modulus of rigidity
I_{min} :	moment of inertia in weak direction
K:	user defined: $K = \sqrt{4 \cdot E \cdot I \cdot m \cdot \omega^2 + N^2}$
l, m, n:	third-order elastic constants (Murnaghan constants)
L:	length
m:	mass per unit length
M:	bending moment
P:	axial compressive load
$P_{buckling}$:	buckling load
$P_{ultimate}$:	ultimate load
r:	the radius of gyration
SL:	signal loss
t:	time
u:	displacement in axial (x) direction
v:	displacement in transverse (y) direction
V:	ultrasonic pulse velocity at an arbitrary stress

V_0 :	initial ultrasonic pulse velocity (at the natural state)
$V_{xx}, V_{xy},$	propagation velocities of the ultrasound waves along x-direction
V_{xz} :	with a particle displacement along x-, y-, z-directions respectively
x:	coordinate axis in axial direction
ω_n :	cyclic fundamental frequency in n-th mode
y:	coordinate axis in transverse direction
Z :	acoustic impedance
α :	user defined: $\alpha = \sqrt{(K + N)/(2 \cdot E \cdot I)}$
β :	user defined: $\beta = \sqrt{(K - N)/(2 \cdot E \cdot I)}$
κ	constant depending on the cross-sectional shape and accounting for the non-uniform distribution of shear stress across the section
λ :	slenderness ratio
λ_e :	elastic constants, Lamé constants
λ_w :	wave length
μ :	shear modulus
ν :	Poisson's ratio
ρ :	density
ρ_0 :	initial density
σ :	axial stress

CHAPTER 1

INTRODUCTION

1.1. Objectives and Scope of the Thesis:

The level of axial compressive load on an existing column is one of the most important parameters that engineers want to know. To determine the level of axial load without an initial reference measurement would be tremendous help to understand structural loading and behavior of a structural system. Estimation of the axial load acting on a column in a non-destructive way is becoming more important.

Two approaches are investigated in order to determine the axial load acting on a column. First approach consists of measurement of transverse natural vibration frequency. The transverse vibration frequencies of a column are expected to decrease under compression. Thus, relationships between the fundamental transverse vibration frequency and compressive axial load are investigated. A series of tests are conducted to investigate effects of axial load on wave propagation velocity and transverse natural vibration frequency.

A scaled (1/3) reinforced concrete shear wall is cast. A steel I120 column is tested. Ultrasonic pulse velocities and first natural mode of vibration frequencies are measured under changing axial loads. Natural frequencies of

columns and shear wall of a full-scale 24 storey R/C building are measured at different floors to see the effects of changing axial dead load.

The second approach that is investigated consists of measurement of the stress wave propagation velocity in anisotropic solids such as concrete. Standard cylinders are cast for BS12, BS16, and BS20 concrete classes. Ultrasound velocity through concrete cylinders is measured under changing axial loads.

The parameters affecting the stress wave propagation velocity are the density, Poisson's ratio, and modulus of elasticity of the medium, and the state of stress. The change in the velocity of mechanical (stress) waves traveling in solids can be an indicator of the level of stress. Standard cylinders are also tested under changing axial loads to capture waveforms. The changes in wave frequencies are also investigated in addition to wave velocities.

Sensitivity analysis is conducted using analytical and finite element models. The results are organized and discussed. Conclusions are drawn.

1.2. General:

The traditional, and still most widely used, test methods for concrete and masonry are destructive methods, such as coring, drilling or otherwise removing part of a structure. While these methods are reliable, they are time consuming, expensive, and the defects they cause often become initiation points of deterioration. Over the past several decades, a range of non-destructive tests (including X-rays, gamma rays, radar, infrared thermographs, and acoustic methods) has become widely used, not only for concrete, but for other structural materials as well.

A non-destructive test (NDT) is one in which there is no impairment of the properties and performance in future use of the object under examination. The subject of NDT has no clearly defined boundaries. It ranges from simple techniques such as visual examination of surfaces, through the well-established methods of radiography, ultrasonic testing, magnetic particle crack detection, to new methods such as the measurement of Barkhausen noise and positron annihilation.

1.3. Commonly Used Non-Destructive Testing Methods:

Most of the available non-destructive testing (NDT) methods are listed below:

According to Method of Use:

- Dynamic (Vibration) Tests
 - Acoustic Emission (AE)
 - Intensity Method
 - Pulse-Echo Methods
 - Ground Penetrating Radar
 - Impact-Echo
 - Resonant Frequency Method
 - Ultrasonic Impulse-Echo
 - Through-Transmission Methods
 - Ultrasonic Pulse Velocity Method
 - Transverse Vibration Technique
- Electrical and Magnetic Methods
 - AC Field Methods
 - Barkhausen Noise Measurement
 - Cover Meter
 - Eddy Current Testing
 - Magnetic Flux Leakage
 - Magnetic Particle Inspection

- Microwave Absorption Method
- Potential Drop
- Holographic Interferometer
- Infrared and Optical Methods
 - Borescope Images
 - Infrared Thermograph (IT)
 - Shearography
- Penetration Tests
 - Laboratory Permeability Tests
 - Absorption Test
 - Chloride Ion Penetration Test
 - Rapid Chloride Permeability Test
 - Field Permeability Tests
 - Figg's Field Permeability Tests
 - Leak Testing
- Radiological/Radiographic Methods
 - Gamma Radiography
 - Neutron Beams
 - Positron Annihilation
 - X-ray
- Visual/Optical Inspection
- Other Methods
 - Break-off Method
 - Maturity Tests
 - Pull-off Tests
 - Pull-out Tests
 - Surface Hardness Methods
 - Penetration Test (Windsor probe)
 - Rebound Test (Schmidt hammer)

Note that some of the methods listed under the category of “other methods” are semi-destructive methods since they result in the inflicting of damage

which, however, may be repaired. Another list is given below in accordance to the objective of use with the available methods.

According to Objective:

- Material Properties
 - Strength
 - Break-off Tests
 - Maturity Tests
 - Penetration Probe
 - Pull-out Methods
 - Rebound Hammer
 - Ultrasonic Pulse Velocity
 - Elasticity
 - Ultrasonic Pulse Velocity
 - Density
 - Gamma Radiography
 - Ultrasonic Pulse Velocity
 - Neutron Density Gage
 - Moisture Content
 - Electrical Resistance Measurements
 - Microwave Absorption Method
 - Permeability
 - Absorption Test
 - Air Permeability Test
 - Chloride Ion Penetration Test
 - Figg's Field Permeability Tests
 - Rapid Chloride Permeability Test
 - Sorptivity
 - Water Permeability
 - General Quality and Uniformity
 - Gamma Radiography

- Penetration Probe
- Rebound Hammer
- Ultrasonic Pulse Echo
- Ultrasonic Pulse Velocity
- Visual Examination
- Topological Data
 - Thickness
 - Gamma Radiography
 - Radar
 - Ultrasonic Pulse Echo
 - Rebar Size and Location
 - Cover meter (Pachometer)
 - Eddy Current (such as Profometer)
 - Gamma Radiography
 - Radar
 - Ultrasonic Pulse Echo
 - X-ray Radiography
- Defects
 - Presence of Subsurface Voids
 - Acoustic Emission
 - Infrared Thermography
 - Radar
 - Ultrasonic Pulse Velocity
 - X-ray Radiography
 - Corrosion State of Reinforcing Steel
 - Electrical Potential Measurement

1.4. Development of Non-Destructive Testing Methods in Turkey:

Non-destructive testing started in Turkey with respect to the inspection of the welding in 1970's. The organized educational program started in the second half of the 1980's by the foundation of commission of NDT as a branch of the

Chamber of Metallurgical Engineers in 1987. With the project between the governments of Turkey and Germany, the “Welding Technology and NDT Center” was founded at the Middle East Technical University (METU) in 1988. In the same year, Turkish Atomic Energy Institution, and after 2 years, İstanbul Technical University with Institution of Nuclear Energy started educational programs on NDT. The commission of the Chamber of Metallurgical Engineers has started a certification program on NDT.

CHAPTER 2

FREE TRANSVERSE VIBRATION OF PRISMATIC COLUMNS UNDER AXIAL COMPRESSION

A series of vibration tests were conducted to relate the free vibration frequency of members to the axial compressive load on them. A concrete shear wall with dimensions of 9 x 91 x 151 cm and a steel I120 beam-column with 160 cm length were tested under changing axial load. Natural frequencies of columns and shear wall of a full-scale 24 storey R/C building were measured at different floors to see effects of changing axial dead load. This chapter discusses the theory of transverse vibration and the analytical calculations done in order to simulate the experiments.

2.1. General:

Transverse vibration of structural members is affected by many structural parameters. In general, following parameters predominantly affect the natural transverse vibration frequencies of an axially loaded member:

- Length of the member
- Material properties
 - Strength
 - Modulus of elasticity
 - Density
- Sectional properties
 - Area

- Second moment of inertia
- Load on the member
- Boundary conditions of the member

Since some of these properties are functions of each other, the problem becomes more complicated. Difficulties experienced with the boundary conditions of the test setups will be discussed later in this Chapter.

2.2. Derivations of Formulas and Different Boundary Conditions:

Dynamic equilibrium and continuity equations are derived for members under lateral and axial load. General equations are then modified for different boundary conditions. Governing equations are used to determine changes in natural vibration frequencies of different members with different boundary conditions.

For a member with arbitrarily chosen boundary conditions (Figure 2.1), a section is taken as shown in Figure 2.2.

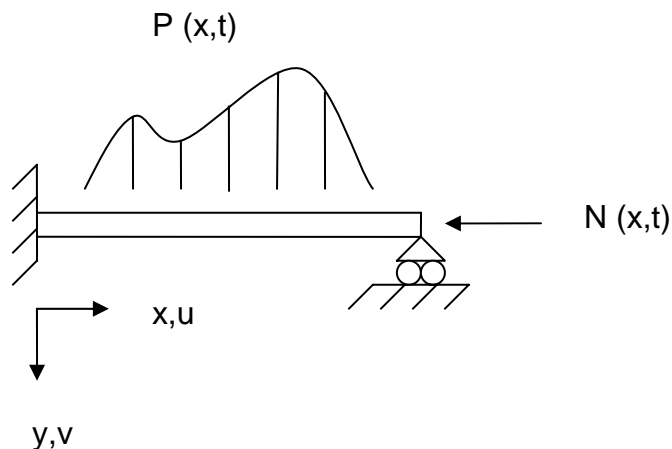


Figure 2.1: 2-D view of the beam

The section shown in Figure 2.2 has an infinitesimal length “dx”. In addition to the member forces, inertial forces also act on the shown member segment.

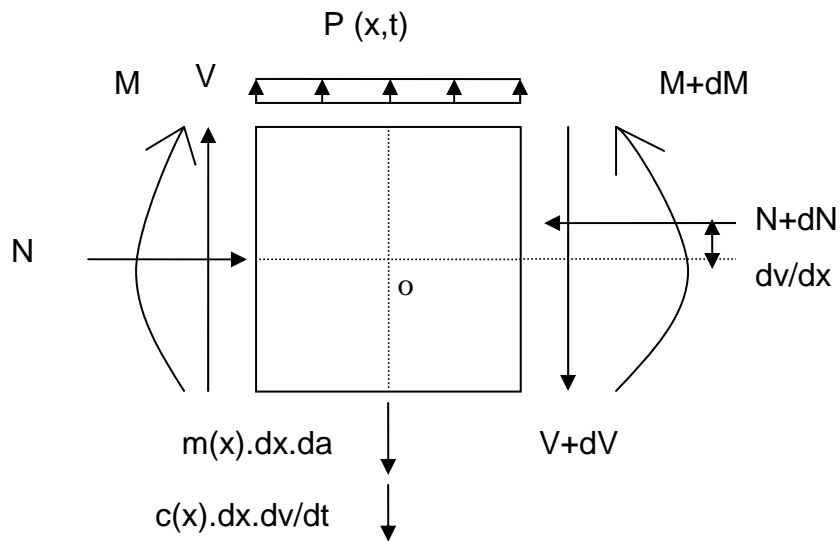


Figure 2.2: A section of the beam

The variables shown in Figure 2.2 are described below:

- N: compressive axial force
- P: force in transverse direction
- x: coordinate axis in axial direction
- u: displacement in x direction
- y: coordinate axis in transverse direction
- v: displacement in y direction
- t: time
- m: mass per unit length
- a: acceleration
- c: critical damping ratio

M: bending moment

V: shear force

d: operator to represent changes. For example:

$$dM = \frac{\partial}{\partial x} M \cdot dx$$

2.2.1. Equilibrium Equations:

The equilibrium equations of the segment shown in Figure 2.2 are written for x, y and rotational degrees of freedom as below.

$$\sum F_x = 0 = N(x, t) - N(x, t) - \frac{\partial}{\partial x} N(x, t) \cdot dx \quad (2.1)$$

$$\frac{\partial}{\partial x} N(x, t) = 0 \quad (2.2)$$

$$\sum F_y = 0 = -P(x, t) \cdot dx - V + V + \frac{\partial}{\partial x} V \cdot dx + m(x) \cdot dx \cdot \frac{\partial^2}{\partial t^2} v(x, t) + c(x) \cdot dx \cdot \frac{\partial}{\partial t} v(x, t) \quad (2.3)$$

$$P(x, t) = m(x) \cdot \frac{\partial^2}{\partial t^2} v(x, t) + c(x) \cdot \frac{\partial}{\partial x} v(x, t) + \frac{\partial}{\partial x} V \quad (2.4)$$

$$\sum M_o = 0 = M + V \cdot \frac{dx}{2} + V \cdot \frac{dx}{2} + \frac{\partial}{\partial x} V \cdot dx \cdot \frac{dx}{2} - M - \frac{\partial}{\partial x} M \cdot dx - N(x, t) \cdot \frac{\partial}{\partial x} v(x, t) \cdot dx \quad (2.5)$$

$$V = \frac{\partial}{\partial x} M + N(x, t) \cdot \frac{\partial}{\partial x} v(x, t) \quad (2.6)$$

Note that, moment acting on a section is equal to curvature times flexural rigidity (EI) of the section. Therefore,

$$\frac{\partial}{\partial x} M = \frac{\partial}{\partial x} \left(EI(x) \cdot \frac{\partial^2}{\partial x^2} v(x, t) \right) \quad (2.7)$$

2.2.2. Equation of Motion:

The equation of motion of the segment shown in Figure 2.2 is written in Equation (2.8).

$$P(x, t) = m(x) \cdot \frac{\partial^2}{\partial t^2} v(x, t) + c(x) \cdot \frac{\partial}{\partial t} v(x, t) + \frac{\partial^2}{\partial x^2} \left(EI(x) \cdot \frac{\partial^2}{\partial x^2} v(x, t) \right) + \frac{\partial}{\partial x} \left(N(x, t) \cdot \frac{\partial}{\partial x} v(x, t) \right) \quad (2.8)$$

Note that during the analysis of column vibration, the effects of rotational inertia and shear deformations are neglected. Further, let:

$$m(x) = m$$

$$EI(x) = EI, \text{ same material \& geometric properties throughout the length}$$

$$N(x) = N$$

The impulse duration is so short that all the modes are excited, i.e.

$$P(x, t) = 0, \text{ free vibration}$$

Undamped vibration is assumed. Thus,

$$c(x) = 0$$

Under the above assumptions the equation of motion becomes:

$$m \cdot \frac{\partial^2}{\partial t^2} v(x, t) + EI \cdot \frac{\partial^4}{\partial x^4} v(x, t) + N \cdot \frac{\partial^2}{\partial x^2} v(x, t) = 0 \quad (2.9)$$

If the effects of rotational inertia and shear deformations are taken into consideration, the “general” equation of motion of the transverse vibration of a beam under axial compression is defined as [1]:

$$m \cdot \frac{\partial^2}{\partial t^2} u + c(x) \cdot \frac{\partial}{\partial t} u + EI \cdot \frac{\partial^4}{\partial x^4} u + \frac{\partial}{\partial x} \left(N(x) \cdot \frac{\partial}{\partial x} u \right) - m \cdot r^2 \cdot \left(1 + \frac{E}{\kappa \cdot G} \right) \cdot \frac{\partial^2}{\partial x^2} \frac{\partial^2}{\partial t^2} u + \frac{m^2 \cdot r^2}{\kappa \cdot G \cdot A} \cdot \frac{\partial^4}{\partial t^4} u = P(x, t) \quad (2.10)$$

where,

κ : constant depending on the cross-sectional shape and accounting for the non-uniform distribution of shear stress across the section

G: the modulus of rigidity

A: the area of cross-section

r: the radius of gyration

Since the test members (like most of the reinforced concrete members) were stocky members, shear deformation and rotational inertia can be neglected [1]. That is;

$$m \cdot r^2 \cdot \left(1 + \frac{E}{\kappa \cdot G} \right) \cdot \frac{d^2}{dx^2} \frac{d^2}{dt^2} u = 0 \quad (2.11)$$

$$\frac{m^2 \cdot r^2}{\kappa \cdot G \cdot A} \cdot \frac{d^4}{dt^4} u = 0 \quad (2.12)$$

A solution is attempted of the form;

$$v(x, t) = \Phi(x) \cdot z(t) \quad (2.13)$$

where $\Phi(x)$ is the shape function and $z(t)$ is the amplitude. Then;

$$\frac{d^2}{dt^2} v(x, t) = \Phi(x) \cdot \frac{d^2}{dt^2} z(t) \quad (2.14)$$

$$\frac{d^2}{dx^2} v(x, t) = \frac{d^2}{dx^2} \Phi(x) \cdot z(t) \quad (2.15)$$

$$\frac{d^4}{dx^4} v(x, t) = \frac{d^4}{dx^4} \Phi(x) \cdot z(t) \quad (2.16)$$

Then, Equation (2.10) becomes,

$$m \cdot \Phi(x) \cdot \frac{d^2}{dt^2} z(t) + \left(EI \cdot \frac{d^4}{dx^4} \Phi(x) + N \cdot \frac{d^2}{dx^2} \Phi(x) \right) \cdot z(t) = 0 \quad (2.17)$$

Then,

$$\frac{d^2}{dt^2} z(t) + \left(\frac{EI \cdot \frac{d^4}{dx^4} \Phi(x) + N \cdot \frac{d^2}{dx^2} \Phi(x)}{m \cdot \Phi(x)} \right) \cdot z(t) = 0 \quad (2.18)$$

or,

$$\frac{-\frac{d^2}{dt^2}z(t)}{z(t)} = \frac{EI \cdot \frac{d^4}{dx^4}\Phi(x) + N \cdot \frac{d^2}{dx^2}\Phi(x)}{m \cdot \Phi(x)} \quad (2.19)$$

The left side of the expression in Equation (2.19) is a function of “t” only, and the right side of the Equation (2.19) depends only on “x”. For the equation to be valid for all values of “x” and “t”, the two expressions must therefore be constants [1]. Assume both sides are equal to ω^2 .

$$\frac{EI \cdot \frac{d^4}{dx^4}\Phi(x) + N \cdot \frac{d^2}{dx^2}\Phi(x)}{m \cdot \Phi(x)} = \omega^2 \quad (2.20)$$

Then,

$$\frac{d^2}{dt^2}z(t) + \omega^2 \cdot z(t) = 0 \quad (2.21)$$

and,

$$0 = EI \cdot \frac{d^4}{dx^4}\Phi(x) + N \cdot \frac{d^2}{dx^2}\Phi(x) - \omega^2 \cdot m \cdot \Phi(x) \quad (2.22)$$

or,

$$0 = \frac{d^4}{dx^4}\Phi(x) + \frac{N}{EI} \cdot \frac{d^2}{dx^2}\Phi(x) - \frac{\omega^2 \cdot m}{EI} \cdot \Phi(x) \quad (2.23)$$

The solution of the fourth-order, linear ordinary differential equation of $\Phi(x)$ shown in Equation (2.23) is in the following form:

$$\Phi(x) = R \cdot e^{rx} \quad (2.24)$$

“R” in Equation (2.24) is an arbitrary constant. When $\Phi(x)$ of Equation (2.24) is substituted in Equation (2.23), the characteristic equation is obtained as shown in Equation (2.25) and (2.26).

$$0 = R \cdot r^4 \cdot e^{rx} + \frac{N}{EI} \cdot R \cdot r^2 \cdot e^{rx} - \frac{\omega^2 \cdot m}{EI} \cdot R \cdot e^{rx} \quad (2.25)$$

or;

$$0 = r^4 + \frac{N}{EI} \cdot r^2 - \frac{\omega^2 \cdot m}{EI} \quad (2.26)$$

A variable “K” is defined as shown in Equation (2.27).

$$K = \sqrt{4 \cdot EI \cdot m \cdot \omega^2 + N^2} \quad (2.27)$$

Then, the four roots of the characteristic equation can be found as follows:

$$r_1 = i \cdot \sqrt{\frac{K + N}{2 \cdot EI}} \quad (2.28)$$

$$r_2 = -i \cdot \sqrt{\frac{K + N}{2 \cdot EI}} \quad (2.29)$$

$$r_3 = \sqrt{\frac{K - N}{2 \cdot EI}} \quad (2.30)$$

$$r_4 = \sqrt{\frac{K - N}{2 \cdot EI}} \quad (2.31)$$

Let,

$$\alpha = \sqrt{\frac{K + N}{2 \cdot EI}} \quad (2.32)$$

$$\beta = \sqrt{\frac{K - N}{2 \cdot EI}} \quad (2.33)$$

Note that,

$$\alpha = \sqrt{\beta^2 + \frac{N}{E \cdot I}} \quad (2.34)$$

If α and β are both positive numbers, then roots r_1 through r_4 are calculated as follows:

$$r_1 = i \cdot \alpha \quad (2.35)$$

$$r_2 = -i \cdot \alpha \quad (2.36)$$

$$r_3 = \beta \quad (2.37)$$

$$r_4 = -\beta \quad (2.38)$$

Shape function becomes,

$$\Phi(x) = R_1 \cdot e^{i\alpha \cdot x} + R_2 \cdot e^{-i\alpha \cdot x} + R_3 \cdot e^{\beta \cdot x} + R_4 \cdot e^{-\beta \cdot x} \quad (2.39)$$

Note that;

$$e^{i\alpha \cdot x} = \cos(\alpha \cdot x) + i \cdot \sin(\alpha \cdot x) \quad (2.40)$$

$$e^{-i\alpha \cdot x} = \cos(\alpha \cdot x) - i \cdot \sin(\alpha \cdot x) \quad (2.41)$$

$$e^{\beta \cdot x} = \cosh(\beta \cdot x) + \sinh(\beta \cdot x) \quad (2.42)$$

$$e^{-\beta \cdot x} = \cosh(\beta \cdot x) - \sinh(\beta \cdot x) \quad (2.43)$$

Then, shape function can be rewritten as,

$$\begin{aligned} \Phi(x) = & R_1 \cdot (\cos(\alpha \cdot x) + i \cdot \sin(\alpha \cdot x)) + \\ & R_2 \cdot (\cos(\alpha \cdot x) - i \cdot \sin(\alpha \cdot x)) + R_3 \cdot (\cosh(\beta \cdot x) + \sinh(\beta \cdot x)) \\ & + R_4 \cdot (\cosh(\beta \cdot x) - \sinh(\beta \cdot x)) \end{aligned} \quad (2.44)$$

or,

$$\begin{aligned} \Phi(x) = & (R_1 + R_2) \cdot \cos(\alpha \cdot x) + i \cdot (R_1 - R_2) \cdot \sin(\alpha \cdot x) + \\ & (R_3 + R_4) \cdot \cosh(\beta \cdot x) + (R_3 - R_4) \cdot \sinh(\beta \cdot x) \end{aligned} \quad (2.45)$$


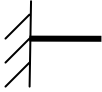
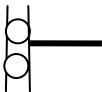
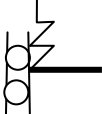
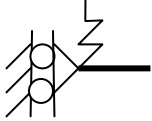
All constants are replaced with the letter “C” to simplify the equation. The shape function is obtained as shown in Equation (2.46).

$$\begin{aligned} \Phi(x) = & C_1 \cdot \cos(\alpha \cdot x) + C_2 \cdot \sin(\alpha \cdot x) + C_3 \cdot \cosh(\beta \cdot x) + \\ & C_4 \cdot \sinh(\beta \cdot x) \end{aligned} \quad (2.46)$$

For a 2-D element four boundary conditions needed to be defined from which four constants (C_1 through C_4) are solved. Four boundary conditions are

grouped by two conditions at each end. The effects of support conditions on $\Phi(x)$ are shown in a tabular form in Table 2.1.

Table 2.1. The effects of support conditions on mode shapes

Support Conditions	Mode Shape Functions
 Pin	$\Phi(0) = 0$ and $\Phi''(0) = 0$
 Fixed	$\Phi(0) = 0$ and $\Phi'(0) = 0$
 Fixed roller	$\Phi(0) = 0$ and $\Phi'''(0) = 0$
 Transverse spring with roller	$\Phi'(0) = 0$ and $\Phi'''(0).E.I = k.\Phi(0)$
 Transverse spring with pin	$\Phi''(0) = 0$ and $\Phi'''(0).E.I = k.\Phi(0)$

Application of the four boundary conditions (two on each side) will provide a solution for “ β ” values and hence for the natural frequency “ ω ” for all modes.

Following boundary conditions will be considered:

- pin ends on both supports
- fixed ends on both supports
- transverse springs with rollers on both ends
- fixed end and spring with roller on other end

Motion with respect to Time:

A similar solution is derived for the amplitude function $z(t)$. Equation (2.21) is used as the starting point. Let:

$$z(t) = A \cdot e^{at} \quad (2.47)$$

Equation (2.21) becomes,

$$A \cdot a^2 \cdot e^{at} + \omega^2 \cdot A \cdot e^{at} = 0 \quad (2.48)$$

Then,

$$a^2 + \omega^2 = 0 \quad (2.49)$$

Where,

$$a_1 = i \cdot \omega \quad (2.50)$$

$$a_2 = -i \cdot \omega \quad (2.51)$$

The amplitude function $z(t)$ becomes:

$$z(t) = A_1 \cdot e^{i\omega t} + A_2 \cdot e^{-i\omega t} \quad (2.52)$$

$$z(t) = A_1 \cdot (\cos(\omega \cdot t) + i \cdot \sin(\omega \cdot t)) + A_2 \cdot (\cos(\omega \cdot t) - i \cdot \sin(\omega \cdot t)) \quad (2.53)$$

or,

$$z(t) = (A_1 + A_2) \cdot \cos(\omega \cdot t) + i \cdot (A_1 - A_2) \cdot \sin(\omega \cdot t) \quad (2.54)$$

If the constants are replaced with the letters “A” and “B”, respectively, the amplitude function becomes;

$$z(t) = A \cdot \cos(\omega \cdot t) + B \cdot \sin(\omega \cdot t) \quad (2.55)$$

The general equations derived in Equation (2.46) and (2.55) are used to derive governing equations for the considered boundary conditions.

2.2.3. Pinned Ends on Both Supports:

If only translations are prevented at both ends (Figure 2.3), i.e. simply supported, at both, $x = 0$ and at $x = L$ the lateral displacements and the moments will be zero.

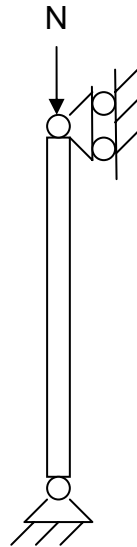


Figure 2.3: The sketch of a simply supported beam

$$\Phi(x) = 0 \quad \text{at } x = 0 \text{ \& at } x = L \quad (2.56)$$

$$M(x) = E \cdot I \cdot \frac{d^2}{dx^2} \Phi(x) = 0 \quad \text{at } x = 0 \text{ \& at } x = L \quad (2.57)$$

Note that,

$$\cosh(0) = 1 \quad (2.58)$$

$$\sinh(0) = 0 \quad (2.59)$$

$$\frac{d}{dx} \cosh(x) = \sinh(x) \quad (2.60)$$

$$\frac{d}{dx} \sinh(x) = \cosh(x) \quad (2.61)$$

When the displacement boundary conditions are inserted in the shape function, following relationships are obtained:

$$\Phi(0) = 0 = C_1 + C_3 \quad (2.62)$$

$$C_3 = -C_1 \quad (2.63)$$

$$M(0) = E \cdot I \cdot \frac{d^2}{dx^2} \Phi(0) = 0 = -\alpha^2 \cdot C_1 + \beta^2 \cdot C_3 \quad (2.64)$$

$$0 = -(\alpha^2 + \beta^2) \cdot C_1 \quad (2.65)$$

Note that,

$$\alpha^2 + \beta^2 = \frac{K}{2 \cdot E \cdot I} = \frac{\sqrt{4 \cdot E \cdot I \cdot m \cdot \omega^2 + N^2}}{2 \cdot E \cdot I} \quad (2.66)$$

Equation (2.66) should not be equal to zero for a nontrivial solution. Therefore, C_1 , and thus C_3 , must both be equal to zero. Boundary conditions at $x=L$ are similarly expressed as shown in Equation (2.67) and (2.68).

$$\Phi(L) = 0 = C_2 \cdot \sin(\alpha \cdot L) + C_4 \cdot \sinh(\beta \cdot L) \quad (2.67)$$

$$M(L) = E \cdot I \cdot \frac{d^2}{dx^2} \Phi(L) = 0 = -\alpha^2 \cdot C_2 \cdot \sin(\alpha \cdot L) + \beta^2 \cdot C_4 \cdot \sinh(\beta \cdot L) \quad (2.68)$$

These two equations can be shown and solved in matrix form,

$$\begin{pmatrix} \sin(\alpha \cdot L) & \sinh(\beta \cdot L) \\ -\alpha^2 \cdot \sin(\alpha \cdot L) & \beta^2 \cdot \sinh(\beta \cdot L) \end{pmatrix} \cdot \begin{pmatrix} C_2 \\ C_4 \end{pmatrix} = \begin{pmatrix} 0 \\ 0 \end{pmatrix} \quad (2.69)$$

For a nontrivial solution, the coefficient matrix must not have an inverse, i.e. the determinant of the coefficient matrix must be zero. That is,

$$(\alpha^2 + \beta^2) \cdot \sin(\alpha \cdot L) \cdot \sinh(\beta \cdot L) = 0 \quad (2.70)$$

Since $(\alpha^2 + \beta^2) \neq 0$ and $\sinh(\beta \cdot L) \neq 0$ (because $\beta > 0$), then $\sin(\alpha \cdot L)$ must be equal to zero. Therefore,

$$\alpha \cdot L = n \cdot \pi$$

where, $n = 1, 2, 3 \dots$

$$\alpha = \sqrt{\frac{K + N}{2 \cdot E \cdot I}} = \frac{n \cdot \pi}{L} \quad (2.71)$$

where,

$$K = \sqrt{4 \cdot EI \cdot m \cdot \omega^2 + N^2} \quad (2.72)$$

The natural cyclic frequency of the n-th mode is,

$$\omega_n = \frac{n \cdot \pi}{L} \cdot \sqrt{\frac{n^2 \cdot \pi^2}{L^2} \cdot \frac{E \cdot I}{m} - \frac{N}{m}} \quad (2.73)$$

The natural frequency of the n-th mode is,

$$f_n = \frac{\omega_n}{2 \cdot \pi} = \frac{n}{2 \cdot L} \cdot \sqrt{\frac{n^2 \cdot \pi^2}{L^2} \cdot \frac{E \cdot I}{m} - \frac{N}{m}} \quad (2.74)$$

where,

ω_n : cyclic fundamental frequency in n-th mode (rad/s)

f_n : fundamental frequency in n-th mode (1/s = Hz)

L: length (m)

EI: flexural rigidity (kN.m²) (1 t.cm² = 9.81 x 10⁻⁴ kN.m²)

N : axial compressive load (kN) (1 ton = 9.81 kN)

m : mass per unit length (tons/m)

In this thesis, the first (fundamental) mode will be considered because it can be seen from the below derivation that the first mode is the most sensitive mode for changes in the axial load. The change in the frequency for the load increase is the highest in the first mode.

$$f_n(0) = \frac{\omega_n}{2 \cdot \pi} = \frac{n}{2 \cdot L} \cdot \sqrt{\frac{n^2 \cdot \pi^2}{L^2} \cdot \frac{E \cdot I}{m}} \quad (2.75)$$

$$f_n(N) = \frac{\omega_n}{2 \cdot \pi} = \frac{n}{2 \cdot L} \cdot \sqrt{\frac{n^2 \cdot \pi^2}{L^2} \cdot \frac{E \cdot I}{m} - \frac{N}{m}} \quad (2.76)$$

$$\frac{\Delta f_n}{f_n} = \frac{f_n(N) - f_n(0)}{f_n(0)} = \frac{\frac{n}{2 \cdot L} \cdot \sqrt{\frac{n^2 \cdot \pi^2}{L^2} \cdot \frac{E \cdot I}{m} - \frac{N}{m}} - \frac{n}{2 \cdot L} \cdot \sqrt{\frac{n^2 \cdot \pi^2}{L^2} \cdot \frac{E \cdot I}{m}}}{\frac{n}{2 \cdot L} \cdot \sqrt{\frac{n^2 \cdot \pi^2}{L^2} \cdot \frac{E \cdot I}{m}}} \quad (2.77)$$

$$\frac{\Delta f_n}{f_n} = \sqrt{1 - \frac{N \cdot L^2}{n^2 \cdot \pi^2 \cdot E \cdot I}} - 1 \quad (2.78)$$

It can be concluded that in higher modes (i.e. as “n” increases), the ratio of the difference in the frequency to the initial vibration frequency gets smaller for changing axial load. Variable “f₁” shown in Equation (2.79) is the first vibration frequency in Hz.

$$f_1 = \frac{\omega_1}{2 \cdot \pi} = \frac{1}{2 \cdot L} \cdot \sqrt{\frac{\pi^2}{L^2} \cdot \frac{E \cdot I}{m} - \frac{N}{m}} \quad (2.79)$$

From Euler buckling,

$$P_{cr} = \frac{\pi^2 \cdot E \cdot I}{L^2} \quad (2.80)$$

When Equation (2.80) is adopted, Equation (2.79) becomes:

$$f_1 = \frac{1}{2 \cdot L} \cdot \sqrt{\frac{P_{cr} - P}{m}} \quad (2.81)$$

Another significant outcome is that the ratio of axial force “N” to “EI” plays an important role on the frequency change. Moreover, as length increases the change in the frequency increases. To summarize, the change in the vibration frequency is high in slender members.

An example is given to illustrate the use of the equations. If a simply supported 25 x 25 cm, slender column (minimum dimensions of reinforced concrete columns) is considered for a “sway-permitted” length of 6 meters:

Let, $E = 25\,000\text{ MPa}$ (250 t/cm^2)

Let, $f_{ck} = 25\text{ MPa}$ (0.25 t/cm^2) (for buckling load calculation)

In Table 2.2, the fundamental frequency ratio (f/f_o in percentages) of the concrete member is calculated for different lengths and load levels.

The results show a reduction of about 35 % of first fundamental vibration frequency between the “no-load” and “buckling load” stages for a 6 m long member (pin-pin connected). A “sway-permitted” analysis of the same cross-section over a length of 2.1 m gives a frequency change of about 4 %. This example demonstrates that the method is more applicable to the slender members, such as “sway-permitted” frames with weak columns.

Mode Shapes:

For a nontrivial solution, $\sin(\alpha \cdot L)$ is equal to zero. In addition, C_1 and C_3 are equal to zero. From Equation (2.67):

$$\Phi(L) = 0 = C_2 \cdot \sin(\alpha \cdot L) + C_4 \cdot \sinh(\beta \cdot L)$$

$C_4 \cdot \sinh(\beta \cdot L)$ must be equal to zero. Since, β is not equal to zero, $\sinh(\beta \cdot L)$ cannot be equal to zero. Thus, C_4 must be equal to zero.

Table 2.2. The fundamental frequency ratio of the concrete member of 25x25 cm (continued)

		Length (m)																						
		0,50	0,75	1,00	1,25	1,50	1,75	2,00	2,25	2,50	2,75	3,00	3,25	3,50	3,75	4,00	4,25	4,50	4,75	5,00	5,25	5,50	5,75	6,00
Load (kN)	9400	99,9	99,7	99,4	99,1	98,7	98,2	97,6	97,0	96,3	95,5	94,6	93,6	92,6	91,4	90,2	88,8	87,4	85,8	84,1	82,3	80,4	78,3	76,1
	9500	99,9	99,7	99,4	99,1	98,7	98,2	97,6	97,0	96,2	95,4	94,5	93,5	92,5	91,3	90,0	88,7	87,2	85,6	83,9	82,1	80,1	78,0	75,8
	9600	99,9	99,7	99,4	99,1	98,6	98,2	97,6	96,9	96,2	95,4	94,5	93,5	92,4	91,2	89,9	88,6	87,1	85,5	83,7	81,9	79,9	77,8	75,5
	9700	99,8	99,7	99,4	99,1	98,6	98,1	97,6	96,9	96,2	95,3	94,4	93,4	92,3	91,1	89,8	88,4	86,9	85,3	83,6	81,7	79,7	77,5	75,2
	9800	99,8	99,7	99,4	99,0	98,6	98,1	97,5	96,9	96,1	95,3	94,3	93,3	92,2	91,0	89,7	88,3	86,8	85,1	83,4	81,5	79,4	77,2	74,9
	9900	99,8	99,7	99,4	99,0	98,6	98,1	97,5	96,8	96,1	95,2	94,3	93,3	92,1	90,9	89,6	88,2	86,6	85,0	83,2	81,3	79,2	77,0	74,6
	10000	99,8	99,6	99,4	99,0	98,6	98,1	97,5	96,8	96,0	95,2	94,2	93,2	92,1	90,8	89,5	88,0	86,5	84,8	83,0	81,0	79,0	76,7	74,3
	10100	99,8	99,6	99,4	99,0	98,6	98,1	97,5	96,8	96,0	95,1	94,2	93,1	92,0	90,7	89,4	87,9	86,3	84,6	82,8	80,8	78,7	76,4	74,0
	10200	99,8	99,6	99,4	99,0	98,6	98,0	97,4	96,7	95,9	95,1	94,1	93,1	91,9	90,6	89,3	87,8	86,2	84,5	82,6	80,6	78,5	76,2	73,7
	10300	99,8	99,6	99,4	99,0	98,5	98,0	97,4	96,7	95,9	95,0	94,1	93,0	91,8	90,5	89,2	87,7	86,0	84,3	82,4	80,4	78,2	75,9	73,4
	10400	99,8	99,6	99,4	99,0	98,5	98,0	97,4	96,7	95,9	95,0	94,0	92,9	91,7	90,4	89,0	87,5	85,9	84,1	82,2	80,2	78,0	75,6	73,1
	10500	99,8	99,6	99,3	99,0	98,5	98,0	97,4	96,6	95,8	94,9	93,9	92,8	91,6	90,3	88,9	87,4	85,7	84,0	82,0	80,0	77,8	75,4	72,8
	10600	99,8	99,6	99,3	99,0	98,5	98,0	97,3	96,6	95,8	94,9	93,9	92,8	91,6	90,2	88,8	87,3	85,6	83,8	81,9	79,8	77,5	75,1	72,4
	10700	99,8	99,6	99,3	99,0	98,5	97,9	97,3	96,6	95,7	94,8	93,8	92,7	91,5	90,1	88,7	87,1	85,5	83,6	81,7	79,5	77,3	74,8	72,1
	10800	99,8	99,6	99,3	99,0	98,5	97,9	97,3	96,5	95,7	94,8	93,8	92,6	91,4	90,1	88,6	87,0	85,3	83,5	81,5	79,3	77,0	74,5	71,8
	10900	99,8	99,6	99,3	98,9	98,5	97,9	97,2	96,5	95,7	94,7	93,7	92,6	91,3	90,0	88,5	86,9	85,2	83,3	81,3	79,1	76,8	74,3	71,5
	11000	99,8	99,6	99,3	98,9	98,4	97,9	97,2	96,5	95,6	94,7	93,6	92,5	91,2	89,9	88,4	86,8	85,0	83,1	81,1	78,9	76,5	74,0	71,2
	11100	99,8	99,6	99,3	98,9	98,4	97,9	97,2	96,4	95,6	94,6	93,6	92,4	91,1	89,8	88,3	86,6	84,9	83,0	80,9	78,7	76,3	73,7	70,9
	11200	99,8	99,6	99,3	98,9	98,4	97,8	97,2	96,4	95,5	94,6	93,5	92,4	91,1	89,7	88,1	86,5	84,7	82,8	80,7	78,5	76,0	73,4	70,6
	11300	99,8	99,6	99,3	98,9	98,4	97,8	97,1	96,4	95,5	94,5	93,5	92,3	91,0	89,6	88,0	86,4	84,6	82,6	80,5	78,2	75,8	73,1	70,3
	11400	99,8	99,6	99,3	98,9	98,4	97,8	97,1	96,3	95,4	94,5	93,4	92,2	90,9	89,5	87,9	86,2	84,4	82,4	80,3	78,0	75,5	72,9	69,9
	11500	99,8	99,6	99,3	98,9	98,4	97,8	97,1	96,3	95,4	94,4	93,3	92,1	90,8	89,4	87,8	86,1	84,3	82,3	80,1	77,8	75,3	72,6	69,6
	11600	99,8	99,6	99,3	98,9	98,4	97,8	97,1	96,3	95,4	94,4	93,3	92,1	90,7	89,3	87,7	86,0	84,1	82,1	79,9	77,6	75,0	72,3	69,3
	11700	99,8	99,6	99,3	98,9	98,3	97,7	97,0	96,2	95,3	94,3	93,2	92,0	90,6	89,2	87,6	85,8	84,0	81,9	79,7	77,4	74,8	72,0	69,0
	11800	99,8	99,6	99,3	98,8	98,3	97,7	97,0	96,2	95,3	94,3	93,2	91,9	90,6	89,1	87,5	85,7	83,8	81,8	79,5	77,1	74,5	71,7	68,6
	11900	99,8	99,6	99,3	98,8	98,3	97,7	97,0	96,2	95,3	94,2	93,1	91,8	90,5	89,0	87,3	85,6	83,7	81,6	79,3	76,9	74,3	71,4	68,3
	12000	99,8	99,6	99,3	98,8	98,3	97,7	97,0	96,1	95,2	94,2	93,0	91,8	90,4	88,9	87,2	85,4	83,5	81,4	79,2	76,7	74,0	71,1	68,0
	12100	99,8	99,6	99,2	98,8	98,3	97,7	96,9	96,1	95,2	94,1	93,0	91,7	90,3	88,8	87,1	85,3	83,4	81,2	79,0	76,5	73,8	70,8	67,7
	12200	99,8	99,6	99,2	98,8	98,3	97,6	96,9	96,1	95,1	94,1	92,9	91,6	90,2	88,7	87,0	85,2	83,2	81,1	78,8	76,2	73,5	70,6	67,3
	12300	99,8	99,6	99,2	98,8	98,3	97,6	96,9	96,0	95,1	94,0	92,9	91,6	90,1	88,6	86,9	85,1	83,1	80,9	78,6	76,0	73,3	70,3	67,0
	12400	99,8	99,6	99,2	98,8	98,2	97,6	96,9	96,0	95,1	94,0	92,8	91,5	90,0	88,5	86,8	84,9	82,9	80,7	78,4	75,8	73,0	70,0	66,6
	12500	99,8	99,6	99,2	98,8	98,2	97,6	96,8	96,0	95,0	93,9	92,7	91,4	90,0	88,4	86,7	84,8	82,8	80,6	78,2	75,6	72,7	69,7	66,3
12600	99,8	99,6	99,2	98,8	98,2	97,6	96,8	95,9	95,0	93,9	92,7	91,3	89,9	88,3	86,5	84,7	82,6	80,4	78,0	75,3	72,5	69,4	66,0	
12700	99,8	99,6	99,2	98,8	98,2	97,5	96,8	95,9	94,9	93,8	92,6	91,3	89,8	88,2	86,4	84,5	82,5	80,2	77,8	75,1	72,2	69,1	65,6	
12800	99,8	99,6	99,2	98,7	98,2	97,5	96,8	95,9	94,9	93,8	92,6	91,2	89,7	88,1	86,3	84,4	82,3	80,0	77,6	74,9	72,0	68,8	65,3	
12900	99,8	99,5	99,2	98,7	98,2	97,5	96,7	95,8	94,8	93,7	92,5	91,1	89,6	88,0	86,2	84,3	82,1	79,9	77,4	74,7	71,7	68,5		
13000	99,8	99,5	99,2	98,7	98,2	97,5	96,7	95,8	94,8	93,7	92,4	91,0	89,5	87,9	86,1	84,1	82,0	79,7	77,2	74,4	71,4	68,2		
13100	99,8	99,5	99,2	98,7	98,1	97,5	96,7	95,8	94,8	93,6	92,4	91,0	89,5	87,8	86,0	84,0	81,8	79,5	77,0	74,2	71,2	67,9		
13200	99,8	99,5	99,2	98,7	98,1	97,5	96,7	95,7	94,7	93,6	92,3	90,9	89,4	87,7	85,9	83,9	81,7	79,3	76,8	74,0	70,9			
13300	99,8	99,5	99,2	98,7	98,1	97,4	96,6	95,7	94,7	93,5	92,2	90,8	89,3	87,6	85,7	83,7	81,5	79,1	76,6	73,7	70,6			
13400	99,8	99,5	99,2	98,7	98,1	97,4	96,6	95,7	94,6	93,5	92,2	90,8	89,2	87,5	85,6	83,6	81,4	79,0	76,3	73,5				
13500	99,8	99,5	99,2	98,7	98,1	97,4	96,6	95,7	94,6	93,4	92,1	90,7	89,1	87,4	85,5	83,5	81,2	78,8	76,1	73,3				
13600	99,8	99,5	99,1	98,7	98,1	97,4	96,6	95,6	94,6	93,4	92,1	90,6	89,0	87,3	85,4	83,3	81,1	78,6	75,9					
13700	99,8	99,5	99,1	98,7	98,1	97,4	96,5	95,6	94,5	93,3	92,0	90,5	88,9	87,2	85,3	83,2	80,9	78,4	75,7					
13800	99,8	99,5	99,1	98,6	98,0	97,3	96,5	95,6	94,5	93,3	91,9	90,5	88,9	87,1	85,2	83,0	80,8	78,3						
13900	99,8	99,5	99,1	98,6	98,0	97,3	96,5	95,5	94,4	93,2	91,9	90,4	88,8	87,0	85,0	82,9	80,6	78,1						
14000	99,8	99,5	99,1	98,6	98,0	97,3	96,5	95,5	94,4	93,2	91,8	90,3	88,7	86,9	84,9	82,8	80,4							
14100	99,8	99,5	99,1	98,6	98,0	97,3	96,4	95,5	94,4	93,1	91,8	90,3	88,6	86,8	84,8	82,6								
14200	99,8	99,5	99,1	98,6	98,0	97,3	96,4	95,4	94,3	93,1	91,7	90,2	88,5	86,7	84,7	82,5								
14300	99,8	99,5	99,1	98,6	98,0	97,2	96,4	95,4	94,3	93,0	91,6	90,1	88,4	86,6	84,6									
14400	99,8	99,5	99,1	98,6	98,0	97,2	96,3	95,4	94,2	93,0	91,6	90,0	88,3	86,5	84,4									
14500	99,8	99,5	99,1	98,6	97,9	97,2	96,3	95,3	94,2	92,9	91,5	90,0	88,3	86,4										
14600	99,8	99,5	99,1	98,6	97,9	97,2	96,3	95,3	94,1	92,9	91,5	89,9	88,2											
14700	99,8	99,5	99,1	98,6	97,9	97,2	96,3	95,3	94,1	92,8	91,4	89,8												
14800	99,8	99,5	99,1	98,5	97,9	97,1	96,2	95,2	94,1	92,8	91,3	89,7												
14900	99,8	99,5	99,1	98,5	97,9	97,1	96,2	95,2	94,0	92,7	91,3													
15000	99,8	99,5	99,1	98,5	97,9	97,1	96,2	95,2	94,0	92,7														
15100	99,8	99,5	99,																					

As a result, shape function for different modes is obtained as shown in Equation (2.82).

$$\Phi_n(x) = C_2 \cdot \sin\left(\frac{n \cdot \pi}{L} \cdot x\right) \quad (2.82)$$

C_2 can be taken as equal to one for unit amplitude. The shape function of the first mode becomes,

$$\Phi_1(x) = \sin\left(\frac{\pi}{L} \cdot x\right) \quad (2.83)$$

2.2.4. Fixed Ends on Both Supports:

After pin-pin condition explained in Section 2.2.3, the governing equations and natural frequencies for fixed-fixed condition are derived similarly. The general view of a fixed-fixed column is shown in Figure 2.4.

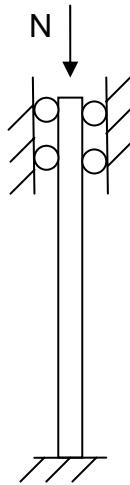


Figure 2.4: The sketch of a fixed ended column

If the beam or column is fixed at both ends, the boundary conditions are such that at $x = 0$ & $x = L$, the lateral displacements and the rotations are equal to zero.

$$\Phi(x) = 0 \quad \text{at } x = 0 \text{ \& } x = L \quad (2.84)$$

$$\frac{d}{dx}\Phi(x) = 0 \quad \text{at } x = 0 \text{ \& } x = L \quad (2.85)$$

Remember from Equation (2.46):

$$\Phi(x) = C_1 \cdot \cos(\alpha \cdot x) + C_2 \cdot \sin(\alpha \cdot x) + C_3 \cdot \cosh(\beta \cdot x) + C_4 \cdot \sinh(\beta \cdot x)$$

The boundary conditions for a fixed-fixed column are shown in Equation (2.86) through (2.93).

At $x = 0$,

$$\Phi(0) = 0 = C_1 + C_3 \quad (2.86)$$

$$C_3 = -C_1 \quad (2.87)$$

$$\frac{d}{dx}\Phi(x) = 0 = \alpha \cdot C_2 + \beta \cdot C_4 \quad (2.88)$$

$$C_4 = \frac{-\alpha}{\beta} \cdot C_2 \quad (2.89)$$

At $x = L$,

$$\Phi(L) = 0 = C_1 \cdot \cos(\alpha \cdot L) + C_2 \cdot \sin(\alpha \cdot L) + C_3 \cdot \cosh(\beta \cdot L) + C_4 \cdot \sinh(\beta \cdot L) \quad (2.90)$$

$$0 = C_1 \cdot (\cos(\alpha \cdot L) - \cosh(\beta \cdot L)) + C_2 \cdot \left(\sin(\alpha \cdot L) - \frac{\alpha}{\beta} \cdot \sinh(\beta \cdot L) \right) \quad (2.91)$$

$$\frac{d}{dx} \Phi(x) = 0 = -\alpha \cdot C_1 \cdot \sin(\alpha \cdot L) + \alpha \cdot C_2 \cdot \cos(\alpha \cdot L) + \beta \cdot C_3 \cdot \sinh(\beta \cdot L) + \beta \cdot C_4 \cdot \cosh(\beta \cdot L) \quad (2.92)$$

$$0 = C_1 \cdot (-\alpha \cdot \sin(\alpha \cdot L) - \beta \cdot \sinh(\beta \cdot L)) + C_2 \cdot (\alpha \cdot \cos(\alpha \cdot L) - \alpha \cdot \cosh(\beta \cdot L)) \quad (2.93)$$

These equations can be shown and solved in matrix form,

$$\begin{pmatrix} \cos(\alpha \cdot L) - \cosh(\beta \cdot L) & \sin(\alpha \cdot L) - \frac{\alpha}{\beta} \cdot \sinh(\beta \cdot L) \\ -\alpha \cdot \sin(\alpha \cdot L) - \beta \cdot \sinh(\beta \cdot L) & \alpha \cdot \cos(\alpha \cdot L) - \alpha \cdot \cosh(\beta \cdot L) \end{pmatrix} \cdot \begin{pmatrix} C_1 \\ C_2 \end{pmatrix} = \begin{pmatrix} 0 \\ 0 \end{pmatrix} \quad (2.94)$$

For a nontrivial solution, the coefficient matrix must not have an inverse, i.e. the determinant of the coefficient matrix should be zero. That is,

$$2 \cdot \alpha - 2 \cdot \alpha \cdot \cos(\alpha \cdot L) \cdot \cosh(\beta \cdot L) - \frac{(\alpha^2 - \beta^2)}{\beta} \cdot \sin(\alpha \cdot L) \cdot \sinh(\beta \cdot L) = 0 \quad (2.95)$$

A solution procedure for this nonlinear function may be iterative:

1. Select β where $\beta > 0$.
2. Enter the length "L" in meters.
3. Enter the flexural rigidity "E.I" and axial compressive force "N".

4. Compute α where $\alpha = \sqrt{\beta^2 + \frac{N}{E \cdot I}}$

N : axial compressive load (kN) (1 ton = 9.81 kN)

EI: flexural rigidity (kN.m²) (1 t.cm² = 9.81 x 10⁻⁴ kN.m²)

5. Calculate Equation (2.95).

$$f(\alpha, \beta) = 2 \cdot \alpha - 2 \cdot \alpha \cdot \cos(\alpha \cdot L) \cdot \cosh(\beta \cdot L) - \frac{(\alpha^2 - \beta^2)}{\beta} \cdot \sin(\alpha \cdot L) \cdot \sinh(\beta \cdot L)$$

6. If the accuracy is not acceptable (i.e. not close to zero), repeat steps (1-5). Note that, precision of the solver function of MS Excel worksheet is “0.000001”.

7. After finding “ β ” and “ α ”, vibration frequencies can be calculated.

Remember the definition of “ α ” from Equation (2.32) and “ K ” from Equation (2.27). Then, vibration frequencies can be computed from Equation (2.96).

$$K = 2 \cdot E \cdot I \cdot \alpha^2 - N = \sqrt{4 \cdot E \cdot I \cdot m \cdot \omega^2 + N^2} \quad (2.96)$$

The cyclic fundamental frequency can be computed by Equation (2.97).

$$\omega = \sqrt{\frac{E \cdot I}{m} \cdot \alpha^4 - \frac{N}{m} \cdot \alpha^2} \quad (2.97)$$

The fundamental frequency can be computed by Equation (2.98).

$$f = \frac{\omega}{2 \cdot \pi} = \frac{\alpha}{2 \cdot \pi} \cdot \sqrt{\frac{E \cdot I}{m} \cdot \alpha^2 - \frac{N}{m}} \quad (2.98)$$

where,

ω : cyclic fundamental frequency (rad/s)

f : fundamental frequency (1/s = Hz)

EI : flexural rigidity (kN.m²) (1 t.cm² = 9.81 x 10⁻⁴ kN.m²)

N : axial compressive load (kN) (1 ton = 9.81 kN)

m : mass per unit length (tons/m)

To illustrate the use of the derived formulas, I120 steel columns (fixed-fixed supported) with different lengths are used to compute the frequency ratios as

shown in Figure 2.5 and Figure 2.6. The fundamental frequency changes are provided in Table 2.3 in percentage and in Table 2.4 in frequencies (Hz) with respect to load (in kN). The frequency ratios for all “I sections” are given in Appendix A.

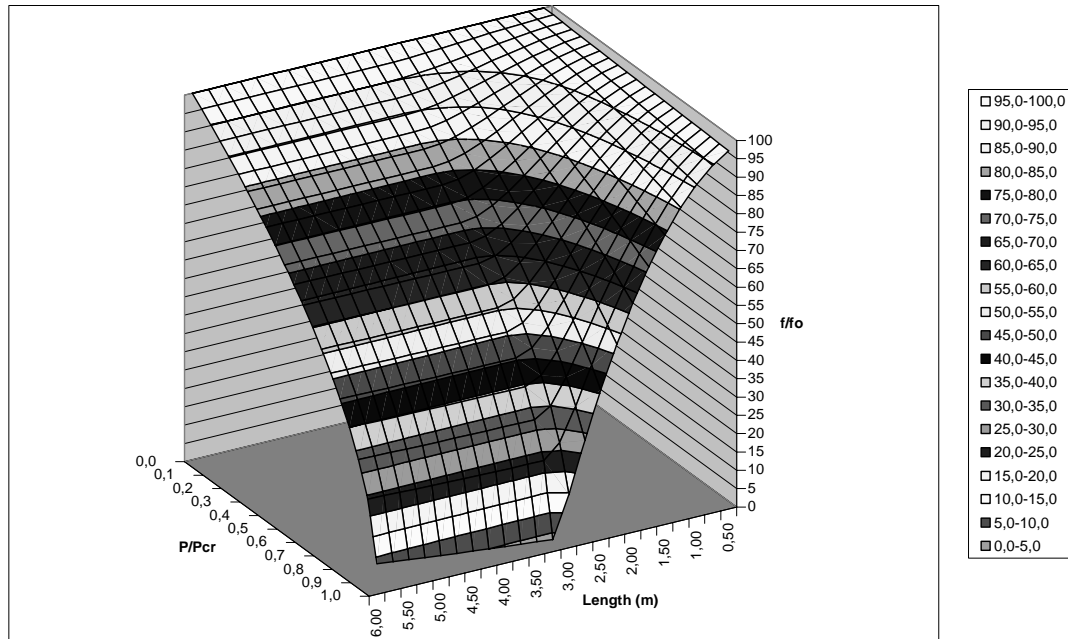


Figure 2.5: 3-D surface chart of the first vibration frequency ratios of the steel I120 beam-column for certain lengths

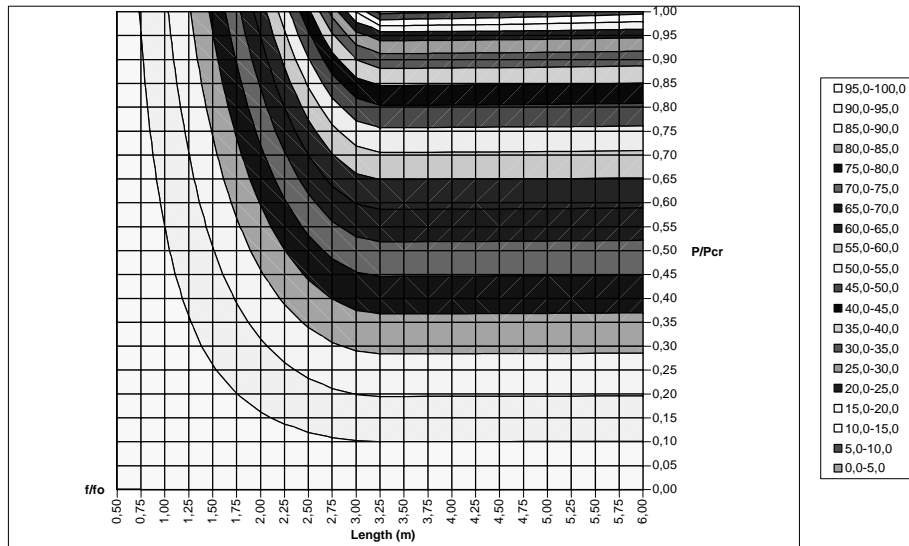


Figure 2.6: Contour chart of the first vibration frequency ratios of the steel I120 beam-column for certain lengths

The results have shown that in elastic buckling range, the relationship between the ratio of the vibration frequency to the unstressed frequency and the ratio of the load to the buckling load becomes insensitive to the changes in length (Figure 2.7). Elastic buckling range starts from 3.25 m for I120.

Figure 2.8 is given as an illustration in order to show the relationship between the ratio of vibration frequency to unstressed frequency and the ratio of the load to buckling load for 5 m.

Table 2.3. Fundamental frequency change in percentage versus axial load level for I120 steel column for different lengths

f/f _o (%)	Length (m)																							
	0,50	0,75	1,00	1,25	1,50	1,75	2,00	2,25	2,50	2,75	3,00	3,25	3,50	3,75	4,00	4,25	4,50	4,75	5,00	5,25	5,50	5,75	6,00	
0	100,0	100,0	100,0	100,0	100,0	100,0	100,0	100,0	100,0	100,0	100,0	100,0	100,0	100,0	100,0	100,0	100,0	100,0	100,0	100,0	100,0	100,0	100,0	100,0
5	100,0	99,9	99,9	99,8	99,7	99,6	99,5	99,3	99,1	99,0	98,8	98,6	98,3	98,1	97,8	97,5	97,2	96,9	96,5	96,2	95,8	95,4	95,0	95,0
10	99,9	99,8	99,7	99,6	99,4	99,2	98,9	98,6	98,3	97,9	97,5	97,1	96,6	96,1	95,5	94,9	94,3	93,6	92,9	92,2	91,4	90,5	89,6	89,6
15	99,9	99,8	99,6	99,4	99,1	98,7	98,4	97,9	97,4	96,9	96,2	95,6	94,9	94,1	93,2	92,3	91,3	90,3	89,2	88,0	86,7	85,3	83,9	83,9
20	99,9	99,7	99,5	99,1	98,8	98,3	97,8	97,2	96,5	95,8	95,0	94,1	93,1	92,0	90,8	89,6	88,2	86,8	85,2	83,5	81,7	79,8	77,7	77,7
25	99,8	99,6	99,3	98,9	98,5	97,9	97,2	96,5	95,6	94,7	93,7	92,5	91,2	89,9	88,4	86,8	85,0	83,1	81,0	78,8	76,4	73,8	71,0	71,0
30	99,8	99,5	99,2	98,7	98,1	97,5	96,7	95,8	94,7	93,6	92,3	90,9	89,4	87,7	85,8	83,8	81,6	79,2	76,6	73,8	70,7	67,2	63,4	63,4
35	99,8	99,5	99,0	98,5	97,8	97,0	96,1	95,0	93,8	92,5	91,0	89,3	87,5	85,5	83,2	80,8	78,1	75,2	71,9	68,3	64,4	59,9	54,8	54,8
40	99,7	99,4	98,9	98,3	97,5	96,6	95,5	94,3	92,9	91,4	89,6	87,7	85,5	83,1	80,5	77,6	74,4	70,9	66,9	62,4	57,3	51,5	44,5	44,5
45	99,7	99,3	98,8	98,1	97,2	96,2	95,0	93,6	92,0	90,2	88,2	86,0	83,5	80,8	77,7	74,3	70,5	66,2	61,4	55,8	49,3	41,3	30,7	30,7
50	99,7	99,2	98,6	97,8	96,9	95,7	94,4	92,8	91,1	89,1	86,8	84,3	81,5	78,3	74,8	70,8	66,4	61,2	55,3	48,3	39,5	27,4	27,4	
55	99,6	99,2	98,5	97,6	96,6	95,3	93,8	92,1	90,1	87,9	85,4	82,5	79,3	75,8	71,7	67,2	61,9	55,8	48,5	39,3	26,2			
60	99,6	99,1	98,4	97,4	96,2	94,9	93,2	91,3	89,2	86,7	83,9	80,7	77,2	73,1	68,5	63,3	57,1	49,7	40,4	27,3				
65	99,6	99,0	98,2	97,2	95,9	94,4	92,6	90,6	88,2	85,5	82,4	78,9	74,9	70,4	65,2	59,1	51,8	42,7	30,2					
70	99,5	98,9	98,1	97,0	95,6	94,0	92,0	89,8	87,2	84,2	80,9	77,0	72,6	67,5	61,6	54,6	45,9	34,3	13,7					
75	99,5	98,8	97,9	96,8	95,3	93,5	91,4	89,0	86,2	83,0	79,3	75,1	70,2	64,5	57,8	49,6	39,1	22,9						
80	99,5	98,8	97,8	96,5	95,0	93,1	90,8	88,2	85,2	81,7	77,7	73,1	67,7	61,4	53,8	44,1	30,7							
85	99,4	98,7	97,7	96,3	94,6	92,6	90,2	87,4	84,2	80,4	76,1	71,0	65,1	58,1	49,3	37,8	18,9							
90	99,4	98,6	97,5	96,1	94,3	92,2	89,6	86,6	83,1	79,1	74,4	68,9	62,4	54,5	44,5	30,2								
95	99,4	98,5	97,4	95,9	94,0	91,7	89,0	85,8	82,1	77,8	72,7	66,7	59,6	50,7	39,0	19,7								
100	99,3	98,5	97,2	95,6	93,7	91,2	88,4	85,0	81,0	76,4	71,0	64,5	56,6	46,6	32,5									
105	99,3	98,4	97,1	95,4	93,3	90,8	87,7	84,2	80,0	75,0	69,2	62,1	53,4	42,0	24,4									
110	99,2	98,3	97,0	95,2	93,0	90,3	87,1	83,3	78,9	73,6	67,3	59,7	50,1	36,9	11,4									
115	99,2	98,2	96,8	95,0	92,7	89,9	86,5	82,5	77,8	72,1	65,4	57,1	46,4	31,0										
120	99,2	98,1	96,7	94,7	92,3	89,4	85,8	81,6	76,6	70,7	63,4	54,4	42,5	23,5										
125	99,1	98,1	96,5	94,5	92,0	88,9	85,2	80,8	75,5	69,1	61,4	51,6	38,1	12,0										
130	99,1	98,0	96,4	94,3	91,7	88,4	84,5	79,9	74,3	67,6	59,3	48,6	33,2											
135	99,1	97,9	96,2	94,1	91,3	88,0	83,9	79,0	73,1	66,0	57,1	45,4	27,3											
140	99,0	97,8	96,1	93,8	91,0	87,5	83,2	78,1	71,9	64,4	54,8	41,9	19,8											
145	99,0	97,8	96,0	93,6	90,6	87,0	82,6	77,2	70,7	62,7	52,4	38,1	6,0											
150	99,0	97,7	95,8	93,4	90,3	86,5	81,9	76,3	69,5	61,0	49,9	33,9												
155	98,9	97,6	95,7	93,2	90,0	86,0	81,2	75,4	68,2	59,2	47,3	29,0												
160	98,9	97,5	95,5	92,9	89,6	85,5	80,5	74,4	66,9	57,3	44,5	23,2												
165	98,9	97,4	95,4	92,7	89,3	85,0	79,8	73,5	65,6	55,4	41,5	15,2												
170	98,8	97,4	95,2	92,5	88,9	84,5	79,1	72,5	64,2	53,5	38,2													
175	98,8	97,3	95,1	92,2	88,6	84,0	78,4	71,5	62,8	51,4	34,7													
180	98,8	97,2	95,0	92,0	88,2	83,5	77,7	70,5	61,4	49,3	30,7													
185	98,7	97,1	94,8	91,8	87,9	83,0	77,0	69,5	59,9	47,0	26,1													
190	98,7	97,0	94,7	91,5	87,5	82,5	76,3	68,5	58,4	44,7	20,5													
195	98,7	97,0	94,5	91,3	87,2	82,0	75,5	67,4	56,9	42,2														
200	98,6	96,9	94,4	91,1	86,8	81,5	74,8	66,4	55,3	39,5														
205	98,6	96,8	94,2	90,8	86,4	80,9	74,0	65,3	53,7	36,7														
210	98,6	96,7	94,1	90,6	86,1	80,4	73,3	64,2	52,0	33,6														
215	98,5	96,6	93,9	90,3	85,7	79,9	72,5	63,0	50,3	30,1														
220	98,5	96,6	93,8	90,1	85,4	79,3	71,7	61,9	48,5															
225	98,5	96,5	93,7	89,9	85,0	78,8	71,0	60,7	46,6															
230	98,4	96,4	93,5	89,6	84,6	78,3	70,2	59,5	44,6															
235	98,4	96,3	93,4	89,4	84,3	77,7	69,4	58,3	42,6															
240	98,4	96,2	93,2	89,2	83,9	77,2	68,5	57,1																
245	98,3	96,2	93,1	88,9	83,5	76,6	67,7	55,8																
250	98,3	96,1	92,9	88,7	83,1	76,1	66,9	54,5																
255	98,2	96,0	92,8	88,4	82,8	75,5	66,0	53,2																
260	98,2	95,9	92,6	88,2	82,4	74,9	65,2																	
265	98,2	95,8	92,5	87,9	82,0	74,4	64,3																	
270	98,1	95,8	92,3	87,7	81,6	73,8	63,4																	
275	98,1	95,7	92,2	87,4	81,2	73,2	62,5																	
280	98,1	95,6	92,0	87,2	80,9	72,6																		
285	98,0	95,5	91,9	87,0	80,5	72,0																		
290	98,0	95,4	91,7	86,7	80,1	71,4																		
295	98,0	95,4	91,6	86,5	79,7																			
300	97,9	95,3	91,4	86,2	79,3																			
305	97,9	95,2	91,3	86,0																				
310	97,9	95,1	91,1	85,7																				
315	97,8	95,0	91,0	85,5																				
320	97,8	95,0	90,8																					
325	97,8	94,9																						
330	97,7	94,8																						
335	97,7																							

Table 2.4. Fundamental frequency versus axial load level
for I120 steel column for different lengths

f (Hz)	Length (m)																						
	0,50	0,75	1,00	1,25	1,50	1,75	2,00	2,25	2,50	2,75	3,00	3,25	3,50	3,75	4,00	4,25	4,50	4,75	5,00	5,25	5,50	5,75	6,00
0	897,8	399,0	224,5	143,7	99,8	73,3	56,1	44,3	35,9	29,7	24,9	21,3	18,3	16,0	14,0	12,4	11,1	9,9	9,0	8,1	7,4	6,8	6,2
5	897,5	398,7	224,2	143,3	99,5	73,0	55,8	44,0	35,6	29,4	24,6	20,9	18,0	15,7	13,7	12,1	10,8	9,6	8,7	7,8	7,1	6,5	5,9
10	897,2	398,4	223,8	143,0	99,1	72,7	55,5	43,7	35,3	29,1	24,3	20,6	17,7	15,3	13,4	11,8	10,5	9,3	8,3	7,5	6,8	6,1	5,6
15	896,9	398,1	223,5	142,7	98,8	72,4	55,2	43,4	35,0	28,7	24,0	20,3	17,4	15,0	13,1	11,5	10,1	9,0	8,0	7,2	6,4	5,8	5,2
20	896,6	397,8	223,2	142,4	98,5	72,1	54,9	43,1	34,7	28,4	23,7	20,0	17,1	14,7	12,7	11,1	9,8	8,6	7,6	6,8	6,1	5,4	4,8
25	896,3	397,5	222,9	142,1	98,2	71,7	54,6	42,8	34,3	28,1	23,4	19,7	16,7	14,3	12,4	10,8	9,4	8,3	7,3	6,4	5,7	5,0	4,4
30	896,0	397,2	222,6	141,8	97,9	71,4	54,2	42,5	34,0	27,8	23,0	19,3	16,4	14,0	12,0	10,4	9,0	7,9	6,9	6,0	5,2	4,6	4,0
35	895,7	396,9	222,3	141,5	97,6	71,1	53,9	42,1	33,7	27,5	22,7	19,0	16,0	13,6	11,7	10,0	8,7	7,5	6,5	5,6	4,8	4,1	3,4
40	895,4	396,6	222,0	141,2	97,3	70,8	53,6	41,8	33,4	27,1	22,3	18,6	15,7	13,3	11,3	9,6	8,2	7,0	6,0	5,1	4,3	3,5	2,8
45	895,1	396,3	221,7	140,9	97,0	70,5	53,3	41,5	33,0	26,8	22,0	18,3	15,3	12,9	10,9	9,2	7,8	6,6	5,5	4,5	3,7	2,8	1,9
50	894,8	396,0	221,4	140,6	96,7	70,2	53,0	41,2	32,7	26,4	21,6	17,9	14,9	12,5	10,5	8,8	7,4	6,1	5,0	3,9	2,9	1,9	
55	894,5	395,7	221,1	140,2	96,3	69,8	52,6	40,8	32,4	26,1	21,3	17,5	14,5	12,1	10,1	8,3	6,9	5,5	4,4	3,2	1,9		
60	894,2	395,4	220,8	139,9	96,0	69,5	52,3	40,5	32,0	25,7	20,9	17,2	14,1	11,7	9,6	7,9	6,3	4,9	3,6	2,2			
65	893,8	395,0	220,4	139,6	95,7	69,2	52,0	40,2	31,7	25,4	20,5	16,8	13,7	11,2	9,1	7,3	5,7	4,2	2,7				
70	893,5	394,7	220,1	139,3	95,4	68,9	51,6	39,8	31,3	25,0	20,2	16,4	13,3	10,8	8,6	6,8	5,1	3,4	1,2				
75	893,2	394,4	219,8	139,0	95,1	68,5	51,3	39,5	31,0	24,6	19,8	16,0	12,9	10,3	8,1	6,2	4,3	2,3					
80	892,9	394,1	219,5	138,7	94,7	68,2	51,0	39,1	30,6	24,3	19,4	15,5	12,4	9,8	7,5	5,5	3,4						
85	892,6	393,8	219,2	138,4	94,4	67,9	50,6	38,8	30,2	23,9	19,0	15,1	11,9	9,3	6,9	4,7	2,1						
90	892,3	393,5	218,9	138,0	94,1	67,5	50,3	38,4	29,9	23,5	18,6	14,6	11,4	8,7	6,2	3,7							
95	892,0	393,2	218,6	137,7	93,8	67,2	49,9	38,0	29,5	23,1	18,1	14,2	10,9	8,1	5,5	2,4							
100	891,7	392,9	218,3	137,4	93,4	66,9	49,6	37,7	29,1	22,7	17,7	13,7	10,4	7,4	4,6								
105	891,4	392,6	217,9	137,1	93,1	66,5	49,2	37,3	28,7	22,3	17,2	13,2	9,8	6,7	3,4								
110	891,1	392,3	217,6	136,8	92,8	66,2	48,9	36,9	28,3	21,8	16,8	12,7	9,2	5,9	1,6								
115	890,8	391,9	217,3	136,4	92,4	65,9	48,5	36,6	27,9	21,4	16,3	12,1	8,5	4,9									
120	890,5	391,6	217,0	136,1	92,1	65,5	48,2	36,2	27,5	21,0	15,8	11,6	7,8	3,7									
125	890,2	391,3	216,7	135,8	91,8	65,2	47,8	35,8	27,1	20,5	15,3	11,0	7,0	1,9									
130	889,8	391,0	216,4	135,5	91,4	64,8	47,4	35,4	26,7	20,1	14,8	10,3	6,1										
135	889,5	390,7	216,0	135,1	91,1	64,5	47,1	35,0	26,3	19,6	14,2	9,6	5,0										
140	889,2	390,4	215,7	134,8	90,8	64,1	46,7	34,6	25,8	19,1	13,7	8,9	3,6										
145	888,9	390,1	215,4	134,5	90,4	63,8	46,3	34,2	25,4	18,6	13,1	8,1	1,1										
150	888,6	389,8	215,1	134,1	90,1	63,4	45,9	33,8	24,9	18,1	12,4	7,2											
155	888,3	389,4	214,8	133,8	89,7	63,0	45,6	33,4	24,5	17,6	11,8	6,2											
160	888,0	389,1	214,4	133,5	89,4	62,7	45,2	33,0	24,0	17,0	11,1	4,9											
165	887,7	388,8	214,1	133,2	89,1	62,3	44,8	32,6	23,5	16,5	10,3	3,2											
170	887,4	388,5	213,8	132,8	88,7	62,0	44,4	32,1	23,1	15,9	9,5												
175	887,1	388,2	213,5	132,5	88,4	61,6	44,0	31,7	22,6	15,3	8,6												
180	886,8	387,9	213,1	132,2	88,0	61,2	43,6	31,3	22,0	14,6	7,7												
185	886,4	387,6	212,8	131,8	87,7	60,8	43,2	30,8	21,5	14,0	6,5												
190	886,1	387,2	212,5	131,5	87,3	60,5	42,8	30,4	21,0	13,3	5,1												
195	885,8	386,9	212,2	131,1	86,9	60,1	42,4	29,9	20,4	12,5													
200	885,5	386,6	211,9	130,8	86,6	59,7	42,0	29,4	19,9	11,7													
205	885,2	386,3	211,5	130,5	86,2	59,3	41,5	28,9	19,3	10,9													
210	884,9	386,0	211,2	130,1	85,9	58,9	41,1	28,5	18,7	10,0													
215	884,6	385,7	210,9	129,8	85,5	58,5	40,7	28,0	18,1	8,9													
220	884,3	385,3	210,5	129,4	85,2	58,2	40,3	27,4	17,4														
225	884,0	385,0	210,2	129,1	84,8	57,8	39,8	26,9	16,7														
230	883,7	384,7	209,9	128,8	84,4	57,4	39,4	26,4	16,0														
235	883,3	384,4	209,6	128,4	84,1	57,0	38,9	25,9	15,3														
240	883,0	384,1	209,2	128,1	83,7	56,6	38,5	25,3															
245	882,7	383,7	208,9	127,7	83,3	56,2	38,0	24,7															
250	882,4	383,4	208,6	127,4	82,9	55,7	37,5	24,2															
255	882,1	383,1	208,2	127,0	82,6	55,3	37,1	23,6															
260	881,8	382,8	207,9	126,7	82,2	54,9	36,6																
265	881,5	382,5	207,6	126,3	81,8	54,5	36,1																
270	881,2	382,1	207,2	126,0	81,4	54,1	35,6																
275	880,9	381,8	206,9	125,6	81,1	53,6	35,1																
280	880,5	381,5	206,6	125,3	80,7	53,2																	
285	880,2	381,2	206,2	124,9	80,3	52,8																	
290	879,9	380,9	205,9	124,6	79,9	52,3																	
295	879,6	380,5	205,6	124,2	79,5																		
300	879,3	380,2	205,2	123,8	79,1																		
305	879,0	379,9	204,9	123,5																			
310	878,7	379,6	204,6	123,1																			
315	878,4	379,3	204,2	122,8																			
320	878,0	378,9	203,9																				
325	877,7	378,6																					
330	877,4	378,3																					
335	877,1																						

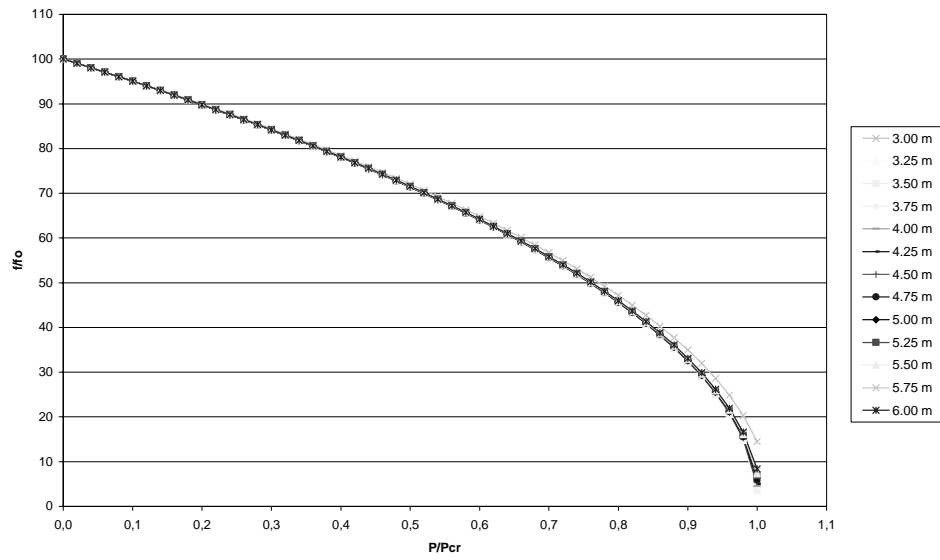


Figure 2.7: The ratio of load to buckling load versus the ratio of vibration frequency to unstressed frequency for I120 for various lengths

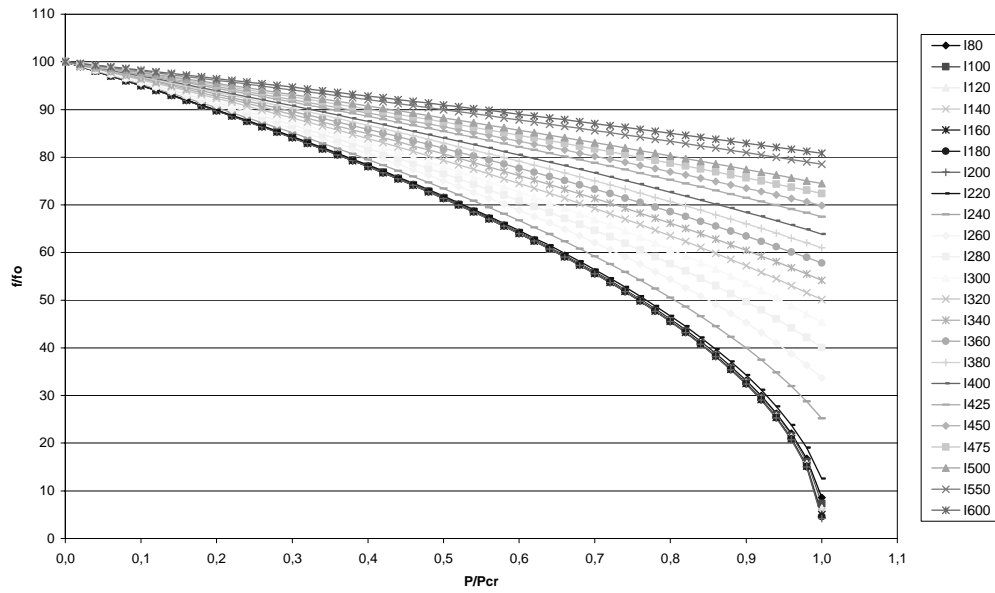


Figure 2.8: Relation between the ratio of the vibration frequency to the unstressed frequency and the ratio of the load to the buckling load for various I sections in 5 m

Mode Shapes:

Mode shapes of the calculated modes are important to check especially for iterative solutions. The converged “ α ” and “ β ” coefficients are often found to belong to second or third mode shapes instead of the first mode since optimization routines can converge to any minimum point.

From Equation (2.87) and (2.89),

$$C_3 = -C_1$$

$$C_4 = \frac{-\alpha}{\beta} \cdot C_2$$

Equation (2.46) becomes;

$$0 = C_1 \cdot (\cos(\alpha \cdot L) - \cosh(\beta \cdot L)) + C_2 \cdot \left(\sin(\alpha \cdot L) - \frac{\alpha}{\beta} \cdot \sinh(\beta \cdot L) \right) \quad (2.100)$$

$$C_2 = \frac{\cos(\alpha \cdot L) - \cosh(\beta \cdot L)}{\sin(\alpha \cdot L) - \frac{\alpha}{\beta} \cdot \sinh(\beta \cdot L)} \cdot C_1 \quad (2.101)$$

No need to use the fourth boundary condition due to trivial solution. Then, the mode shape $\Phi(x)$ is equal to Equation (2.102).

$$\begin{aligned} \Phi(x) = C_1 \cdot \cos(\alpha \cdot x) + \frac{\cos(\alpha \cdot L) - \cosh(\beta \cdot L)}{\sin(\alpha \cdot L) - \frac{\alpha}{\beta} \cdot \sinh(\beta \cdot L)} \cdot C_1 \cdot \sin(\alpha \cdot x) - \\ C_1 \cdot \cosh(\beta \cdot x) - \frac{\alpha}{\beta} \cdot \frac{\cos(\alpha \cdot L) - \cosh(\beta \cdot L)}{\sin(\alpha \cdot L) - \frac{\alpha}{\beta} \cdot \sinh(\beta \cdot L)} \cdot C_1 \cdot \sinh(\beta \cdot x) \end{aligned} \quad (2.102)$$

C_1 can be taken as “one” for maximum amplitude. After simplification, Equation (2.103) is obtained for the mode shapes.

$$\Phi(x) = \cos(\alpha \cdot x) - \cosh(\beta \cdot x) + \frac{\cos(\alpha \cdot L) - \cosh(\beta \cdot L)}{\sin(\alpha \cdot L) - \frac{\alpha}{\beta} \cdot \sinh(\beta \cdot L)} \cdot \left(\sin(\alpha \cdot x) + \frac{\alpha}{\beta} \cdot \sinh(\beta \cdot x) \right) \quad (2.103)$$

When substituted in Equation (2.103), the “ β ” values calculated from Equation (2.95) with corresponding “ α ” values calculated from Equation (2.32) will give the corresponding mode shapes.

2.2.5. Transverse Springs with Rollers on Both Ends:

The test setup for the shear wall and steel column caused formation of lateral springs at the upper and lower support levels. The derivation of the analytical formulas became essential to correlate the measured modal frequencies to the generated modal frequencies. The equations defining boundary conditions are listed below with the general view of the analytical model (Figure 2.9).

At $x = 0$,

$$M(x) = E \cdot I \cdot \frac{d^2}{dx^2} \Phi(x) = 0 \quad (2.104)$$

$$V(x) = E \cdot I \cdot \frac{d^3}{dx^3} \Phi(x) = k_1 \cdot \Phi(x) \quad (2.105)$$

At $x = L$,

$$M(x) = E \cdot I \cdot \frac{d^2}{dx^2} \Phi(x) = 0 \quad (2.106)$$

$$V(x) = E \cdot I \cdot \frac{d^3}{dx^3} \Phi(x) = k_2 \cdot \Phi(x) \quad (2.107)$$

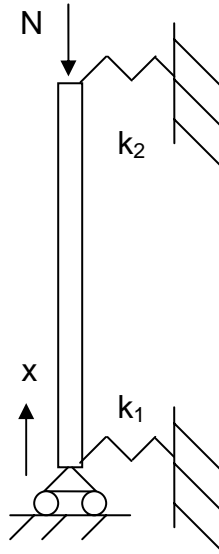


Figure 2.9: The sketch of the beam with springs at the ends

The equations defining the relationship between constants are derived using the boundary conditions and listed below.

$$0 = -\alpha^2 \cdot C_1 + \beta^2 \cdot C_3 \quad (2.108)$$

$$0 = -k_1 \cdot C_1 - E \cdot I \cdot \alpha^3 \cdot C_2 - k_1 \cdot C_3 + E \cdot I \cdot \beta^3 \cdot C_4 \quad (2.109)$$

$$0 = -C_1 \cdot \cos(\alpha \cdot L) \cdot \alpha^2 - C_2 \cdot \sin(\alpha \cdot L) \cdot \alpha^2 + C_3 \cdot \cosh(\beta \cdot L) \cdot \beta^2 + C_4 \cdot \sinh(\beta \cdot L) \cdot \beta^2 \quad (2.110)$$

$$0 = C_1 \cdot E \cdot I \cdot \sin(\alpha \cdot L) \cdot \alpha^3 - C_2 \cdot E \cdot I \cdot \cos(\alpha \cdot L) \cdot \alpha^3 + C_3 \cdot E \cdot I \cdot \sinh(\beta \cdot L) \cdot \beta^3 + C_4 \cdot E \cdot I \cdot \cosh(\beta \cdot L) \cdot \beta^3 - k_2 \cdot C_1 \cdot \cos(\alpha \cdot L) - k_2 \cdot C_2 \cdot \sin(\alpha \cdot L) - k_2 \cdot C_3 \cdot \cosh(\beta \cdot L) - k_2 \cdot C_4 \cdot \sinh(\beta \cdot L) \quad (2.111)$$

The matrix form of the relations (2.108 to 2.111) is given in Equation (2.112). The matrix is divided into blocks for better print quality.

$$(k_{11} \quad k_{12}) \cdot \begin{pmatrix} C_1 \\ C_2 \\ C_3 \\ C_4 \end{pmatrix} = \begin{pmatrix} 0 \\ 0 \\ 0 \\ 0 \end{pmatrix} \quad (2.112)$$

where,

$$k_{11} = \begin{pmatrix} -\alpha^2 & 0 \\ -k_1 & -\alpha^3 \cdot E \cdot I \\ -\cos(\alpha \cdot L) \cdot \alpha^2 & -\sin(\alpha \cdot L) \cdot \alpha^2 \\ E \cdot I \cdot \sin(\alpha \cdot L) \cdot \alpha^3 - k_2 \cdot \cos(\alpha \cdot L) & -E \cdot I \cdot \cos(\alpha \cdot L) \cdot \alpha^3 - k_2 \cdot \sin(\alpha \cdot L) \end{pmatrix} \quad (2.113)$$

$$k_{12} = \begin{pmatrix} \beta^2 & 0 \\ -k_1 & \beta^3 \cdot E \cdot I \\ \cosh(\beta \cdot L) \cdot \beta^2 & \sinh(\beta \cdot L) \cdot \beta^2 \\ E \cdot I \cdot \sinh(\beta \cdot L) \cdot \beta^3 - k_2 \cdot \cosh(\beta \cdot L) & E \cdot I \cdot \cosh(\beta \cdot L) \cdot \beta^3 - k_2 \cdot \sinh(\beta \cdot L) \end{pmatrix} \quad (2.114)$$

For a nontrivial solution, the coefficient matrix must not have an inverse (i.e. the determinant of the coefficient matrix should be zero). That is,

$$\begin{aligned}
 0 = & 2 \cdot \alpha^5 \cdot \beta^5 \cdot E^2 \cdot I^2 \cdot [(\cos(\alpha \cdot L) \cdot \cosh(\beta \cdot L)) - 1] + \\
 & \alpha^3 \cdot \beta^2 \cdot (\alpha^2 + \beta^2) \cdot E \cdot I \cdot (k_1 - k_2) \cdot \cos(\alpha \cdot L) \cdot \sinh(\beta \cdot L) + \\
 & \alpha^2 \cdot \beta^3 \cdot (\alpha^2 + \beta^2) \cdot E \cdot I \cdot (k_2 - k_1) \cdot \sin(\alpha \cdot L) \cdot \cosh(\beta \cdot L) + \\
 & \left[\alpha^4 \cdot \beta^4 \cdot E^2 \cdot I^2 \cdot (\alpha^2 - \beta^2) + k_1 \cdot k_2 \cdot (\alpha^2 + \beta^2)^2 \right] \cdot \sin(\alpha \cdot L) \cdot \sinh(\beta \cdot L) \quad (2.115)
 \end{aligned}$$

A solution procedure for this nonlinear function may be iterative:

1. Select β where $\beta > 0$.
2. Enter the length "L" in meters.
3. Enter the flexural rigidity "E.I" and axial compressive force "N".
4. Enter the spring constants k1 and k2 (kN/m).

5. Compute α where $\alpha = \sqrt{\beta^2 + \frac{N}{E \cdot I}}$

N : axial compressive load (kN) (1 ton = 9.81 kN)

EI: flexural rigidity (kN.m²) (1 t.cm² = 9.81 x 10⁻⁴ kN.m²)

6. Calculate Equation (2.115).

$$\begin{aligned}
 f(\alpha, \beta) = & 2 \cdot \alpha^5 \cdot \beta^5 \cdot E^2 \cdot I^2 \cdot [(\cos(\alpha \cdot L) \cdot \cosh(\beta \cdot L)) - 1] + \\
 & \alpha^3 \cdot \beta^2 \cdot (\alpha^2 + \beta^2) \cdot E \cdot I \cdot (k_1 - k_2) \cdot \cos(\alpha \cdot L) \cdot \sinh(\beta \cdot L) + \\
 & \alpha^2 \cdot \beta^3 \cdot (\alpha^2 + \beta^2) \cdot E \cdot I \cdot (k_2 - k_1) \cdot \sin(\alpha \cdot L) \cdot \cosh(\beta \cdot L) + \\
 & \left[\alpha^4 \cdot \beta^4 \cdot E^2 \cdot I^2 \cdot (\alpha^2 - \beta^2) + k_1 \cdot k_2 \cdot (\alpha^2 + \beta^2)^2 \right] \cdot \sin(\alpha \cdot L) \cdot \sinh(\beta \cdot L)
 \end{aligned}$$

7. If the accuracy is not acceptable (i.e. not close to zero), repeat steps (1-6).
8. After finding " β " and " α ", vibration frequencies can be calculated from Equation (2.98).

Mode Shapes:

Matrix condensation will be used to simplify the calculations. General form of the matrix is given in Equation (2.116).

$$\begin{pmatrix} k_{aa} & k_{ab} \\ k_{ba} & k_{bb} \end{pmatrix} \cdot \begin{pmatrix} C_a \\ C_b \end{pmatrix} = \begin{pmatrix} 0 \\ 0 \end{pmatrix} \quad (2.116)$$

Equation (2.117) and (2.118) can be extracted from Equation (2.116) as follows:

$$k_{aa} \cdot C_a + k_{ab} \cdot C_b = 0 \quad (2.117)$$

$$k_{ba} \cdot C_a + k_{bb} \cdot C_b = 0 \quad (2.118)$$

From Equation (2.118), C_b can be written in terms of C_a .

$$C_b = -(k_{bb})^{-1} \cdot k_{ba} \cdot C_a \quad (2.119)$$

After substituting C_b , Equation (2.117) can be rewritten as follows:

$$C_a \cdot \left[k_{aa} - k_{ab} \cdot (k_{bb})^{-1} \cdot k_{ba} \right] = 0 \quad (2.120)$$

Using matrix condensation principle, Equation (2.112) can be reconsidered as below.

$$\begin{pmatrix} -\alpha^2 & 0 & \beta^2 & 0 \\ -k_1 & -\alpha^3 \cdot E \cdot I & -k_1 & \beta^3 \cdot E \cdot I \\ -\cos(\alpha \cdot L) \cdot \alpha^2 & -\sin(\alpha \cdot L) \cdot \alpha^2 & \cosh(\beta \cdot L) \cdot \beta^2 & \sinh(\beta \cdot L) \cdot \beta^2 \\ E \cdot I \cdot \sin(\alpha \cdot L) \cdot \alpha^3 - k_2 \cdot \cos(\alpha \cdot L) & E \cdot I \cdot \cos(\alpha \cdot L) \cdot \alpha^3 - k_2 \cdot \sin(\alpha \cdot L) & E \cdot I \cdot \sinh(\beta \cdot L) \cdot \beta^3 - k_2 \cdot \cosh(\beta \cdot L) & E \cdot I \cdot \cosh(\beta \cdot L) \cdot \beta^3 - k_2 \cdot \sinh(\beta \cdot L) \end{pmatrix} \begin{pmatrix} C_1 \\ C_2 \\ C_3 \\ C_4 \end{pmatrix} = \begin{pmatrix} 0 \\ 0 \\ 0 \\ 0 \end{pmatrix}$$

If Equation (2.120) is directly adapted to Equation (2.112), the shape function can be written in Equation (2.121).

$$\Phi(x) = C_1 \cdot \left[-\alpha^2 - \left[\begin{pmatrix} 0 & \beta^2 & 0 \end{pmatrix} \cdot (k_{11} \ k_{12})^{-1} \cdot M \right] \right] \quad (2.121)$$

where,

$$k_{11} = \begin{pmatrix} -\alpha^3 \cdot E \cdot I \\ -\sin(\alpha \cdot x) \cdot \alpha^2 \\ -E \cdot I \cdot \cos(\alpha \cdot x) \cdot \alpha^3 - k_2 \cdot \sin(\alpha \cdot x) \end{pmatrix} \quad (2.122)$$

$$k_{12} = \begin{pmatrix} -k_1 & \beta^3 \cdot E \cdot I \\ \cosh(\beta \cdot x) \cdot \beta^2 & \sinh(\beta \cdot x) \cdot \beta^2 \\ E \cdot I \cdot \sinh(\beta \cdot x) \cdot \beta^3 - k_2 \cdot \cosh(\beta \cdot x) & E \cdot I \cdot \cosh(\beta \cdot x) \cdot \beta^3 - k_2 \cdot \sinh(\beta \cdot x) \end{pmatrix} \quad (2.123)$$

$$M = \begin{pmatrix} -k_1 \\ -\cos(\alpha \cdot x) \cdot \alpha^2 \\ E \cdot I \cdot \sin(\alpha \cdot x) \cdot \alpha^3 - k_2 \cdot \cos(\alpha \cdot x) \end{pmatrix} \quad (2.124)$$

After simplifications, the mode shape function for the boundary condition of transverse springs with rollers on both ends is given in Equation (2.125).

$$\Phi(x) = -C_1 \cdot \left[\alpha^2 + \beta^2 \cdot \left[\frac{(X6 \cdot X7 - X4 \cdot X9) \cdot X2 + (X1 \cdot X9 - X7 \cdot X3) \cdot X7 + (X4 \cdot X3 - X1 \cdot X6) \cdot X8}{X1 \cdot (X5 \cdot X9 - X6 \cdot X8) - X2 \cdot (X4 \cdot X9 + X6 \cdot X7) + X3 \cdot (X4 \cdot X8 - X5 \cdot X7)} \right] \right] \quad (2.125)$$

where,

$$X1 = -\alpha^3 \cdot E \cdot I \quad (2.126)$$

$$X2 = -k_1 \quad (2.127)$$

$$X3 = \beta^3 \cdot E \cdot I \quad (2.128)$$

$$X4 = -\sin(\alpha \cdot L) \cdot \alpha^2 \quad (2.129)$$

$$X5 = \cosh(\beta \cdot L) \cdot \beta^2 \quad (2.130)$$

$$X6 = \sinh(\beta \cdot L) \cdot \beta^2 \quad (2.131)$$

$$X7 = -E \cdot I \cdot \cos(\alpha \cdot L) \cdot \alpha^3 - k_2 \cdot \sin(\alpha \cdot L) \quad (2.132)$$

$$X8 = E \cdot I \cdot \sinh(\beta \cdot L) \cdot \beta^3 - k_2 \cdot \cosh(\beta \cdot L) \quad (2.133)$$

$$X9 = E \cdot I \cdot \cosh(\beta \cdot L) \cdot \beta^3 - k_2 \cdot \sinh(\beta \cdot L) \quad (2.134)$$

C_1 can be taken as “minus one” for maximum amplitude.

2.2.6. Fixed End and Spring with Roller on Other End:

This type is considered because the test setup has also caused similar boundary conditions. The equations defining boundary conditions are listed below with the general view of the analytical model (Figure 2.10).

At $x=0$,

$$\Phi(x) = 0 \quad \text{at } x = 0, \quad (2.135)$$

$$\frac{d}{dx}\Phi(x) = 0 \quad \text{at } x = 0, \quad (2.136)$$

At $x=L$,

$$M(x) = E \cdot I \cdot \frac{d^2}{dx^2}\Phi(x) = 0 \quad \text{at } x = L, \quad (2.137)$$

$$V(x) = E \cdot I \cdot \frac{d^3}{dx^3} \Phi(x) = k \cdot \Phi(x) \quad \text{at } x = L, \quad (2.138)$$

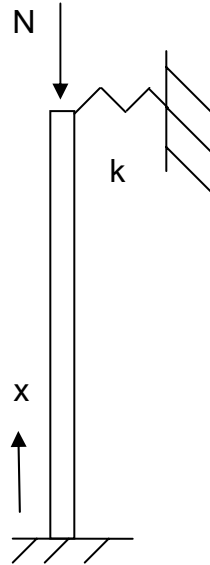


Figure 2.10: The sketch of the beam with fix support at one end and spring at the other end

The equations defining the relationship between constants are derived using the boundary conditions and listed below.

$$0 = C_1 + C_3 \quad (2.139)$$

$$0 = \alpha \cdot C_2 + \beta \cdot C_4 \quad (2.140)$$

$$0 = -C_1 \cdot \cos(\alpha \cdot L) \cdot \alpha^2 - C_2 \cdot \sin(\alpha \cdot L) \cdot \alpha^2 + C_3 \cdot \cosh(\beta \cdot L) \cdot \beta^2 + C_4 \cdot \sinh(\beta \cdot L) \cdot \beta^2 \quad (2.141)$$

$$\begin{aligned}
0 = & C_1 \cdot E \cdot I \cdot \sin(\alpha \cdot L) \cdot \alpha^3 - C_2 \cdot E \cdot I \cdot \cos(\alpha \cdot L) \cdot \alpha^3 + \\
& C_3 \cdot E \cdot I \cdot \sinh(\beta \cdot L) \cdot \beta^3 + C_4 \cdot E \cdot I \cdot \cosh(\beta \cdot L) \cdot \beta^3 - \\
& k \cdot C_1 \cdot \cos(\alpha \cdot L) - k \cdot C_2 \cdot \sin(\alpha \cdot L) - k \cdot C_3 \cdot \cosh(\beta \cdot L) - \\
& k \cdot C_4 \cdot \sinh(\beta \cdot L)
\end{aligned} \tag{2.142}$$

In the matrix form of the same relations are given in Equation (2.143). The matrix is divided into blocks for better print quality as follows:

$$(k_{11} \quad k_{12}) \cdot \begin{pmatrix} C_1 \\ C_2 \\ C_3 \\ C_4 \end{pmatrix} = \begin{pmatrix} 0 \\ 0 \\ 0 \\ 0 \end{pmatrix} \tag{2.143}$$

where,

$$k_{11} = \begin{pmatrix} 1 & 0 \\ 0 & \alpha \\ -\cos(\alpha \cdot L) \cdot \alpha^2 & -\sin(\alpha \cdot L) \cdot \alpha^2 \\ E \cdot I \cdot \sin(\alpha \cdot L) \cdot \alpha^3 - k \cdot \cos(\alpha \cdot L) & -E \cdot I \cdot \cos(\alpha \cdot L) \cdot \alpha^3 - k \cdot \sin(\alpha \cdot L) \end{pmatrix} \tag{2.144}$$

$$k_{12} = \begin{pmatrix} 1 & 0 \\ 0 & \beta \\ \cosh(\beta \cdot L) \cdot \beta^2 & \sinh(\beta \cdot L) \cdot \beta^2 \\ E \cdot I \cdot \sinh(\beta \cdot L) \cdot \beta^3 - k \cdot \cosh(\beta \cdot L) & E \cdot I \cdot \cosh(\beta \cdot L) \cdot \beta^3 - k \cdot \sinh(\beta \cdot L) \end{pmatrix} \tag{2.145}$$

For a nontrivial solution, the coefficient matrix must not have an inverse (i.e. the determinant of the coefficient matrix should be zero). That is,

$$\begin{aligned}
0 = & \alpha \cdot \beta \cdot E \cdot I \cdot (\alpha^4 + \beta^4) + 2 \cdot \alpha^3 \cdot \beta^3 \cdot E \cdot I \cdot \cos(\alpha \cdot L) \cdot \cosh(\beta \cdot L) + \\
& \alpha^2 \cdot \beta^2 \cdot (\alpha^2 - \beta^2) \cdot E \cdot I \cdot \sin(\alpha \cdot L) \cdot \sinh(\beta \cdot L) - \\
& \alpha \cdot k \cdot (\alpha^2 + \beta^2) \cdot \cos(\alpha \cdot L) \cdot \sinh(\beta \cdot L) + \\
& \beta \cdot k \cdot (\alpha^2 + \beta^2) \cdot \sin(\alpha \cdot L) \cdot \cosh(\beta \cdot L)
\end{aligned} \tag{2.146}$$

A solution procedure for this nonlinear function may be iterative:

1. Select β where $\beta > 0$.
2. Enter the length "L" in meters.
3. Enter the flexural rigidity "E.I" and axial compressive force "N".
4. Enter the spring constant k (kN/m).
5. Compute α where $\alpha = \sqrt{\beta^2 + \frac{N}{E \cdot I}}$
N: axial compressive load (kN) (1 ton = 9.81 kN)
EI: flexural rigidity (kN.m²) (1 t.cm² = 9.81 x 10⁻⁴ kN.m²)
6. Calculate Equation (2.146).
7. If the accuracy is not acceptable (i.e. not close to zero), repeat steps (1-6).
8. After finding " β " and " α ", vibration frequencies can be calculated from Equation (2.98).

Mode Shapes:

To apply matrix condensation Equation (2.143) can be reconsidered as below.

$$\left(\begin{array}{cc|cc} 1 & 0 & 1 & 0 \\ \hline 0 & \alpha & 0 & \beta \\ \hline -\cos(\alpha \cdot L) \cdot \alpha^2 & -\sin(\alpha \cdot L) \cdot \alpha^2 & \cosh(\beta \cdot L) \cdot \beta^2 & \sinh(\beta \cdot L) \cdot \beta^2 \\ \hline E \cdot I \cdot \sin(\alpha \cdot L) \cdot \alpha^3 - k \cdot \cos(\alpha \cdot L) & -E \cdot I \cdot \cos(\alpha \cdot L) \cdot \alpha^3 - k \cdot \sin(\alpha \cdot L) & E \cdot I \cdot \sinh(\beta \cdot L) \cdot \beta^3 - k \cdot \cosh(\beta \cdot L) & E \cdot I \cdot \cosh(\beta \cdot L) \cdot \beta^3 - k \cdot \sinh(\beta \cdot L) \end{array} \right) \cdot \begin{pmatrix} C_1 \\ C_2 \\ C_3 \\ C_4 \end{pmatrix} = \begin{pmatrix} 0 \\ 0 \\ 0 \\ 0 \end{pmatrix}$$

As a result, shape function can be calculated from Equation (2.147).

$$\Phi(x) = C_1 \cdot \left[1 - \left[(0 \ 1 \ 0) \cdot (k_{11} \ k_{22})^{-1} \cdot M \right] \right] \quad (2.147)$$

where,

$$k_{11} = \begin{pmatrix} \alpha & & \\ & -\sin(\alpha \cdot L) \cdot \alpha^2 & \\ & & -E \cdot I \cdot \cos(\alpha \cdot L) \cdot \alpha^3 - k \cdot \sin(\alpha \cdot L) \end{pmatrix} \quad (2.148)$$

$$k_{12} = \begin{pmatrix} 0 & \beta & \\ \cosh(\beta \cdot L) \cdot \beta^2 & \sinh(\beta \cdot L) \cdot \beta^2 & \\ E \cdot I \cdot \sinh(\beta \cdot L) \cdot \beta^3 - k \cdot \cosh(\beta \cdot L) & E \cdot I \cdot \cosh(\beta \cdot L) \cdot \beta^3 - k \cdot \sinh(\beta \cdot L) \end{pmatrix} \quad (2.149)$$

$$M = \begin{pmatrix} 0 & & \\ & -\cos(\alpha \cdot L) \cdot \alpha^2 & \\ & & E \cdot I \cdot \sin(\alpha \cdot L) \cdot \alpha^3 - k \cdot \cos(\alpha \cdot L) \end{pmatrix} \quad (2.150)$$

After simplifications, the mode shape function for the boundary condition of transverse springs with rollers on both ends is given in Equation (2.151).

$$\Phi(x) = C_1 \cdot \left[1 + \frac{(\alpha \cdot X_6 - \beta \cdot X_4) \cdot \alpha^2 \cdot \cos(\alpha \cdot L)}{\alpha \cdot (X_2 \cdot X_6 - X_3 \cdot X_5) + \beta \cdot (X_1 \cdot X_5 - X_4 \cdot X_2)} + \frac{(\alpha \cdot X_3 - \beta \cdot X_1) \cdot k \cdot \cos(\alpha \cdot L) + (\alpha \cdot X_3 - \beta \cdot X_1) \cdot E \cdot I \cdot \alpha^3 \cdot \sin(\alpha \cdot L)}{\alpha \cdot X_2 \cdot X_6 - \alpha \cdot X_3 \cdot X_5 + X_1 \cdot \beta \cdot X_5 - X_4 \cdot \beta \cdot X_2} \right] \quad (2.151)$$

where,

$$X_1 = -\sin(\alpha \cdot L) \cdot \alpha^2 \quad (2.152)$$

$$X_2 = \cosh(\beta \cdot L) \cdot \beta^2 \quad (2.153)$$

$$X3 = \sinh(\beta \cdot L) \cdot \beta^2 \quad (2.154)$$

$$X4 = -E \cdot I \cdot \cos(\alpha \cdot L) \cdot \alpha^3 - k \cdot \sin(\alpha \cdot L) \quad (2.155)$$

$$X5 = E \cdot I \cdot \sinh(\beta \cdot L) \cdot \beta^3 - k \cdot \cosh(\beta \cdot L) \quad (2.156)$$

$$X6 = E \cdot I \cdot \cosh(\beta \cdot L) \cdot \beta^3 - k \cdot \sinh(\beta \cdot L) \quad (2.157)$$

C_1 can be taken as “one” for maximum amplitude.

CHAPTER 3

ULTRASONIC TESTING

3.1. General:

Ultrasound is sound with a pitch too high to be detected by the human ear, i.e. of frequencies greater than about 20 kHz. Ultrasonic waves have a wide variety of applications including non-destructive testing, cutting, cleaning, and destruction of tissues in medical field.

Ultrasonics is the name given to the study and application of ultrasound. The main difference between the basic methods of “ultrasonics” and the more specialized ones used in “ultrasonic non-destructive testing” is in the approach to the elastic medium. In ultrasonics, the material is usually assumed to be ideal (isotropic, homogeneous, linear, attenuation-free, dispersion-free, temperature-independent, etc.) in order to study the basic laws of elastic wave propagation in their simplest form. In ultrasonic non-destructive testing, real materials with more complex elastic properties (anisotropy, inhomogeneity, nonlinearity, attenuation, dispersion, temperature dependence, etc.) are considered.

Ultrasonic is used instead of audible frequencies because of the fact that wavelengths decrease inversely with increase in frequency. Use of ultrasonic

waves is advantageous for smaller sample size tests since sample size and wave lengths are of the same order of magnitude. The use of short wavelengths enables the employment of shorter pulses, thus provides higher degrees of resolution for defect detection. Furthermore, the degree of sound beam spread (dispersion) decreases with rise in frequency and hence causes an increase in directivity, which is of great importance for locating defects. However, loss of signal due to path length (attenuation) generally increases with frequency.

Ultrasonic testing is generally used to determine:

- the homogeneity of concrete
- the thickness of a layer of inferior quality concrete, the presence of voids, cracks, or other imperfections
- the changes in the concrete which may occur over time (such as the hydration of cement) or through the action of fire, frost, or chemical attack
- the mechanical properties (generally strength) of concrete in relation to specified standard requirements

The relationship [2] between the ultrasonic pulse velocity and concrete uniformity is given in Table 3.1.

3.2. Historical Perspective of the Use of Ultrasonic Testing:

Blitz [3] made a brief explanation on the first development and use of ultrasonic waves in his book as below:

“The application of ultrasound to non-destructive testing was first made possible by the discovery of the piezoelectric effect by the brothers Pierre and Jacques Curie in 1880. However, it was not until the discovery of radar, that any effective progress was possible. Sokolov studied the use of ultrasonic waves in detecting metal objects. Mulhauser obtained a patent for

using ultrasonic waves, using two transducers to detect flaws in solids. Then, Firestone in the USA and Sproule in the UK, working independently of one another, developed the pulse-echo ultrasonic flaw detector. The first ultrasonic instruments used an “A-mode presentation” with blips on an oscilloscope screen. That was followed by a “B-mode presentation” with a two dimensional, gray scale imaging”.

Table 3.1. Pulse velocity vs. concrete quality [2]

Pulse velocity (m/s)	General conditions
Above 4575	Excellent
3660-4575	Good
3050-3660	Questionable
2135-3050	Poor
Below 2135	Very poor

Razi [4] explained the developments in the ultrasonic testing in his article as below:

“In 40's the principal need of the civil engineers were the in situ determination of the homogeneity and the compressive strength of fresh concrete to be able, for example, to remove the formworks. The majorities of these techniques (rebound hammer, pull-out test, Windsor probe test, etc.) are standardized and are based on the measurement of the surface hardness of the concrete. With the progressive ageing of the structures, the needs of the engineers evolved to the search for tools allowing the estimation of the mechanical properties of old materials, as well as the detection and the characterization of hidden defects. This request was at the origin of the

appearance of many investigation techniques in the construction industry, and this from the 70's. The majority of these techniques are based on those used successfully in geophysics for the exploration of basements and soils. They can be distinguished according to the nature of the phenomena exploited (acoustic, electromagnetic, thermal, electric, etc.), and have a common principle: the response of a medium to a given excitation is a function of the characteristics of this medium. Acoustic techniques, such as the impact-echo, the sonic test or the spectral analysis of surface (Rayleigh) waves, can bring information on the elastic parameters of materials as well as on the presence of discontinuities, whereas the other techniques find their principal application in the detection of defects”.

An assessment of recent developments in use of ultrasound and NDT methods starting with 1970's is made in the internet site “www.ndt-ed.org” [5] as below:

“In the early 1970's, two events occurred which caused a major change. The continued improvement of the technology, in particular its ability to detect small flaws, led to the unsatisfactory situation that more and more parts had to be rejected, even though the probability of failure had not changed. However, the discipline of fracture mechanics emerged, which enabled one to predict whether a crack of a given size would fail under a particular load if a material property, fracture toughness, were known. Other laws were developed to predict the rate of growth of cracks under cyclic loading (fatigue). With the advent of these tools, it became possible to accept structures containing defects if the sizes of those defects were known. This formed the basis for new philosophy of "fail safe" or "damage tolerant" design. Components having known defects could continue in service as long as it could be established that those defects would not grow to a critical, failure producing size. A new challenge was thus presented to the non-destructive testing community. Detection was not enough. One needed to also obtain quantitative information about flaw size to serve as an input to

fracture mechanics based predictions of remaining life. These concerns, which were felt particularly strongly in the defense and nuclear power industries, led to the creation of a number of research programs around the world and the emergence of quantitative non-destructive evaluation (QNDE) as a new discipline. Quantitative descriptions of NDE performance, such as the probability of detection (POD), have become an integral part of statistical risk assessment. Measurement procedures initially developed for metals have been extended to engineered materials, such as composites, where anisotropy and inhomogeneity have become important issues. The rapid advances in digitization and computing capabilities have totally changed the faces of many instruments and the type of algorithms that are used in processing the resulting data. Goals range from the determination of fundamental micro structural characteristics such as grain size, porosity and texture (preferred grain orientation) to material properties related to such failure mechanisms as fatigue, creep, and fracture toughness determination”.

3.3. Theory of Ultrasonic Testing:

The propagation velocities of ultrasonic waves within an elastic, “unstressed” material depend only on the second order elastic constants and material density [6]. In the case of an isotropic material, the pulse velocity (V_p) is expressed as shown in Equation (3.1).

$$V_p = \sqrt{\frac{\lambda + 2 \cdot \mu}{\rho}} \quad (3.1)$$

The variable V_p is the longitudinal (compressional) wave velocity, ρ is the material density; λ and μ are the *Lamé* constants.

The constants λ and μ are calculated using Equations (3.2) and (3.3), respectively.

$$\lambda = \frac{\nu \cdot E}{(1 + \nu) \cdot (1 - 2 \cdot \nu)} \quad (3.2)$$

$$\mu = G = \frac{E}{2 \cdot (1 + \nu)} \quad (3.3)$$

Where “E” is the material’s elastic modulus and “ ν ” is Poisson’s ratio.

The pulse velocity equation can be rewritten as shown in Equation (3.4). [7]

$$V_p = \sqrt{\frac{E \cdot (1 - \nu)}{\rho \cdot (1 + \nu) \cdot (1 - 2 \cdot \nu)}} \quad (3.4)$$

V_p : Primary (compressional) wave velocity (km/s)

E: Modulus of elasticity (MPa)

ρ : Density (kg/m^3)

ν : Poisson’s ratio

Typical propagation velocity values for various materials are given in Table 3.2. [8]

Table 3.2. Typical propagation velocities for various materials [8]

Medium	Density, ρ (kg/m^3)	Compression Wave Velocity, V_p (m/s)	Shear Wave Velocity, V_s (m/s)
Air	1.2	340	-
Water	1000	1480	-
Concrete	2400	3500-4500	2500-3400
Steel	7800	5900	3200

When the material is “stressed”, the relation shown in Equation 3.4 cannot describe the change in the ultrasonic wave velocities due to the applied stress. New equations, taking these changes into account, are indispensable for every mechanical behavior.

Acoustoelastic Equations:

Study of materials under stress is described by the “Acoustoelasticity Theory”. The propagation equation given in stressed case, is the same as the one given in the unstressed case, except that the acoustoelasticity tensor depends on (a) the second and third order elastic constants, (b) applied stresses, and (c) ultrasonic wave direction of propagation.

The application of uniaxial stress on an initially isotropic material, induces a directional anisotropy in the material as shown in the Figure 3.1 [6].

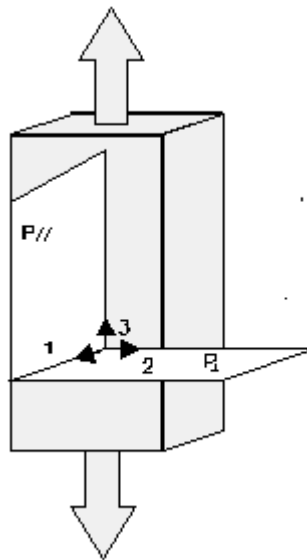


Figure 3.1: Planes of isotropy P_{\perp} and anisotropy $P_{//}$ [6]

The relative variations of the ultrasonic wave velocities (for both in the presence and absence of stress) expressed in perpendicular and parallel planes are given by Equations (3.5) through (3.8). [9]

In perpendicular plane to the loading plane:

$$\frac{\Delta V_L}{V_{L0}} = \left[\frac{v_1}{2} + v_2 - \mu - (5 \cdot \mu + 2 \cdot \lambda + 2 \cdot v_2 + 4 \cdot v_3) \cdot \frac{\lambda}{2 \cdot \mu} \right] \cdot \frac{\sigma}{(\lambda + 2 \cdot \mu) \cdot (3 \cdot \lambda + 2 \cdot \mu)} \quad (3.5)$$

$$\frac{\Delta V_T}{V_{T0}} = \left[v_2 + 2 \cdot v_3 - 2 \cdot \lambda - \mu - 2 \cdot v_3 \cdot \left(1 + \frac{\lambda}{\mu} \right) \right] \cdot \frac{\sigma}{2 \cdot \mu \cdot (3 \cdot \lambda + 2 \cdot \mu)} \quad (3.6)$$

In parallel plane to the loading plane:

$$\begin{aligned} \frac{\Delta V_L}{V_{L0}} = & \left[\frac{v_1}{2} + v_2 - (5 \cdot \mu + 2 \cdot \lambda + 2 \cdot v_2 + 4 \cdot v_3) \cdot \frac{\lambda}{2 \cdot \mu} \right] \cdot \frac{\sigma}{(\lambda + 2 \cdot \mu) \cdot (3 \cdot \lambda + 2 \cdot \mu)} + \\ & \frac{5 \cdot \mu + 2 \cdot \lambda + 2 \cdot v_2 + 4 \cdot v_3}{2 \cdot \mu \cdot (\lambda + 2 \cdot \mu)} \cdot (n_3)^2 \cdot \sigma \end{aligned} \quad (3.7)$$

$$\frac{\Delta V_T}{V_{T0}} = \left[\frac{4 \cdot \mu \cdot (\lambda + \mu + v_2 + 2 \cdot v_3) + 4 \cdot \lambda \cdot v_3}{8 \cdot \mu^2 \cdot (3 \cdot \lambda + 2 \cdot \mu)} + \frac{1}{2 \cdot \mu} \cdot (n_3)^2 \right] \cdot \sigma \quad (3.8)$$

where V_L and V_{L0} are the longitudinal ultrasonic velocities with and without stress, respectively. Similarly, V_T and V_{T0} are transverse ultrasonic velocities with and without stress, respectively. “ v_1 , v_2 and v_3 ” are the third order Lamé constants and “ n_3 ” is the direction of propagation projection along the applied stress axis.

3.4. Factors Influencing the Ultrasonic Testing:

The pulse velocity in concrete may be affected by any one of the following factors:

- pulse frequency,
- transducer arrangement,
- transducer diameter,
- couplants,
- path length,
- thickness of the specimen,
- lateral dimensions of the specimen,
- reinforcing steel bars,
- temperature of the concrete,
- moisture content,
- age of the concrete,
- water/cement ratio,
- retarders,
- cement type,
- state of stress,
- discontinuities,
- surface conditions, and
- orientation of the cable used for pulse transmission.

Frequency Selection:

The pulse frequency used for testing concrete must be much lower than those used for metals. Because the higher the frequency, the greater the attenuation of the pulse vibrations. On the other hand, use of lower pulse frequency affects the width of beam pulse in a negative way (causing large dispersion).

Attenuation, generally, means the loss of the signal's amplitude as the propagation distance increases. The loss defined in Equation (3.9) is usually expressed in decibels (dB).

$$SL = 20 \cdot \log\left(\frac{A_2}{A_1}\right) \quad (3.9)$$

SL: signal loss for a specific frequency

A_1 : amplitude of input signal (without attenuation)

A_2 : amplitude of output signal (with attenuation)

Attenuation coefficient given in Equation (3.10) is the signal loss per unit length.

$$\alpha_a = \frac{SL}{L} \quad (3.10)$$

α_a : attenuation coefficient

SL: signal loss

L: path length

Sound beam dispersion, absorption by the material, and scattering (i.e. diffusion during the interactions with the diffusers on the ultrasonic wave's route such as grains, pores, cracks and bars) are three major causes of attenuation phenomena. The following parameters determine the attenuation level in a heterogeneous medium:

- the wavelength " λ "
- the frequency "f"
- the size of the specimen

In order to have waves traveling long distances in concrete, low frequency signals causing high wavelengths are preferred. The frequencies suitable for the heterogeneous materials range from about 20 kHz to 250 kHz, with 50 kHz being appropriate for the field testing of concrete. These frequencies correspond to wavelengths ranging from about 20 cm for the lower frequency

to about 1,6 cm at the higher frequency. Wavelengths in concrete are in the order of 7~8 cm calculated using Equation (3.11).

$$\lambda = c / f \quad (3.11)$$

λ : wave length (m)

c: velocity (m/s)

f: frequency (Hz = 1/s)

Test specimen size and grain size should also be taken in consideration to determine wavelength. Generally, wavelength should be greater than 3 times of the maximum aggregate size to disregard inhomogeneity of concrete.

Transducer Arrangement:

Three basic test configurations are generally used as shown in Figure 3.2.

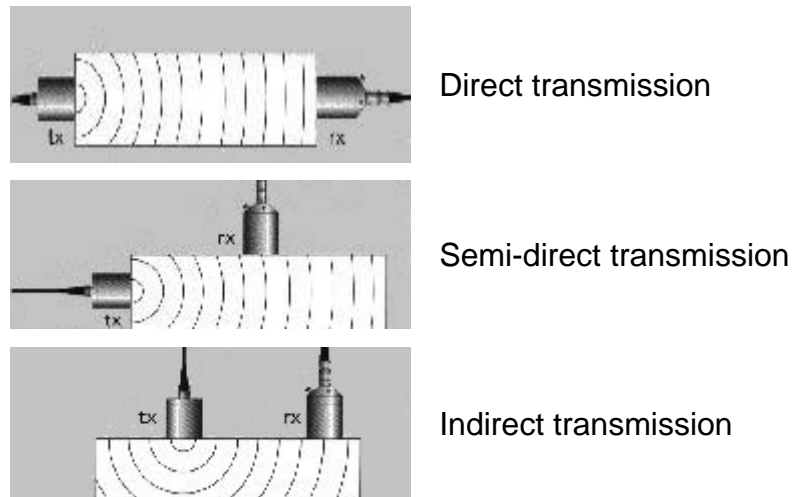


Figure 3.2: Transducer arrangement alternatives

The best and preferred method is direct transmission. The semi-direct and indirect methods are alternatives when access to only one side of a structure is available. However, in the indirect method, the receiving transducer sees less portion of the transmitted signal as compared to the direct method.

The accuracy of the typical schemes of testing shown in Figure 3.3 [10] may be calculated as shown in Table 3.3 [10]. Note that:

L: distance between the transducers plates centers,

D: diameter of the transducer plate,

m, n: distances between the transducers centers and the material corner,

t: transmission time.

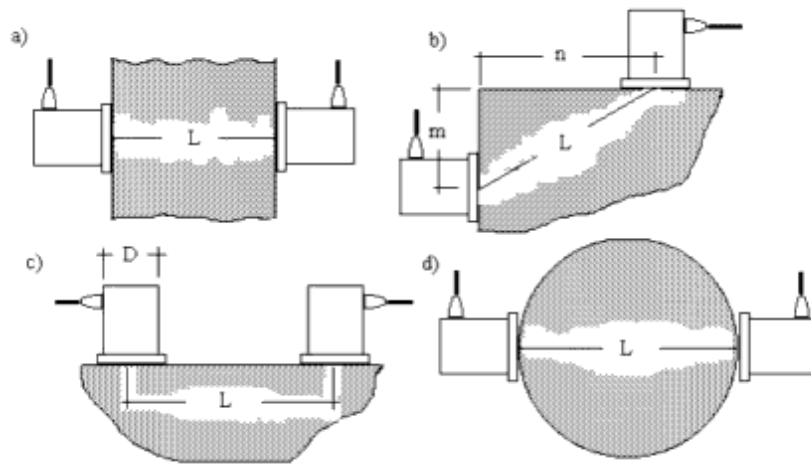


Figure 3.3. Typical schemes of ultrasonic testing [10]

Table 3.3. Path length error in typical transducer arrangements [10]

	Fig. 3.3.a	Fig. 3.3.b	Fig. 3.3.c	Fig. 3.3.d
V_{\max}	$V_{\max} = \frac{\sqrt{L^2 + D^2}}{t}$	$V_{\max} = \frac{\sqrt{\left(m + \frac{D}{2}\right)^2 + \left(n + \frac{D}{2}\right)^2}}{t}$	$V_{\max} = \frac{L + D}{t}$	similar to Fig. 3.3.a
V_{\min}	$V_{\min} = \frac{L}{t}$	$V_{\min} = \frac{\sqrt{\left(m - \frac{D}{2}\right)^2 + \left(n - \frac{D}{2}\right)^2}}{t}$	$V_{\min} = \frac{L - D}{t}$	
$\% \text{ error} = (V_{\max} - V_{\min}) / V_{\max}$				

Indirect arrangement is the least satisfactory arrangement. Because indirect arrangement is less sensitive and gives pulse velocity measurements which are usually influenced by the concrete layer near the surface. Near surface layer may not be representative of the concrete in deeper layers. Furthermore, the length of the path is less well defined because the distance from centre to centre of the transducers may not be the exact path.

Instead, the method shown in the Figure 3.4 [11] should be adopted for indirect arrangement to determine the effective path length.

In this method, the transmitting transducer is placed on a suitable point on the surface and the receiving transducer is placed on the surface at successive positions along a line and the centre to centre distance is plotted against the transit time. The slope of the straight line drawn through these points gives the mean pulse velocity at the surface (Figure 3.5). [11]

In general, the pulse velocity determined by the indirect method of testing will be lower than that using the direct method. If it is possible to employ both

methods of measurement then a relationship may be established between them and a correction factor derived. Compressional wave velocities which were obtained from the one-sided (indirect) technique are typically 93% to 95% of those measured with the through-thickness (direct) ultrasonic measurements. [12]

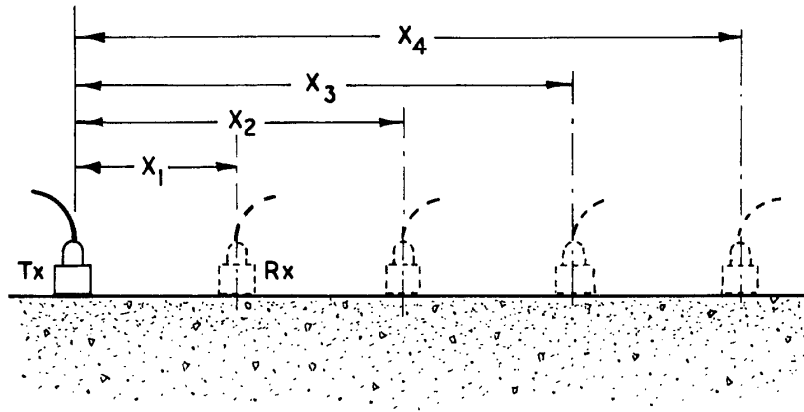


Figure 3.4: Indirect measurement method [11]

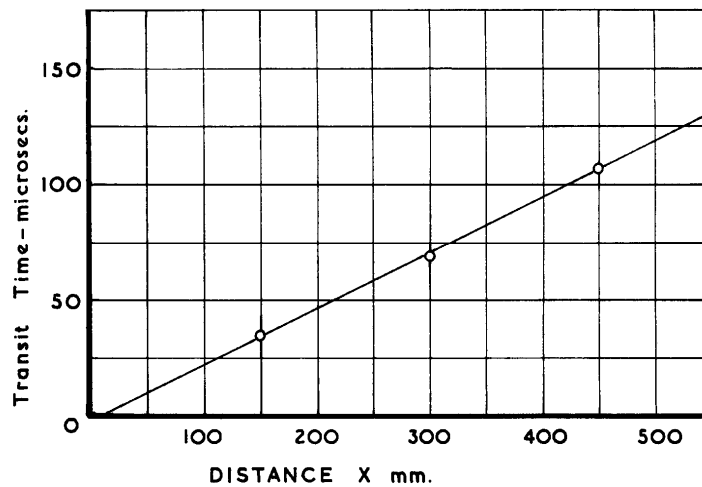


Figure 3.5: Mean pulse velocity at the surface [11]

If the points do not lie in a straight line, it is an indication either that the concrete near the surface is of variable quality or that a crack exists in the concrete within the line of the test position (Figure 3.6) [11]. A change of slope as shown in Figure 3.7 [11] could indicate that the pulse velocity near the surface is much lower than it is deeper down in the concrete.

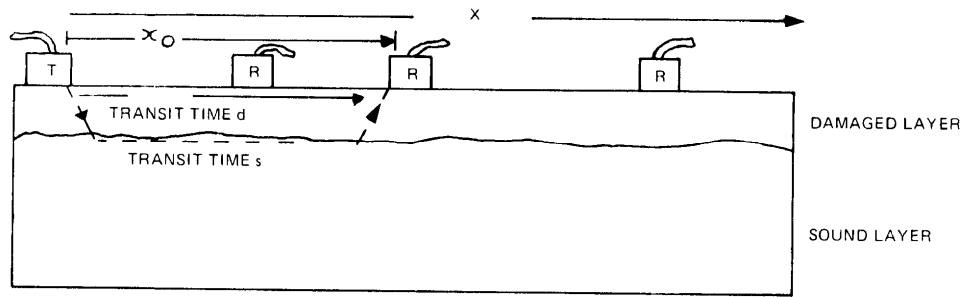


Figure 3.6: Inferior quality surface concrete [11]

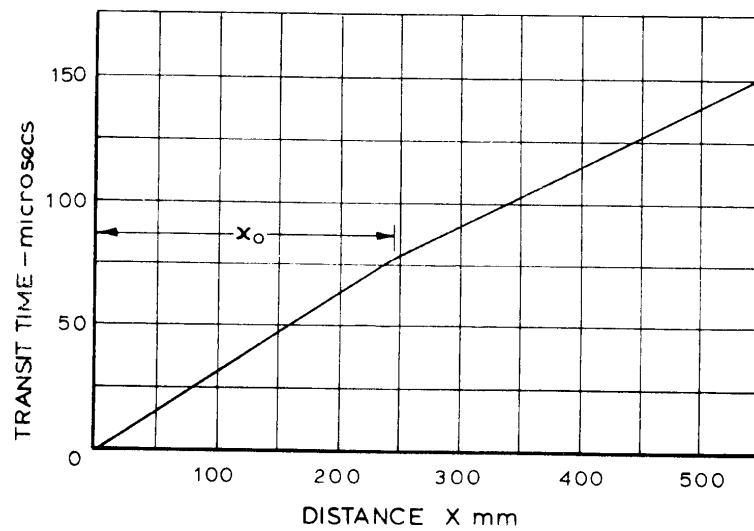


Figure 3.7: Ultrasonic pulse velocity at inferior quality surface concrete [11]

For transducer separation distances up to X_0 , the pulse travels through the damaged surface layer and the slope of the line gives the pulse velocity in this layer. Beyond X_0 , the pulse has traveled along the surface of the underlying sound concrete and the slope of the line beyond X_0 gives the higher velocity in the sound concrete. The thickness of the affected surface layer may be estimated from Equation (3.12).

$$T = \frac{X_0 \cdot (V_s - V_d)}{2 \cdot (V_s + V_d)} \quad (3.12)$$

where;

- V_d is the pulse velocity in the damaged concrete (km/s)
- V_s is the pulse velocity in the underlying sound concrete (km/s)
- T is the thickness of the layer of damaged concrete (mm)
- X_0 is the distance at which the change of slope occurs (mm)

Transducer Diameter:

Transducer diameter is also important from the path length point of view (Figure 3.8 and Figure 3.9). [13]

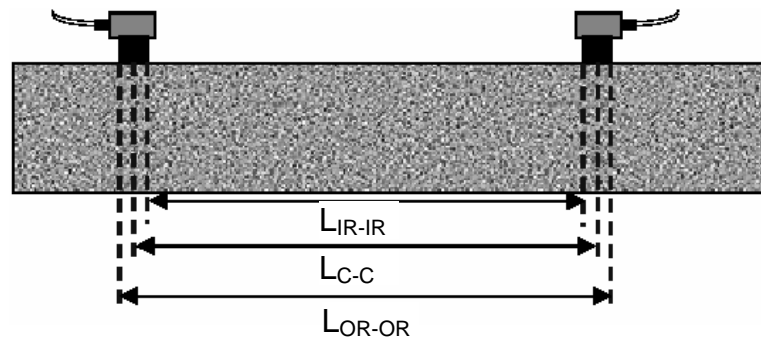


Figure 3.8: Transducer diameter effect on indirect UPV measurement [13]

The transducer diameter affects the wave type. As the transducer diameter is smaller compared to the wavelength, the transducer can be treated as a point source in which case the wave front is spherical.

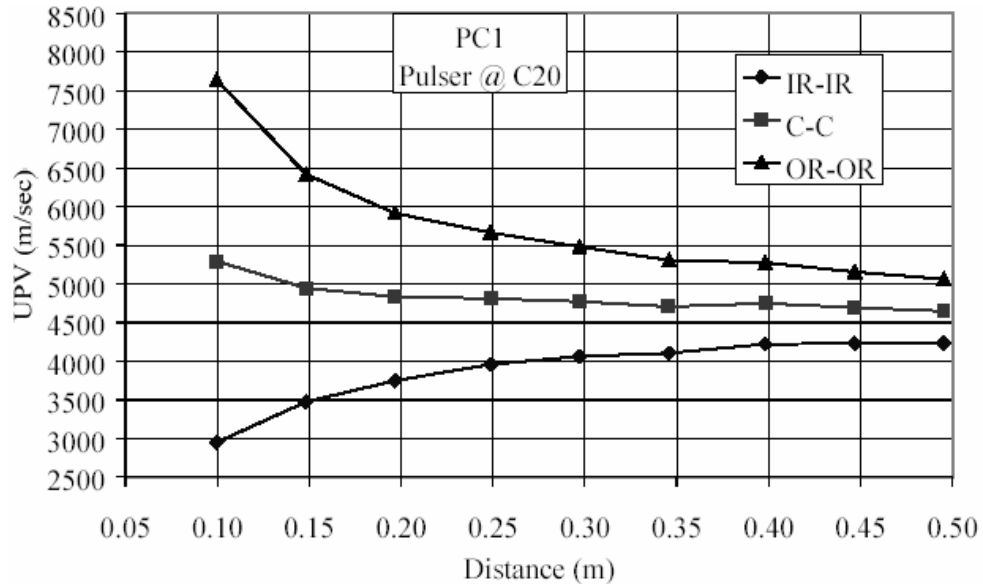


Figure 3.9: Indirect UPV evaluation procedure using different wave path lengths [13]

Couplants:

The ultrasonic transducer must be in contact with the material in such a way that the air voids should be filled and permit the transmission of the waves. The material (gel or grease) used between the transducer and the test material is called “couplants”. The couplant may form a layer between a transducer and a test material causing errors in the measurement of ultrasonic velocity by increasing the path length and causing attenuation. Therefore, couplant should be applied as a thin layer as possible.

Wave propagation between different mediums depends on the acoustic impedance of the layers. The acoustic impedance “Z” of a surface or medium is the ratio of the amplitude of the sound pressure “s” to the amplitude of the particle velocity “v” of an acoustic wave that make an impression on the surface or medium [14]. See Equation (3.13).

$$Z = \frac{s}{v} \quad (3.13)$$

In the same cross-sectional area, impedance can also be expressed by Equation (3.14).

$$Z = \rho \cdot v \quad (3.14)$$

ρ : density (t/m³)

v : velocity (km/s)

Z : acoustic impedance (1 t/(m². s) = 10⁶ Rayls = 1 MRayls)

As an example:

$$Z_{\text{Steel}} = 46.7 \text{ MRayls}$$

$$Z_{\text{Water}} = 1.48 \text{ MRayls}$$

$$Z_{\text{Air}} = 0.0004 \text{ MRayls}$$

While passing to a different medium (or layer) plane waves reflects and refracts. The transmitted and reflected energy may be computed from Equation (3.15) and (3.16), respectively. [15]

E_T : transmitted energy in percentage

$$E_T = \frac{4 \cdot Z_1 \cdot Z_2}{(Z_1 + Z_2)^2} \cdot 100 \quad (3.15)$$

E_R : reflected energy in percentage

$$E_R = \left(\frac{Z_1 - Z_2}{Z_1 + Z_2} \right)^2 \cdot 100 = 100 - E_T \quad (3.16)$$

The portion of an incident longitudinal wave that is reflected at an interface between two media depends on the specific impedances of each medium. The amplitude of the reflected stress wave, A_R , relative to the amplitude of the normal incident stress wave, A_I , can be found from Equation (3.17). [16]

$$\frac{A_R}{A_I} = \frac{Z_2 - Z_1}{Z_2 + Z_1} = \frac{\rho_2 \cdot v_2 - \rho_1 \cdot v_1}{\rho_2 \cdot v_2 + \rho_1 \cdot v_1} \quad (3.17)$$

where Z_1 and Z_2 are the specific mechanical impedances of media 1 and 2, respectively.

The amplitude of the transmitted stress wave, A_T , relative to the amplitude of the normal incident stress wave, A_I , is determined from Equation (3.18).

$$\frac{A_T}{A_I} = \frac{2Z_1}{Z_2 + Z_1} = \frac{2\rho_1 \cdot v_1}{\rho_2 \cdot v_2 + \rho_1 \cdot v_1} \quad (3.18)$$

Also, note that the pressure applied to transducers to hold them in place also affects the level of contact, hence affects the transmitted wave portion.

Path Length:

Since the higher frequency components of the pulse are attenuated more, the electronic timing apparatus may indicate a tendency for velocity to reduce slightly with increasing path length. It is, therefore, preferable to use high frequency transducers for short path lengths and low frequency transducers for long path lengths.

The influence of path length will be negligible provided that the path length is not less than 100 mm when 20 mm size aggregate is used, or not less than 150 mm for 40 mm size aggregate [11]. It is recommended that the first measurement is made at approximately two to three wavelengths from the transmitting transducer. [17]

The path length is also important from the sound energy point of view. The sound field of a transducer is divided into two zones; the near field and the far field (Figure 3.10). [18]

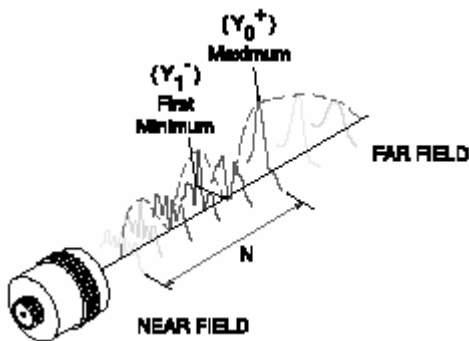


Figure 3.10: Sound fields of a transducer [18]

The “near field” is the region directly in front of the transducer. The echo amplitude goes through a series of maxima and minima and ends at the last maximum, at distance N from the transducer. The location of the last maximum is known as the near field distance (N or Y_0^+) and is the natural focus of the transducer. The “far field” is the area beyond N where the sound field pressure gradually drops to zero. Because of the variations within the near field, it can be difficult to accurately evaluate flaws using amplitude based techniques.

The near field distance is a function of the transducer frequency, element diameter, and sound velocity of the test material as shown by Equation (3.19) and (3.20). [18]

$$N = D^2 \cdot f / 4 \cdot c \quad (3.19)$$

$$N = D^2 / 4 \cdot \lambda \quad (3.20)$$

N: near field distance

D: element diameter

f: frequency

c: material sound velocity

λ : wavelength

Thickness of the Specimen:

Where the thickness of the test material is much greater than the wavelength of the transmission, the effective velocity is the group velocity (i.e., the velocity of the group of waves included in the pulse envelope). [19]

Lateral Dimension of the Specimen:

If the dimensions of the specimen perpendicular to the direction of the wave's propagation (i.e., lateral dimensions) are close to the wavelength, the specimen can vibrate radially. The shift from an infinite medium into a finite one then generates so-called 'guided' waves and their group velocity may differ from the one recorded on the unlimited structure.

The wavelength of the pulse vibrations is inversely proportional to the frequency. For pulses of 50 kHz frequency, this corresponds to a least lateral dimension of about 80 mm. Otherwise, the pulse velocity may be reduced

and the results of pulse velocity measurements should be used with caution (see Table 3.4). [20]

Table 3.4. Effect of specimen dimensions on pulse transmission [20]

Transducer frequency	Pulse velocity in concrete (in km/s)		
	V _c = 3.5	V _c = 4.0	V _c = 4.5
	Minimum permissible lateral specimen dimension		
<u>kHz</u>	<u>mm</u>	<u>mm</u>	<u>mm</u>
24	146	167	188
54	65	74	83
82	43	49	55
150	23	27	30

Reinforcing Steel Bars:

The pulse velocity in steel may be up to twice the velocity in plain concrete. Since the first pulse to arrive at the receiving transducer travels partly in concrete and partly in steel, there will be an apparent increase in pulse velocity. The diameter and number of bars and their orientation with respect to the propagation path affect the pulse velocity.

Figure 3.11 [11] shows how this influence may be allowed when the bar diameter lies directly along the pulse path. If the ratio L_s/L is known, the measured pulse velocity may be corrected by multiplying it by the correction factor corresponding to the ratio and the quality of the concrete. It is,

however, preferable to avoid such a path arrangement and to choose a path which is not in a direct line with the bar diameters.

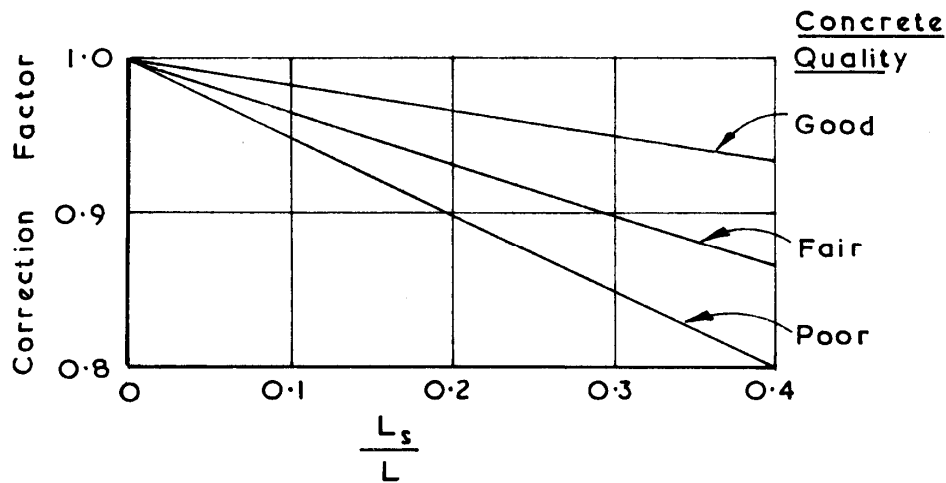


Figure 3.11: Correction factor for pulse velocity in case of directly lying reinforcing bars [11]

When the steel bars lie in a direction parallel to the pulse path, the influence of the steel may be more difficult to avoid as seen in Figure 3.12. [11]

Making reliable corrections is not easy for the influence of the steel. The correction factors given in Figure 3.13 [11] should be regarded as approximate only.

It is generally found that these values represent an upper limit of the steel influence. Again, it is advisable to choose pulse paths, which avoid the influence of the steel as far as possible. More detailed information and usage of correction factors can be found in BS 1881: Part 203: 1986. [20]

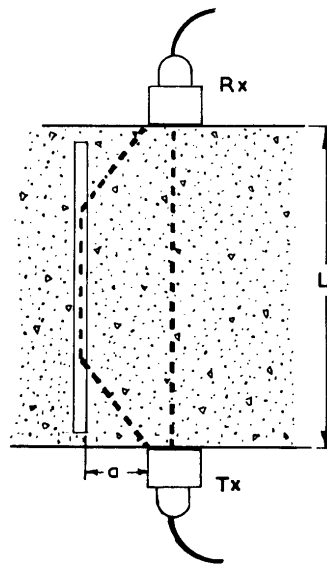


Figure 3.12: Reinforcing steel bar that do not directly lie under the path [11]

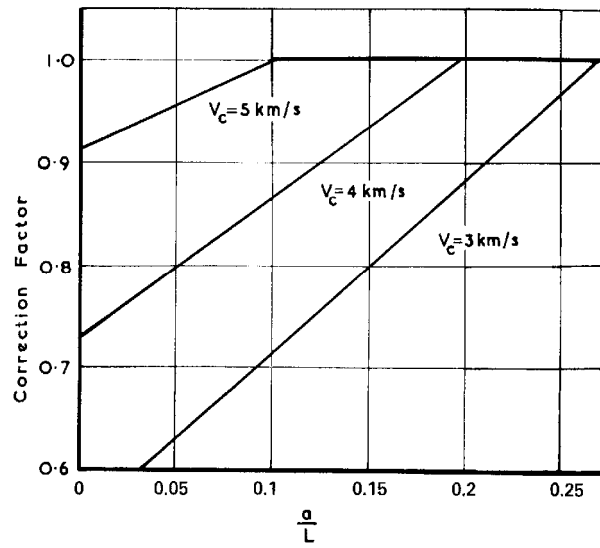


Figure 3.13: Velocity correction factor for far lying steel bars [11]

Temperature of the Concrete:

As the temperature increases, the pulse velocity decreases. The temperature of the concrete has no significant effect on pulse velocity over the range from 10°C to 30°C without the occurrence of corresponding changes in strength or elastic properties (Table 3.5) [20]. Therefore, except extreme temperatures, temperature influence may be disregarded.

Table 3.5. Effect of temperature on pulse transmission [20]

Temperature (°C)	Correction to the measured pulse velocity	
	Air-dried concrete (%)	Water-saturated concrete (%)
60	+5	+4
40	+2	+1.7
20	0	0
0	-0.5	-1
-4	-1.5	-7.5

Moisture Content:

The moisture content of concrete can have a small but significant influence on the pulse velocity. In general, the velocity is increased with increased moisture content, the influence being more marked for lower quality concrete. In saturated concrete, modulus of elasticity increases by 5-12 % and the strength reduces about 5 %. The pulse velocity of saturated concrete may be up to 2% higher than that in dry concrete of the same composition and quality. [11]

Age of the Concrete:

The compressional velocity increases continuously with the age of the concrete. (Figure 3.14) [21].

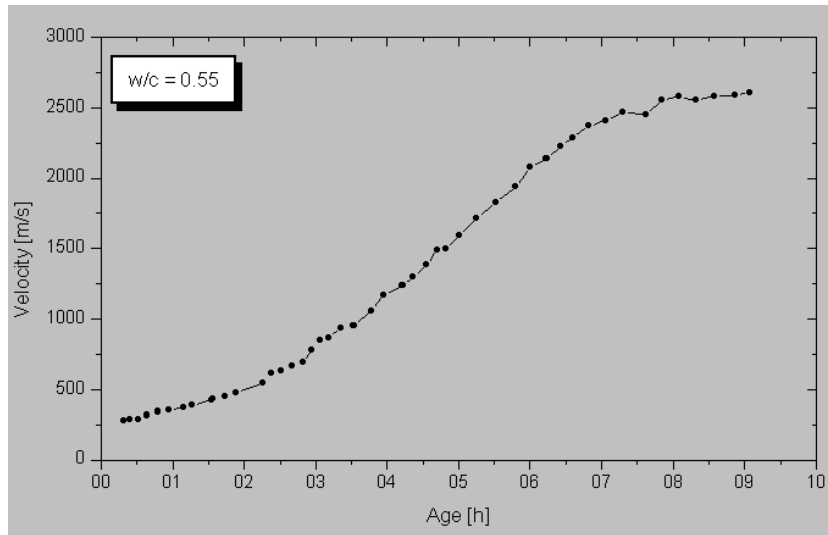


Figure 3.14: Velocity of the compressional wave versus age of the concrete [21]

After about 9 hours, the velocity increases only slowly (Figure 3.14). This facility is particularly useful for following the hardening process during the first two days after casting and it is sometimes possible to take measurements through formwork before it is removed at very early ages. Figure 3.15 [11] shows some typical experimental results of pulse velocity measurements of early ages.

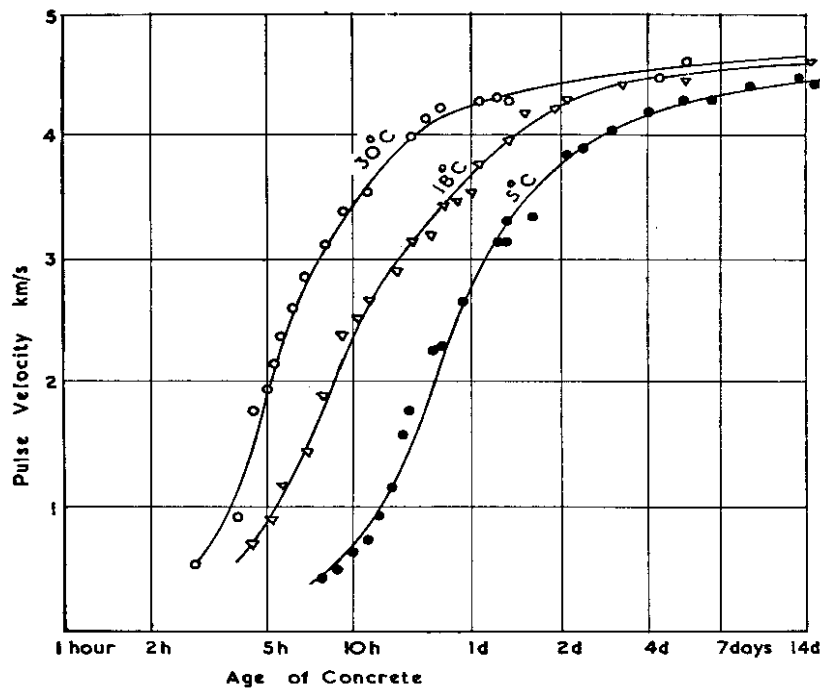


Figure 3.15: Pulse velocity versus age of concrete for different temperature values [11]

Water/Cement Ratio:

A plot of the results of tests with four water-cement ratios is shown in Figure 3.16. [21]

The lines start at about 300 m/s and develop continuously to values between 2500 and 3500 m/s after 8 hours. The lower the water-cement ratio the faster the velocity increases. This feature is well known from measurements of the compressive strength and the elastic modulus of young concrete. If a certain wave velocity is reached, the concrete is not workable any more. Van der Winden considered a velocity of 1000 to 1500 m/s as the end of workability. Regarding the Figure 3.16 the concrete with $w/c = 0.40$ would reach this after about 2.5 hours and the concrete with $w/c = 0.55$ at about 4.5 hours. The dosage of a commercial retarder can be applied such that the duration of

workability can be adjusted to the need of the construction site. [21]

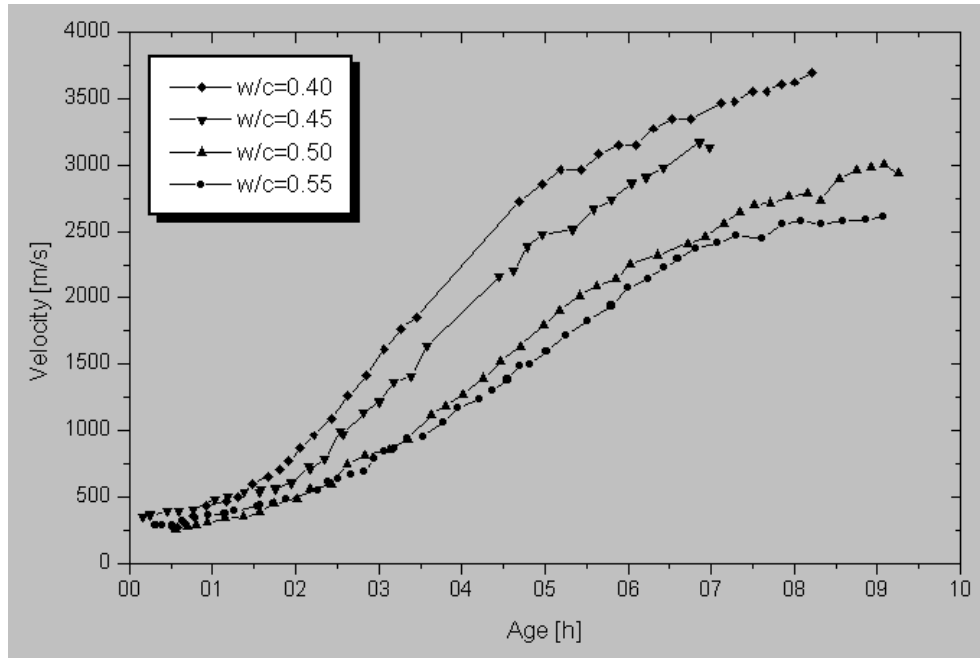


Figure 3.16: Velocity of the compressional wave as function of age and water/cement ratio [21]

Retarders:

Figure 3.17 [21] shows that the increase of velocity depends strongly on the dosage of retarder.

When 25 mg per kilogram of cement are used the velocity after 30 hours stays at a value which is only about two third of the value reached without or with little retarder. The super retarder is aimed to stop hydration for many hours or even several days. When concrete cannot be placed on a certain day it would be possible to store it to a later time and to use it when needed.

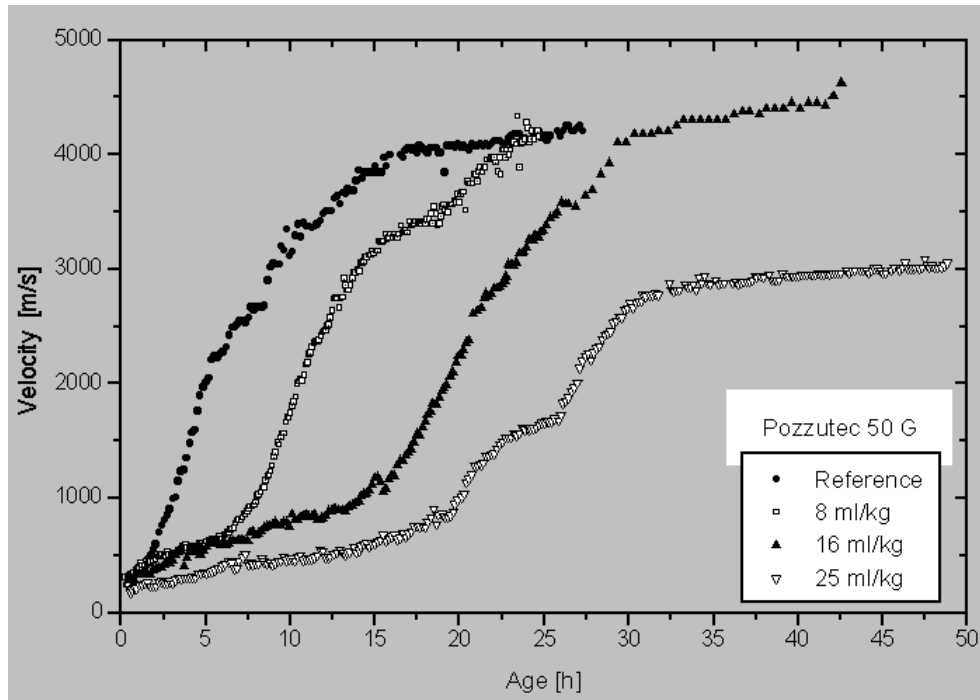


Figure 3.17: Velocity of the compressional wave as function of age and dosage of retarder [21]

Figure 3.18 [21] shows that the super retarder has a great effect already at a dosage of 11 ml per kilogram of cement. With 33 ml, the end of workability can be delayed until about 3 days.

Cement Type:

The effect of the cement type on the wave velocity is shown in Figure 3.19 [21]. There is almost no difference until 8 h. After that time the CEM I concrete develops the wave velocity faster than CEM III does.

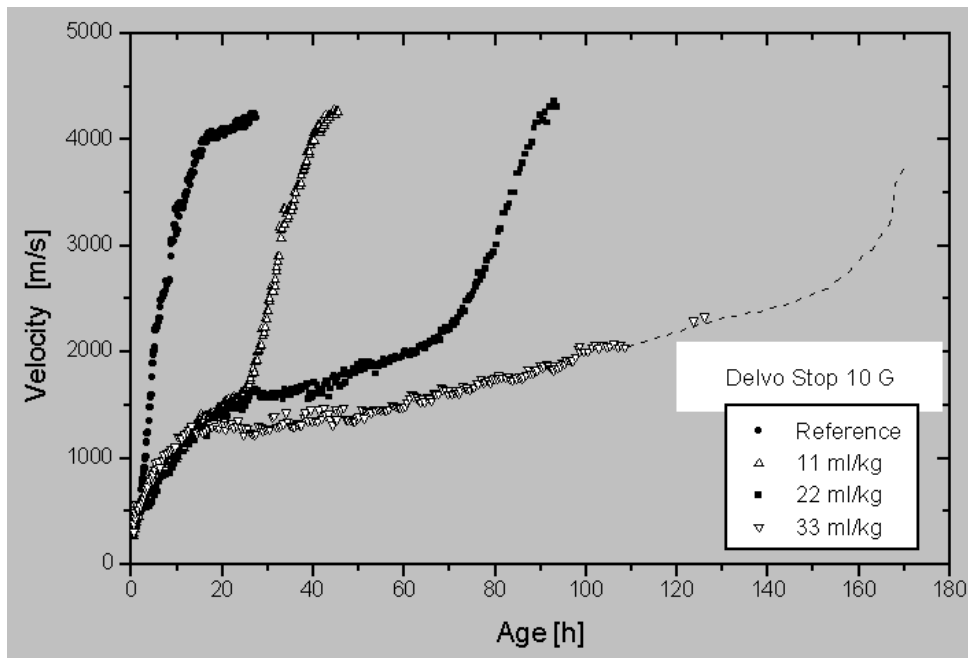


Figure 3.18: Velocity of the compressional wave as function of age and dosage of super retarder [21]

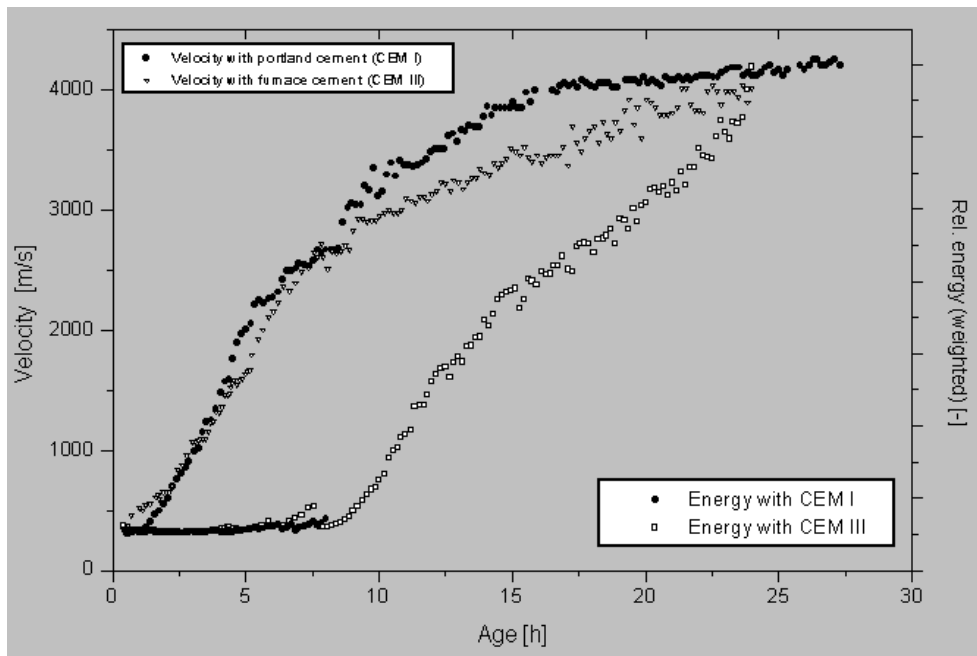


Figure 3.19: Velocity of compressional wave in concrete with CEM III and CEM I as function of age [21]

State of Stress:

Figure 3.20 [22] is an example of force, velocity and transmitted energy as function of deflection. The force-deflection line starts as a straight line up to the cracking force. Then, the inclination of the line decreases but keeps absolutely increasing up to about 12 kN.

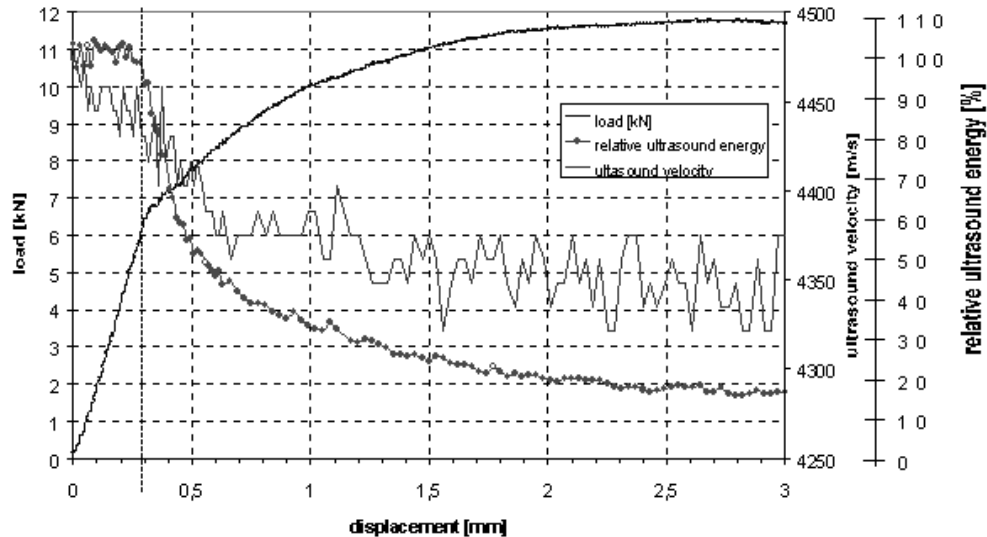


Figure 3.20: Force, velocity and transmitted energy as function of deflection [22]

The velocity starts at about 4450 m/s and drops to 4430 m/s at the cracking point. With increasing deflection, the velocity decreases finally to 4350 m/s. This is a relative decrease by about 2%. The transmitted energy is given in relative terms and drops from 90 % at the cracking point, ending up at a value of below 20 % after maximum load. This result also means that the decay of energy transfer is much more sensitive to damage in the zone around the notch than the velocity decrease.

Age of loading, residual stresses, and polarization will affect the current-state stresses, which will also change the pulse velocity.

Discontinuities:

When an ultrasonic pulse traveling through concrete meets a concrete-air interface, there is a negligible transmission of energy across this interface so that any air-filled crack or void lying directly between the transducers will obstruct the direct beam of ultrasound when the void has a projected area larger than the area of the transducer faces. The first pulse to arrive at the receiving transducer will have been diffracted around the periphery of the defect and the transit time will be longer than in similar concrete with no defect. Discontinuity normal to sound beam gives large reflected signal from discontinuity whereas discontinuity at an angle from the normal gives smaller reflected signal from discontinuity. [11]

Surface Conditions:

The surface moisture content, surface cracks, etc. affect the indirect measurements by changing the velocity of surface waves and weak edge compressional waves. Roughness, coating, and curvature at the test point also will affect the wave coupling.

Pulse velocity measurements may be used to assess the extent of damage to concrete after a fire. Figure 3.21 and Figure 3.22 [11] show some typical results as obtained by Watkeys [23] who showed that a good correlation existed between the maximum temperature reached by the concrete and the percentage reduction in pulse velocity due to heating. It is also showed that a useful correlation could be obtained to estimate the residual crushing strength of the concrete after heating from pulse velocity tests.

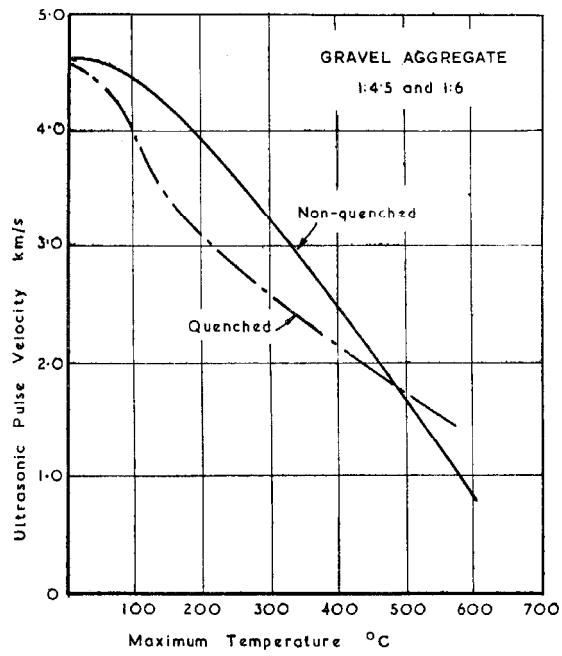


Figure 3.21: Ultrasonic pulse velocity as a function of temperature and quenching [11]

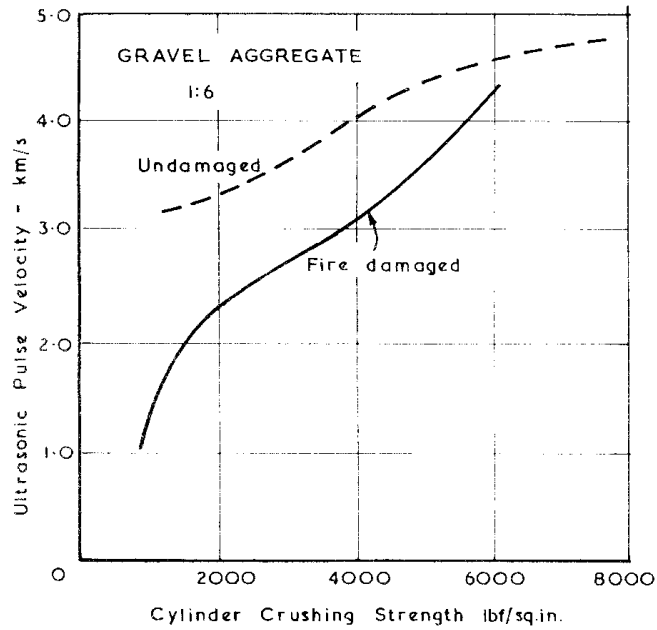


Figure 3.22: Ultrasonic pulse velocity as a function of cylinder crushing strength and fire damage [11]

In Figure 3.21, the two curves are for two sets of concrete specimens, which had been heated and cooled down either by spraying with water (quenched) or by loss of heat slowly in air (non-quenched).

Figure 3.22 shows that, for a given residual strength, the pulse velocity is apparently less than that for undamaged concrete. These results are for concrete made with gravel aggregate and are typical of normal concrete although no information is available regarding the effect of different types of aggregate on the correlations.

Cable Effect:

The cable used for the pulse transmission also affects the signal due to reflections in it.

3.5. Related Standards:

Some of the related standards are listed below:

- BS 1881: Part 203: 1986, "Testing Concrete - Recommendations for Measurement of Velocity of Ultrasonic Pulses in Concrete", British Standard Institute
- ASTM C 597-83 (91), "Standard Test Method for Pulse Velocity Through Concrete".
- DIN/ISO 8047 (Entwurf), "Hardened Concrete - Determination of Ultrasonic Pulse Velocity", in German.
- "Testing of Concrete - Recommendations and Commentary" by N. Burke in Deutscher Ausschuss für Stahlbeton (DAfStb), Heft 422, 1991, as a supplement to DIN/ISO 1048 in German.
- RILEM/NDT 1 1972, "Testing of Concrete by the Ultrasonic Pulse Method", (Réunion Internationale des Laboratoires et Experts des Matériaux, systèmes de construction et ouvrages) International Union

of Laboratories and Experts in Construction Materials, Systems and Structures.

- GOST 17624-87, "Concrete - Ultrasonic Method for Strength Determination", in Russian.
- STN 73 1371, "Method for Ultrasonic Pulse Testing of Concrete", in Slovak (Identical with the Czech CSN 73 1371).
- MI 07-3318-94, "Testing of Concrete Pavements and Concrete Structures by Rebound Hammer and by Ultrasound", Technical Guidelines in Hungarian.

Several standards use the term "measurement" (messung) or equivalent, for pulse velocity. This is not exactly correct because the distance between the two transducers and the transit time are the only measured variables (the transit time is the time taken for the onset of the pulse to pass through the concrete). The pulse velocity is calculated from these two. Nevertheless, this misnaming does not cause much confusion.

3.6. Advantages and Drawbacks of Ultrasonic Testing:

The main advantages of the test are:

- It is not a destructive measurement
- It is applicable to wide range of materials and members
- It is portable for field inspection

The principal drawbacks are:

- The length covered by the wave is not perfectly measured. In indirect UPV measurement, the transducer diameter introduces uncertainty in the path length for shorter intervals. Moreover, the measurements can not be made at large spacing due to the attenuation of waves in concrete and length limitations.

- The transducers and the structure should have a good contact in between (usage of coupling paste, clean surface, etc.).
- Reinforcement affects the wave propagation.

There are some ways to eliminate the drawbacks: There are “*point contact*” transducers available in the market, which can solve the actual length and coupling problems. There are also other non-destructive equipments, which give the layout of the reinforcement and bar diameters including the cover thickness of the concrete but still needs velocity corrections.

There are also additional drawbacks for ultrasonic testing:

- Only a small part of a surface can be scanned at a time with manual operation over a large surface area. Usage of transducer arrays can improve the ease and operation time.
- Samples must be taken from the structure for calibration.
- In some cases, more than one operator is needed to operate the instrument.
- Geometric acoustic method, which considers only linear wave propagation, introduces serious errors into estimation of the velocity values.
- High level of acoustic attenuation existing in these materials gives velocity dispersion, which hinders estimation of frequency characteristics of propagating waves
- There is also uncertainty in the definition of velocity. Physically, only "phase" or "group" wave velocities can be considered, but for materials with high level of attenuation and dispersion, these definitions do not fit.
- Fairly extensive research has been done in an attempt to correlate the pulse velocity with the compressive strength. The idea is that pulse velocity is a function of material density and stiffness, both of which have been correlated with compressive strength. In practice, however,

the results have been mixed. The number of variables that affect concrete compressive strength is large. Water-cement ratio, aggregate size and shape, size of sample, and cement content all directly relate to the strength. However, the pulse velocity is not affected by all of these variables. Thus, it is difficult to find universal pulse velocity methods for concrete. It is generally well accepted that pulse velocity can be a good indicator of strength gain of concrete at early ages (up to a few days). Pulse velocity techniques can also be applied in order to evaluate uniformity of the concrete in a structure. This type of measurement is generally qualitative in nature, and yields little quantitative information.

CHAPTER 4

THE EXPERIMENTS AND RESULTS

4.1. Transverse Vibration Measurement Tests:

Transverse vibration technique is considered to estimate the uniaxial compressive load on a structural member. For this purpose, concrete shearwall test and steel I120 beam-column tests are conducted in the laboratory. Furthermore, a real life application is carried out on a 24 storey high reinforced concrete building columns and shearwalls.

4.1.1. Concrete Shearwall Test:

Construction Stages:

A concrete shearwall with reinforcement is cast with dimensions of 9 x 91 x 151 cm (Figure 4.1). The properties of the shear wall are given in Table 4.1.

The poured concrete is shown in Figure 4.2.

Test Setup:

The shear wall is placed into a steel frame to test the transverse vibration frequencies. Front view of the concrete shear wall test setup is given in Figure 4.3.



Figure 4.1: The reinforcement of the concrete shearwall

Table 4.1. The properties of the concrete shearwall

Dimensions	: 9 x 91 x 151 cm
Concrete class	: C12
Maximum aggregate size	: 30 mm
Slump	: 75-100 mm
Water/Cement ratio	: 0,80
Weight	: ~ 2.94 kN
Estimated modulus of elasticity	: 25 000 MPa
Estimated buckling load	: 922 kN



Figure 4.2: The fresh concrete of the shearwall

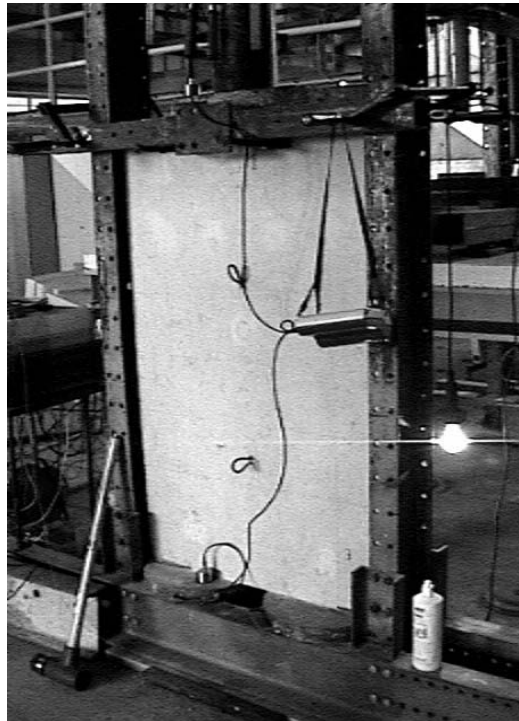


Figure 4.3: Front view of the concrete shearwall test setup

The shear wall is loaded from one point at the top (Figure 4.4). The shear wall is restrained at two points by rods connected to the box girder both at the front and back (Figure 4.4 and Figure 4.5). The girders are hold in place by pressure.

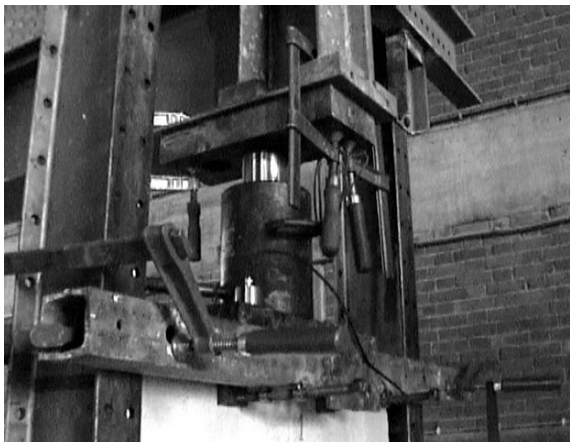


Figure 4.4: Front-top view of the concrete shearwall test setup

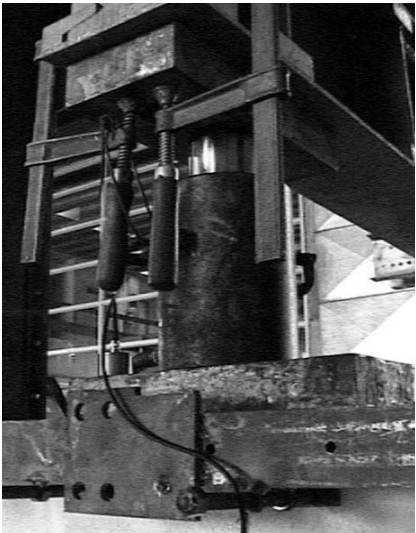


Figure 4.5: Back-top view of the concrete shearwall test setup

At the bottom, the shear wall is placed on two steel plates in order to have a non-uniform stress distribution (Figure 4.6 and Figure 4.7).

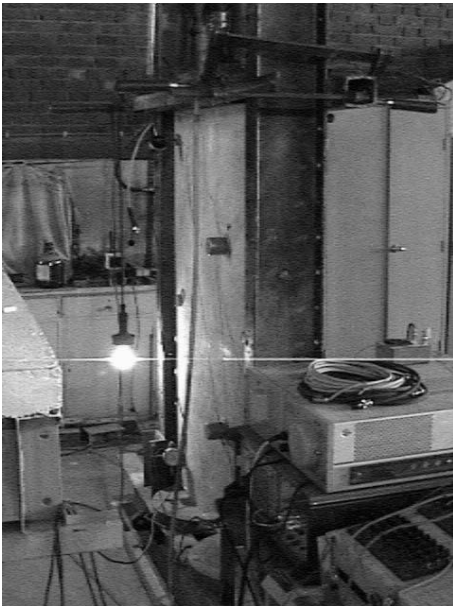


Figure 4.6: Back view of the concrete shearwall test setup



Figure 4.7: Back-bottom view of the concrete shearwall test setup

Testing Instruments:

HP 3582A Spectrum Analyzer and Tektronix 5110 Oscilloscope with 5A15N Amplifier are used (Figure 4.8).

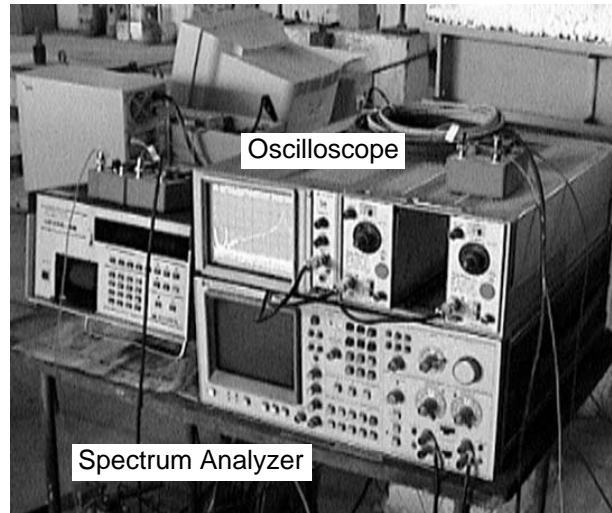


Figure 4.8: General view of the test equipments

Spectrum analyzer separates the frequency content of different waves superimposed on each other. The acceleration received from the accelerometers are plotted on the screen of spectrum analyzer. Since the screen of spectrum analyzer was out of order accelerometer readings are plotted on the screen of the oscilloscope (Figure 4.8).

Peaks indicate possible mode shapes and their resonant frequencies. Using the knob located on the spectrum analyzer, it is possible to move a tracer on a peak and read the corresponding frequency of the peak. To illustrate the accelerometer readings Figure 4.9 and Figure 4.10 are given.

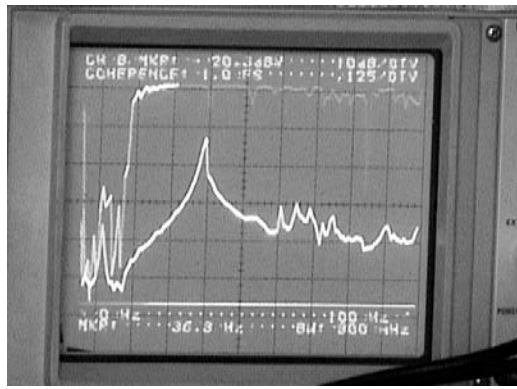


Figure 4.9: Accelerometer readings and coherence

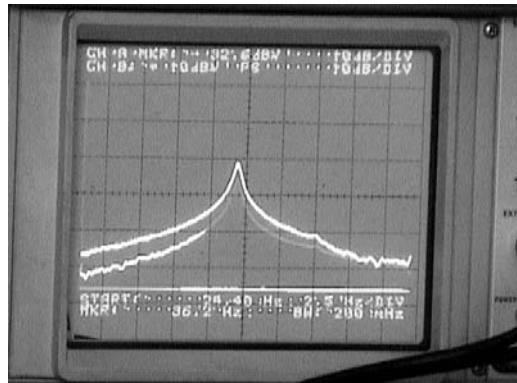


Figure 4.10: Two accelerometer readings

Before the test results are compared against analytical studies, validation checks are carried out for the assumptions made in Chapter 2. The two checked assumptions are; i) shear deformation neglect, ii) damping neglect. These checks are shown under separate heading below. The properties of the test specimen for these validity checks are listed below.

L = 1.40 m
 E = 25 000 MPa

$f_{ck} =$	12	MPa
$A =$	819	cm^2
$I_{\min} =$	5528.3	cm^4
$m =$	1.93	kN/m
$\lambda =$	53.9	
$P_{\text{ultimate}} =$	964.1	kN
$P_{\text{buckling}} =$	882.9	kN

Shear deformation neglection check:

The ratio of the radius of gyration to the length is calculated to see the shear effect. [1]

$$\frac{r}{L} = \frac{\sqrt{\frac{I_{\min}}{A}}}{L} = \frac{\sqrt{\frac{5528.3}{819}}}{140} = 0.019$$

where,

r: radius of gyration (cm)

L: length (cm)

I_{\min} : moment of inertia in weak direction (cm^4)

A: area (cm^2)

When 0.019 value is entered to the chart given in Chopra's text book [1]

ω'_n / ω_n is found to be approximately equal to 0.99 for the first mode (n=1).

As a result, influence of shear deformation and rotational inertia on natural frequencies can be neglected. Although the figure in Chopra's text book [1] is prepared for simply supported beams, computations are done for a comparison.

Effect of neglect of damping:

Response curve shown in Figure 4.11 is used to compute the damping ratio using the frequency-response curve method described in Chopra's book [1]. The response curve at 27.12 tons is selected as an example. The critical frequencies and amplitudes are shown in Figure 4.11.

The peak of the frequency-response curve occurs at 76.25 Hz. The peak value (in logarithmic scale) is 3.15. A horizontal line is drawn at "3.15 – $\log(\sqrt{2}) = 3.00$ " as shown in Figure 4.11. This line intersects the frequency-response curve at 76.86 Hz and 75.51 Hz.

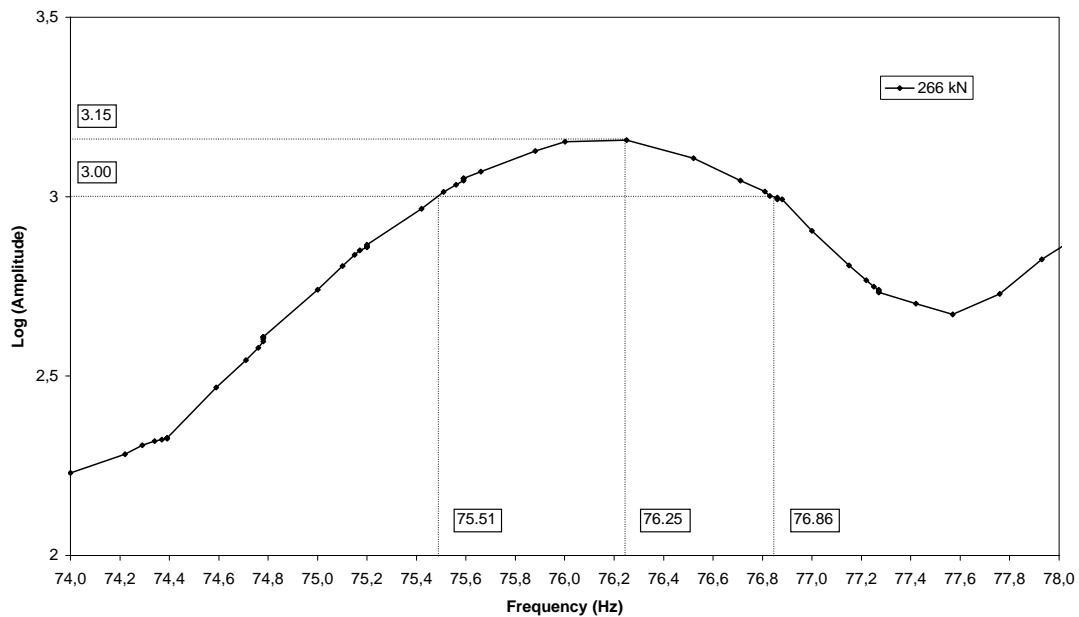


Figure 4.11: Evaluating damping from frequency-response curve of concrete shear wall

The damping ratio is computed as below:

$$\zeta = \frac{76.86 - 75.51}{2 \cdot 76.25} = 0,9 \%$$

From the following equation [1]:

$$\omega_{\text{damped}} = \omega_{\text{natural}} \cdot \sqrt{1 - \zeta^2} \quad (4.1)$$

$$76.25 = \omega_n \cdot \sqrt{1 - (0.009)^2}$$

$\omega_n = 76.25$ rad/s is obtained.

Therefore, the damping effect can be neglected.

Shear Wall Test and the Results:

The shear wall was loaded monotonically after it is placed in a steel frame. At each load increment, transverse vibration frequencies of the first mode and the ultrasonic pulse velocities (parallel to the load direction) are measured. Vibrations are generated by a hammer and pulse velocities are measured by "TICO", respectively (Figure 4.3).

The test results was too complicated to analyze due to the contribution of different vibration frequencies coming from different modes of the steel frame. While collecting the data, the vibration frequencies of the whole system (i. e. concrete shear wall and the steel frame) are taken between the range of 0-150 Hz in three windows (0-50 Hz, 50-100 Hz and 100-150 Hz) in order to increase the accuracy. 50-100 Hz window was the appropriate one for investigation of the results Figure 4.12 because the first bending mode

frequency of the shear wall existed around 76 Hz. These frequencies have a trend to decrease and are close to the analytical solutions.

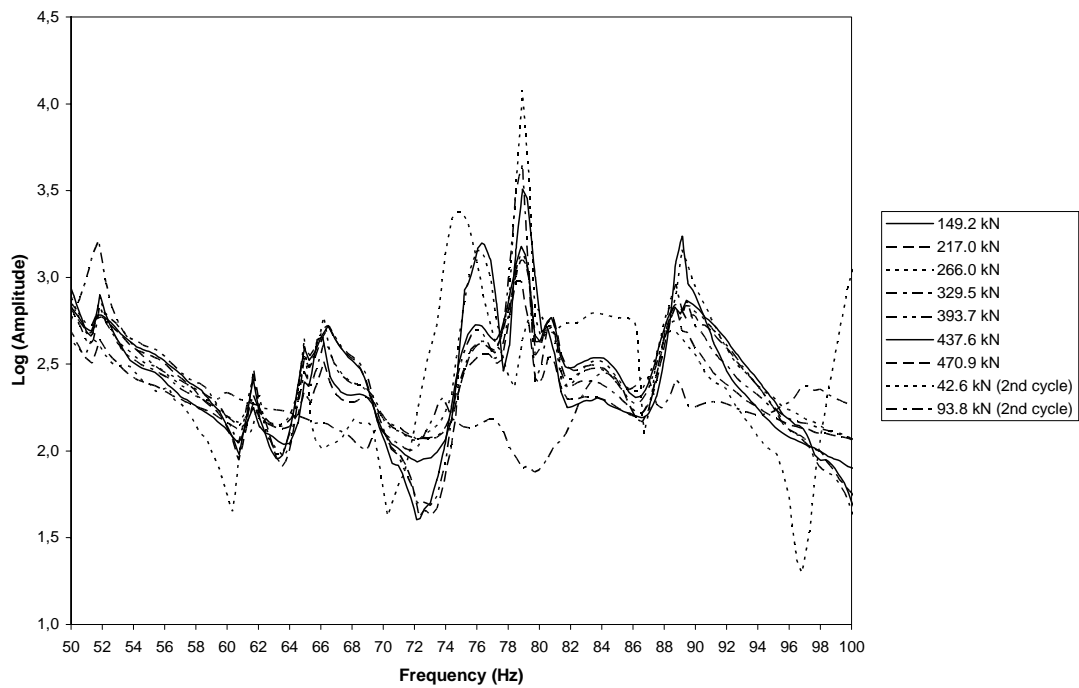


Figure 4.12: Vibration frequencies of the concrete shearwall and the test setup under different axial load levels

A closer view of 74 Hz to 78 Hz range is given in Figure 4.13. The results of the transverse vibration of the concrete shear wall are given in a tabular form in Table 4.2.

In addition, results of ultrasonic pulse velocity measurements are given in Figure 4.14. At 1.86 MPa pulse velocity was 3170 m/s.

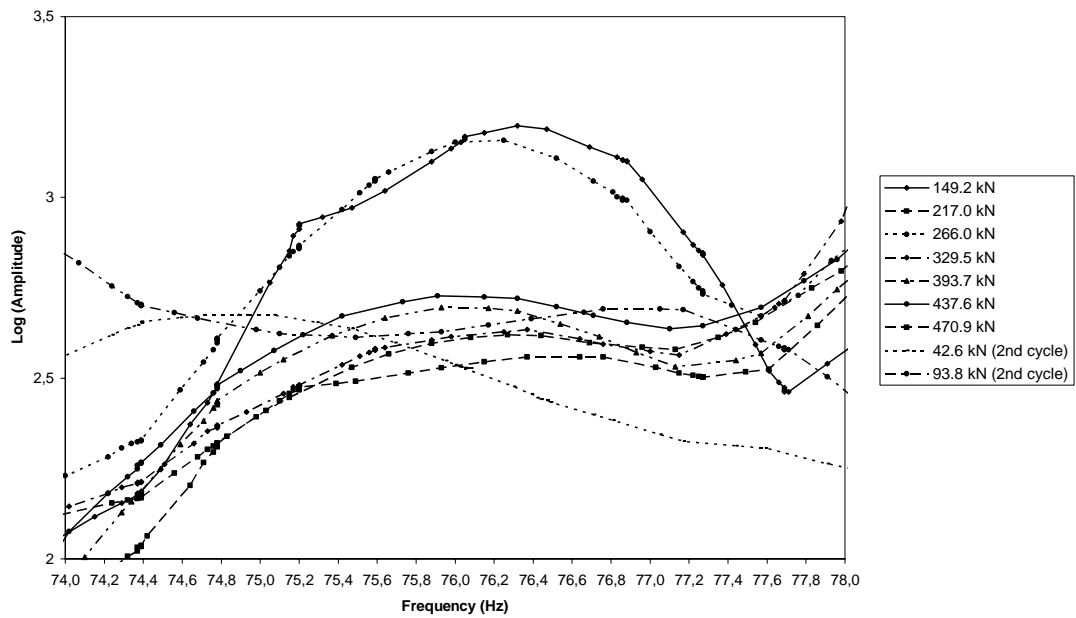


Figure 4.13: Closer view of the vibration frequencies of the concrete shearwall under different axial load levels

Table 4.2. Measured fundamental frequencies of the concrete shear wall

P (kN)	f (Hz)	Change (Hz)	Change (%)
149.2	76,32	0,00	0,00
217.0	76,70	0,38	0,50
266.0	76,25	-0,07	-0,09
329.5	76,37	0,05	0,07
393.7	76,05	-0,27	-0,35
437.6	75,91	-0,41	-0,54
470.9	76,27	-0,05	-0,07
42.6 (2 nd cycle)	74,93	-1,39	-1,82
93.8 (2 nd cycle)	77,05	0,73	0,96

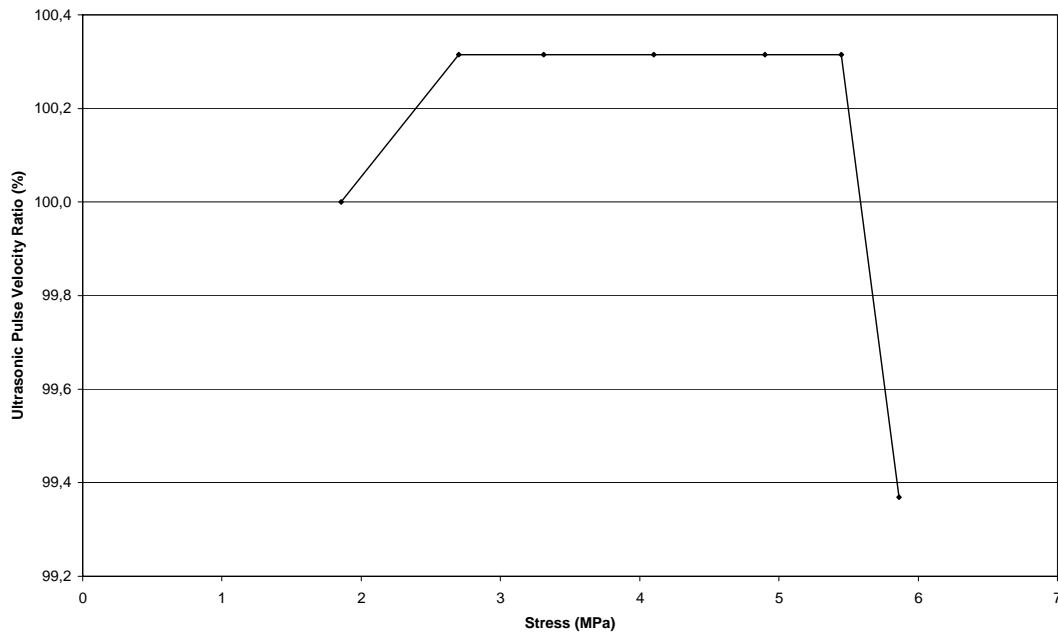


Figure 4.14: The ultrasonic pulse velocity ratio versus stress in parallel direction on C12 concrete shearwall

Since the boundary conditions were not so clear, several analytical solutions are performed to check the test results.

Analytical Solution for Pinned Ends on Both Supports:

Using the derivations from Section 2.2.3 for pin-ended boundary conditions, the expected fundamental frequency of the shear wall is calculated (Table 4.3).

Analytical Solution for Fixed Ends on Both Supports:

Analytical calculations are carried out using derivations from Section 2.2.4. The expected fundamental frequencies are given in Table 4.4.

Table 4.3. Expected fundamental frequencies of the concrete shear wall from the model with pinned ends on both supports

P (kN)	P/P _{buckling} (%)	f (Hz)	Change (Hz)	Change (%)
0.00	0.00	66.56	0.00	0.00
42.6	4.82	66.35	-0.21	-0.31
93.8	10.62	66.10	-0.46	-0.69
149.2	16.90	65.83	-0.73	-1.10
217.0	24.58	65.49	-1.07	-1.60
266.0	30.13	65.25	-1.31	-1.97
329.5	37.32	64.93	-1.63	-2.44
393.7	44.59	64.61	-1.95	-2.93
437.6	49.57	64.39	-2.17	-3.26
470.9	53.33	64.22	-2.34	-3.51

Table 4.4. Expected fundamental frequencies of the concrete shear wall from the model with fixed ends on both supports

P (kN)	P/P _{buckling} (%)	f (Hz)	Change (Hz)	Change (%)
0.00	0.00	150.89	0.00	0.00
42.6	4.82	150.77	-0.12	-0.08
93.8	10.62	150.63	-0.26	-0.17
149.2	16.90	150.48	-0.41	-0.27
217.0	24.58	150.30	-0.59	-0.39
266.0	30.13	150.17	-0.72	-0.48
329.5	37.32	150.00	-0.89	-0.59
393.7	44.59	149.83	-1.06	-0.70
437.6	49.57	149.71	-1.18	-0.78
470.9	53.33	149.62	-1.27	-0.84

Analytical Solution for Fixed End and Spring with Roller on Other End:

Analytical calculations are carried out using derivations from Section 2.2.6. The spring is assumed to be linearly elastic. The spring constant is solved by trial and error method in order to match the test results. The stiffness of the springs are given in Table 4.5.

Table 4.5. Analytical fundamental frequencies of the concrete shear wall with fixed and spring with roller supports

P (kN)	k (kN/cm)	f (Hz)
0.00	210.9	76.32
42.6	198.2	74.94
93.8	220.7	77.09
149.2	213.9	76.33
217.0	219.7	76.77
266.0	214.8	76.21
329.5	217.8	76.37
393.7	215.8	76.06
437.6	215.8	75.98
470.9	219.7	76.28

SAP2000 Model of the Shear Wall:

For the comparison of analytical and experimental results, shear wall is modeled by the structural analysis program “SAP2000 Nonlinear version 7.12” (Figure 4.15).

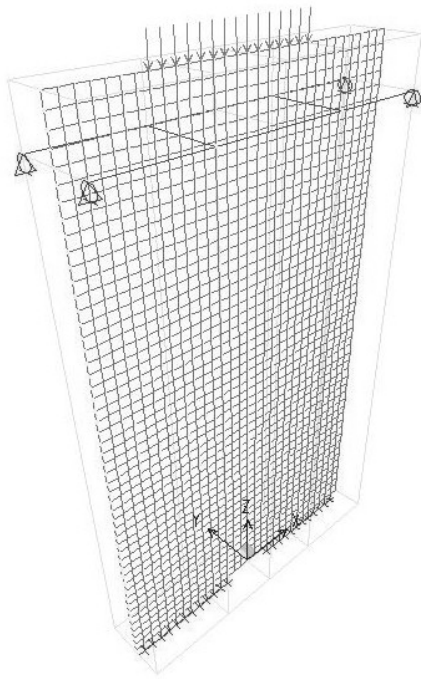


Figure 4.15: SAP2000 model of the concrete shearwall

In SAP2000 model, the properties of the test specimen is taken as below in order to compare with the other analytical solutions.

$$\begin{aligned} L &= 1.38 \text{ m} \\ E &= 25\,310 \text{ MPa} \\ f_{ck} &= 12 \text{ MPa} \\ A &= 819 \text{ cm}^2 \\ I_{min} &= 5528.3 \text{ cm}^4 \\ m &= 1.93 \text{ kN/m} \end{aligned}$$

The stress distribution at the maximum applied load (470.9 kN) is given in Figure 4.16.

The frequency in the first mode (first bending mode) is computed to be 78.98 Hz by taking the spring constant at the supports as a value of 182.2 kN/cm.

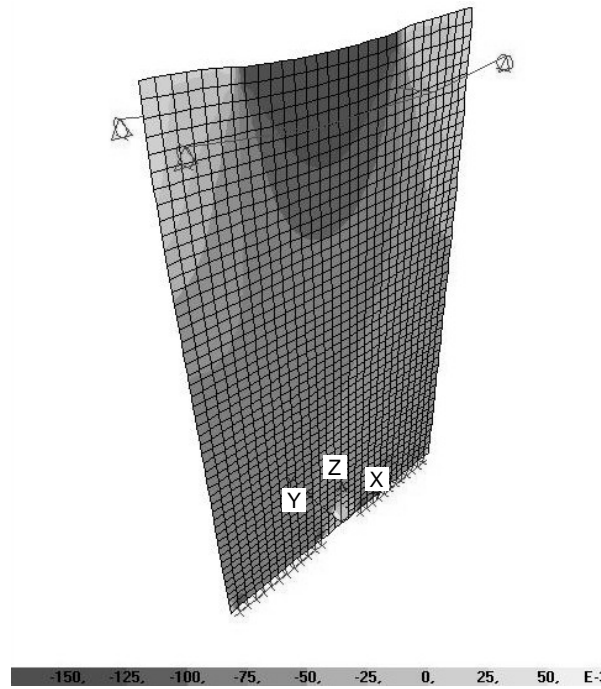


Figure 4.16: Stress distribution on the concrete shearwall at 470.9 kN

In order to calculate the spring constant in SAP2000 model, the stiffness of the I-beams are computed. The model of the beams is given in Figure 4.17.

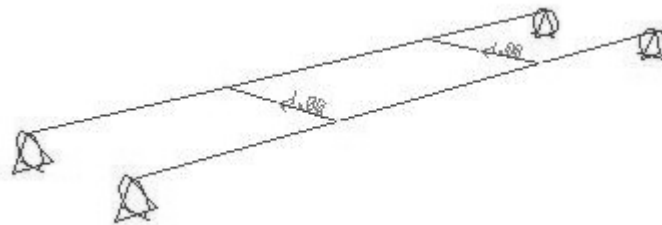


Figure 4.17: Model for computing I-beam stiffness

For 19.62 kN the translation of the beams in global y-direction is 0.0661 cm. Thus, the stiffness of the beam is 19.62 kN / 0.0661 cm = 296.8 kN/cm. If the analytical solution is assumed to be correct (Table 4.5), the spring constants in y-direction at the supports can be calculated as below.

$$\frac{1}{4 \cdot k_{\text{spring}}} + \frac{1}{k_{\text{beam}}} = \frac{1}{k} \quad (4.2)$$

$$\frac{1}{4 \cdot k_{\text{spring}}} + \frac{1}{296.8} = \frac{1}{210.9}$$

$k_{\text{spring}} = 182.2$ kN/cm is obtained.

According to these analytical SAP2000 model the figures of the first five vibration modes are given below.

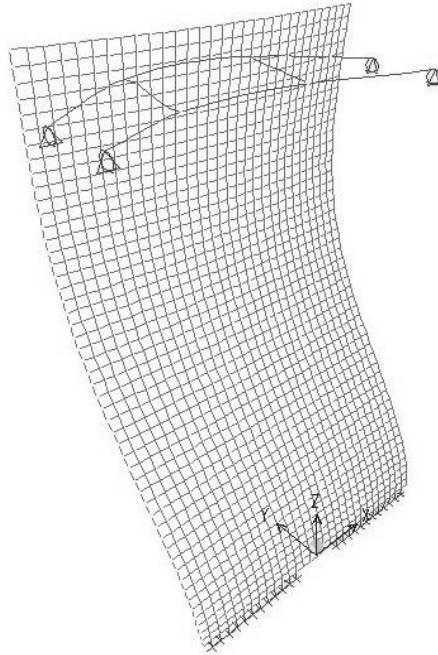


Figure 4.18: First vibration mode of the concrete shearwall

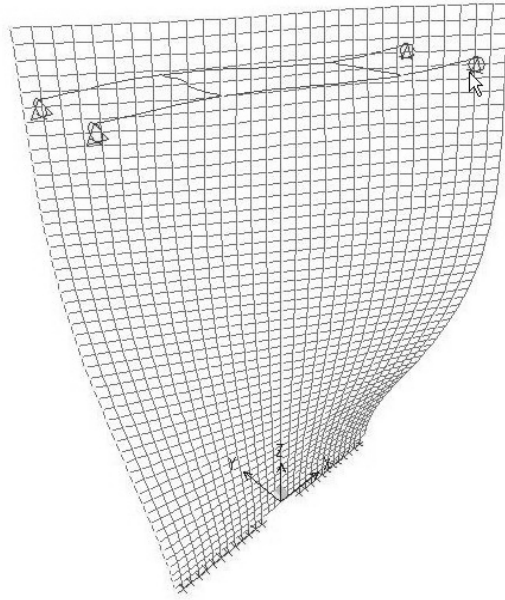


Figure 4.19: Second vibration mode of the concrete shearwall

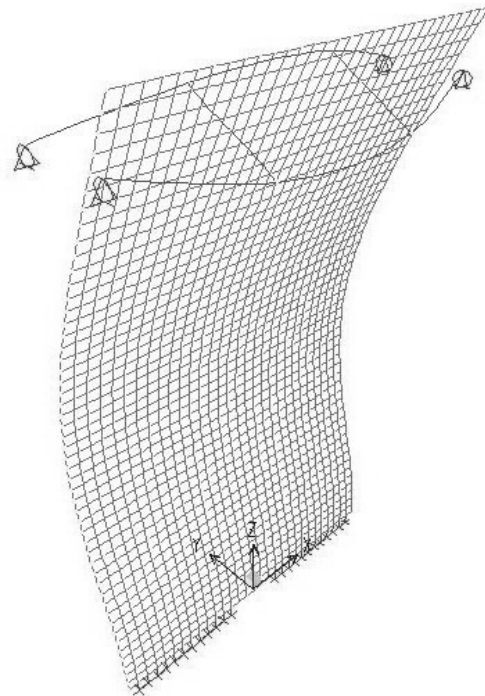


Figure 4.20: Third vibration mode of the concrete shearwall

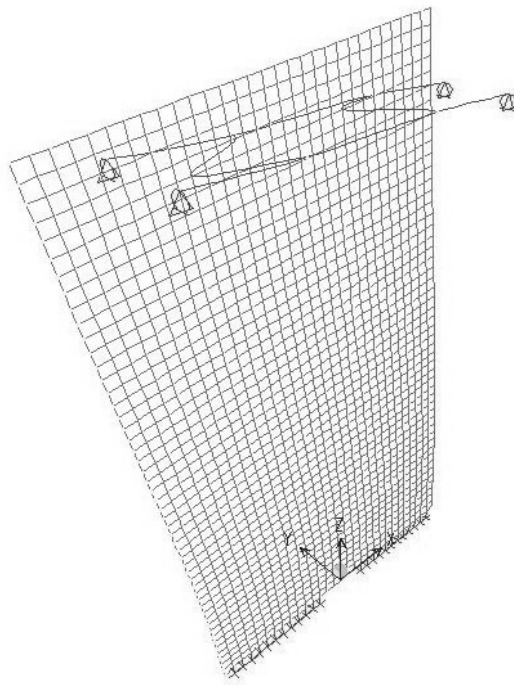


Figure 4.21: Fourth vibration mode of the concrete shearwall

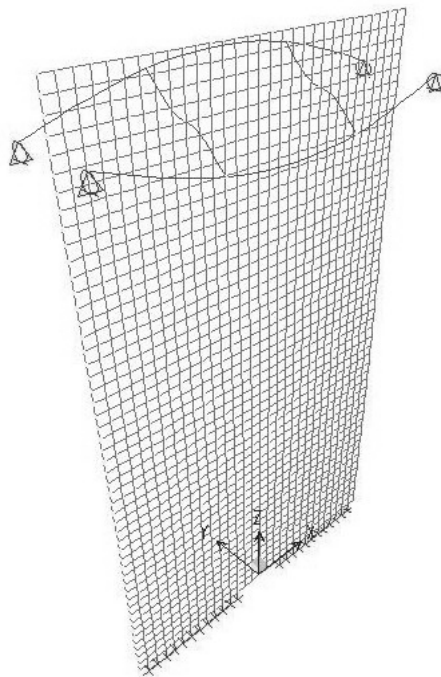


Figure 4.22: Fifth vibration mode of the concrete shearwall

The modal frequencies and participating mass ratios are given in Table 4.6 and Table 4.7, respectively.

Table 4.6. Analytical modal periods and frequencies of SAP2000 concrete shear wall model

MODE	PERIOD (TIME)	FREQUENCY (CYC/TIME)	FREQUENCY (RAD/TIME)	EIGENVALUE (RAD/TIME)**2
1	0.01266	78.981	496.253	2.46E+05
2	0.00711	140.675	883.888	7.81E+05
3	0.00688	145.445	913.858	8.35E+05
4	0.00482	207.484	1303.659	1.70E+06
5	0.00415	240.983	1514.139	2.29E+06

Table 4.7. Analytical modal participating mass ratios of SAP2000 concrete shear wall model

MODE	PERIOD	INDIVIDUAL MODE (PERCENT)			CUMULATIVE SUM (PERCENT)		
		UX	UY	UZ	UX	UY	UZ
1	0.012661	0.00	79.31	0.00	0.00	79.31	0.00
2	0.007109	0.00	0.00	0.00	0.00	79.31	0.00
3	0.006875	0.00	1.32	0.00	0.00	80.63	0.00
4	0.004820	62.91	0.00	0.00	62.91	80.63	0.00
5	0.004150	0.00	0.26	0.00	62.91	80.89	0.00

Comparison of the Shear Wall Results:

The results related to the concrete shear wall are given in Table 4.8 in a tabular form. The results for the shear wall is also compared in Figure 4.23.

Since the shear wall member was not much slender to observe a high frequency change and the boundary (support) conditions of the shear wall was not so clear, this test did not yield much information.

Table 4.8. Comparison of experimental modal frequencies versus analytical results for different boundary conditions

Load (kN)	Fundamental Vibration Frequency (Hz)				
	Test Results	Analytical Results			
		with spring	pin-ended	fix-ended	SAP2000 model
0.00	-	76.32	66.56	150.89	78.98
42.6 (2 nd cycle)	74.93	74.94	66.35	150.77	
93.8 (2 nd cycle)	77.05	77.09	66.10	150.63	
149.2	76.32	76.33	65.83	150.48	
217.0	76.70	76.77	65.49	150.30	
266.0	76.25	76.21	65.25	150.17	
329.5	76.37	76.37	64.93	150.00	
393.7	76.05	76.06	64.61	149.83	
437.6	75.91	75.98	64.39	149.71	
470.9	76.27	76.28	64.22	149.62	

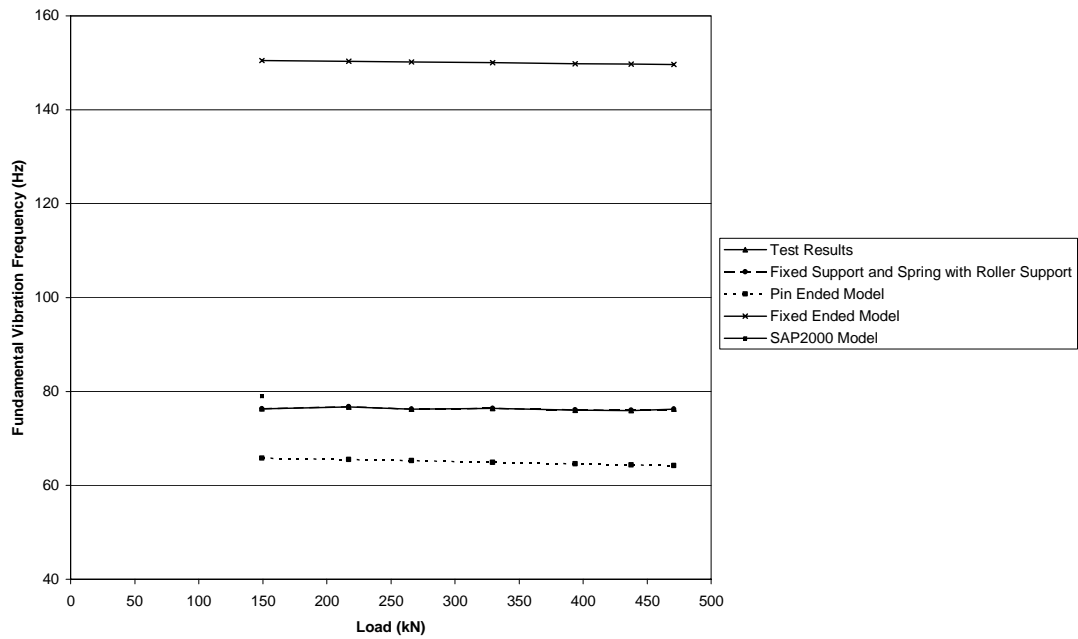


Figure 4.23: Comparison of concrete shear wall test and analytical solution results

4.1.2. Simply Supported I120 Steel Beam-Column Test:

After concrete shear wall tests, I120 steel beam-column vibration tests are conducted. Such a slender member is selected to observe much changes in the vibration frequency. To check the validation of the assumptions done in Chapter 2, following calculations are done. The member properties are listed below.

$$\begin{aligned}
 L &= 1.60 \text{ m} \\
 E &= 210\,000 \text{ MPa} \\
 \sigma_y &= 240 \text{ MPa} \\
 A &= 14.2 \text{ cm}^2 \\
 I_{\min} &= 21.5 \text{ cm}^4
 \end{aligned}$$

$$m = 0.109 \text{ kN/m}$$

In addition, the buckling properties are:

$$\lambda = 126.0$$

$$P_{cr} = 180.5 \text{ kN}$$

The two checked assumptions are; i) shear deformation neglection, ii) damping neglection. These checks are shown under separate heading below.

Shear deformation neglection check:

The ratio of the radius of gyration to the length is calculated to see the shear effect. [1]

$$\frac{r}{L} = \frac{\sqrt{\frac{I_{min}}{A}}}{L} = \frac{\sqrt{\frac{21.5}{14.2}}}{160} = 7.691 \cdot 10^{-3} < 0.008$$

where,

r: radius of gyration (cm)

L: length (cm)

I_{min} : moment of inertia in weak direction (cm⁴)

A: area (cm²)

When 0.008 is entered to the chart given in Chopra's text book [1]

ω'_n / ω_n is found to be greater than 0.99 for the first mode (n=1).

Therefore, influence of shear deformation and rotational inertia on natural frequencies can be neglected. Note that, the result was for simply supported beam.

Effect of neglect of damping:

Response curve shown in Figure 4.24 is used to compute the damping ratio using the frequency-response curve method described in Chopra's book [1].

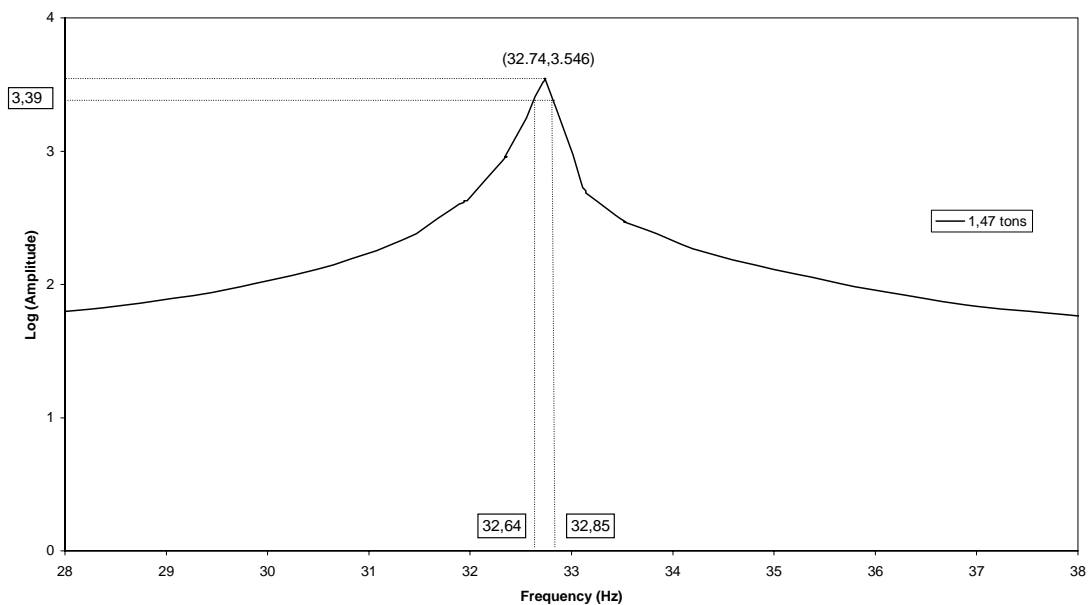


Figure 4.24: Evaluating damping from frequency-response curve of steel I120 beam-column

The peak of the frequency-response curve occurs at 32.74 Hz (Figure 4.24). The peak value (in logarithmic scale) is 3.546. A horizontal line is drawn at

" $3.546 - \log(\sqrt{2}) = 3.395$ ". This line intersects the frequency-response curve at 32.64 Hz and 32.85 Hz.

The damping ratio can be calculated as below.

$$\zeta = \frac{32.85 - 32.64}{2 \cdot 32.74} = 0.3 \% \quad [1]$$

Then,

$$32.74 = \omega_n \cdot \sqrt{1 - (0.003)^2} \quad [1]$$

$\omega_n = 32.74$ rad/s is obtained.

Therefore, the damping effect can be neglected.

1120 Steel Column Test and the Results:

1120 steel column is tested in the same steel frame where the concrete shear wall has been tested. The length and the sectional properties of the steel column are selected in a manner that the fundamental vibration frequency falls between the range of 0-50 Hz where the steel frame has the least contributions.

As a result, it was easy to identify the transverse vibration frequencies of 1120 steel column clearly. The test results are given in Table 4.9 and Figure 4.25.

Since the boundary conditions were not so clear, several analytical solutions are performed to check the test results.

Table 4.9. Measured first bending frequencies during I120 steel column compression test

Load (kN)	Frequency (Hz)
14.42	33.0
28.84	33.0
43.26	32.2
57.68	31.4
72.89	30.2
88.78	28.6
103.20	27.0
118.41	25.4
132.83	24.6

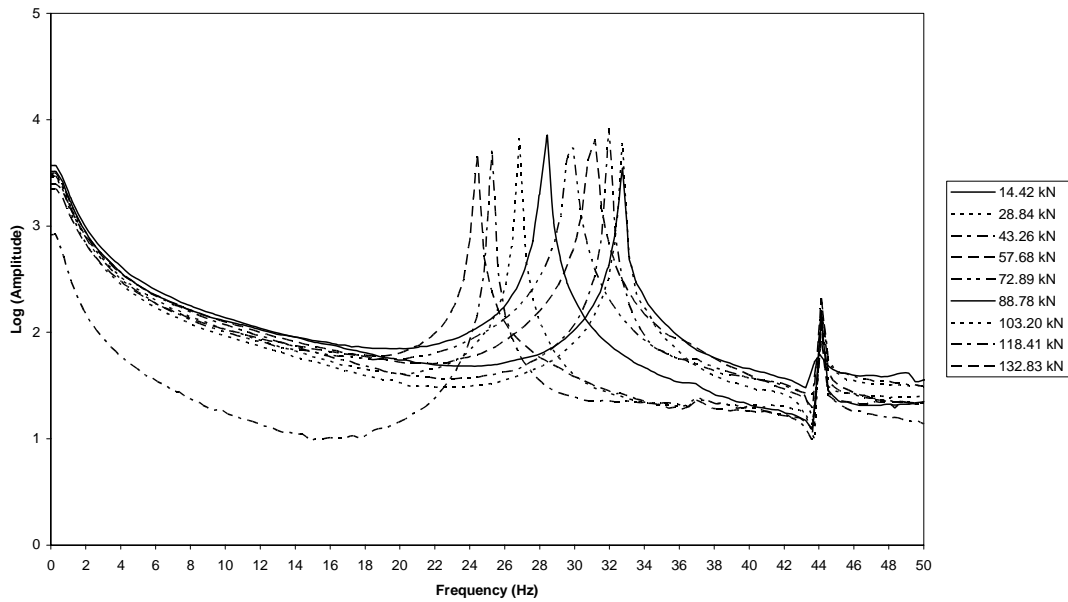


Figure 4.25. Change in the transverse vibration frequency of steel I120 column in the first mode under monotonic axial compression

Analytical Solution for Transverse Springs with Rollers on Both Ends:

Analytical calculations are carried out using derivations from Section 2.2.5. The spring constants are arranged according to fit the test results. The stiffness of the springs are given in Table 4.10.

Table 4.10. The expected (analytical) fundamental frequencies steel I120 column (simply supported, L= 160 cm, transverse springs at the two ends)

Load (kN)	k_1 (kN/cm)	k_2 (kN/cm)	f (Hz)
14.42	18.15	5.79	33.04
28.84	31.88	10.20	33.00
43.26	57.39	18.34	32.22
57.68	500.31	159.71	31.40
72.89	7 848.00	2 504.69	29.34
88.78	68 670.00	21 915.90	26.86
103.20	68 670.00	21 915.90	24.38
118.41	68 670.00	21 915.90	21.46
132.83	68 670.00	21 915.90	18.27

Analytical Solution for Pinned Ends on Both Supports:

Using the derivations from Section 2.2.3 for pin-ended boundary conditions, the expected fundamental frequency of the steel I120 beam-column is calculated (Table 4.11).

Table 4.11. The expected (analytical) fundamental frequencies of steel I120 column (simply supported, L= 160 cm, no springs)

Load (kN)	P/P _{buckling} (%)	f (Hz)	Change (Hz)	Change (%)
14.42	7.99	37.09	0.00	0.00
28.84	15.98	35.34	-1.75	-4.72
43.26	23.97	33.49	-3.60	-9.69
57.68	31.96	31.54	-5.55	-14.95
72.89	40.38	29.34	-7.74	-20.88
88.78	49.18	26.86	-10.23	-27.59
103.20	57.17	24.38	-12.71	-34.26
118.41	65.60	21.46	-15.63	-42.13
132.83	73.59	18.27	-18.82	-50.74

SAP2000 Model of I120 Steel Column:

To compare the results a model is prepared with the structural analysis program “SAP2000 Nonlinear version 7.12” (Figure 4.26). The frequency in the first mode (translation in y-direction) is computed to be “33.12 Hz” with the spring constants 5.30 kN/cm and 1.67 kN/cm in y-direction. In the model:

L= 1.60 m
 E= 203 900 MPa
 σ_y = 240 MPa
 A= 13.2 cm²
 I_{min} = 27.7 cm⁴
 m= 0.101 kN/m

When the moment of inertia and mass values of SAP2000 are used in analytical model (analytical model for transverse springs with rollers on both

ends) the fundamental frequency is calculated as 31.14 Hz which is close to the 33.12 Hz of SAP2000 result.

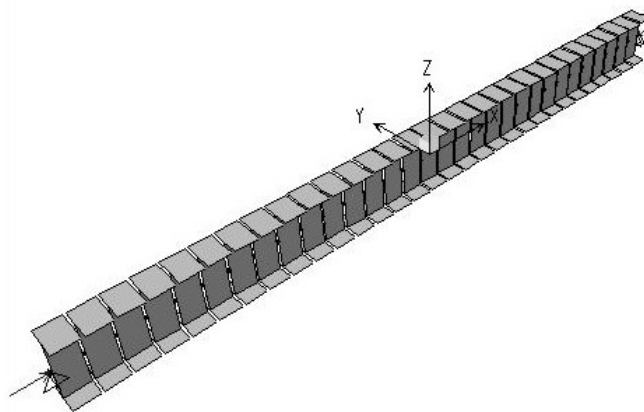


Figure 4.26: The SAP2000 model of steel I120 beam-column

The first three mode shapes of the I120 steel column are given in the following figures.

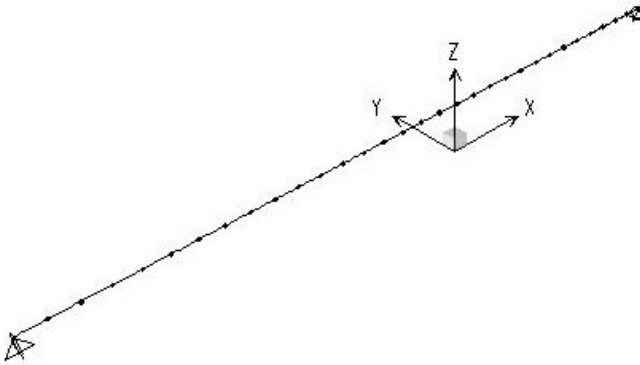


Figure 4.27: First vibration mode of the steel I120 beam-column

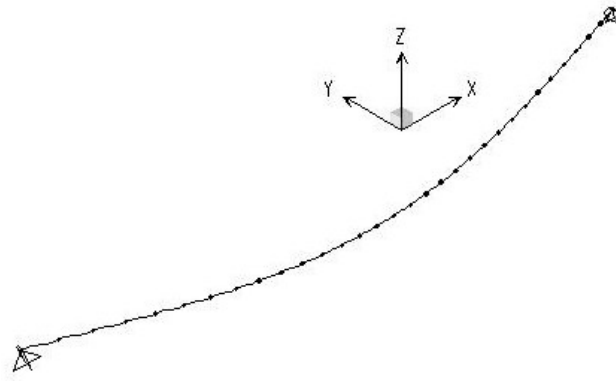


Figure 4.28: Second vibration mode of the steel I120 beam-column

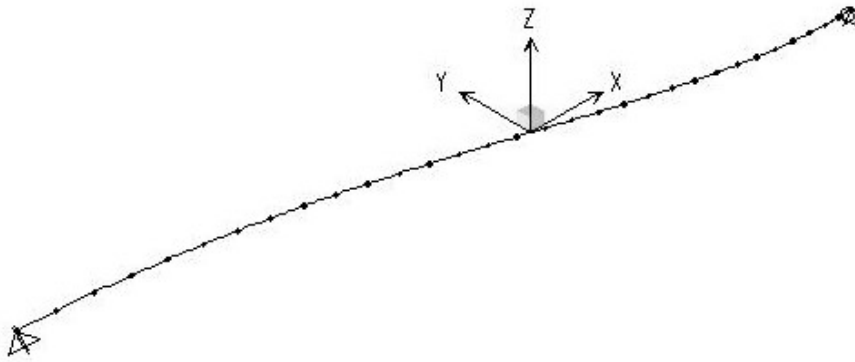


Figure 4.29: Third vibration mode of the steel I120 beam-column

The modal frequencies and participating mass ratios are given in Table 4.12 and Table 4.13, respectively.

Table 4.12. Analytical modal periods and frequencies of SAP2000 steel I120 beam-column model

MODE	PERIOD (TIME)	FREQUENCY (CYC/TIME)	FREQUENCY (RAD/TIME)	EIGENVALUE (RAD/TIME)**2
1	0.03019	33.125	208.13	4.33E+04
2	0.00158	635.03	3990.02	1.59E+07
3	0.00151	661.54	4156.56	1.73E+07

Table 4.13. Analytical modal participating mass ratios of SAP2000 steel I120 beam-column model

MODE	PERIOD	INDIVIDUAL MODE (PERCENT)			CUMULATIVE SUM (PERCENT)		
		UX	UY	UZ	UX	UY	UZ
1	0.03019	0.00	100.00	0.00	0.00	100.00	0.00
2	0.00158	0.00	0.00	83.62	0.00	100.00	83.62
3	0.00151	0.00	0.00	0.00	0.00	100.00	83.62

Comparison of the I120 Steel Column Results:

The all results are given in Table 4.14 and compared in Figure 4.30. Note that the spring constants in the analytical model is taken as 3500 kN/m and 1000 kN/m.

The correlation between the test results and the analytical pin ended results is given in Table 4.15.

Table 4.14. Comparison of I120 steel column test and analytical results

Load (kN)	Fundamental Vibration Frequency (Hz)				
	Test Results	Analytical Results			
		with springs	pin-ended	fix ended	SAP2000 model
14.42	33.0	40.36	37.09	86.78	33.12 (at "0" kN)
28.84	33.0	38.91	35.34	85.86	
43.26	32.2	37.41	33.49	84.94	
57.68	31.4	35.84	31.54	84.00	
72.89	30.2	34.12	29.34	83.00	
88.78	28.6	32.22	26.86	81.94	
103.20	27.0	30.39	24.38	80.97	
118.41	25.4	28.34	21.46	79.93	
132.83	24.6	26.25	18.27	78.93	

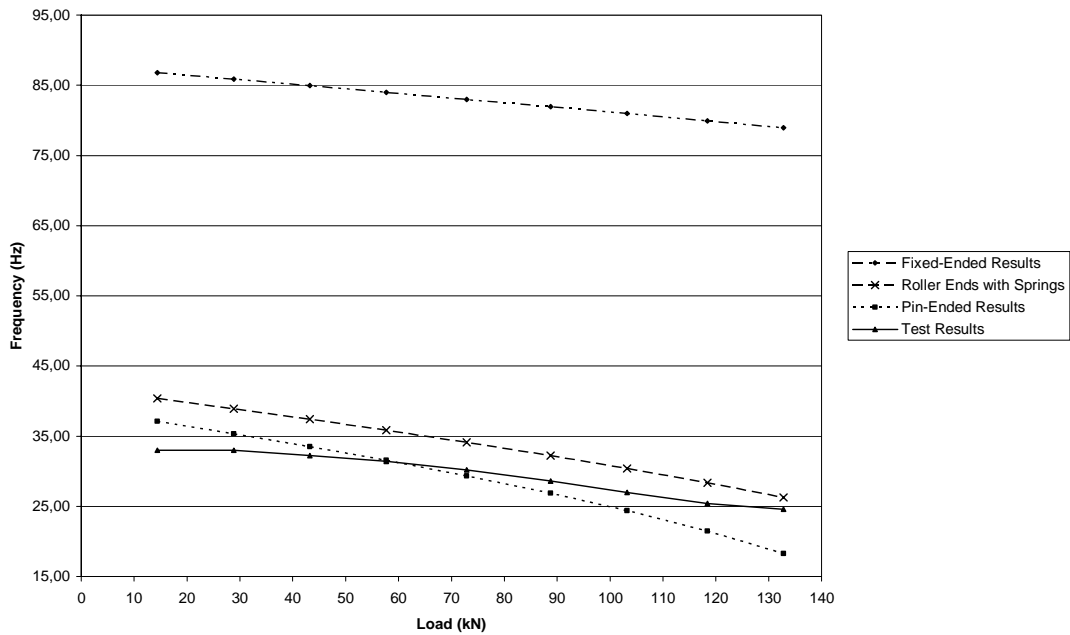


Figure 4.30: Comparison of I120 beam-column test and analytical solution results

Table 4.15. Correlation between the results of I120 steel column test

	Test Results	Pin-Ended Analytical Results
Test Results	1	
Pin-Ended Analytical Results	0,991	1

4.1.3. Full Size 24-Storey High Building Test:

A 24-storey high building without finishing is tested. An interior column (Figure 4.31), an exterior column (Figure 4.32) and an interior shearwall (Figure 4.33) are selected to test.



Figure 4.31. Interior column of the 24-storey high building

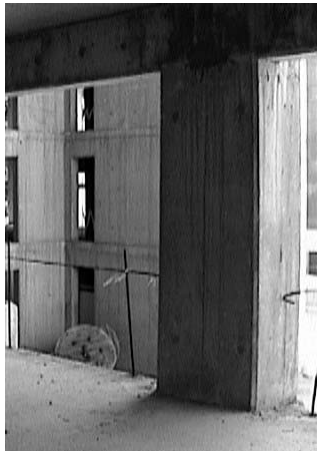


Figure 4.32. Exterior column of the 24-storey high building



Figure 4.33. Shearwall (interior) of the 24-storey high building

Reinforcement plan of the columns and the shearwall is given in Figure 4.34.

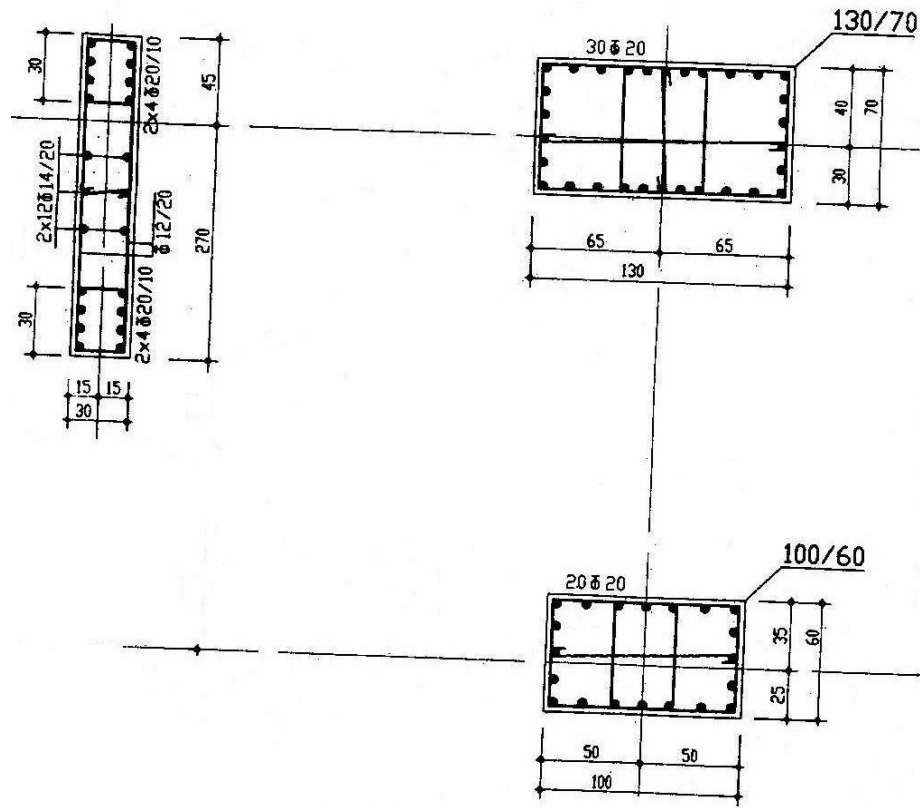


Figure 4.34: Typical reinforcement plan of the 24-storey high building

A typical floor plan is also given (Figure 4.36).

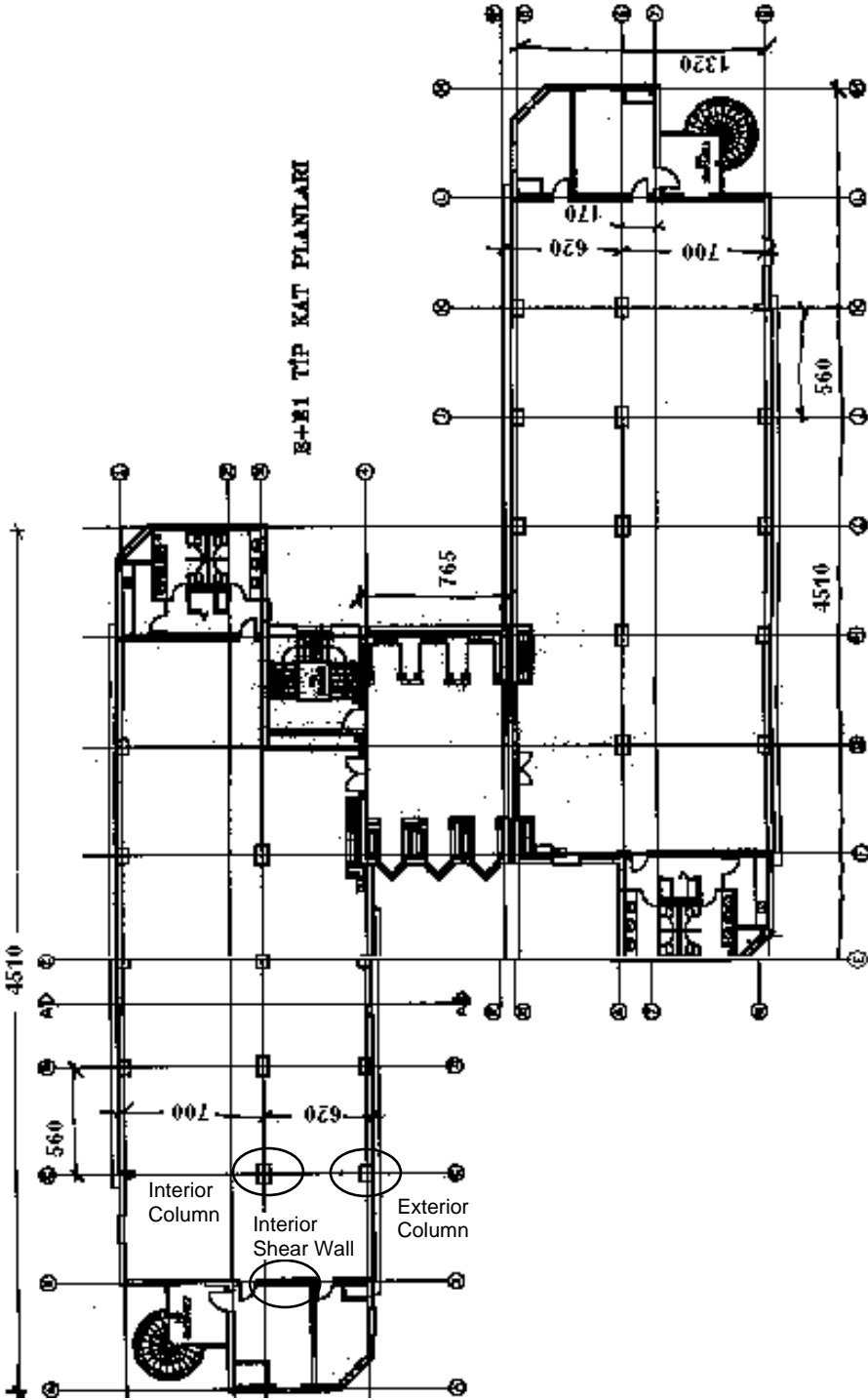


Figure 4.36: Typical floor plan of the 24-storey high building

Member properties and approximate axial load on the members of the full size 24-storey high building is given in Table 4.16.

Table 4.16. Member properties and axial load on the members of the full size 24-storey high building

	Interior Column	Exterior Column	Shearwall (interior)
Dimensions (cm)	130x70 cm	100x60 cm	315x30 cm
Braced Length (m)	3.60 m	3.18 m	2.40 m
Concrete class	C25	C25	C25
Tributary area (cm ²)	560 x 660	560x310	560x395
Floor weight (kN/m ²) (approximately)	21.6 kN/m ²	21.6 kN/m ²	21.6 kN/m ²
Specific gravity of reinforced concrete (kN/m ³) (approx.)	24.5 kN/m ³	24.5 kN/m ³	24.5 kN/m ³
Axial Load (kN) (approximately)			
Sixth Storey	16 054.2	7 862.3	10 354.5
Third Storey	18 715.0	9 162.9	12 064.8
First Storey	20 488.9	10 029.9	13 205.0

The axial load affecting the fundamental vibration frequency is calculated approximately using tributary area method. To illustrate, the calculation of the axial load on interior column at the third storey is given below.

$$\begin{aligned}
 N &= (5.6 \text{ m}).(6.6 \text{ m}).(21.6 \text{ kN/m}^2).(24-3) + (0.7 \text{ m}).(1.3 \text{ m}).(4 \text{ m}).(24.5 \text{ kN/m}^3).(24-3+1) \\
 &= 18 715.0 \text{ kN}
 \end{aligned}$$

The natural frequencies measured on the exterior column on 1st, 3rd and 6th storeys and corresponding analytical results are given in Table 4.17. Note that, in Turkey storey numbers start with ground floor (Z) and go on like 1,2,3.

Table 4.17. Measured fundamental frequencies and expected analytical frequencies of the full size 24-storey high building members

Storey Number	Interior Column	Exterior Column	Shear Wall (interior)
Measured Fundamental Frequencies (Hz)			
Sixth Storey	167.4	252.2 257.4	190.2
Third Storey	123.2 137.4	247.0 257.0 268.0	182.2 184.0
First Storey	117.6	251.0	182.4
Expected Analytical Fundamental Frequencies for Fixed Ends (Hz)			
Sixth Storey	190.05	208.87	183.04
Third Storey	189.97	208.81	182.94
First Storey	189.92	208.76	182.86

The beams on the exterior columns show different lay outs (i.e. at some storeys the beams are at the outer face of the column whereas at other storeys the beams are at the inner face of the column). Thus, the boundary condition of the exterior columns differs.

The fundamental frequencies computed from analytical simulations show deviations because of the boundary condition assessment. The lower and upper part of these members might be vibrating during the tests. Therefore, the length used in analytical computations may not be the same as the member length on corresponding floor.

Similar analytical computations are performed in order to find the required braced lengths for fixed-ended boundary condition in order to match the test results (Table 4.18, 4.19, and 4.20).

Table 4.18. Required braced lengths for fixed-ended boundary condition in order to match the test results for the interior column

Storey Number	Braced Length (fixed-fixed)	Vibration Frequency (Analytical)	Averages of Measured Frequencies
First Storey	4.57 m	117.76. Hz	117.6 Hz
Third Storey	4.34 m	130.55 Hz	130.3 Hz
Sixth Storey	3.83 m	167.73 Hz	167.4 Hz

Table 4.19. Required braced lengths for fixed-ended boundary condition in order to match the test results for the exterior column

Storey Number	Braced Length (fixed-fixed)	Vibration Frequency (Analytical)	Averages of Measured Frequencies
First Storey	2.90 m	251.12. Hz	251.0 Hz
Third Storey	2.87 m	256.45 Hz	257.3 Hz
Sixth Storey	2.88 m	254.74 Hz	254.8 Hz

Table 4.20. Required braced lengths for fixed-ended boundary condition in order to match the test results for the interior shear wall

Storey Number	Braced Length (fixed-fixed)	Vibration Frequency (Analytical)	Averages of Measured Frequencies
First Storey	2.40 m	186.63 Hz	182.4 Hz
Third Storey	2.42 m	183.62 Hz	183.3 Hz
Sixth Storey	2.38 m	189.98 Hz	190.2 Hz

In addition to transverse vibration technique, following ultrasonic methods are applied to estimate the axial load on the structural members.

4.2. Ultrasonic Pulse Velocity Measurement During a Standard Cylinder Compression Test:

In order to test the effect of stress on ultrasonic pulse velocity, standard cylinders (30 cm high and 15 cm in diameter) are prepared in concrete classes C12, C16 and C20 (represented by BS in Turkish Standards). The properties of the cylinders are given in Table 4.21.

Table 4.21. Properties of the standard cylinders for ultrasonic tests

Concrete class	C12 (BS12)	C16 (BS16)	C20 (BS20)
Maximum aggregate size	30 mm	30 mm	30 mm
Slump	75-100 mm	75-100 mm	75-100 mm
Water/Cement ratio	0.80	0.65	0.60
Weight	124.6 N	124.6 N	124.6 N
Estimated modulus of elasticity	18 500 MPa	20 500 Mpa	22 500 MPa
Estimated 28-days load capacity	208 kN	278 kN	347 kN

The ultrasonic wave velocities in cylinders are measured in parallel and perpendicular directions to the applied axial load. The ultrasonic pulse velocity is measured three times in each direction at each incremental load.

The setup prepared together with the laboratory personnel is shown in Figure 4.37. A closer view of the test cylinder instrumentation is given in Figure 4.38.

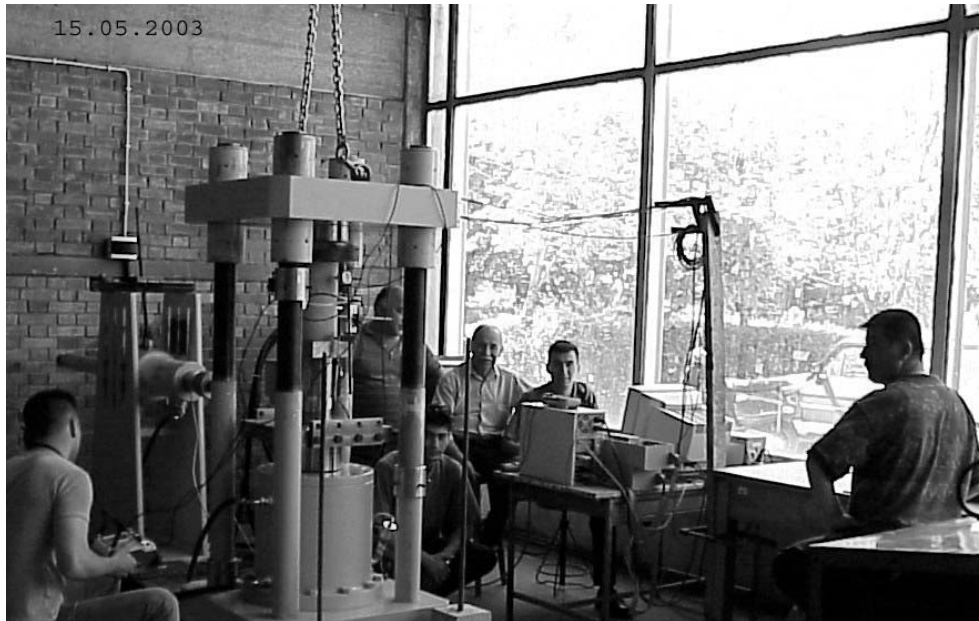


Figure 4.37: Cylinder tests setup

“TICO Ultrasonic Instrument” is used during the tests to measure the ultrasonic pulse velocity. A detailed information about the device (TICO) is given in Appendix B. TICO sends ultrasonic pulse three times per second. During these tests, relationships between the axial load and pulse velocity are investigated. Several test rounds are conducted to try different specimens, transducer orientation, and couplants.

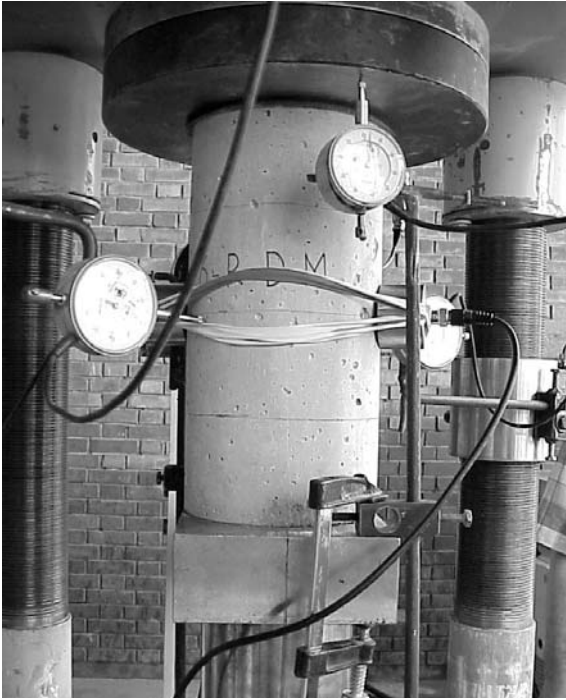


Figure 4.38: Closer view of the cylinder test setup

The change in ultrasonic pulse velocity is defined as the ratio of the initial velocity.

$$\text{Ultrasonic Pulse Velocity Ratio (\%)} = V \cdot 100 / V_0 \quad (4.3)$$

where “V” is the velocity at an arbitrary stress, and “V₀” is the initial velocity at the natural state (i.e. zero stress).

Test 1:

The properties of the test cylinder is given in the Table 4.22. The transducers were placed on concrete surface using rubber bands (Figure 4.38).

Table 4.22. Properties of cylinder for ultrasonic test no 1

Concrete composition	: C12
Curing condition	: Water cured
Age	: 28 days
The testing apparatus	: TICO ultrasonic instrument
Arrangement of the transducers	: Direct measurement
Properties of the concrete surface	: Smoothened for transducer contact
Path length	: ~15 cm
Visual observations	: Normal

The first test using pulse velocity measurement method in transverse direction showed large change in pulse velocity under changing axial load (Figure 4.39). There is 18.8% decrease in the pulse velocity beyond the 88.8% of the ultimate strength (79.5 % of the crushing strain). The crushing strain is 0.0015.

However, it is seen that the change in pulse velocity was largely affected by the couplant (gel) amount used between the concrete and the instruments. As a sensitivity check, the same transverse pulse velocity test is carried out without applying axial load.

Test 2:

When the ultrasonic pulse velocity was measured in unstressed state, there were still changes in velocity values in time. The concrete specimen had a dry surface which started to soak the water based gel as a function of time. The transducers were fixed throughout the test after the gel is applied. The change in the ultrasonic pulse velocity is given in percentage as a function of time in Figure 4.40.

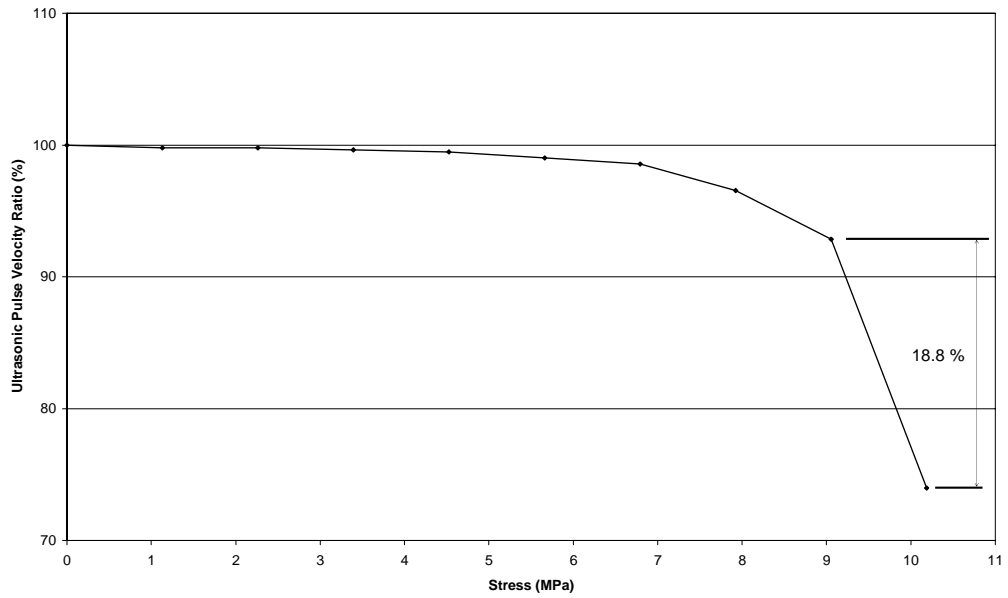


Figure 4.39: Ultrasonic pulse velocity reduction measured perpendicular to the load under axial compression

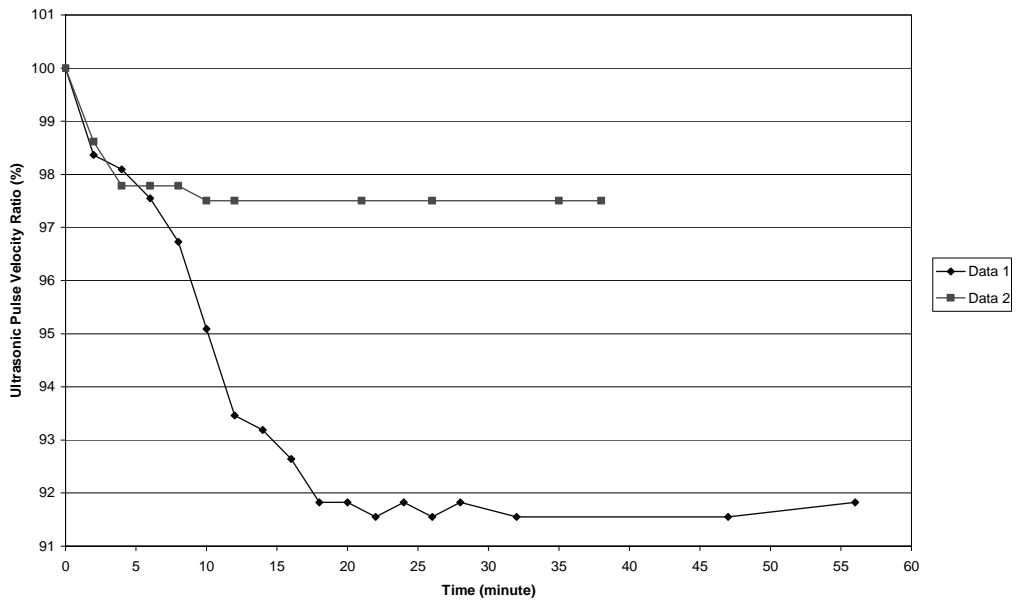


Figure 4.40: Time versus ultrasonic pulse velocity ratio in unstressed case

Another test (Test 3) is conducted to see the gel application effect under application of load.

Test 3:

C16 type concrete cylinder is used for the second test. Pulse velocity is measured perpendicular to the loading direction similar to the first test. The cylinder specimen was dry and 28-days old. Initial velocity was measured as 3990 m/s. The test result is given in Figure 4.41.

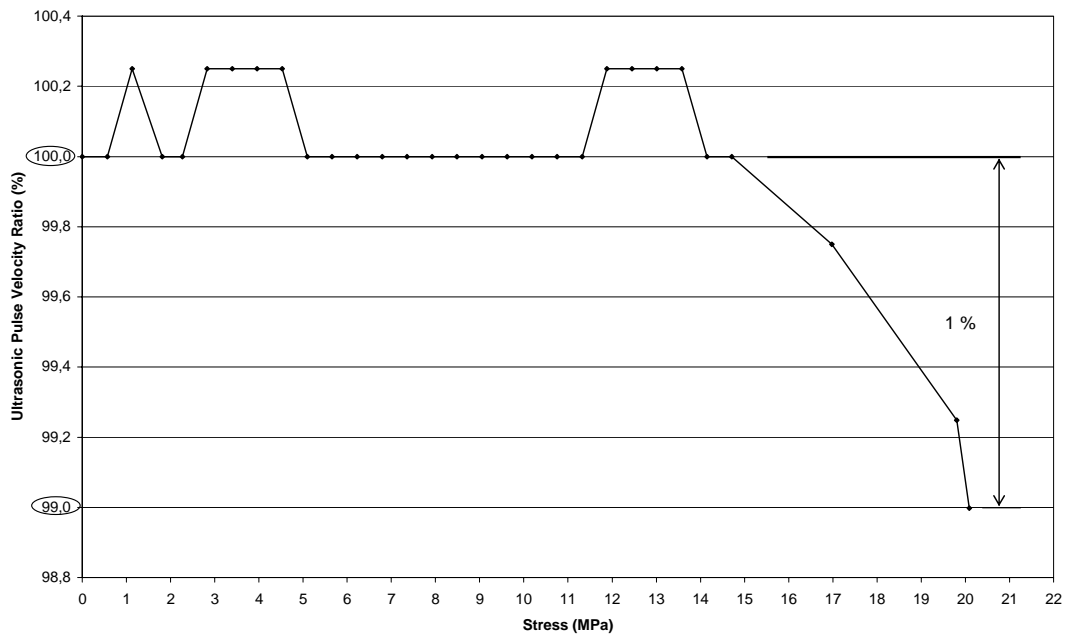


Figure 4.41: The ultrasonic pulse velocity ratio versus stress in perpendicular direction on C16 standard cylinder

As the couplant is properly applied, the pulse velocity (in perpendicular direction to the loading) remained fairly constant up to 70 % of the crushing stress (20.1 MPa).

Test 4:

C16 type concrete cylinder is used for the fourth test. Pulse velocity is measured both parallel and perpendicular to the loading direction. The cylinder was saturated (48 hours waited in water before testing) and 28-days old. The initial velocities were measured about 4450 m/s in perpendicular direction and 3245 m/s in parallel direction. There was unloading and loading at 11.3 MPa and 19.8 MPa. The result of perpendicular and parallel direction is given in Figure 4.42 and Figure 4.43, respectively.

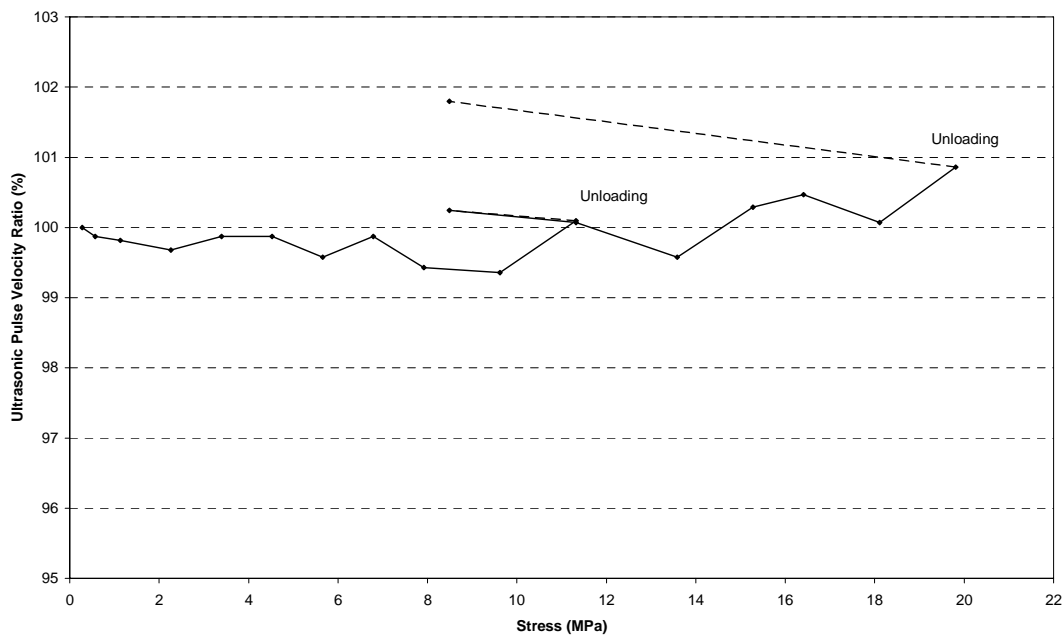


Figure 4.42: The ultrasonic pulse velocity ratio versus stress in perpendicular direction on C16 standard cylinder

In parallel direction the first high decrement is due to the contact achievement between the steel plates of the testing instrument and the concrete cylinder specimen.

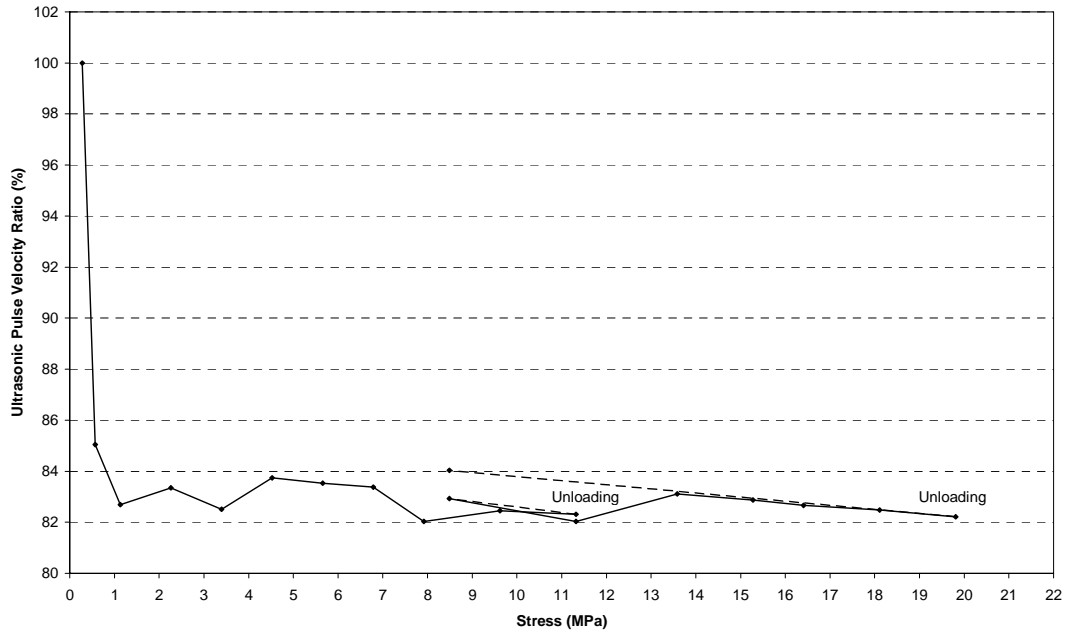


Figure 4.43: The ultrasonic pulse velocity ratio versus stress in parallel direction on C16 standard cylinder

Test 5:

A new series of cylinders were tested using “honey” as couplant. The relation between stress on the cylinders and ultrasonic pulse velocity ratio of 6 cylinders is given in Figure 4.44.

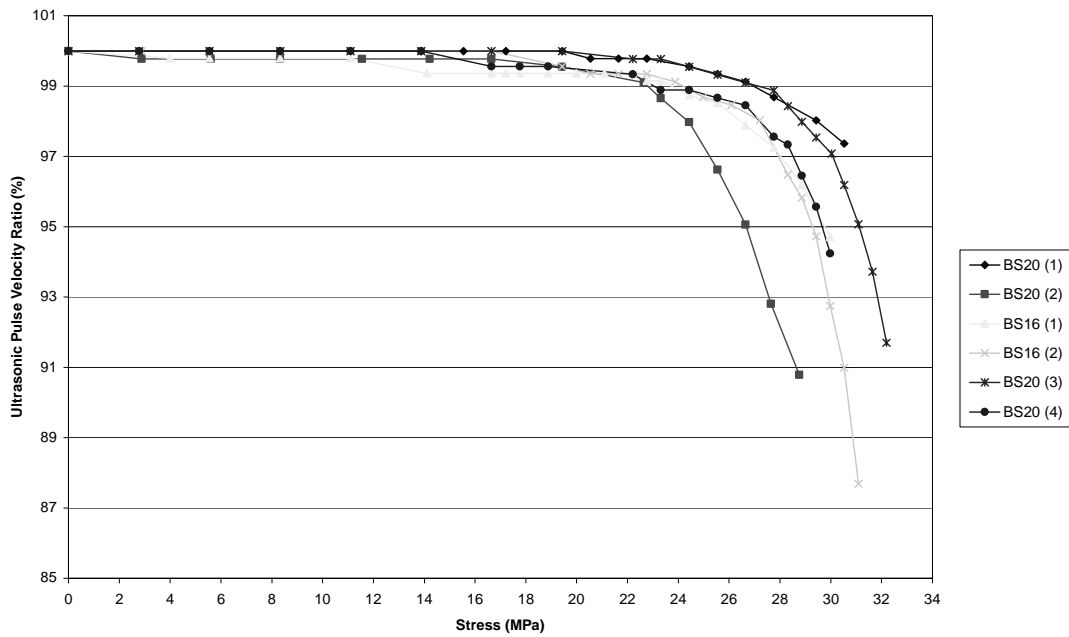


Figure 4.44: The relation between stress on the cylinders and ultrasonic pulse velocity ratio

The relation between strain and ultrasonic pulse velocity ratio of 5 cylinders is given in Figure 4.45.

A logarithmic relationship is searched between strain and ultrasonic pulse velocity ratio as described in Equation (4.4). The constants “a” and “b” are given in Table 4.23.

$$\frac{V}{V_0} \cdot 100 = 100 - a \cdot e^{b \cdot \epsilon} \quad (4.4)$$

where,

V: ultrasonic pulse velocity at an arbitrary stress

V₀: V: ultrasonic pulse velocity at unstressed state

a,b: arbitrary constants

e: exponential function

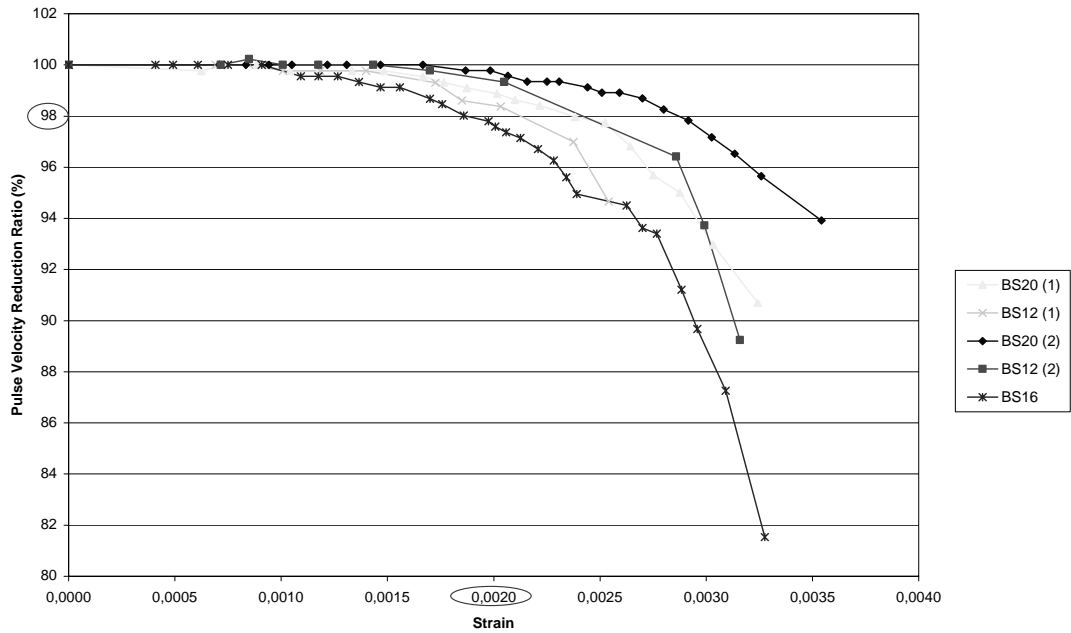


Figure 4.45: The relation between strain and ultrasonic pulse velocity ratio

Table 4.23. Constants of the logarithmic relationship between strain and ultrasonic pulse velocity

Test No	Concrete Class	f_{ck} (MPa)	a	b
1	BS12	23,3	0,01286	2355,78
2	BS12	23,9	0,00021	3432,45
3	BS16	32,0	0,07521	1668,43
4	BS20	32,8	0,01200	2078,53
5	BS20	36,1	0,01371	1736,62

It seems there is no apparent relationship between ultrasonic pulse velocity and loading. This may be due to the chance that the first wave reaching the other edge of the specimen travels through an uncracked path (similar to the unstressed case).

Because of the inconveniences associated with the changing gel property and inconsistencies in the decrement of the pulse velocity, waveform and frequency content of the ultrasound waves is examined in order to find a relationship with the loading. Scattering of the wave due to crack formations will definitely change the waveforms.

4.3. Waveform and Frequency Evaluation of Transmitted Ultrasound Wave during an Axial Compression Test of a Concrete Cylinder:

The changes in the waveform in time and frequency domain are explored to estimate the load level. The time space can also be used to calculate the time of flight to compute the ultrasonic pulse velocity. The time of flight can be determined as the time when the amplitude of the first point of the signal reaches a fixed preset threshold (3% of first cycle peak amplitude) [17].

Ultrasonic waveforms are recorded from the tests of two standard cylinder specimens cast in concrete class C12 (Figure 4.46) using the digital storage oscilloscope Gould DataSys 740 with 150 MHz sampling rate. The signals are recorded and Fast Fourier Transforms (FFT) are taken to see scattering and frequency content in the ultrasonic waves.

Test 1:

The cylinder is loaded until 10 kN at the initial state in order to achieve good contact between the steel plates and the specimen. Other waveforms are obtained at the load level of 100 kN. Test results are given in Figure 4.47, Figure 4.48 and Figure 4.49.

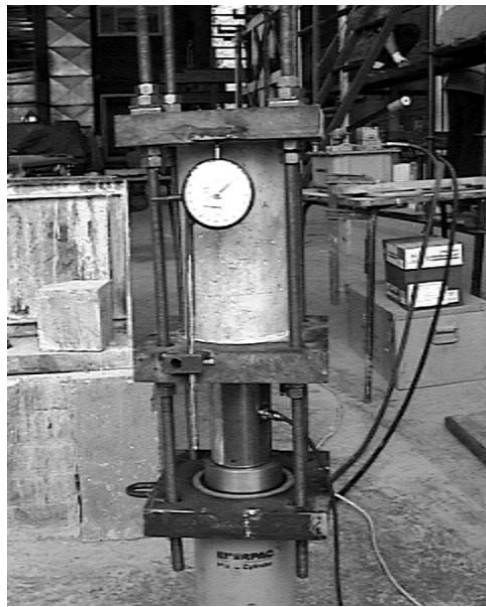


Figure 4.46: The loading setup of the C12 standard cylinder for waveform evaluation

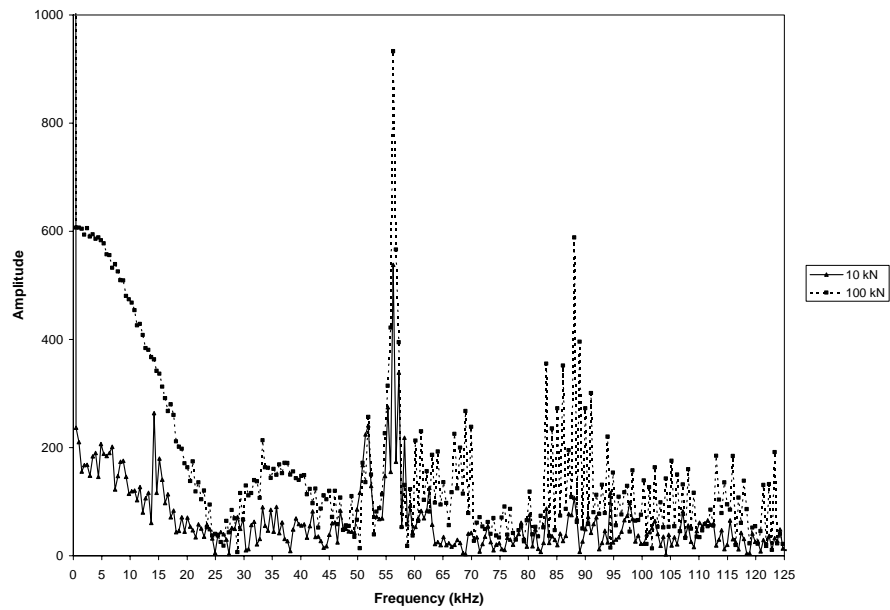


Figure 4.47: The frequency content of ultrasonic waves measured directly across 15 cm

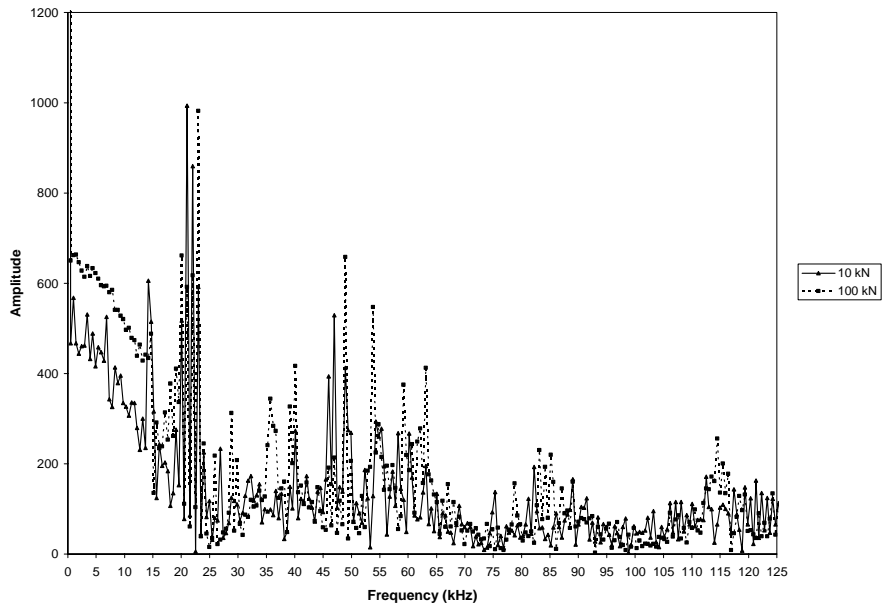


Figure 4.48: The frequency content of the ultrasonic waves measured directly across 30 cm

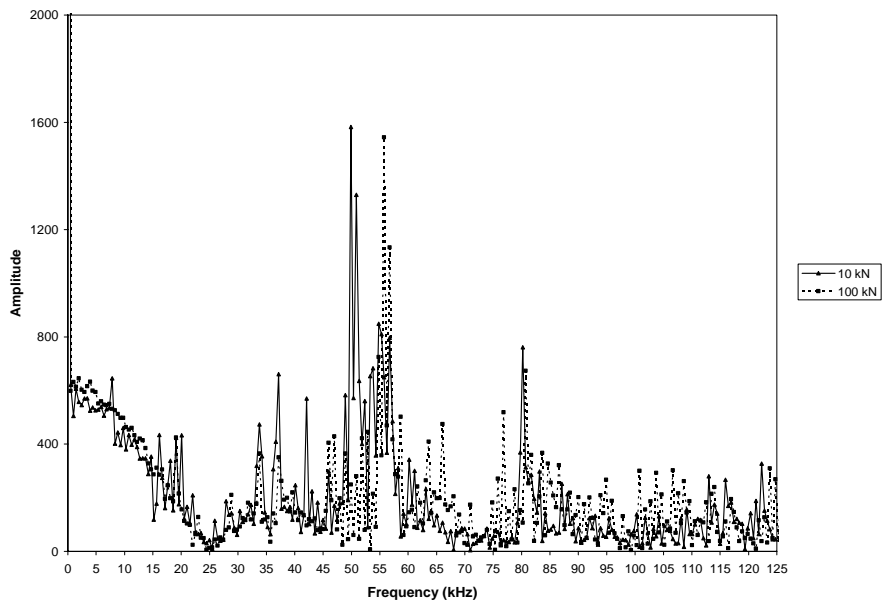


Figure 4.49: The frequency content of the ultrasonic waves measured indirectly across 30 cm

One load increment has not yield much information about the changes. Another test is conducted with more load increments in order to see the changes more clearly.

Test 2:

Further experiment with nine increment steps in load is conducted to observe the relationship between the frequency change and the increase in load. The load increments are given as “turn” instead of “kN” because the cylinder is loaded by turning the bolts (Figure 4.46) manually in nine steps. The relation between the number of turns and the strain is given in Figure 4.50.

In order to increase the resolution the results are given in three windows as 0-42, 42-84, 84-125 kHz. Figure 4.51, Figure 4.52, and Figure 4.53 gives the results of the measurement done across 15 cm directly.

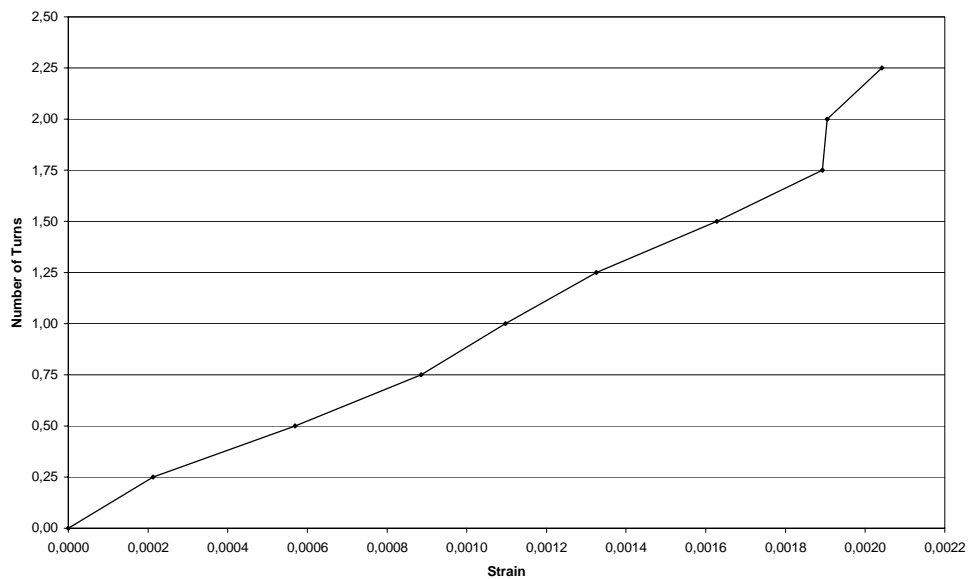


Figure 4.50: The relation between the number of turns and the strain

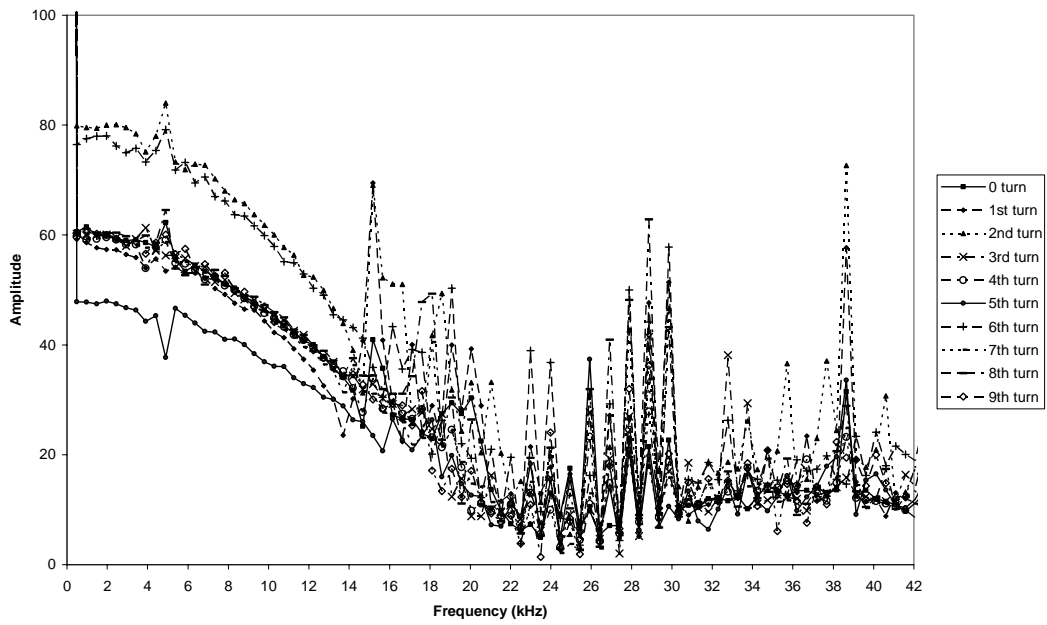


Figure 4.51: Frequency versus load levels in direct measurement across 15 cm between 0-42 kHz

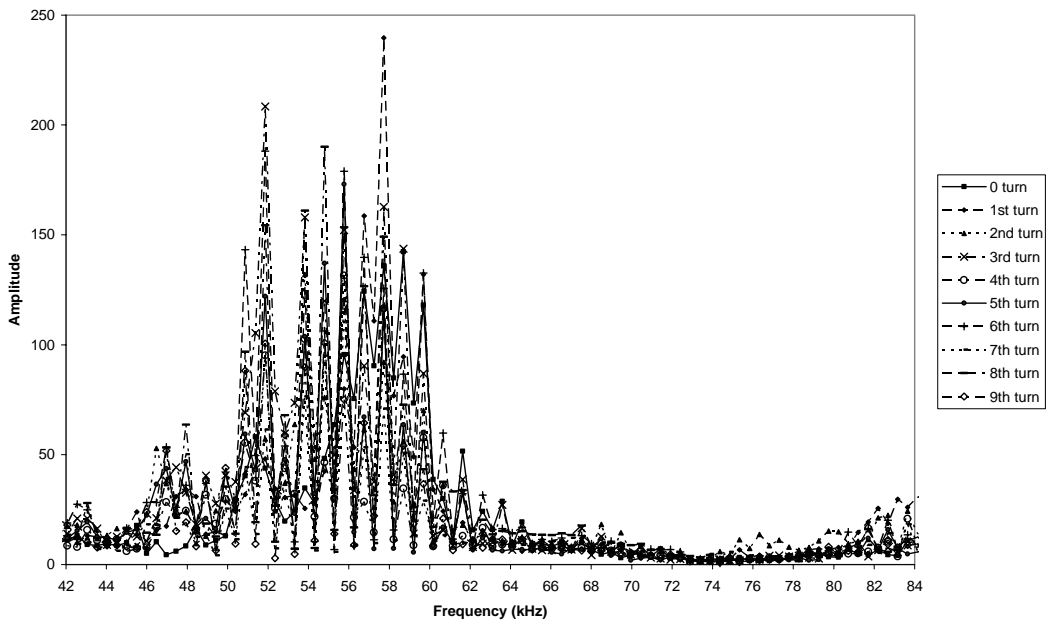


Figure 4.52: Frequency versus load levels in direct measurement across 15 cm between 42-84 kHz

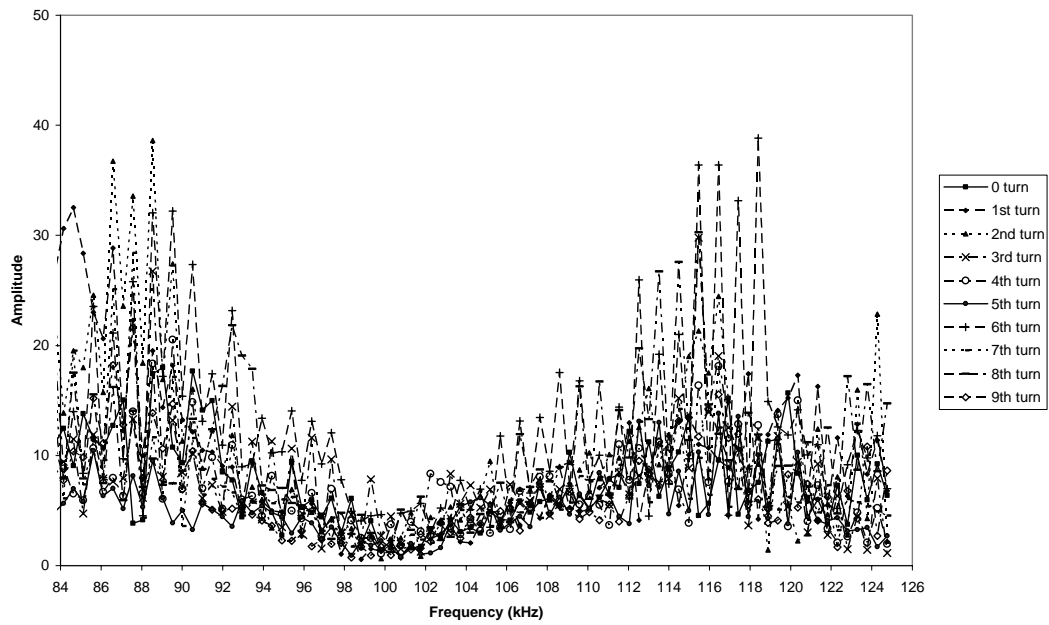


Figure 4.53: Frequency versus load levels in direct measurement
across 15 cm between 84-125 kHz

The results of the direct measurement across 30 cm are given in Figure 4.54,
Figure 4.55, and Figure 4.56.

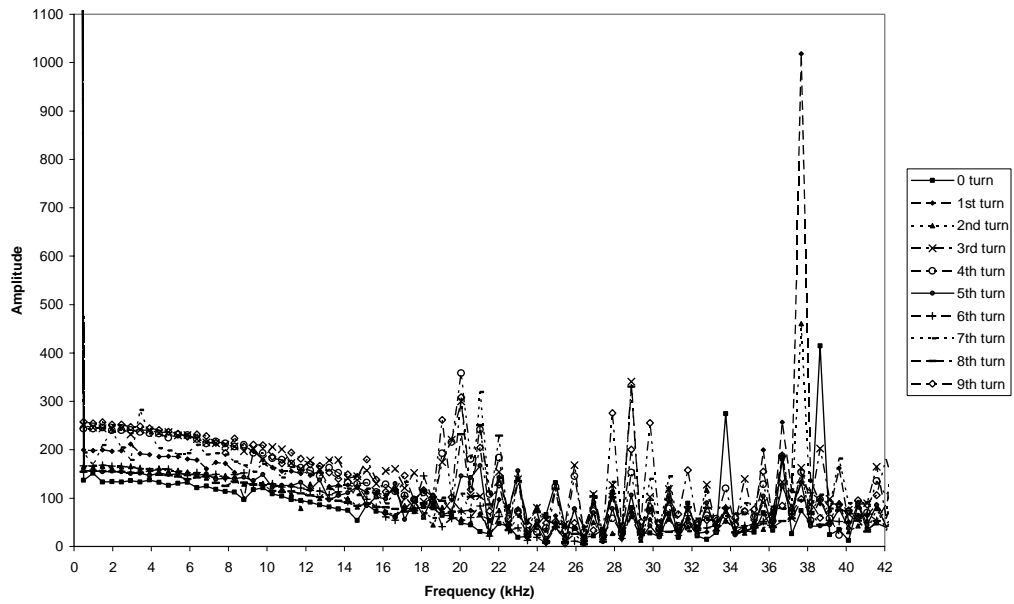


Figure 4.54: Frequency versus load levels in direct measurement across 30 cm between 0-42 kHz

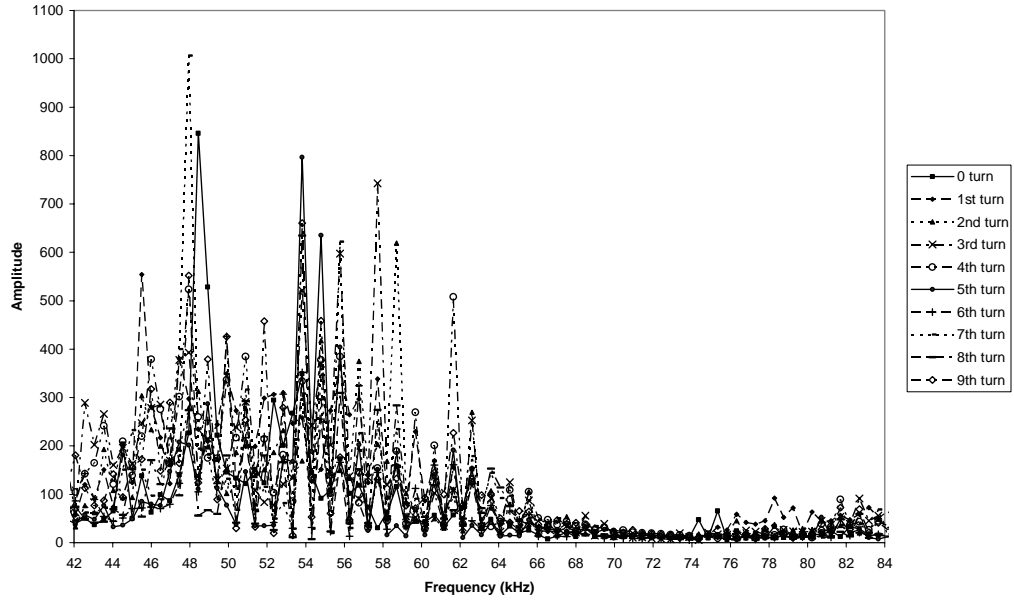


Figure 4.55: Frequency versus load levels in direct measurement across 30 cm between 42-84 kHz

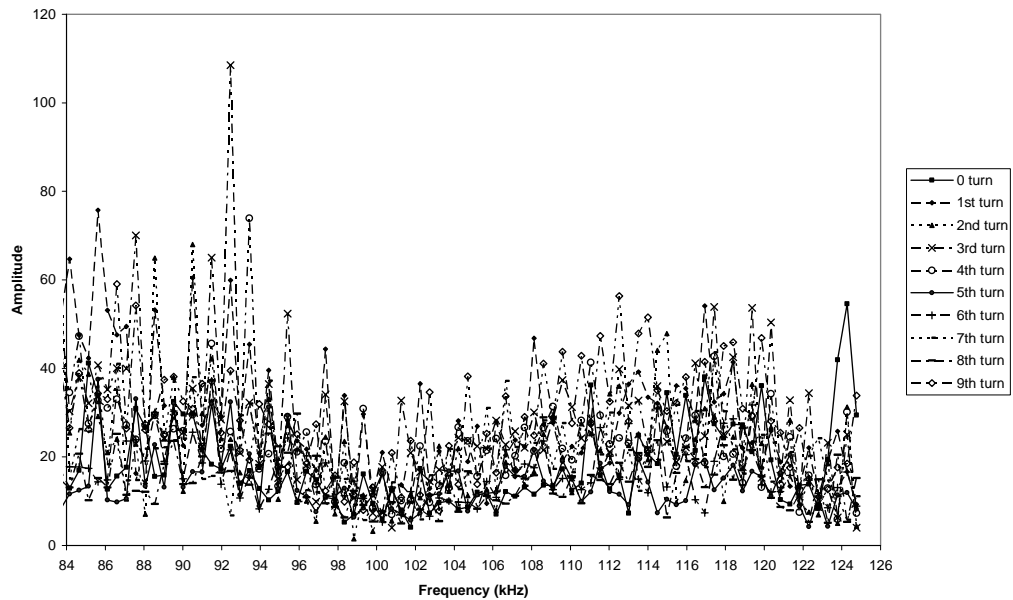


Figure 4.56: Frequency versus load levels in direct measurement across 30 cm between 84-125 kHz

In the second test, where more load increments are performed, the results have showed that the relationship between the frequency of dominant ultrasound waves and the loading is complex. A 3D surface graph is plotted to see changes more clearly (Figure 4.57 and 4.58).

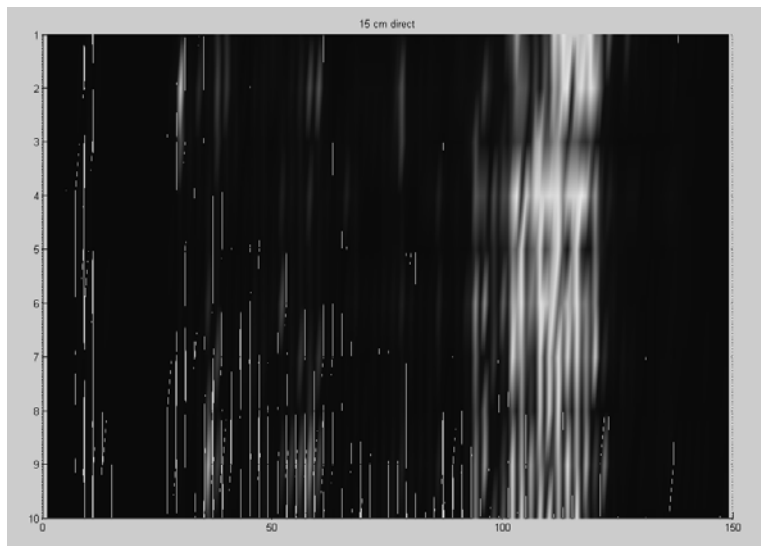


Figure 4.57: 3D surface plot of the two times of frequencies measured directly across 15 cm

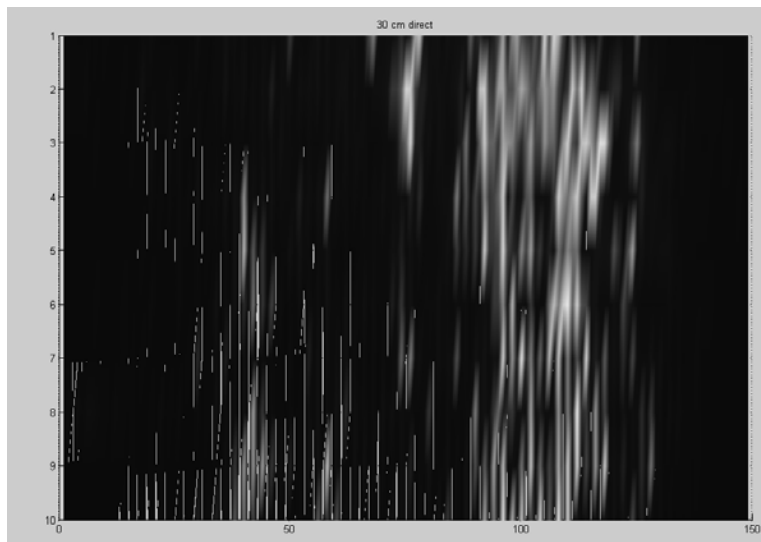


Figure 4.58: 3D surface plot of the two times of frequencies measured directly across 30 cm

When a closer view to the 3D surface plot of the frequencies measured across 15 cm is taken, there seems to be decrease in the frequency around 5 kHz in 15 cm direction (Figure 4.59).

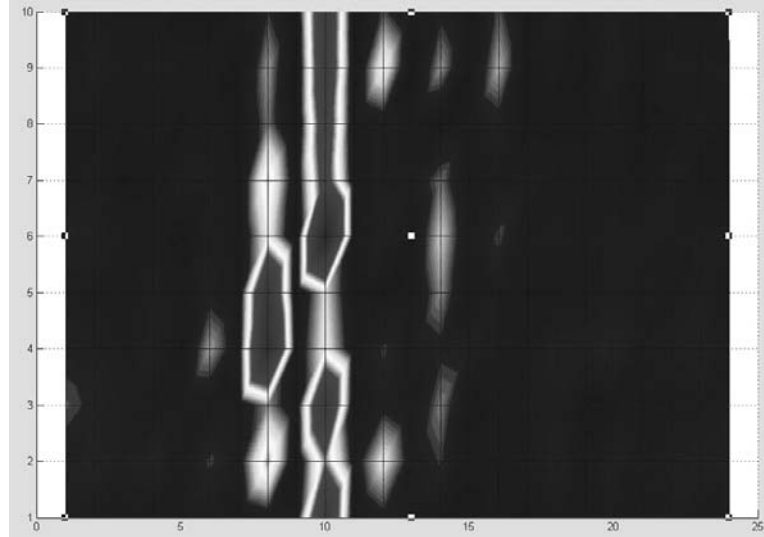


Figure 4.59: Closer view to the 3D surface plot of the two times of frequencies measured across 15 cm

SAP2000 Nonlinear (version 7.12) modelling is done (Figure 4.60) in order to check the vibration frequencies around 5 kHz.

It is seen that fourth vibration mode has frequency of 5,2 kHz (Figure 4.61 and Table 4.24). 1kHz wave generation might have created resonance. During the test, standard concrete cylinder (15x30 cm), four steel rods with 2 cm diameter, and two steel plates (25x25x3 cm) are used.

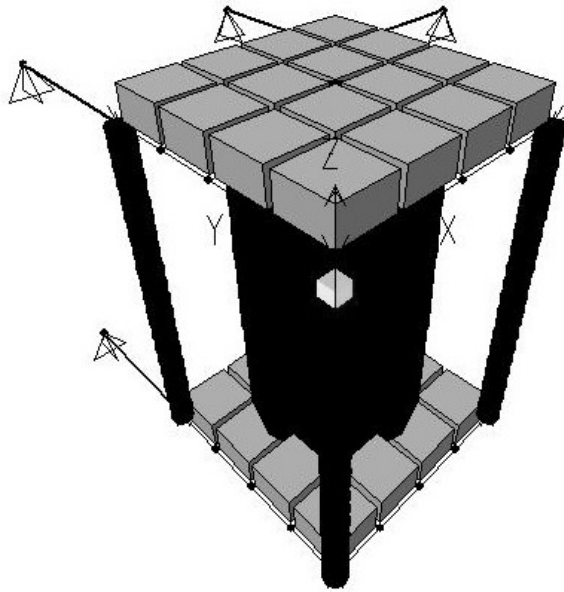


Figure 4.60: SAP2000 model of the standard cylinder

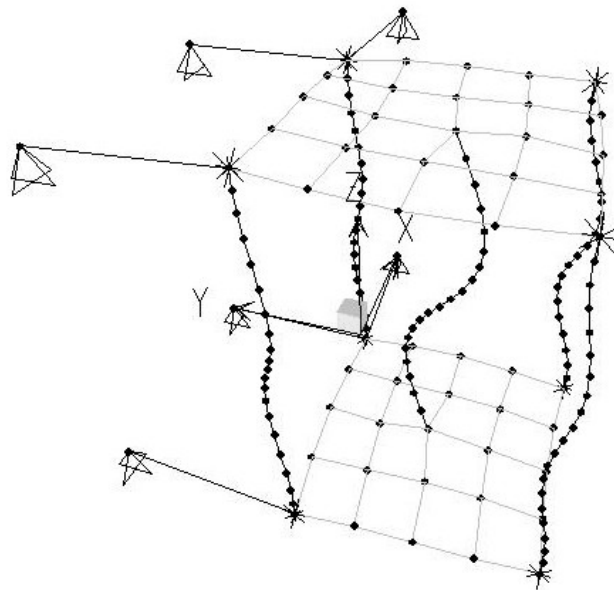


Figure 4.61: Fourty third vibration mode of the standard cylinder

Table 4.24. Analytical modal periods and frequencies of SAP2000 model of the standard cylinder

MODE	PERIOD (TIME)	FREQUENCY (CYC/TIME)	FREQUENCY (RAD/TIME)	EIGENVALUE (RAD/TIME)**2
1	0,081355	12,292	77,232	5,96E+03
5	0,002419	413,358	2597,206	6,75E+06
10	0,001022	978,441	6147,727	3,78E+07
15	0,000876	1141,200	7170,373	5,14E+07
20	0,000383	2610,486	16402,167	2,69E+08
25	0,000363	2756,058	17316,820	3,00E+08
30	0,000263	3801,968	23888,468	5,71E+08
35	0,000205	4879,936	30661,545	9,40E+08
40	0,000199	5024,860	31572,125	9,97E+08
43	0,000194	5159,640	32418,975	1,05E+09
44	0,000178	5616,202	35287,639	1,25E+09

After the 3D surface plots, regression analysis is performed in measurement across 15 cm in order to see if there is any relationship between load level on the specimen and correlation factor (R) of the vibration frequencies (Table 4.25). 3D surface plot of the correlation factor (R) of the vibration frequencies of the cylinder for different load levels is given in Figure 4.62.

Table 4.25. Correlation factor (R) of the vibration frequencies of the cylinder for different load levels in measurement across 15 cm

1	0,8831	0,8091	0,8440	0,8395	0,7918	0,7883	0,7861	0,7955	0,7960
0,8831	1	0,8435	0,8176	0,8242	0,8088	0,7647	0,8099	0,7760	0,8143
0,8091	0,8435	1	0,8475	0,8652	0,8375	0,7491	0,8443	0,7564	0,8301
0,8440	0,8176	0,8475	1	0,9188	0,9011	0,8347	0,8247	0,8002	0,8110
0,8395	0,8242	0,8652	0,9188	1	0,9001	0,8765	0,8913	0,8446	0,8630
0,7918	0,8088	0,8375	0,9011	0,9001	1	0,8494	0,8778	0,8399	0,8641
0,7883	0,7647	0,7491	0,8347	0,8765	0,8494	1	0,8899	0,8802	0,8605
0,7861	0,8099	0,8443	0,8247	0,8913	0,8778	0,8899	1	0,8973	0,9227
0,7955	0,7760	0,7564	0,8002	0,8446	0,8399	0,8802	0,8973	1	0,8876
0,7960	0,8143	0,8301	0,8110	0,8630	0,8641	0,8605	0,9227	0,8876	1

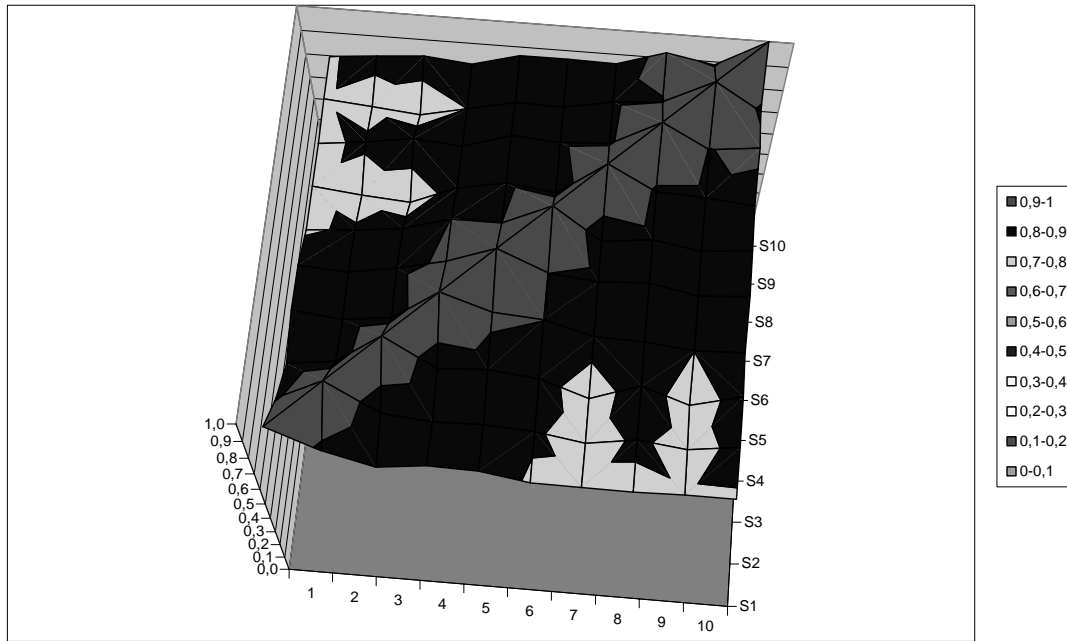


Figure. 4.62: 3D surface plot of the correlation factor (R) of the cylinder vibration frequencies for different load levels across 15 cm

Across 30, direct and indirect, the relationship between the load level on the specimen and the correlation factor (R) of the vibration frequencies are given in Table 4.26 and Table 4.27, respectively. 3D surface plot of the correlation factor (R) of the vibration frequencies of the cylinder for different load levels is given in Figure 4.63 and Figure 4.64.

The estimated relationship between the number of turns and the load level is given in Figure 4.65 by using the Hognestad [24] stress-strain curve model for concrete. Therefore, the load level on a new specimen can be estimated from its correlation coefficient by entering to the charts.

Table 4.26. Correlation factor (R) of the vibration frequencies of the cylinder for different load levels in direct measurement across 30 cm

1	0,8121	0,8010	0,7682	0,7851	0,7585	0,7695	0,7297	0,6950	0,7183
0,8121	1	0,8779	0,8540	0,8355	0,7914	0,8046	0,7671	0,7339	0,7273
0,8010	0,8779	1	0,8704	0,8532	0,8004	0,8088	0,8081	0,7616	0,7528
0,7682	0,8540	0,8704	1	0,9065	0,8547	0,8288	0,8327	0,8030	0,8059
0,7851	0,8355	0,8532	0,9065	1	0,8741	0,8730	0,8683	0,8396	0,8476
0,7585	0,7914	0,8004	0,8547	0,8741	1	0,8482	0,8344	0,8288	0,8255
0,7695	0,8046	0,8088	0,8288	0,8730	0,8482	1	0,8905	0,8772	0,8894
0,7297	0,7671	0,8081	0,8327	0,8683	0,8344	0,8905	1	0,8968	0,8891
0,6950	0,7339	0,7616	0,8030	0,8396	0,8288	0,8772	0,8968	1	0,9041
0,7183	0,7273	0,7528	0,8059	0,8476	0,8255	0,8894	0,8891	0,9041	1

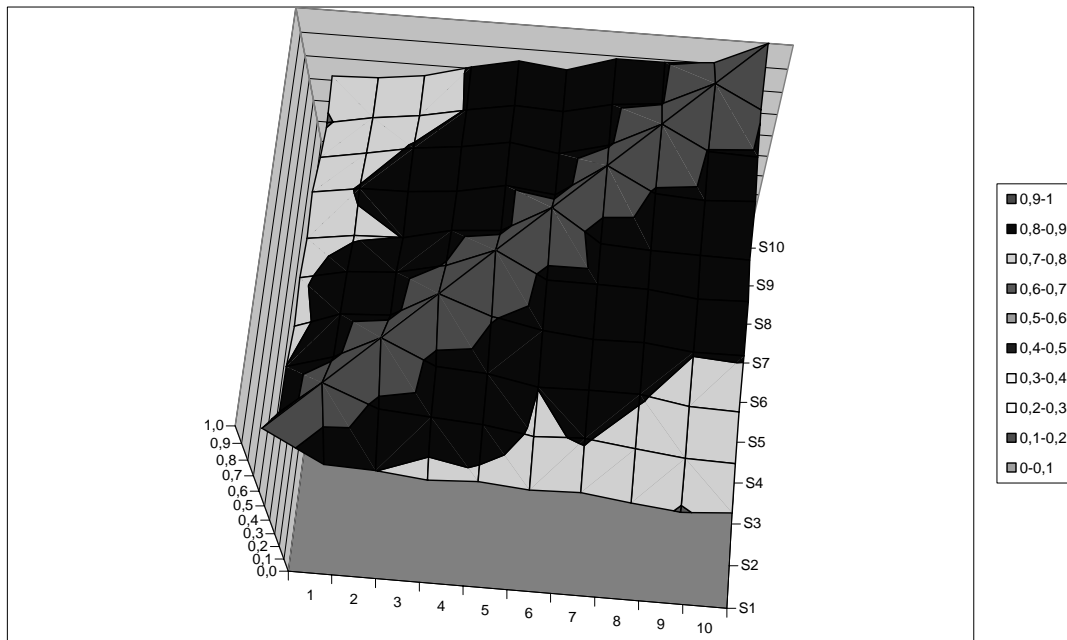


Figure. 4.63: 3D surface plot of the correlation factor (R) of the cylinder vibration frequencies for different load levels directly measured across 30 cm

Table 4.27. Correlation factor (R) of the vibration frequencies of the cylinder for different load levels in indirect measurement across 30 cm

1	0,7739	0,7243	0,7623	0,7901	0,7318	0,6473	0,6992	0,6219	0,6943
0,7739	1	0,8444	0,8541	0,8422	0,8042	0,7022	0,7259	0,7301	0,7469
0,7243	0,8444	1	0,8532	0,8414	0,8209	0,7458	0,7632	0,7611	0,7856
0,7623	0,8541	0,8532	1	0,8679	0,8513	0,7899	0,7689	0,7874	0,8133
0,7901	0,8422	0,8414	0,8679	1	0,8475	0,8080	0,8057	0,7793	0,8080
0,7318	0,8042	0,8209	0,8513	0,8475	1	0,8103	0,8371	0,7772	0,8111
0,6473	0,7022	0,7458	0,7899	0,8080	0,8103	1	0,8000	0,7991	0,7794
0,6992	0,7259	0,7632	0,7689	0,8057	0,8371	0,8000	1	0,8338	0,8341
0,6219	0,7301	0,7611	0,7874	0,7793	0,7772	0,7991	0,8338	1	0,8824
0,6943	0,7469	0,7856	0,8133	0,8080	0,8111	0,7794	0,8341	0,8824	1

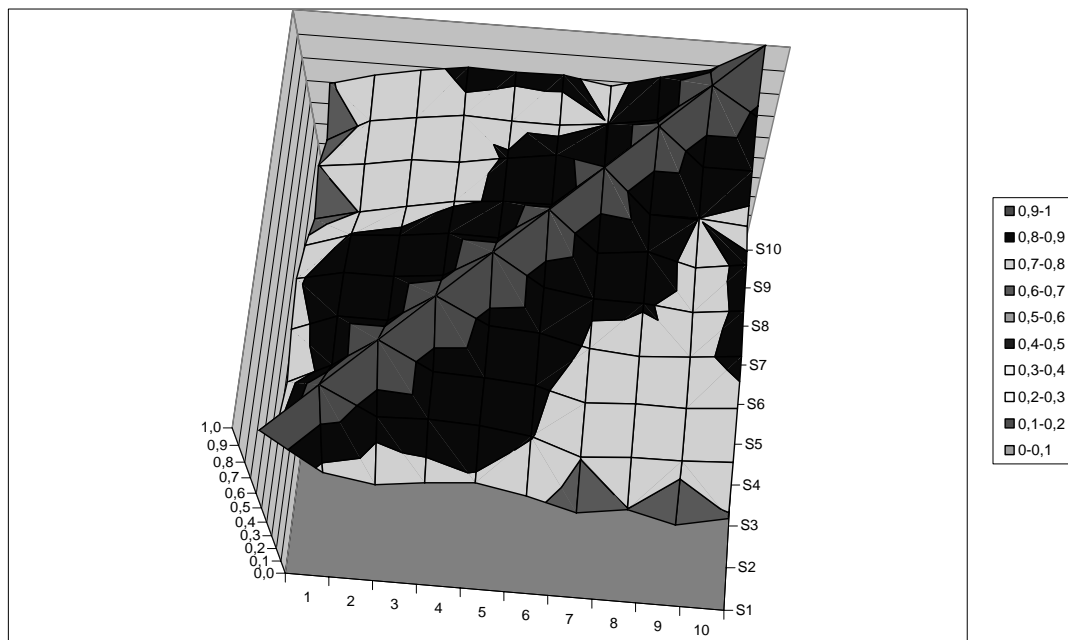


Figure. 4.64: 3D surface plot of the correlation factor (R) of the cylinder vibration frequencies for different load levels indirectly measured across 30 cm

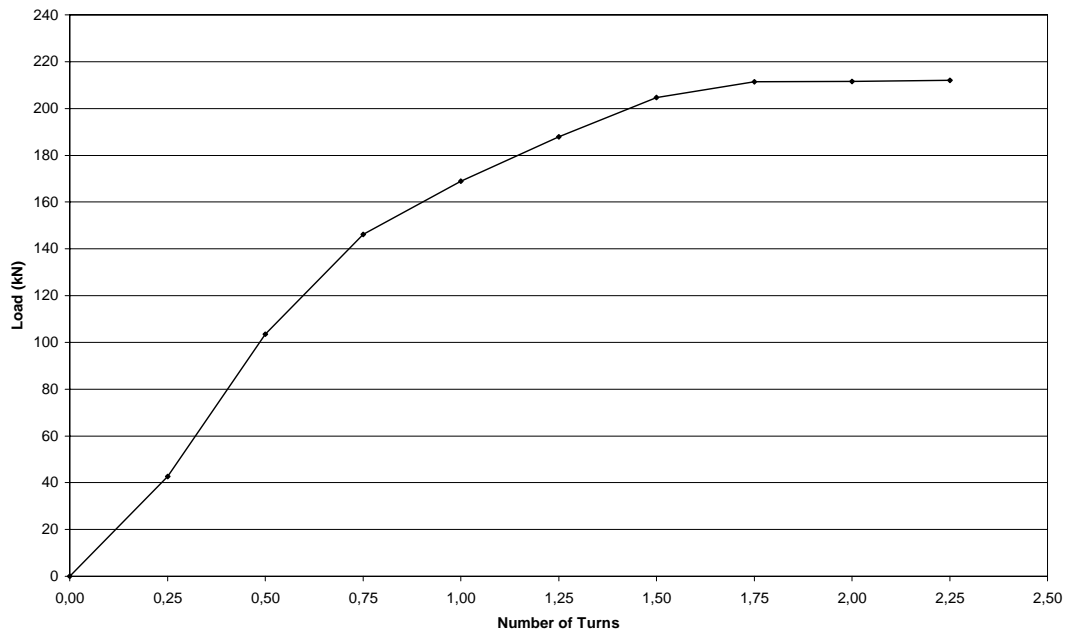


Figure 4.65: Number of turns versus load level

CHAPTER 5

DISCUSSION OF RESULTS AND CONCLUSION

This thesis aims to investigate alternative ways to measure the level of axial compressive load on structural members without an initial reference point and in a non-destructive way. Measurement of axial load level in a structural member would yield better understanding of the behavior of an existing structural system (such as degradation and load redistribution).

Both experimental and analytical studies are conducted throughout the thesis work. *Transverse vibration technique* is investigated and applied to a number of structural systems including 1) 9x91x151 cm shear wall specimen, 2) 160 cm long I120 steel column, and 3) members of a 24-storey high reinforced concrete building on three different floors (two columns and one shear wall on each floor). Five series of cylinder tests are conducted to investigate effects of different parameters and ultimately relate the *ultrasonic pulse velocity* to the axial stress on the test specimens. Finally, *frequency content changes* of transmitted ultrasound waves (dispersion) are investigated through two standard cylinder tests under changing axial load. Analytical formulation derivations and SAP2000 Nonlinear (version 7.12) analyses are also performed in order to support the test results.

This chapter discusses the results and conclusions under three major headings as transverse vibration measurement tests, ultrasonic pulse velocity method, and waveform & frequency content evaluation of transmitted

ultrasound waves, and gives guidelines for future studies.

5.1. Transverse Vibration Measurement Tests:

The effect of axial load on transverse vibration frequency is investigated by testing 1) reinforced concrete shear wall specimen, 2) I120 steel column, and 3) a 24-storey high R/C building's axial load carrying members. In order to capture major modal vibration frequencies an "HP 3582A Spectrum Analyzer" is used during these tests.

Analytical solutions to formulate the transverse vibration frequencies of columns are derived for different boundary conditions before conducting experiments. The Equations 2.74, and 2.81 are obtained for pin-pin connection boundary conditions.

The analytical and experimental results have shown that transverse vibration technique can be successfully used on slender structural members, such as slender members of steel buildings, truss bridge members, energy transmission line towers, slender columns (such as long bridge piers), chimneys, elevated water tanks, etc. The results have also shown that the first (fundamental) vibration frequency is the most sensitive one (compared to the higher modes' transverse vibration frequencies) for axial load changes.

The Equations 2.95, 2.98, and 2.103 are obtained for fixed-fixed boundary conditions. The analytical results have shown that frequencies are very sensitive to small changes in length for stocky columns. In "elastic buckling" range, the relationship between the ratio of the transverse vibration frequency to the unstressed frequency and the ratio of the load on the member to the buckling load of the member becomes insensitive to the length changes. Another significant outcome is that the ratio of axial force to the flexural rigidity ($E.I$) also plays an important role on the frequency change (see Equation 2.78)

Equations 2.115, 2.125 to 2.134 are obtained for lateral springs at both ends boundary condition. The boundary conditions at the supports complicate the analytical solution as well as behavior of a member. Equations 2.146, 2.151 to 2.157 are obtained for “fixed-end and spring with roller on other end” boundary condition.

Before the tests of laboratory shear wall (with a dimensions of 9x91x151 cm), a number of analytical solutions are carried out for different boundary conditions (i.e., pin ends on both supports, fixed ends on both supports, and fixed end and spring with roller on other end). The analytical and experimental results are compared against each other. Since the test member (shear wall) is not very slender, the changes in the transverse vibration frequencies are not expected to be obtained clearly. However, adequate measurements are obtained showing acceptable correlations to the analytical models. Measured natural vibration frequencies are decreased as the axial load in the shear wall is increased. The response of the shear wall is coupled by the response of the testing frame further complicating measurement results.

After the shear wall test, a slender member (I120 steel column with a length of 160 cm) is tested. For I120 steel column, analytical computations are carried out for different boundary conditions (i.e., rollers on both ends with transverse springs, pin ends on both supports. SAP2000 analysis is performed to check the experimental and analytical results. The natural frequencies obtained for the unloaded test case and SAP2000 results for pin-ended boundary condition found to be as close as 99.1%. The theoretical results for natural frequency changes and experimentally obtained values had overall agreement. The variations are denoted to uncertainties in the boundary conditions.

In the 24 storey high R/C building test, the fundamental frequencies computed from the analytical simulations show very small deviations for

different loading levels. However, the actual test results show large deviations in the measured natural frequencies. Analytical simulations show that the natural frequencies of stocky columns are highly sensitive to length changes. Furthermore, the actual boundary conditions may be different than the idealized analytical boundary conditions. The lower and upper part of the members (an interior column, an exterior column, and a shear wall) may also be vibrating during the tests. In addition, the beams connecting to the exterior columns show different layouts (i.e., at some storey the beams are at the outer face of the column whereas at other storey the beams are at the inner face of the column). Therefore, the length used in analytical computations may not be the same as the member length on corresponding floor. Similar analytical computations are performed in order to find the required braced lengths for fixed-ended boundary condition in order to match the test results (Table 4.18, 4.19, and 4.20). The calibrated column lengths for interior columns are found to be larger than the measured length (for fixed-fixed condition simulation). The difference is attributed to limited rotational degrees of freedom at each end of the column at storey levels. The calculated length values are 6% to 27% larger than the measured column lengths. Shear wall expected and measured frequencies had better overall agreement. Exterior column frequency comparisons have given unsatisfactory results. The difference in measurement and simulations are attributed to uncertainties at the boundary conditions due to connecting beams.

The transverse vibration method has the advantage of obtaining “existing axial load” on a slender member without taking a reference point such as initial condition before loading. If the boundary conditions are well defined and controlled, the method will tremendously help to understand structural loading and behavior of a structural system. In steel structures or bridge piers, for example, the axial loads on identical members can be compared against each other, or a damaged/suspicious member on the same floor can be detected easily.

Transverse vibration technique is an easy measurement technique. The method can be applied simply by vibrating the member and measuring the transverse vibration frequency using a spectrum analyzer. In addition, the technique is based on a theory and is not empirical. The measurements are not affected from local defects (whereas strain transducers can be easily affected by local defects such as improper bonding, cracking at the measurement location, rebar being close to surface, etc.) This method considers global behavior of a member and might better estimate the load carried by the member as a whole provided that the member is slender enough to achieve required sensitivity.

Controlled loading on a structural slender member might help to calibrate the uncertainties associated with the boundary conditions. In other words, the member can be loaded by a known additional load. The measured vibration frequency change can be used to calibrate the “effective length” of the member preventing any errors associated with unclear boundary conditions.

5.2. Ultrasonic Pulse Velocity Measurement:

The propagation velocity of ultrasonic stress waves depends on the density, Poisson’s ratio, modulus of elasticity of the medium, and the state of stress. The presence of stress changes the propagation properties of elastic waves in a body. When the material is “stressed”, the relationship shown in Equation 3.4 cannot describe the change in the ultrasonic wave velocities. New equations should be derived to consider the level of stress. Study of materials under stress is described by the “Acoustoelasticity Theory”. The propagation equation given in stressed case depends on (a) the second and third order elastic constants, (b) applied stresses, and (c) ultrasonic wave direction of propagation.

Pulse velocity is measured based on the travel time between initiation and the arrival of the first wave. Five groups of cylinder tests are conducted in an

attempt to relate the ultrasonic pulse velocity to the stress on the specimens. "TICO Ultrasonic Instrument" is used during the tests. The water based gel couplant used between the pulse velocity transducers and concrete surface is found to be time dependent and not suitable for pulse velocity measurements for concrete. The gel which is soaked by the dry concrete surface not only changes the ultrasonic properties of concrete but also loses its couplant properties. At the unstressed states, changes in the pulse velocity are also detected. It is concluded that the gel has to be re-applied each time before taking an ultrasonic pulse velocity reading. However, increasing amounts of gel absorbed by the concrete starts to affect the velocity readings by changing the properties of the specimen. Efforts to eliminate couplant effect by soaking cylinder in water before testing yielded no successful results as the pulse velocities remained fairly constant until final stages of crushing. Velocity changes remained inconsistent using water based gel as a couplant.

Investigations on alternative couplants resulted with eleven additional cylinder tests using "honey" as a couplant. Ultrasonic pulse velocities of concrete cylinder remained constant over two hours of unstressed testing time with no variations at all. The velocities obtained in transverse direction to the loading direction have showed at most 2% decrease when concrete strain is smaller than 0.002 (strain corresponding to the maximum stress). There are about 10% exponential decreases beyond the strain of 0.002.

Insignificant changes in pulse velocity measured parallel to the loading direction may be due to existence of an uncracked path between the two ends of the specimen. Scattering of the ultrasonic wave is not considered by the pulse velocity measurement instrument.

The orientation of the loading direction to wave propagation direction, the couplant uniformity, the accuracy problem of measurement instrument, and the modeling of Poisson's ratio affect the accuracy of test results. The

existence of reinforcement also influences the pulse velocity and requires corrections.

As a result, the pulse velocity change studies in concrete cylinders remained mostly inconclusive. The changes in ultrasonic pulse velocity become significant (larger than 2%) beyond 0.002 strain in concrete. Therefore, the ultrasonic pulse velocity might have limited use to detect concrete regions passing 0.002 strain.

In non-destructive tests, ultrasonic pulse velocity method (portable for field inspections) is commonly used for other purposes in order to determine 1) the homogeneity and the quality of concrete, 2) the thickness of a layer of inferior quality concrete, the presence of voids, cracks, or other imperfections, 3) the changes in the concrete which may occur over time (such as the hydration of cement) or through the action of fire, frost, or chemical attack, and 4) the mechanical properties (generally strength) of concrete.

5.3. Waveform and Frequency Content Evaluation of Transmitted Ultrasound Waves:

In the experiments of ultrasonic wave velocity, the velocity changes have not been clearly detectable at lower stress levels. However, the changes in the wave signal form of the transmitted ultrasound wave is expected to change due to micro crack formation in concrete. If detected, quantification of frequency changes/shifts would have been used for axial load level estimation studies.

Ultrasonic waveforms are recorded from the tests of two C12 standard cylinder specimens with the help of a digital storage oscilloscope ("Gould DataSys 740" 150 MHz maximum sampling rate). Frequency and waveform content of ultrasonic waves traveling in concrete cylinders are investigated

under changing axial loads. The frequency content of the transmitted (recorded) wave is obtained by FFT (Fast Fourier Transformation) and changes are compared against each other using linear regression analysis.

The results have shown that there is a fair relationship between the correlation factors (R) of the ultrasonic wave frequencies and the number of turns (Figure 4.62, 4.63, and 4.64). The estimated relationship between the number of turns and the load level is given in Figure 4.65 by using the Hognestad [24] stress-strain curve model for concrete. Therefore, the load level on a new specimen can be estimated from its correlation coefficient by entering to the charts. Additional tests would be necessary to reach a generalized conclusion. However, the results obtained from the initial tests are very promising.

5.4. Future Studies:

Work items listed below can be helpful for future researches in the field of ultrasonic pulse velocity and transverse vibration measurements.

- Different couplants would be investigated,
- Contact surface and direction of the transducers are important. Instead of surface contact transducers, use of point contact transducers can be investigated,
- Test setup design can be improved to eliminate ultrasound wave propagation through test setup,
- Phaser arrays of transducers can be used to focus and pin-point specific locations in a continuum,
- Test setup design can be improved to eliminate vibration modes of the test setup itself for transverse direction vibration tests,
- Boundary condition determination can be achieved by controlled incremental loading tests. Uncertainties associated with the boundary conditions can be cleared out by incremental load tests.

REFERENCES

- [1] Chopra, A. K., "Dynamics of Structures: Theory and Application to Earthquake Engineering", Prentice Hall Inc., 1995.
- [2] Malhotra, V. M., "Testing of Hardened Concrete: Non-destructive Methods", ACI Monograph No. 9, The Iowa State University Press & American Concrete Institute, 1976.
- [3] Blitz, J., and Simpson, G., "Ultrasonic Methods of Non-destructive Testing", Chapman & Hall London, 1996.
- [4] Rhazi, J., "NDT in Civil Engineering: The Case of Concrete Bridge Decks", NDT.net, May 2001.
- [5] <http://www.ndt-ed.org/EducationResources/CommunityCollege/Ultrasonics/Introduction/history.htm>
- [6] Bentahar, M., et al., "Second and Third Order Elastic Constants Determination of an Isotropic Metal", 15th World Conference on Nondestructive Testing, Roma (Italy), 15-21 October 2000.
- [7] Timoshenko, S. P., and Goodier J. N., "Theory of Elasticity", International Edition, McGraw-Hill Book Co., 1970.
- [8] Achenbach, J. D., "Wave Propagation in Elastic Solids", Elsevier Science Ltd; 01 June 1975.
- [9] Dubuget, M., et al., "Characterization of the Nonlinear Elastic Properties of Aluminum Alloys Using Ultrasonic Evaluation Under Load", ICAA5, Fifth International Conference on Aluminum Alloys, Grenoble, pp. 951-956, July 1-5, 1996.
- [10] Nesvijski, E. G., "On Design of Ultrasonic Transducers and Accuracy of Velocity Measurements", NDT.net, February 2000.
- [11] CNS Farnell Limited, "http://www.cnsfarnell.co.uk/CNSF_English/pundit_support2.htm".

- [12] Qixian, L., and Bungey, J. H., "Using Compression Wave Ultrasonic Transducers to Measure the Velocity of Surface Waves and hence Determine Dynamic Modulus of Elasticity for Concrete", *Construction and Building Materials*, Volume 10, pp. 237-242, 1996.
- [13] Yaman, I. O., et al., "Early-Age Durability Assessment of Cast-in-Place R/C Bridge Decks, Proc. Conference on New Frontiers and Challenges, AIT, Thailand, November 8-12, 1999.
- [14] http://www.sfu.ca/sonic-studio/handbook/Acoustic_Impedance.html
- [15] http://www.ndt.net/article/az/ut_idx.htm
- [16] Graff, K. F., "Wave Motion in Elastic Solids", Oxford University Press, 1975.
- [17] Yaman, I. O., et al., "Ultrasonic Pulse Velocity in Concrete Using Direct and Indirect Transmission", *ACI Materials Journal*, V. 98, No. 6, November-December 2001.
- [18] http://www.gepower.com/panametrics/en_us/pdf/transducers/transducer_technotes.pdf
- [19] <http://www.ndt.net/article/az/ut/vel.htm>
- [20] British Standard Institute, "Recommendations for Measurement of Velocity of Ultrasonic Pulses in Concrete, BS 1881: Part 203: 1986".
- [21] Reinhardt, H. W., and Grosse, C. U., "Setting and Hardening of Concrete Continuously Monitored by Elastic Waves", *NDT.net*, July 1996.
- [22] Reinhardt, H. W., et al., "Material Characterization of Steel Fiber Reinforced Concrete Using Neutron CT, Ultrasound and Quantitative Acoustic Emission Techniques", *NDT.net*, May 2001.
- [23] Watkeys, D. G., "Non-destructive Testing of Concrete Subject to Fire Attack", M.Sc. (Eng) Thesis, University of London, 1955.
- [24] Hognestad, E., "A Study of Combined Bending and Axial Load in R. C. Members", *University of Illinois Engineering Exp. Sta. Bull. No. 339*, Nov. 1951.
- [25] Proceq Co., "www.proceq.com".

APPENDIX A

FUNDAMENTAL FREQUENCY CHANGE IN PERCENTAGE VERSUS AXIAL LOAD LEVEL FOR I SECTION STEEL COLUMNS FOR DIFFERENT LENGTHS

Table A.1. Fundamental frequency change in percentage versus axial load level for I80 steel column for different lengths for load level

		P _{cr} (tons)																											
		17,8	17,3	16,6	15,7	14,6	13,3	11,8	10,2	8,3	6,9	5,8	4,9	4,2	3,7	3,2	2,9	2,6	2,3	2,1	1,9	1,7	1,6	1,4					
		Length (m)																											
P (tons)	f/f ₀ (%)	0,50	0,75	1,00	1,25	1,50	1,75	2,00	2,25	2,50	2,75	3,00	3,25	3,50	3,75	4,00	4,25	4,50	4,75	5,00	5,25	5,50	5,75	6,00					
		4										8,3	6,9	5,8															
6										8,3	6,9	5,8	4,9	4,2	3,7														
8										8,3	6,9	5,8	4,9	4,2	3,7	3,2	2,9	2,6	2,3										
10										8,3	6,8	5,7	4,9	4,2	3,7	3,2	2,9	2,5	2,3	2,1	1,9	1,7							
12										8,2	6,8	5,7	4,9	4,2	3,7	3,2	2,8	2,5	2,3	2,1	1,9	1,7	1,6	1,4					
14								10,1		8,2	6,8	5,7	4,8	4,2	3,6	3,2	2,8	2,5	2,3	2,0	1,9	1,7	1,5	1,4					
16								10,0		8,1	6,7	5,7	4,8	4,2	3,6	3,2	2,8	2,5	2,3	2,0	1,8	1,7	1,5	1,4					
18								10,0		8,1	6,7	5,6	4,8	4,1	3,6	3,2	2,8	2,5	2,2	2,0	1,8	1,7	1,5	1,4					
20								9,9		8,0	6,6	5,6	4,7	4,1	3,6	3,1	2,8	2,5	2,2	2,0	1,8	1,7	1,5	1,4					
22								9,8		8,0	6,6	5,5	4,7	4,1	3,5	3,1	2,7	2,5	2,2	2,0	1,8	1,6	1,5	1,4					
24								9,7		7,9	6,5	5,5	4,7	4,0	3,5	3,1	2,7	2,4	2,2	2,0	1,8	1,6	1,5	1,4					
26								9,6		7,8	6,4	5,4	4,6	4,0	3,5	3,0	2,7	2,4	2,2	1,9	1,8	1,6	1,5	1,4					
28								9,5		7,7	6,4	5,4	4,6	3,9	3,4	3,0	2,7	2,4	2,1	1,9	1,8	1,6	1,5	1,3					
30								9,4		7,6	6,3	5,3	4,5	3,9	3,4	3,0	2,6	2,3	2,1	1,9	1,7	1,6	1,4	1,3					
32								11,7	9,3	7,5	6,2	5,2	4,5	3,8	3,3	2,9	2,6	2,3	2,1	1,9	1,7	1,6	1,4	1,3					
34								11,6	9,1	7,4	6,1	5,1	4,4	3,8	3,3	2,9	2,6	2,3	2,1	1,9	1,7	1,5	1,4	1,3					
36								11,4	9,0	7,3	6,0	5,1	4,3	3,7	3,2	2,9	2,5	2,3	2,0	1,8	1,7	1,5	1,4	1,3					
38								11,2	8,9	7,2	5,9	5,0	4,2	3,7	3,2	2,8	2,5	2,2	2,0	1,8	1,6	1,5	1,4	1,2					
40								11,0	8,7	7,1	5,8	4,9	4,2	3,6	3,1	2,8	2,4	2,2	2,0	1,8	1,6	1,5	1,3	1,2					
42								10,8	8,5	6,9	5,7	4,8	4,1	3,5	3,1	2,7	2,4	2,1	1,9	1,7	1,6	1,4	1,3	1,2					
44								10,6	8,4	6,8	5,6	4,7	4,0	3,5	3,0	2,6	2,3	2,1	1,9	1,7	1,5	1,4	1,3	1,2					
46								10,4	8,2	6,6	5,5	4,6	3,9	3,4	2,9	2,6	2,3	2,0	1,8	1,7	1,5	1,4	1,3	1,1					
48								13,2	10,1	8,0	6,5	5,4	4,5	3,8	3,3	2,9	2,5	2,2	2,0	1,8	1,6	1,5	1,3	1,2	1,1				
50								12,9	9,9	7,8	6,3	5,2	4,4	3,7	3,2	2,8	2,5	2,2	1,9	1,8	1,6	1,4	1,3	1,2	1,1				
52								12,5	9,6	7,6	6,1	5,1	4,3	3,6	3,1	2,7	2,4	2,1	1,9	1,7	1,5	1,4	1,3	1,2	1,1				
54								12,2	9,3	7,4	6,0	4,9	4,1	3,5	3,0	2,7	2,3	2,1	1,8	1,7	1,5	1,4	1,2	1,1	1,0				
56								11,8	9,0	7,1	5,8	4,8	4,0	3,4	3,0	2,6	2,3	2,0	1,8	1,6	1,4	1,3	1,2	1,1	1,0				
58								11,4	8,7	6,9	5,6	4,6	3,9	3,3	2,9	2,5	2,2	1,9	1,7	1,6	1,4	1,3	1,2	1,1	1,0				
60								11,0	8,4	6,7	5,4	4,5	3,8	3,2	2,8	2,4	2,1	1,9	1,7	1,5	1,4	1,2	1,1	1,0	0,9				
62								14,5	10,6	8,1	6,4	5,2	4,3	3,6	3,1	2,7	2,3	2,0	1,8	1,6	1,4	1,3	1,2	1,1	1,0	0,9			
64								13,9	10,2	7,8	6,2	5,0	4,1	3,5	3,0	2,6	2,2	2,0	1,7	1,5	1,4	1,2	1,1	1,0	0,9	0,9			
66								13,3	9,8	7,5	5,9	4,8	4,0	3,3	2,8	2,4	2,1	1,9	1,7	1,5	1,3	1,2	1,1	1,0	0,9	0,8			
68								12,7	9,3	7,1	5,6	4,6	3,8	3,2	2,7	2,3	2,0	1,8	1,6	1,4	1,3	1,1	1,0	0,9	0,8	0,8			
70								12,0	8,8	6,8	5,3	4,3	3,6	3,0	2,6	2,2	1,9	1,7	1,5	1,3	1,2	1,1	1,0	0,9	0,8	0,8			
72								11,4	8,3	6,4	5,0	4,1	3,4	2,8	2,4	2,1	1,8	1,6	1,4	1,3	1,1	1,0	0,9	0,8	0,7				
74								15,4	10,7	7,8	6,0	4,7	3,8	3,2	2,7	2,3	2,0	1,7	1,5	1,3	1,2	1,1	1,0	0,9	0,8	0,7	0,7		
76								14,4	10,0	7,3	5,6	4,4	3,6	3,0	2,5	2,1	1,8	1,6	1,4	1,2	1,1	1,0	0,9	0,8	0,7	0,6	0,6		
78								13,3	9,3	6,8	5,2	4,1	3,3	2,8	2,3	2,0	1,7	1,5	1,3	1,2	1,0	0,9	0,8	0,8	0,7	0,6	0,6		
80								12,3	8,5	6,3	4,8	3,8	3,1	2,5	2,1	1,8	1,6	1,4	1,2	1,1	0,9	0,9	0,8	0,7	0,6	0,5	0,5		
82								11,2	7,8	5,7	4,4	3,4	2,8	2,3	1,9	1,7	1,4	1,2	1,1	1,0	0,9	0,8	0,7	0,6	0,5	0,5	0,5		
84								15,7	10,0	7,0	5,1	3,9	3,1	2,5	2,1	1,7	1,5	1,3	1,1	1,0	0,9	0,8	0,7	0,6	0,5	0,5	0,4	0,4	
86								13,9	8,9	6,2	4,5	3,5	2,7	2,2	1,8	1,5	1,3	1,1	1,0	0,9	0,8	0,7	0,6	0,5	0,5	0,4	0,4	0,4	
88								12,1	7,7	5,4	3,9	3,0	2,4	1,9	1,6	1,3	1,1	1,0	0,9	0,8	0,7	0,6	0,5	0,5	0,4	0,4	0,4	0,3	
90								10,2	6,5	4,5	3,3	2,5	2,0	1,6	1,3	1,1	1,0	0,8	0,7	0,6	0,6	0,5	0,5	0,4	0,4	0,3	0,3	0,3	
92								14,6	8,2	5,3	3,7	2,7	2,1	1,6	1,3	1,1	0,9	0,8	0,7	0,6	0,5	0,5	0,4	0,4	0,3	0,3	0,2	0,2	0,2
94								11,1	6,2	4,0	2,8	2,0	1,6	1,2	1,0	0,8	0,7	0,6	0,5	0,4	0,4	0,3	0,3	0,2	0,2	0,2	0,2	0,2	0,2
96	16,8	7,5	4,2	2,7	1,9	1,4	1,1	0,8	0,7	0,6	0,5	0,4	0,3	0,3	0,3	0,3	0,2	0,2	0,2	0,2	0,2	0,1	0,1	0,1	0,1	0,1	0,1	0,1	
98	8,5	3,8	2,1	1,4	0,9	0,7	0,5	0,4	0,3	0,3	0,2	0,2	0,2	0,2	0,2	0,2	0,1	0,1	0,1	0,1	0,1	0,1	0,1	0,1	0,1	0,1	0,1	0,1	
100	0,0	0,0	0,0	0,0	0,0	0,0	0,0	0,0	0,0	0,0	0,0	0,0	0,0	0,0	0,0	0,0	0,0	0,0	0,0	0,0	0,0	0,0	0,0	0,0	0,0	0,0	0,0	0,0	

Table A.2. Fundamental frequency change in percentage versus axial load level for I80 steel column for different lengths for frequency change

f/f _o (%)	Length (m)																									
	0,50	0,75	1,00	1,25	1,50	1,75	2,00	2,25	2,50	2,75	3,00	3,25	3,50	3,75	4,00	4,25	4,50	4,75	5,00	5,25	5,50	5,75	6,00			
0,0	100,0	100,0	100,0	100,0	100,0	100,0	100,0	100,0	100,0	100,0	100,0	100,0	100,0	100,0	100,0	100,0	100,0	100,0	100,0	100,0	100,0	100,0	100,0	100,0		
0,5	99,9	99,7	99,5	99,3	98,9	98,6	98,1	97,6	97,0	96,4	95,7	94,9	94,1	93,2	92,2	91,2	90,0	88,8	87,5	86,1	84,6	83,1	81,4			
1,0	99,8	99,5	99,1	98,5	97,9	97,1	96,2	95,2	94,0	92,7	91,2	89,6	87,8	85,8	83,7	81,3	78,7	75,9	72,7	69,3	65,4	61,2	56,3			
1,5	99,7	99,2	98,6	97,8	96,8	95,6	94,2	92,6	90,8	88,8	86,4	83,8	80,9	77,7	74,0	69,9	65,3	59,9	53,7	46,2	36,6	22,5				
2,0	99,5	98,9	98,1	97,0	95,7	94,1	92,2	90,0	87,5	84,6	81,4	77,6	73,4	68,5	62,8	56,1	47,9	37,3	20,7							
2,5	99,4	98,7	97,6	96,3	94,6	92,6	90,2	87,4	84,1	80,3	75,9	70,8	64,9	57,7	48,9	37,2	17,4									
3,0	99,3	98,4	97,2	95,5	93,5	91,0	88,1	84,6	80,5	75,7	70,0	63,3	55,0	44,3	28,7											
3,5	99,2	98,1	96,7	94,8	92,4	89,4	85,9	81,7	76,7	70,8	63,6	54,6	42,8	24,1												
4,0	99,1	97,9	96,2	94,0	91,2	87,8	83,7	78,7	72,7	65,4	56,3	44,2	25,0													
4,5	98,9	97,6	95,7	93,2	90,0	86,1	81,4	75,6	68,5	59,6	47,9	30,2														
5,0	98,8	97,3	95,2	92,4	88,9	84,4	79,0	72,3	63,9	53,1	37,6															
5,5	98,7	97,1	94,7	91,6	87,7	82,7	76,6	68,9	59,0	45,6	22,9															
6,0	98,6	96,8	94,2	90,8	86,4	80,9	74,0	65,3	53,7	36,6																
6,5	98,5	96,5	93,7	90,0	85,2	79,1	71,4	61,4	47,7	24,4																
7,0	98,4	96,3	93,2	89,2	83,9	77,3	68,7	57,3	40,7																	
7,5	98,2	96,0	92,7	88,4	82,7	75,3	65,8	52,8	32,3																	
8,0	98,1	95,7	92,2	87,5	81,4	73,4	62,8	47,9	20,7																	
8,5	98,0	95,4	91,7	86,7	80,0	71,4	59,7	42,4																		
9,0	97,9	95,2	91,2	85,8	78,7	69,3	56,3	36,1																		
9,5	97,8	94,9	90,7	85,0	77,3	67,1	52,7	28,4																		
10,0	97,6	94,6	90,2	84,1	75,9	64,9	48,9	17,4																		
10,5	97,5	94,3	89,6	83,2	74,5	62,6	44,7																			
11,0	97,4	94,0	89,1	82,3	73,0	60,2	40,1																			
11,5	97,3	93,8	88,6	81,4	71,6	57,6	34,9																			
12,0	97,2	93,5	88,1	80,5	70,0	55,0																				
12,5	97,0	93,2	87,5	79,6	68,5	52,2																				
13,0	96,9	92,9	87,0	78,6	66,9	49,3																				
13,5	96,8	92,6	86,4	77,7	65,3																					
14,0	96,7	92,4	85,9	76,7	63,6																					
14,5	96,6	92,1	85,3	75,7	61,8																					
15,0	96,4	91,8	84,8	74,7																						
15,5	96,3	91,5	84,2	73,7																						
16,0	96,2	91,2	83,7																							
16,5	96,1	90,9	83,1																							
17,0	96,0	90,6																								
17,5	95,8																									

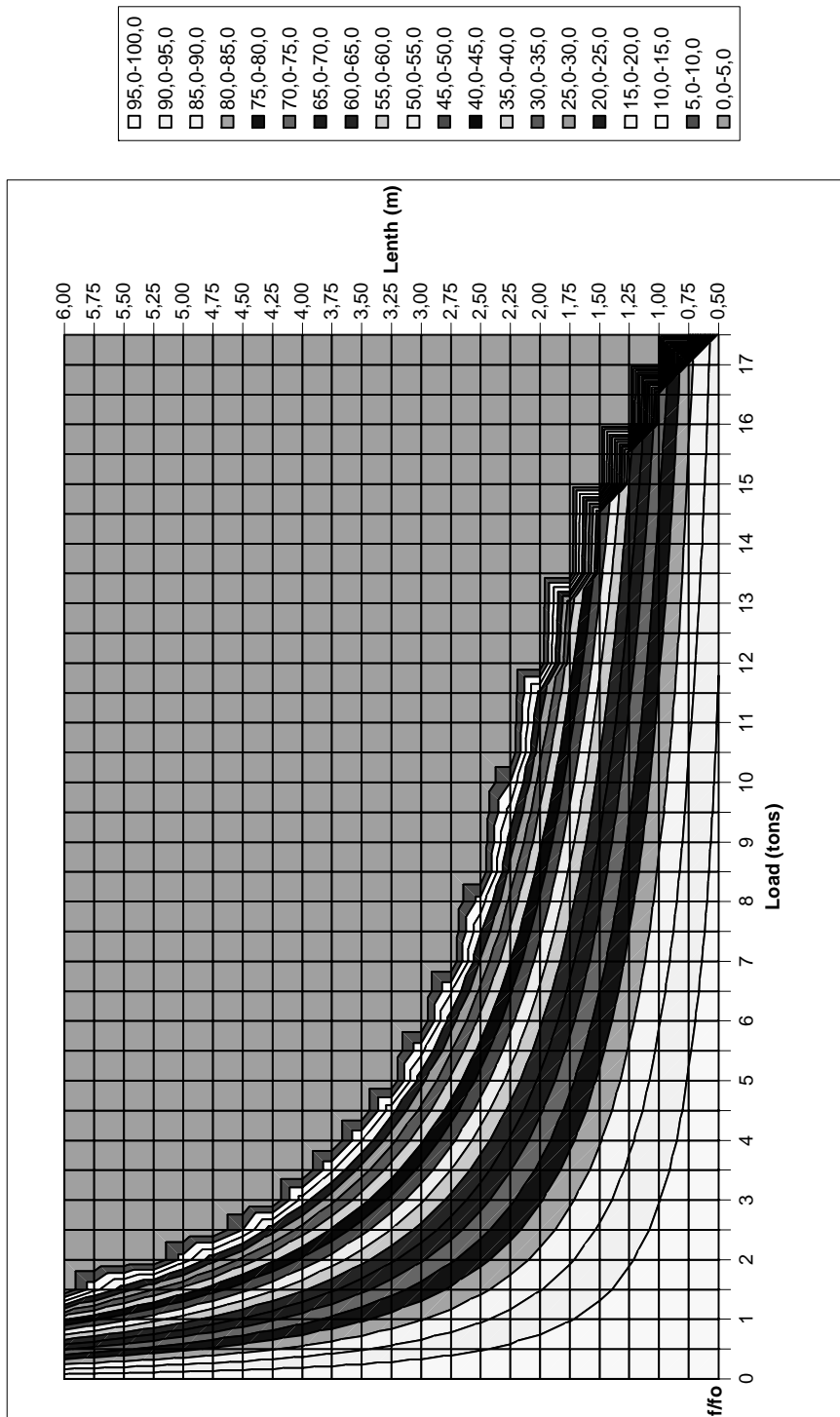


Figure A.1: Contour lines of the first vibration frequency ratios of the I80 steel column (in percentage) for certain lengths and loads

Table A.3. Fundamental frequency change in percentage versus axial load level for I100 steel column for different lengths for load level

P (tons)		P _{cr} (tons)																													
		25,0	24,5	23,8	22,9	21,8	20,5	19,0	17,3	15,4	13,3	11,2	9,6	8,2	7,2	6,3	5,6	5,0	4,5	4,0	3,6	3,3	3,0	2,8							
		Length (m)																													
l (m)	f/f ₀ (%)	0,50	0,75	1,00	1,25	1,50	1,75	2,00	2,25	2,50	2,75	3,00	3,25	3,50	3,75	4,00	4,25	4,50	4,75	5,00	5,25	5,50	5,75	6,00							
		4												11,2	9,6																
6												13,3	11,2	9,5	8,2	7,2	6,3	5,6													
8												13,3	11,2	9,5	8,2	7,1	6,3	5,6	5,0	4,5	4,0	3,6									
10												13,2	11,1	9,5	8,2	7,1	6,3	5,5	4,9	4,4	4,0	3,6	3,3	3,0	2,8						
12												13,2	11,1	9,4	8,1	7,1	6,2	5,5	4,9	4,4	4,0	3,6	3,3	3,0	2,8						
14												13,1	11,0	9,4	8,1	7,1	6,2	5,5	4,9	4,4	4,0	3,6	3,3	3,0	2,8						
16												13,0	11,0	9,3	8,1	7,0	6,2	5,5	4,9	4,4	3,9	3,6	3,3	3,0	2,7						
18												13,0	10,9	9,3	8,0	7,0	6,1	5,4	4,8	4,3	3,9	3,6	3,2	3,0	2,7						
20												12,9	10,8	9,2	7,9	6,9	6,1	5,4	4,8	4,3	3,9	3,5	3,2	2,9	2,7						
22												15,4	12,7	10,7	9,1	7,9	6,9	6,0	5,3	4,8	4,3	3,9	3,5	3,2	2,9	2,7					
24												15,3	12,6	10,6	9,0	7,8	6,8	6,0	5,3	4,7	4,2	3,8	3,5	3,2	2,9	2,7					
26												15,1	12,5	10,5	9,0	7,7	6,7	5,9	5,2	4,7	4,2	3,8	3,4	3,1	2,9	2,6					
28												15,0	12,4	10,4	8,8	7,6	6,6	5,8	5,2	4,6	4,1	3,7	3,4	3,1	2,8	2,6					
30												14,8	12,2	10,3	8,7	7,5	6,6	5,8	5,1	4,6	4,1	3,7	3,4	3,1	2,8	2,6					
32												14,6	12,0	10,1	8,6	7,4	6,5	5,7	5,0	4,5	4,0	3,6	3,3	3,0	2,8	2,5					
34												14,4	11,9	10,0	8,5	7,3	6,4	5,6	5,0	4,4	4,0	3,6	3,3	3,0	2,7	2,5					
36												14,2	11,7	9,8	8,4	7,2	6,3	5,5	4,9	4,4	3,9	3,5	3,2	2,9	2,7	2,5					
38												13,9	11,5	9,7	8,2	7,1	6,2	5,4	4,8	4,3	3,9	3,5	3,2	2,9	2,6	2,4					
40												16,9	13,7	11,3	9,5	8,1	7,0	6,1	5,3	4,7	4,2	3,8	3,4	3,1	2,8	2,6	2,4				
42												16,6	13,4	11,1	9,3	7,9	6,8	6,0	5,2	4,6	4,1	3,7	3,4	3,0	2,8	2,5	2,3				
44												16,2	13,1	10,9	9,1	7,8	6,7	5,8	5,1	4,5	4,1	3,6	3,3	3,0	2,7	2,5	2,3				
46												15,9	12,9	10,6	8,9	7,6	6,6	5,7	5,0	4,4	4,0	3,6	3,2	2,9	2,7	2,4	2,2				
48												15,5	12,6	10,4	8,7	7,4	6,4	5,6	4,9	4,3	3,9	3,5	3,1	2,8	2,6	2,4	2,2				
50												15,1	12,2	10,1	8,5	7,2	6,2	5,4	4,8	4,2	3,8	3,4	3,1	2,8	2,5	2,3	2,1				
52												18,6	14,7	11,9	9,8	8,3	7,1	6,1	5,3	4,7	4,1	3,7	3,3	3,0	2,7	2,5	2,3	2,1			
54												18,1	14,3	11,6	9,6	8,0	6,9	5,9	5,1	4,5	4,0	3,6	3,2	2,9	2,6	2,4	2,2	2,0			
56												17,5	13,9	11,2	9,3	7,8	6,6	5,7	5,0	4,4	3,9	3,5	3,1	2,8	2,5	2,3	2,1	1,9			
58												17,0	13,4	10,9	9,0	7,5	6,4	5,5	4,8	4,2	3,8	3,4	3,0	2,7	2,5	2,2	2,1	1,9			
60												16,4	12,9	10,5	8,7	7,3	6,2	5,3	4,7	4,1	3,6	3,2	2,9	2,6	2,4	2,2	2,0	1,8			
62												15,8	12,5	10,1	8,3	7,0	6,0	5,1	4,5	3,9	3,5	3,1	2,8	2,5	2,3	2,1	1,9	1,8			
64												19,8	15,1	12,0	9,7	8,0	6,7	5,7	4,9	4,3	3,8	3,4	3,0	2,7	2,4	2,2	2,0	1,8	1,7		
66												18,9	14,5	11,4	9,3	7,7	6,4	5,5	4,7	4,1	3,6	3,2	2,9	2,6	2,3	2,1	1,9	1,8	1,6		
68												18,0	13,8	10,9	8,8	7,3	6,1	5,2	4,5	3,9	3,5	3,1	2,7	2,4	2,2	2,0	1,8	1,7	1,5		
70												17,1	13,1	10,4	8,4	6,9	5,8	5,0	4,3	3,7	3,3	2,9	2,6	2,3	2,1	1,9	1,7	1,6	1,5		
72												16,2	12,4	9,8	7,9	6,6	5,5	4,7	4,0	3,5	3,1	2,7	2,4	2,2	2,0	1,8	1,6	1,5	1,4		
74												20,7	15,2	11,6	9,2	7,5	6,2	5,2	4,4	3,8	3,3	2,9	2,6	2,3	2,1	1,9	1,7	1,5	1,4	1,3	
76												19,3	14,2	10,9	8,6	7,0	5,8	4,8	4,1	3,6	3,1	2,7	2,4	2,1	1,9	1,7	1,6	1,4	1,3	1,2	
78												18,0	13,2	10,1	8,0	6,5	5,3	4,5	3,8	3,3	2,9	2,5	2,2	2,0	1,8	1,6	1,5	1,3	1,2	1,1	
80												16,5	12,1	9,3	7,3	5,9	4,9	4,1	3,5	3,0	2,6	2,3	2,1	1,8	1,6	1,5	1,3	1,2	1,1	1,0	
82												21,7	15,0	11,1	8,5	6,7	5,4	4,5	3,8	3,2	2,8	2,4	2,1	1,9	1,7	1,5	1,4	1,2	1,1	1,0	0,9
84												19,5	13,5	9,9	7,6	6,0	4,9	4,0	3,4	2,9	2,5	2,2	1,9	1,7	1,5	1,3	1,2	1,1	1,0	0,9	0,8
86												17,3	12,0	8,8	6,7	5,3	4,3	3,6	3,0	2,6	2,2	1,9	1,7	1,5	1,3	1,2	1,1	1,0	0,9	0,8	0,7
88												23,4	15,0	10,4	7,6	5,8	4,6	3,7	3,1	2,6	2,2	1,9	1,7	1,5	1,3	1,2	1,0	0,9	0,8	0,7	0,6
90												19,7	12,6	8,8	6,4	4,9	3,9	3,2	2,6	2,2	1,9	1,6	1,4	1,2	1,1	1,0	0,9	0,8	0,7	0,6	0,5
92												15,9	10,2	7,1	5,2	4,0	3,2	2,6	2,1	1,8	1,5	1,3	1,1	1,0	0,9	0,8	0,7	0,6	0,5	0,4	0,3
94												21,5	12,1	7,7	5,4	4,0	3,0	2,4	1,9	1,6	1,3	1,1	1,0	0,9	0,8	0,7	0,6	0,5	0,4	0,3	0,2
96												14,5	8,2	5,2	3,6	2,7	2,0	1,6	1,3	1,1	0,9	0,8	0,7	0,6	0,5	0,4	0,4	0,3	0,3	0,2	0,2
98	16,5	7,3	4,1	2,6	1,8	1,3	1,0	0,8	0,7	0,5	0,5	0,4	0,3	0,3	0,3	0,3	0,2	0,2	0,2	0,2	0,1	0,1	0,1	0,1	0,1	0,1	0,1	0,1	0,1	0,1	
100	0,0	0,0	0,0	0,0	0,0	0,0	0,0	0,0	0,0	0,0	0,0	0,0	0,0	0,0	0,0	0,0	0,0	0,0	0,0	0,0	0,0	0,0	0,0	0,0	0,0	0,0	0,0	0,0	0,0	0,0	0,0

Table A.4. Fundamental frequency change in percentage versus axial load level for I100 steel column for different lengths for frequency change

Load (tons)	f/f ₀ (%)	Length (m)																						
		0,50	0,75	1,00	1,25	1,50	1,75	2,00	2,25	2,50	2,75	3,00	3,25	3,50	3,75	4,00	4,25	4,50	4,75	5,00	5,25	5,50	5,75	6,00
0,0	100,0	100,0	100,0	100,0	100,0	100,0	100,0	100,0	100,0	100,0	100,0	100,0	100,0	100,0	100,0	100,0	100,0	100,0	100,0	100,0	100,0	100,0	100,0	100,0
0,5	99,9	99,9	99,8	99,6	99,5	99,3	99,0	98,8	98,5	98,2	97,8	97,4	97,0	96,6	96,1	95,6	95,0	94,4	93,8	93,1	92,4	91,7	90,9	
1,0	99,9	99,7	99,5	99,2	98,9	98,5	98,1	97,5	97,0	96,3	95,6	94,8	93,9	93,0	92,0	90,9	89,7	88,4	87,1	85,7	84,1	82,5	80,7	
1,5	99,8	99,6	99,3	98,9	98,4	97,8	97,1	96,3	95,4	94,4	93,3	92,1	90,7	89,3	87,7	85,9	84,0	82,0	79,8	77,4	74,8	72,0	68,9	
2,0	99,8	99,5	99,0	98,5	97,8	97,0	96,1	95,0	93,8	92,4	90,9	89,2	87,4	85,3	83,1	80,6	77,9	75,0	71,7	68,1	64,0	59,5	54,3	
2,5	99,7	99,3	98,8	98,1	97,3	96,3	95,1	93,7	92,2	90,4	88,5	86,3	83,9	81,2	78,2	74,9	71,3	67,1	62,5	57,1	50,9	43,4	33,7	
3,0	99,6	99,2	98,5	97,7	96,7	95,5	94,1	92,4	90,5	88,4	86,0	83,3	80,3	76,9	73,1	68,7	63,8	58,2	51,5	43,3	32,6	14,2		
3,5	99,6	99,1	98,3	97,3	96,1	94,7	93,0	91,1	88,8	86,3	83,4	80,1	76,4	72,2	67,4	61,9	55,4	47,5	37,3	21,9				
4,0	99,5	98,9	98,1	97,0	95,6	93,9	92,0	89,7	87,1	84,1	80,7	76,8	72,4	67,2	61,3	54,1	45,3	33,4	10,8					
4,5	99,5	98,8	97,8	96,6	95,0	93,1	90,9	88,3	85,3	81,9	77,9	73,4	68,1	61,8	54,3	44,9	32,0							
5,0	99,4	98,6	97,6	96,2	94,4	92,3	89,8	86,9	83,5	79,6	75,0	69,7	63,4	55,9	46,4	33,3								
5,5	99,3	98,5	97,3	95,8	93,9	91,5	88,8	85,5	81,7	77,2	72,0	65,9	58,4	49,2	36,6	13,6								
6,0	99,3	98,4	97,1	95,4	93,3	90,7	87,7	84,0	79,8	74,8	68,9	61,8	52,9	41,3	22,9									
6,5	99,2	98,2	96,8	95,0	92,7	89,9	86,5	82,6	77,9	72,3	65,6	57,3	46,8	31,5										
7,0	99,2	98,1	96,6	94,6	92,1	89,1	85,4	81,1	75,9	69,6	62,1	52,5	39,6	16,7										
7,5	99,1	98,0	96,3	94,2	91,5	88,2	84,3	79,5	73,8	66,9	58,3	47,2	30,8											
8,0	99,0	97,8	96,1	93,8	90,9	87,4	83,1	77,9	71,7	64,0	54,3	41,2	17,9											
8,5	99,0	97,7	95,8	93,4	90,3	86,5	81,9	76,3	69,5	61,0	50,0	34,1												
9,0	98,9	97,5	95,6	93,0	89,7	85,7	80,7	74,7	67,2	57,9	45,3	24,9												
9,5	98,9	97,4	95,3	92,6	89,1	84,8	79,5	73,0	64,9	54,5	39,9	9,1												
10,0	98,8	97,3	95,1	92,2	88,5	83,9	78,2	71,3	62,5	50,9	33,7													
10,5	98,7	97,1	94,8	91,8	87,9	83,0	77,0	69,5	59,9	47,0	26,1													
11,0	98,7	97,0	94,6	91,3	87,2	82,1	75,7	67,7	57,3	42,8	14,8													
11,5	98,6	96,8	94,3	90,9	86,6	81,2	74,4	65,8	54,5	38,0														
12,0	98,5	96,7	94,1	90,5	86,0	80,3	73,1	63,8	51,5	32,6														
12,5	98,5	96,6	93,8	90,1	85,3	79,3	71,7	61,8	48,4	26,0														
13,0	98,4	96,4	93,5	89,7	84,7	78,4	70,3	59,8	45,0	17,0														
13,5	98,4	96,3	93,3	89,3	84,0	77,4	68,9	57,6	41,3															
14,0	98,3	96,1	93,0	88,8	83,4	76,4	67,4	55,4	37,3															
14,5	98,2	96,0	92,8	88,4	82,7	75,4	65,9	53,0	32,8															
15,0	98,2	95,9	92,5	88,0	82,1	74,4	64,4	50,6	27,5															
15,5	98,1	95,7	92,2	87,5	81,4	73,4	62,9	48,0																
16,0	98,1	95,6	92,0	87,1	80,7	72,4	61,3	45,3																
16,5	98,0	95,4	91,7	86,7	80,0	71,3	59,6	42,3																
17,0	97,9	95,3	91,4	86,2	79,3	70,3	57,9	39,2																
17,5	97,9	95,1	91,2	85,8	78,6	69,2	56,2																	
18,0	97,8	95,0	90,9	85,3	77,9	68,1	54,3																	
18,5	97,8	94,9	90,6	84,9	77,2	66,9	52,5																	
19,0	97,7	94,7	90,4	84,4	76,5	65,8	50,5																	
19,5	97,6	94,6	90,1	84,0	75,8	64,6																		
20,0	97,6	94,4	89,8	83,5	75,0	63,4																		
20,5	97,5	94,3	89,6	83,1	74,3	62,2																		
21,0	97,4	94,1	89,3	82,6	73,6																			
21,5	97,4	94,0	89,0	82,2	72,8																			
22,0	97,3	93,9	88,8	81,7																				
22,5	97,3	93,7	88,5	81,2																				
23,0	97,2	93,6	88,2																					
23,5	97,1	93,4	87,9																					
24,0	97,1	93,3																						
24,5	97,0	93,1																						
25,0	97,0																							

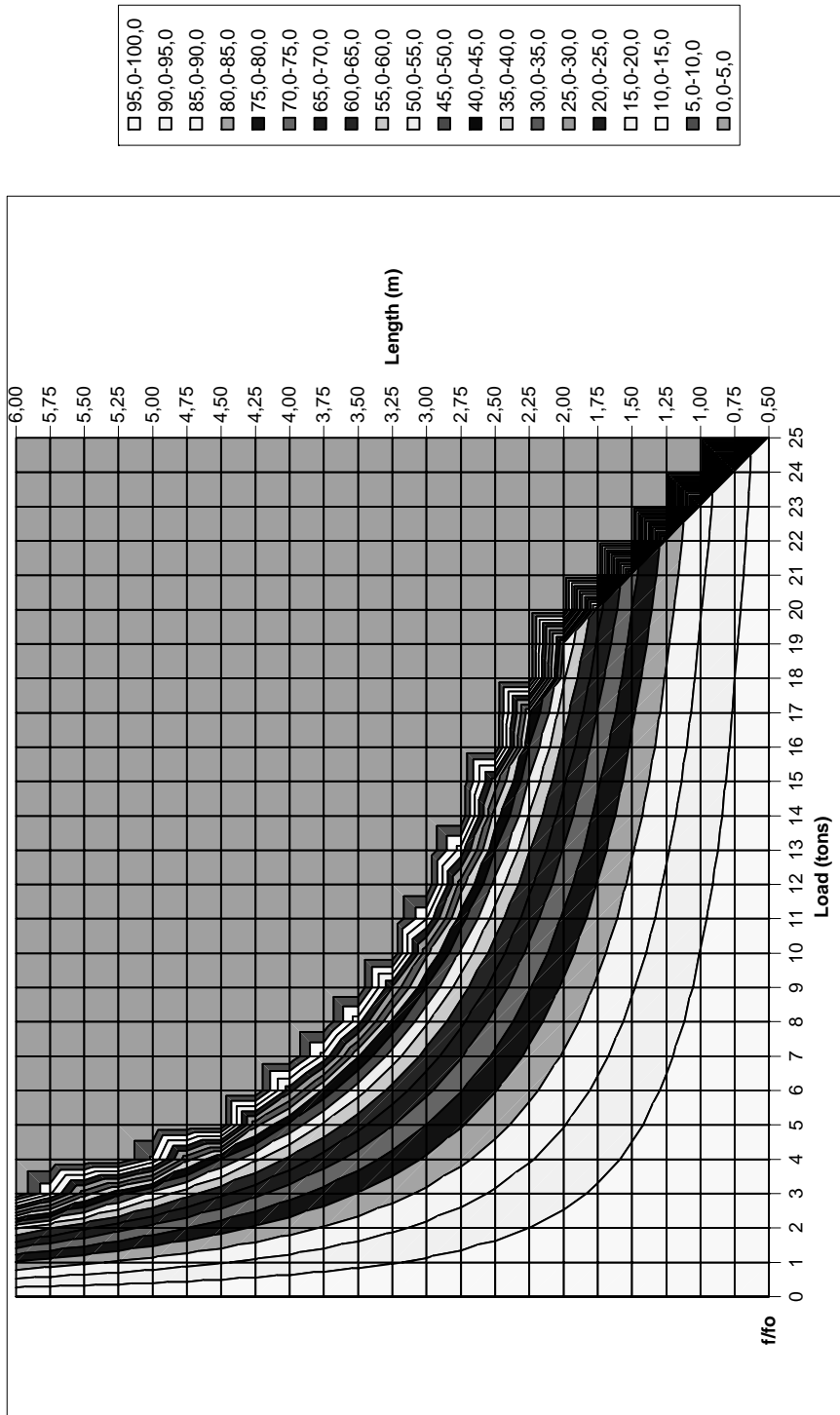


Figure A.2: Contour lines of the first vibration frequency ratios of the I100 steel column (in percentage) for certain lengths and loads

Table A.5. Fundamental frequency change in percentage versus axial load level for I120 steel column for different lengths for load level

		P _r (tons)																						
		33,7	33,2	32,4	31,5	30,4	29,1	27,6	25,8	23,9	21,7	19,4	16,9	14,5	12,7	11,1	9,8	8,8	7,9	7,1	6,4	5,9	5,4	4,9
P (tons)	l/f ₀ (%)	Length (m)																						
		0,50	0,75	1,00	1,25	1,50	1,75	2,00	2,25	2,50	2,75	3,00	3,25	3,50	3,75	4,00	4,25	4,50	4,75	5,00	5,25	5,50	5,75	6,00
4													16,8	14,5										
6													16,8	14,5	12,6	11,1	9,8	8,8	7,9					
8													16,8	14,5	12,6	11,1	9,8	8,7	7,9	7,1	6,4	5,9	5,4	
10													16,7	14,4	12,6	11,0	9,8	8,7	7,8	7,1	6,4	5,8	5,3	4,9
12													16,6	14,3	12,5	11,0	9,7	8,7	7,8	7,0	6,4	5,8	5,3	4,9
14													16,6	14,3	12,4	10,9	9,7	8,6	7,8	7,0	6,3	5,8	5,3	4,9
16												19,3	16,5	14,2	12,4	10,9	9,6	8,6	7,7	7,0	6,3	5,7	5,3	4,8
18												19,2	16,3	14,1	12,3	10,8	9,6	8,5	7,7	6,9	6,3	5,7	5,2	4,8
20												19,0	16,2	14,0	12,2	10,7	9,5	8,5	7,6	6,9	6,2	5,7	5,2	4,8
22												18,9	16,1	13,9	12,1	10,6	9,4	8,4	7,5	6,8	6,2	5,6	5,1	4,7
24												18,7	15,9	13,7	12,0	10,5	9,3	8,3	7,5	6,7	6,1	5,6	5,1	4,7
26												18,5	15,8	13,6	11,8	10,4	9,2	8,2	7,4	6,7	6,0	5,5	5,0	4,6
28												18,3	15,6	13,4	11,7	10,3	9,1	8,1	7,3	6,6	6,0	5,4	5,0	4,6
30											21,5	18,1	15,4	13,3	11,6	10,2	9,0	8,0	7,2	6,5	5,9	5,4	4,9	4,5
32											21,2	17,8	15,2	13,1	11,4	10,0	8,9	7,9	7,1	6,4	5,8	5,3	4,9	4,5
34											20,9	17,6	15,0	12,9	11,3	9,9	8,8	7,8	7,0	6,3	5,7	5,2	4,8	4,4
36											20,6	17,3	14,8	12,7	11,1	9,7	8,6	7,7	6,9	6,2	5,7	5,2	4,7	4,3
38											20,3	17,0	14,5	12,5	10,9	9,6	8,5	7,6	6,8	6,1	5,6	5,1	4,6	4,3
40											19,9	16,7	14,3	12,3	10,7	9,4	8,3	7,4	6,7	6,0	5,5	5,0	4,6	4,2
42											23,6	19,5	16,4	14,0	12,1	10,5	9,2	8,2	7,3	6,5	5,9	5,4	4,9	4,5
44											23,2	19,1	16,1	13,7	11,8	10,3	9,0	8,0	7,1	6,4	5,8	5,3	4,8	4,4
46											22,7	18,7	15,7	13,4	11,6	10,1	8,8	7,8	7,0	6,3	5,7	5,1	4,7	4,3
48											22,1	18,3	15,4	13,1	11,3	9,8	8,6	7,7	6,8	6,1	5,5	5,0	4,6	4,2
50											21,6	17,8	15,0	12,8	11,0	9,6	8,4	7,5	6,7	6,0	5,4	4,9	4,5	4,1
52											21,0	17,4	14,6	12,4	10,7	9,3	8,2	7,3	6,5	5,8	5,3	4,8	4,3	4,0
54											25,2	20,4	16,9	14,2	12,1	10,4	9,1	8,0	7,1	6,3	5,7	5,1	4,6	4,2
56											24,4	19,8	16,4	13,7	11,7	10,1	8,8	7,7	6,8	6,1	5,5	4,9	4,5	4,1
58											23,6	19,1	15,8	13,3	11,3	9,8	8,5	7,5	6,6	5,9	5,3	4,8	4,3	4,0
60											22,8	18,5	15,3	12,8	10,9	9,4	8,2	7,2	6,4	5,7	5,1	4,6	4,2	3,8
62											22,0	17,8	14,7	12,4	10,5	9,1	7,9	6,9	6,2	5,5	4,9	4,4	4,0	3,7
64											26,7	21,1	17,1	14,1	11,9	10,1	8,7	7,6	6,7	5,9	5,3	4,7	4,3	3,9
66											25,5	20,2	16,3	13,5	11,3	9,7	8,3	7,3	6,4	5,7	5,0	4,5	4,1	3,7
68											24,3	19,2	15,6	12,9	10,8	9,2	7,9	6,9	6,1	5,4	4,8	4,3	3,9	3,5
70											23,1	18,3	14,8	12,2	10,3	8,7	7,5	6,6	5,8	5,1	4,6	4,1	3,7	3,4
72											28,5	21,8	17,2	14,0	11,5	9,7	8,3	7,1	6,2	5,5	4,8	4,3	3,9	3,5
74											26,8	20,5	16,2	13,1	10,9	9,1	7,8	6,7	5,8	5,1	4,5	4,1	3,6	3,3
76											25,1	19,2	15,2	12,3	10,1	8,5	7,3	6,3	5,5	4,8	4,2	3,8	3,4	3,1
78											23,2	17,8	14,1	11,4	9,4	7,9	6,7	5,8	5,1	4,4	3,9	3,5	3,2	2,8
80											29,1	21,4	16,4	12,9	10,5	8,7	7,3	6,2	5,3	4,7	4,1	3,6	3,2	2,9
82											26,5	19,5	14,9	11,8	9,5	7,9	6,6	5,6	4,9	4,2	3,7	3,3	2,9	2,6
84											23,9	17,5	13,4	10,6	8,6	7,1	6,0	5,1	4,4	3,8	3,4	3,0	2,7	2,4
86											30,4	21,1	15,5	11,9	9,4	7,6	6,3	5,3	4,5	3,9	3,4	3,0	2,6	2,3
88											26,4	18,3	13,5	10,3	8,1	6,6	5,4	4,6	3,9	3,4	2,9	2,6	2,3	2,0
90											22,2	15,4	11,3	8,7	6,9	5,6	4,6	3,9	3,3	2,8	2,5	2,2	1,9	1,7
92											28,1	18,0	12,5	9,2	7,0	5,6	4,5	3,7	3,1	2,7	2,3	2,0	1,8	1,6
94											21,3	13,6	9,5	7,0	5,3	4,2	3,4	2,8	2,4	2,0	1,7	1,5	1,3	1,2
96											25,6	14,4	9,2	6,4	4,7	3,6	2,8	2,3	1,9	1,6	1,4	1,2	1,0	0,9
98	29,1	12,9	7,3	4,7	3,2	2,4	1,8	1,4	1,2	1,0	0,8	0,7	0,6	0,5	0,5	0,4	0,4	0,3	0,3	0,3	0,3	0,2	0,2	
100	0,0	0,0	0,0	0,0	0,0	0,0	0,0	0,0	0,0	0,0	0,0	0,0	0,0	0,0	0,0	0,0	0,0	0,0	0,0	0,0	0,0	0,0	0,0	

Table A.6. Fundamental frequency change in percentage versus axial load level for I120 steel column for different lengths for frequency change

Load (tons)	f/f _o (%)	Length (m)																						
		0,50	0,75	1,00	1,25	1,50	1,75	2,00	2,25	2,50	2,75	3,00	3,25	3,50	3,75	4,00	4,25	4,50	4,75	5,00	5,25	5,50	5,75	6,00
0,0	100,0	100,0	100,0	100,0	100,0	100,0	100,0	100,0	100,0	100,0	100,0	100,0	100,0	100,0	100,0	100,0	100,0	100,0	100,0	100,0	100,0	100,0	100,0	100,0
0,5	100,0	99,9	99,9	99,8	99,7	99,6	99,5	99,3	99,1	99,0	98,8	98,6	98,3	98,1	97,8	97,5	97,2	96,9	96,5	96,2	95,8	95,4	95,0	
1,0	99,9	99,8	99,7	99,6	99,4	99,2	98,9	98,6	98,3	97,9	97,5	97,1	96,6	96,1	95,5	94,9	94,3	93,6	92,9	92,2	91,4	90,5	89,6	
1,5	99,9	99,8	99,6	99,4	99,1	98,7	98,4	97,9	97,4	96,9	96,2	95,6	94,9	94,1	93,2	92,3	91,3	90,3	89,2	88,0	86,7	85,3	83,9	
2,0	99,9	99,7	99,5	99,1	98,8	98,3	97,8	97,2	96,5	95,8	95,0	94,1	93,1	92,0	90,8	89,6	88,2	86,8	85,2	83,5	81,7	79,8	77,7	
2,5	99,8	99,6	99,3	98,9	98,5	97,9	97,2	96,5	95,6	94,7	93,7	92,5	91,2	89,9	88,4	86,8	85,0	83,1	81,0	78,8	76,4	73,8	71,0	
3,0	99,8	99,5	99,2	98,7	98,1	97,5	96,7	95,8	94,7	93,6	92,3	90,9	89,4	87,7	85,8	83,8	81,6	79,2	76,6	73,8	70,7	67,2	63,4	
3,5	99,8	99,5	99,0	98,5	97,8	97,0	96,1	95,0	93,8	92,5	91,0	89,3	87,5	85,5	83,2	80,8	78,1	75,2	71,9	68,3	64,4	59,9	54,8	
4,0	99,7	99,4	98,9	98,3	97,5	96,6	95,5	94,3	92,9	91,4	89,6	87,7	85,5	83,1	80,5	77,6	74,4	70,9	66,9	62,4	57,3	51,5	44,5	
4,5	99,7	99,3	98,8	98,1	97,2	96,2	95,0	93,6	92,0	90,2	88,2	86,0	83,5	80,8	77,7	74,3	70,5	66,2	61,4	55,8	49,3	41,3	30,7	
5,0	99,7	99,2	98,6	97,8	96,9	95,7	94,4	92,8	91,1	89,1	86,8	84,3	81,5	78,3	74,8	70,8	66,4	61,2	55,3	48,3	39,5	27,4		
5,5	99,6	99,2	98,5	97,6	96,6	95,3	93,8	92,1	90,1	87,9	85,4	82,5	79,3	75,8	71,7	67,2	61,9	55,8	48,5	39,3	26,2			
6,0	99,6	99,1	98,4	97,4	96,2	94,9	93,2	91,3	89,2	86,7	83,9	80,7	77,2	73,1	68,5	63,3	57,1	49,7	40,4	27,3				
6,5	99,6	99,0	98,2	97,2	95,9	94,4	92,6	90,6	88,2	85,5	82,4	78,9	74,9	70,4	65,2	59,1	51,8	42,7	30,2					
7,0	99,5	98,9	98,1	97,0	95,6	94,0	92,0	89,8	87,2	84,2	80,9	77,0	72,6	67,5	61,6	54,6	45,9	34,3	13,7					
7,5	99,5	98,8	97,9	96,8	95,3	93,5	91,4	89,0	86,2	83,0	79,3	75,1	70,2	64,5	57,8	49,6	39,1	22,9						
8,0	99,5	98,8	97,8	96,5	95,0	93,1	90,8	88,2	85,2	81,7	77,7	73,1	67,7	61,4	53,8	44,1	30,7							
8,5	99,4	98,7	97,7	96,3	94,6	92,6	90,2	87,4	84,2	80,4	76,1	71,0	65,1	58,1	49,3	37,8	18,9							
9,0	99,4	98,6	97,5	96,1	94,3	92,2	89,6	86,6	83,1	79,1	74,4	68,9	62,4	54,5	44,5	30,2								
9,5	99,4	98,5	97,4	95,9	94,0	91,7	89,0	85,8	82,1	77,8	72,7	66,7	59,6	50,7	39,0	19,7								
10,0	99,3	98,5	97,2	95,6	93,7	91,2	88,4	85,0	81,0	76,4	71,0	64,5	56,6	46,6	32,5									
10,5	99,3	98,4	97,1	95,4	93,3	90,8	87,7	84,2	80,0	75,0	69,2	62,1	53,4	42,0	24,4									
11,0	99,2	98,3	97,0	95,2	93,0	90,3	87,1	83,3	78,9	73,6	67,3	59,7	50,1	36,9	11,4									
11,5	99,2	98,2	96,8	95,0	92,7	89,9	86,5	82,5	77,8	72,1	65,4	57,1	46,4	31,0										
12,0	99,2	98,1	96,7	94,7	92,3	89,4	85,8	81,6	76,6	70,7	63,4	54,4	42,5	23,5										
12,5	99,1	98,1	96,5	94,5	92,0	88,9	85,2	80,8	75,5	69,1	61,4	51,6	38,1	12,0										
13,0	99,1	98,0	96,4	94,3	91,7	88,4	84,5	79,9	74,3	67,6	59,3	48,6	33,2											
13,5	99,1	97,9	96,2	94,1	91,3	88,0	83,9	79,0	73,1	66,0	57,1	45,4	27,3											
14,0	99,0	97,8	96,1	93,8	91,0	87,5	83,2	78,1	71,9	64,4	54,8	41,9	19,8											
14,5	99,0	97,8	96,0	93,6	90,6	87,0	82,6	77,2	70,7	62,7	52,4	38,1	6,0											
15,0	99,0	97,7	95,8	93,4	90,3	86,5	81,9	76,3	69,5	61,0	49,9	33,9												
15,5	98,9	97,6	95,7	93,2	90,0	86,0	81,2	75,4	68,2	59,2	47,3	29,0												
16,0	98,9	97,5	95,5	92,9	89,6	85,5	80,5	74,4	66,9	57,3	44,5	23,2												
16,5	98,9	97,4	95,4	92,7	89,3	85,0	79,8	73,5	65,6	55,4	41,5	15,2												
17,0	98,8	97,4	95,2	92,5	88,9	84,5	79,1	72,5	64,2	53,5	38,2													
17,5	98,8	97,3	95,1	92,2	88,6	84,0	78,4	71,5	62,8	51,4	34,7													
18,0	98,8	97,2	95,0	92,0	88,2	83,5	77,7	70,5	61,4	49,3	30,7													
18,5	98,7	97,1	94,8	91,8	87,9	83,0	77,0	69,5	59,9	47,0	26,1													
19,0	98,7	97,0	94,7	91,5	87,5	82,5	76,3	68,5	58,4	44,7	20,5													
19,5	98,7	97,0	94,5	91,3	87,2	82,0	75,5	67,4	56,9	42,2														
20,0	98,6	96,9	94,4	91,1	86,8	81,5	74,8	66,4	55,3	39,5														
20,5	98,6	96,8	94,2	90,8	86,4	80,9	74,0	65,3	53,7	36,7														
21,0	98,6	96,7	94,1	90,6	86,1	80,4	73,3	64,2	52,0	33,6														
21,5	98,5	96,6	93,9	90,3	85,7	79,9	72,5	63,0	50,3	30,1														
22,0	98,5	96,6	93,8	90,1	85,4	79,3	71,7	61,9	48,5															
22,5	98,5	96,5	93,7	89,9	85,0	78,8	71,0	60,7	46,6															
23,0	98,4	96,4	93,5	89,6	84,6	78,3	70,2	59,5	44,6															
23,5	98,4	96,3	93,4	89,4	84,3	77,7	69,4	58,3	42,6															
24,0	98,4	96,2	93,2	89,2	83,9	77,2	68,5	57,1																
24,5	98,3	96,2	93,1	88,9	83,5	76,6	67,7	55,8																
25,0	98,3	96,1	92,9	88,7	83,1	76,1	66,9	54,5																
25,5	98,2	96,0	92,8	88,4	82,8	75,5	66,0	53,2																
26,0	98,2	95,9	92,6	88,2	82,4	74,9	65,2																	
26,5	98,2	95,8	92,5	87,9	82,0	74,4	64,3																	
27,0	98,1	95,8	92,3	87,7	81,6	73,8	63,4																	
27,5	98,1	95,7	92,2	87,4	81,2	73,2	62,5																	
28,0	98,1	95,6	92,0	87,2	80,9	72,6																		
28,5	98,0	95,5	91,9	87,0	80,5	72,0																		
29,0	98,0	95,4	91,7	86,7	80,1	71,4																		
29,5	98,0	95,4	91,6	86,5	79,7																			
30,0	97,9	95,3	91,4	86,2	79,3																			
30,5	97,9	95,2	91,3	86,0																				
31,0	97,9	95,1	91,1	85,7																				
31,5	97,8	95,0	91,0	85,5																				
32,0	97,8	95,0	90,8																					
32,5	97,8	94,9																						
33,0	97,7	94,8																						
33,5	97,7																							

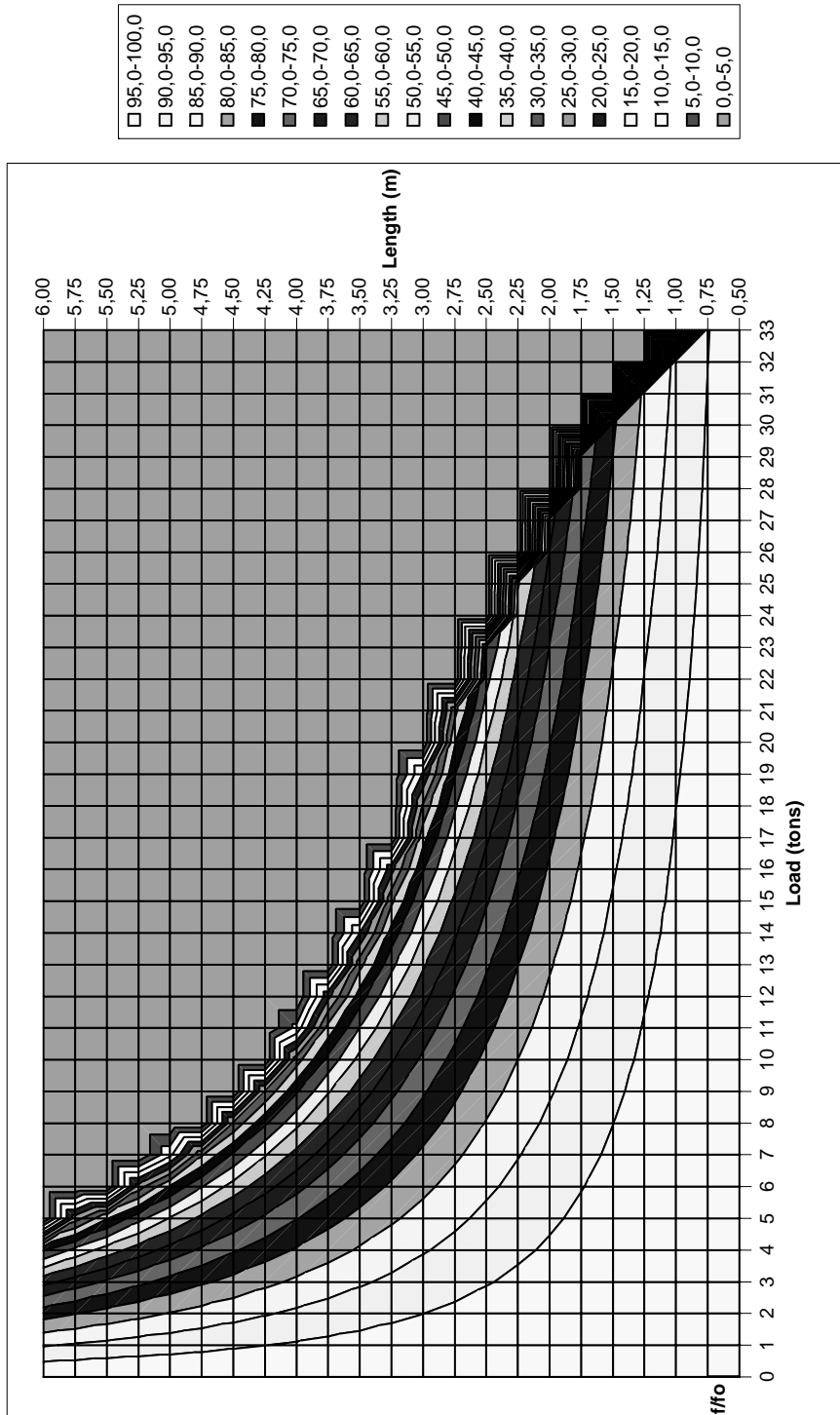


Figure A.3: Contour lines of the first vibration frequency ratios of the I120 steel column (in percentage) for certain lengths and loads

Table A.8. Fundamental frequency change in percentage versus axial load level for I140 steel column for different lengths for frequency change

Load (tons)	f/f ₀ (%)	Length (m)																						
		0,50	0,75	1,00	1,25	1,50	1,75	2,00	2,25	2,50	2,75	3,00	3,25	3,50	3,75	4,00	4,25	4,50	4,75	5,00	5,25	5,50	5,75	6,00
0,0	100,0	100,0	100,0	100,0	100,0	100,0	100,0	100,0	100,0	100,0	100,0	100,0	100,0	100,0	100,0	100,0	100,0	100,0	100,0	100,0	100,0	100,0	100,0	100,0
0,5	100,0	100,0	99,9	99,9	99,8	99,7	99,7	99,6	99,5	99,4	99,2	99,1	99,0	98,8	98,7	98,5	98,3	98,1	97,9	97,7	97,4	97,2	97,0	97,0
1,0	100,0	99,9	99,8	99,7	99,6	99,5	99,3	99,2	99,0	98,7	98,5	98,2	97,9	97,6	97,3	96,9	96,6	96,2	95,7	95,3	94,8	94,3	93,8	93,8
1,5	99,9	99,9	99,8	99,6	99,4	99,2	99,0	98,7	98,4	98,1	97,7	97,3	96,9	96,4	95,9	95,4	94,8	94,2	93,5	92,8	92,1	91,3	90,5	90,5
2,0	99,9	99,8	99,7	99,5	99,2	99,0	98,7	98,3	97,9	97,4	97,0	96,4	95,8	95,2	94,5	93,8	93,0	92,2	91,3	90,3	89,3	88,3	87,1	87,1
2,5	99,9	99,8	99,6	99,3	99,1	98,7	98,3	97,9	97,4	96,8	96,2	95,5	94,8	94,0	93,1	92,2	91,2	90,1	88,9	87,7	86,4	85,0	83,6	83,6
3,0	99,9	99,7	99,5	99,2	98,9	98,5	98,0	97,4	96,8	96,1	95,4	94,6	93,7	92,7	91,6	90,5	89,3	88,0	86,5	85,0	83,4	81,7	79,8	79,8
3,5	99,9	99,7	99,4	99,1	98,7	98,2	97,6	97,0	96,3	95,5	94,6	93,6	92,6	91,4	90,2	88,8	87,3	85,8	84,1	82,2	80,3	78,2	75,9	75,9
4,0	99,8	99,6	99,3	99,0	98,5	97,9	97,3	96,6	95,7	94,8	93,8	92,7	91,5	90,1	88,7	87,1	85,4	83,5	81,5	79,4	77,0	74,5	71,8	71,8
4,5	99,8	99,6	99,2	98,8	98,3	97,7	97,0	96,1	95,2	94,2	93,0	91,7	90,3	88,8	87,1	85,3	83,3	81,2	78,9	76,4	73,6	70,6	67,3	67,3
5,0	99,8	99,5	99,2	98,7	98,1	97,4	96,6	95,7	94,6	93,5	92,2	90,8	89,2	87,5	85,6	83,5	81,3	78,8	76,1	73,2	70,0	66,5	62,6	62,6
5,5	99,8	99,5	99,1	98,6	97,9	97,2	96,3	95,2	94,1	92,8	91,4	89,8	88,0	86,1	84,0	81,7	79,1	76,3	73,3	69,9	66,2	62,0	57,4	57,4
6,0	99,8	99,4	99,0	98,4	97,7	96,9	95,9	94,8	93,5	92,1	90,5	88,8	86,8	84,7	82,3	79,8	76,9	73,8	70,3	66,5	62,1	57,3	51,6	51,6
6,5	99,7	99,4	98,9	98,3	97,5	96,6	95,6	94,4	93,0	91,4	89,7	87,8	85,6	83,3	80,7	77,8	74,6	71,1	67,2	62,8	57,8	52,0	45,1	45,1
7,0	99,7	99,3	98,8	98,2	97,3	96,4	95,2	93,9	92,4	90,7	88,8	86,8	84,4	81,8	79,0	75,8	72,3	68,3	63,9	58,9	53,0	46,1	37,5	37,5
7,5	99,7	99,3	98,7	98,0	97,2	96,1	94,9	93,5	91,8	90,0	88,0	85,7	83,2	80,4	77,2	73,8	69,9	65,5	60,4	54,7	47,8	39,4	27,8	27,8
8,0	99,7	99,2	98,7	97,9	97,0	95,8	94,5	93,0	91,3	89,3	87,1	84,7	81,9	78,9	75,5	71,6	67,3	62,4	56,8	50,1	41,9	31,1	11,7	11,7
8,5	99,6	99,2	98,6	97,8	96,8	95,6	94,2	92,5	90,7	88,6	86,3	83,6	80,7	77,3	73,6	69,4	64,7	59,2	52,8	45,0	35,0	19,6	19,6	
9,0	99,6	99,2	98,5	97,6	96,6	95,3	93,8	92,1	90,1	87,9	85,4	82,5	79,4	75,8	71,8	67,2	61,9	55,8	48,5	39,3	26,3	12,6	12,6	
9,5	99,6	99,1	98,4	97,5	96,4	95,0	93,4	91,6	89,5	87,2	84,5	81,4	78,0	74,2	69,8	64,8	59,0	52,2	43,8	32,6	12,6	12,6	12,6	
10,0	99,6	99,1	98,3	97,4	96,2	94,8	93,1	91,2	88,9	86,4	83,6	80,3	76,7	72,6	67,8	62,4	56,0	48,3	38,4	24,0	9,3	9,3	9,3	
10,5	99,6	99,0	98,2	97,2	96,0	94,5	92,7	90,7	88,3	85,7	82,7	79,2	75,3	70,9	65,8	59,8	52,8	44,0	32,2	12,4	12,4	12,4	12,4	
11,0	99,5	99,0	98,2	97,1	95,8	94,2	92,4	90,2	87,8	84,9	81,7	78,1	73,9	69,2	63,6	57,2	49,3	39,3	24,4	9,3	9,3	9,3	9,3	
11,5	99,5	98,9	98,1	97,0	95,6	93,9	92,0	89,7	87,2	84,2	80,8	76,9	72,5	67,4	61,4	54,4	45,6	33,8	12,4	12,4	12,4	12,4	12,4	
12,0	99,5	98,9	98,0	96,8	95,4	93,7	91,6	89,3	86,5	83,4	79,8	75,7	71,0	65,6	59,1	51,4	41,5	27,3	12,4	12,4	12,4	12,4	12,4	
12,5	99,5	98,8	97,9	96,7	95,2	93,4	91,3	88,8	85,9	82,6	78,9	74,5	69,5	63,7	56,8	48,2	37,0	18,6	12,4	12,4	12,4	12,4	12,4	
13,0	99,5	98,8	97,8	96,6	95,0	93,1	90,9	88,3	85,3	81,9	77,9	73,3	68,0	61,8	54,3	44,8	31,8	12,4	12,4	12,4	12,4	12,4	12,4	
13,5	99,4	98,7	97,7	96,4	94,8	92,8	90,5	87,8	84,7	81,1	76,9	72,1	66,5	59,8	51,6	41,2	25,6	12,4	12,4	12,4	12,4	12,4	12,4	
14,0	99,4	98,7	97,6	96,3	94,6	92,6	90,2	87,3	84,1	80,3	75,9	70,8	64,8	57,7	48,9	37,1	17,2	12,4	12,4	12,4	12,4	12,4	12,4	
14,5	99,4	98,6	97,6	96,2	94,4	92,3	89,8	86,9	83,4	79,5	74,9	69,5	63,2	55,6	45,9	32,5	12,4	12,4	12,4	12,4	12,4	12,4	12,4	
15,0	99,4	98,6	97,5	96,0	94,2	92,0	89,4	86,4	82,8	78,7	73,9	68,2	61,5	53,3	42,8	27,2	12,4	12,4	12,4	12,4	12,4	12,4	12,4	
15,5	99,4	98,5	97,4	95,9	94,0	91,7	89,0	85,9	82,2	77,9	72,8	66,9	59,8	51,0	39,3	20,5	12,4	12,4	12,4	12,4	12,4	12,4	12,4	
16,0	99,3	98,5	97,3	95,7	93,8	91,5	88,7	85,4	81,5	77,0	71,8	65,5	58,0	48,5	35,6	10,0	12,4	12,4	12,4	12,4	12,4	12,4	12,4	
16,5	99,3	98,4	97,2	95,6	93,6	91,2	88,3	84,9	80,9	76,2	70,7	64,1	56,1	45,9	31,4	12,4	12,4	12,4	12,4	12,4	12,4	12,4	12,4	
17,0	99,3	98,4	97,1	95,5	93,4	90,9	87,9	84,4	80,2	75,3	69,6	62,7	54,2	43,1	26,5	12,4	12,4	12,4	12,4	12,4	12,4	12,4	12,4	
17,5	99,3	98,3	97,0	95,3	93,2	90,6	87,5	83,9	79,5	74,5	68,5	61,2	52,2	40,2	20,5	12,4	12,4	12,4	12,4	12,4	12,4	12,4	12,4	
18,0	99,2	98,3	97,0	95,2	93,0	90,3	87,1	83,3	78,9	73,6	67,3	59,7	50,1	37,0	11,7	12,4	12,4	12,4	12,4	12,4	12,4	12,4	12,4	
18,5	99,2	98,3	96,9	95,1	92,8	90,0	86,7	82,8	78,2	72,7	66,2	58,1	47,9	33,5	12,4	12,4	12,4	12,4	12,4	12,4	12,4	12,4	12,4	
19,0	99,2	98,2	96,8	94,9	92,6	89,8	86,3	82,3	77,5	71,8	65,0	56,5	45,6	29,5	12,4	12,4	12,4	12,4	12,4	12,4	12,4	12,4	12,4	
19,5	99,2	98,2	96,7	94,8	92,4	89,5	86,0	81,8	76,8	70,9	63,8	54,9	43,2	25,0	12,4	12,4	12,4	12,4	12,4	12,4	12,4	12,4	12,4	
20,0	99,2	98,1	96,6	94,6	92,2	89,2	85,6	81,3	76,1	70,0	62,6	53,2	40,7	19,4	12,4	12,4	12,4	12,4	12,4	12,4	12,4	12,4	12,4	
20,5	99,1	98,1	96,5	94,5	92,0	88,9	85,2	80,7	75,4	69,1	61,3	51,5	37,9	11,2	12,4	12,4	12,4	12,4	12,4	12,4	12,4	12,4	12,4	
21,0	99,1	98,0	96,4	94,4	91,8	88,6	84,8	80,2	74,7	68,1	60,0	49,6	35,0	12,4	12,4	12,4	12,4	12,4	12,4	12,4	12,4	12,4	12,4	
21,5	99,1	98,0	96,4	94,2	91,6	88,3	84,4	79,7	74,0	67,2	58,7	47,7	31,7	12,4	12,4	12,4	12,4	12,4	12,4	12,4	12,4	12,4	12,4	
22,0	99,1	97,9	96,3	94,1	91,4	88,0	84,0	79,1	73,3	66,2	57,4	45,8	28,1	12,4	12,4	12,4	12,4	12,4	12,4	12,4	12,4	12,4	12,4	
22,5	99,1	97,9	96,2	94,0	91,2	87,7	83,6	78,6	72,6	65,2	56,0	43,7	24,0	12,4	12,4	12,4	12,4	12,4	12,4	12,4	12,4	12,4	12,4	
23,0	99,0	97,8	96,1	93,8	90,9	87,4	83,2	78,0	71,8	64,2	54,6	41,5	18,9	12,4	12,4	12,4	12,4	12,4	12,4	12,4	12,4	12,4	12,4	
23,5	99,0	97,8	96,0	93,7	90,7	87,1	82,8	77,5	71,1	63,2	53,1	39,2	11,8	12,4	12,4	12,4	12,4	12,4	12,4	12,4	12,4	12,4	12,4	
24,0	99,0	97,7	95,9	93,5	90,5	86,8	82,3	76,9	70,3	62,1	51,6	36,8	12,4	12,4	12,4	12,4	12,4	12,4	12,4	12,4	12,4	12,4	12,4	
24,5	99,0	97,7	95,8	93,4	90,3	86,5	81,9	76,4	69,5	61,1	50,1	34,2	12,4	12,4	12,4	12,4	12,4	12,4	12,4	12,4	12,4	12,4	12,4	
25,0	99,0	97,6	95,7	93,3	90,1	86,2	81,5	75,8	68,8	60,0	48,5	31,4	12,4	12,4	12,4	12,4	12,4	12,4	12,4	12,4	12,4	12,4	12,4	
25,5	98,9	97,6	95,7	93,1	89,9	85,9	81,1	75,2	68,0	58,9	46,9	28,2	12,4	12,4	12,4	12,4	12,4	12,4	12,4	12,4	12,4	12,4	12,4	
26,0	98,9	97,5	95,6	93,0	89,7	85,6	80,7	74,6	67,2	57,8	45,1	24,7	12,4	12,4	12,4	12,4	12,4	12,4	12,4	12,4	12,4	12,4	12,4	
26,5	98,9	97,5	95,5	92,8	89,5	85,3	80,3	74,1	66,4	56,6	43,4	12,4	12,4	12,4	12,4									

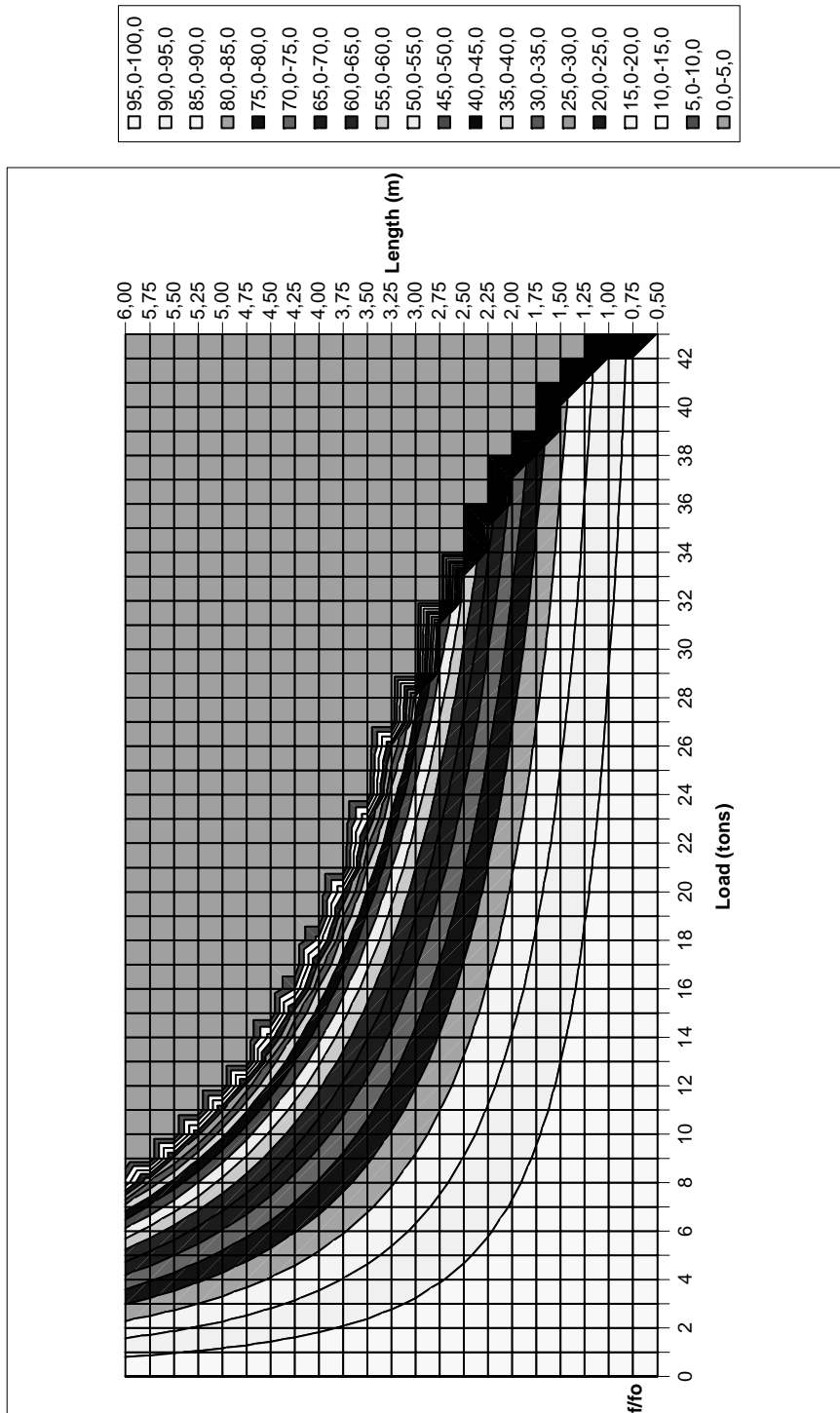


Figure A.4: Contour lines of the first vibration frequency ratios of the I140 steel column (in percentage) for certain lengths and loads

Table A.9. Fundamental frequency change in percentage versus axial load level for I160 steel column for different lengths for load level

		P _{cr} (tons)																																			
		54,3	53,8	53,1	52,1	51,0	49,6	48,1	46,3	44,4	42,2	39,8	37,3	34,5	31,5	28,3	25,1	22,4	20,1	18,1	16,4	14,9	13,7	12,5													
P (tons)	f/f ₀ (%)	Length (m)																																			
		0,50	0,75	1,00	1,25	1,50	1,75	2,00	2,25	2,50	2,75	3,00	3,25	3,50	3,75	4,00	4,25	4,50	4,75	5,00	5,25	5,50	5,75	6,00													
4																	25,1																				
6																28,2	25,0	22,3	20,0	18,1	16,4	14,9															
8																28,2	25,0	22,3	20,0	18,0	16,4	14,9	13,6	12,5													
10																28,1	24,9	22,2	19,9	18,0	16,3	14,8	13,6	12,5													
12																27,9	24,8	22,1	19,8	17,9	16,2	14,8	13,5	12,4													
14																27,8	24,6	22,0	19,7	17,8	16,1	14,7	13,5	12,4													
16																31,5	27,6	24,5	21,8	19,6	17,7	16,0	14,6	13,4	12,3												
18																31,2	27,5	24,3	21,7	19,5	17,6	15,9	14,5	13,3	12,2												
20																31,0	27,2	24,1	21,5	19,3	17,4	15,8	14,4	13,2	12,1												
22																30,7	27,0	23,9	21,3	19,2	17,3	15,7	14,3	13,1	12,0												
24																30,5	26,8	23,7	21,1	19,0	17,1	15,5	14,2	13,0	11,9												
26																30,1	26,5	23,5	20,9	18,8	17,0	15,4	14,0	12,8	11,8												
28																34,2	29,8	26,2	23,2	20,7	18,6	16,8	15,2	13,9	12,7	11,6											
30																33,8	29,4	25,9	22,9	20,4	18,3	16,6	15,0	13,7	12,5	11,5											
32																33,4	29,1	25,5	22,6	20,2	18,1	16,3	14,8	13,5	12,4	11,3											
34																32,9	28,6	25,2	22,3	19,9	17,8	16,1	14,6	13,3	12,2	11,2											
36																32,4	28,2	24,8	22,0	19,6	17,6	15,9	14,4	13,1	12,0	11,0											
38																31,8	27,7	24,4	21,6	19,3	17,3	15,6	14,1	12,9	11,8	10,8											
40																36,3	31,3	27,2	23,9	21,2	18,9	17,0	15,3	13,9	12,7	11,6	10,6										
42																35,6	30,7	26,7	23,5	20,8	18,6	16,7	15,0	13,6	12,4	11,4	10,4										
44																34,9	30,1	26,2	23,0	20,4	18,2	16,3	14,7	13,4	12,2	11,1	10,2										
46																34,1	29,4	25,6	22,5	19,9	17,8	16,0	14,4	13,1	11,9	10,9	10,0										
48																39,1	33,3	28,7	25,0	22,0	19,5	17,4	15,6	14,1	12,8	11,6	10,6	9,8									
50																38,1	32,5	28,0	24,4	21,4	19,0	16,9	15,2	13,7	12,4	11,3	10,4	9,5									
52																37,1	31,6	27,3	23,7	20,9	18,5	16,5	14,8	13,4	12,1	11,0	10,1	9,3									
54																36,1	30,7	26,5	23,1	20,3	18,0	16,0	14,4	13,0	11,8	10,7	9,8	9,0									
56																41,6	35,0	29,8	25,7	22,4	19,7	17,4	15,5	13,9	12,6	11,4	10,4	9,5	8,7								
58																40,3	33,8	28,8	24,8	21,6	19,0	16,9	15,0	13,5	12,2	11,0	10,1	9,2	8,5								
60																38,8	32,6	27,8	24,0	20,9	18,4	16,3	14,5	13,0	11,8	10,7	9,7	8,9	8,2								
62																37,4	31,4	26,8	23,1	20,1	17,7	15,7	14,0	12,5	11,3	10,3	9,3	8,6	7,9								
64																43,4	35,9	30,2	25,7	22,2	19,3	17,0	15,0	13,4	12,0	10,9	9,8	9,0	8,2	7,5							
66																41,6	34,3	28,9	24,6	21,2	18,5	16,2	14,4	12,8	11,5	10,4	9,4	8,6	7,9	7,2							
68																39,6	32,7	27,5	23,4	20,2	17,6	15,5	13,7	12,2	11,0	9,9	9,0	8,2	7,5	6,9							
70																37,6	31,1	26,1	22,3	19,2	16,7	14,7	13,0	11,6	10,4	9,4	8,5	7,8	7,1	6,5							
72																43,9	35,5	29,4	24,7	21,0	18,1	15,8	13,9	12,3	11,0	9,8	8,9	8,1	7,3	6,7	6,2						
74																41,3	33,4	27,6	23,2	19,8	17,1	14,9	13,1	11,6	10,3	9,3	8,4	7,6	6,9	6,3	5,8						
76																38,6	31,2	25,8	21,7	18,5	15,9	13,9	12,2	10,8	9,6	8,7	7,8	7,1	6,5	5,9	5,4						
78																45,3	35,8	29,0	23,9	20,1	17,1	14,8	12,9	11,3	10,0	8,9	8,0	7,2	6,6	6,0	5,5	5,0					
80																41,7	32,9	26,7	22,0	18,5	15,8	13,6	11,9	10,4	9,2	8,2	7,4	6,7	6,0	5,5	5,0	4,6					
82																49,6	37,9	30,0	24,3	20,1	16,9	14,4	12,4	10,8	9,5	8,4	7,5	6,7	6,1	5,5	5,0	4,6	4,2				
84																44,6	34,1	27,0	21,8	18,1	15,2	12,9	11,1	9,7	8,5	7,6	6,7	6,1	5,5	5,0	4,5	4,1	3,8				
86																39,5	30,2	23,9	19,3	16,0	13,4	11,4	9,9	8,6	7,6	6,7	6,0	5,4	4,8	4,4	4,0	3,7	3,4				
88																46,6	34,2	26,2	20,7	16,8	13,9	11,6	9,9	8,6	7,5	6,6	5,8	5,2	4,6	4,2	3,8	3,5	3,2	2,9			
90																39,3	28,9	22,1	17,5	14,1	11,7	9,8	8,4	7,2	6,3	5,5	4,9	4,4	3,9	3,5	3,2	2,9	2,7	2,5			
92																45,8	31,8	23,3	17,9	14,1	11,4	9,5	7,9	6,8	5,8	5,1	4,5	4,0	3,5	3,2	2,9	2,6	2,4	2,2	2,0		
94																34,7	24,1	17,7	13,6	10,7	8,7	7,2	6,0	5,1	4,4	3,9	3,4	3,0	2,7	2,4	2,2	2,0	1,8	1,6	1,5		
96																36,6	23,4	16,3	11,9	9,1	7,2	5,9	4,8	4,1	3,5	3,0	2,6	2,3	2,0	1,8	1,6	1,5	1,3	1,2	1,1	1,0	
98																32,9	18,5	11,8	8,2	6,0	4,6	3,7	3,0	2,4	2,1	1,8	1,5	1,3	1,2	1,0	0,9	0,8	0,7	0,7	0,6	0,6	0,5
100																0,0	0,0	0,0	0,0	0,0	0,0	0,0	0,0	0,0	0,0	0,0	0,0	0,0	0,0	0,0	0,0	0,0	0,0	0,0	0,0	0,0	0,0

Table A.10. Fundamental frequency change in percentage versus axial load level for I160 steel column for different lengths for frequency change

f/f ₀ (%)	Length (m)																							
	0.50	0.75	1.00	1.25	1.50	1.75	2.00	2.25	2.50	2.75	3.00	3.25	3.50	3.75	4.00	4.25	4.50	4.75	5.00	5.25	5.50	5.75	6.00	
0.0	100.0	100.0	100.0	100.0	100.0	100.0	100.0	100.0	100.0	100.0	100.0	100.0	100.0	100.0	100.0	100.0	100.0	100.0	100.0	100.0	100.0	100.0	100.0	100.0
0.5	100.0	100.0	99.9	99.9	99.9	99.9	99.8	99.7	99.7	99.6	99.5	99.4	99.3	99.2	99.1	99.0	98.9	98.8	98.7	98.5	98.4	98.2	98.1	98.1
1.0	100.0	99.9	99.8	99.8	99.8	99.8	99.7	99.6	99.5	99.3	99.2	99.0	98.9	98.7	98.5	98.3	98.0	97.8	97.6	97.3	97.0	96.7	96.4	96.1
1.5	100.0	99.9	99.8	99.7	99.6	99.5	99.4	99.2	99.0	98.8	98.5	98.3	98.0	97.7	97.4	97.1	96.7	96.3	95.9	95.5	95.0	94.5	94.0	94.0
2.0	99.9	99.9	99.8	99.7	99.5	99.3	99.1	98.9	98.7	98.4	98.1	97.7	97.3	96.9	96.5	96.0	95.6	95.0	94.5	94.0	93.5	93.0	92.6	91.9
2.5	99.9	99.8	99.7	99.6	99.4	99.2	98.9	98.6	98.3	98.0	97.6	97.1	96.7	96.2	95.6	95.0	94.4	93.8	93.0	92.1	91.1	90.1	89.7	89.8
3.0	99.9	99.8	99.7	99.5	99.3	99.0	98.7	98.4	98.0	97.5	97.1	96.5	96.0	95.4	94.7	94.0	93.3	92.4	91.6	90.7	89.7	89.7	89.7	89.6
3.5	99.9	99.8	99.6	99.4	99.2	98.8	98.5	98.1	97.6	97.1	96.6	96.0	95.3	94.6	93.8	93.0	92.1	91.1	90.1	89.0	87.9	86.6	85.4	85.4
4.0	99.9	99.8	99.6	99.3	99.0	98.7	98.3	97.8	97.3	96.7	96.1	95.4	94.6	93.8	92.9	91.9	90.9	89.8	88.6	87.3	86.0	84.6	83.0	83.0
4.5	99.9	99.7	99.5	99.2	98.9	98.5	98.1	97.5	96.9	96.3	95.5	94.8	93.9	93.0	91.9	90.8	89.7	88.4	87.1	85.8	84.1	82.4	80.6	80.6
5.0	99.9	99.5	99.2	98.8	98.3	97.8	97.3	96.6	95.9	95.1	94.2	93.2	92.1	91.0	89.8	88.4	87.0	85.5	83.8	82.1	80.2	78.2	76.2	76.2
5.5	99.9	99.7	99.4	99.1	98.7	98.2	97.6	97.0	96.2	95.4	94.5	93.6	92.5	91.3	90.0	88.7	87.2	85.6	83.9	82.0	80.0	77.9	75.6	75.6
6.0	99.8	99.6	99.4	99.0	98.5	98.0	97.4	96.7	95.9	95.0	94.0	92.9	91.8	90.5	89.1	87.6	85.9	84.2	82.2	80.2	77.9	75.5	72.9	72.9
6.5	99.8	99.6	99.3	98.9	98.4	97.8	97.2	96.4	95.5	94.6	93.5	92.3	91.0	89.6	88.1	86.4	84.6	82.7	80.6	78.3	75.8	73.1	70.2	70.2
7.0	99.8	99.6	99.2	98.8	98.3	97.7	97.0	96.1	95.2	94.1	93.0	91.7	90.3	88.8	87.1	85.3	83.3	81.2	78.9	76.3	73.6	70.6	67.3	67.3
7.5	99.8	99.5	99.2	98.7	98.2	97.5	96.7	95.8	94.8	93.7	92.5	91.1	89.6	87.9	86.1	84.1	82.0	79.6	77.1	74.3	71.3	67.9	64.3	64.3
8.0	99.8	99.5	99.1	98.7	98.1	97.3	96.5	95.6	94.5	93.3	91.9	90.5	88.8	87.1	85.1	83.0	80.6	78.1	75.3	72.3	68.9	65.2	61.1	61.1
8.5	99.8	99.5	99.1	98.6	97.9	97.2	96.3	95.3	94.1	92.8	91.4	89.8	88.1	86.2	84.1	81.8	79.2	76.5	73.5	70.1	66.4	62.3	57.7	57.7
9.0	99.8	99.5	99.0	98.5	97.8	97.0	96.1	95.0	93.8	92.4	90.9	89.2	87.3	85.3	83.0	80.6	77.8	74.9	71.6	67.9	63.9	59.3	54.1	54.1
9.5	99.7	99.4	99.0	98.4	97.7	96.8	95.8	94.7	93.4	92.0	90.3	88.5	86.6	84.4	82.0	79.3	76.4	73.2	69.6	65.6	61.2	56.1	50.2	50.2
10.0	99.7	99.4	98.9	98.3	97.6	96.7	95.6	94.4	93.0	91.5	89.7	87.9	85.8	83.5	80.9	78.1	74.9	71.5	67.6	63.3	58.4	52.7	46.0	46.0
10.5	99.7	99.4	98.9	98.2	97.4	96.5	95.4	94.1	92.7	91.1	89.3	87.2	85.0	82.5	79.8	76.8	73.4	69.7	65.5	60.8	55.4	49.1	41.4	41.4
11.0	99.7	99.3	98.8	98.1	97.3	96.3	95.2	93.8	92.3	90.6	88.7	86.6	84.2	81.6	78.7	75.5	71.9	67.9	63.4	58.2	52.3	45.1	36.2	36.2
11.5	99.7	99.3	98.8	98.1	97.2	96.2	94.9	93.5	92.0	90.2	88.2	85.9	83.4	80.7	77.6	74.2	70.3	66.0	61.2	55.5	48.9	40.8	30.0	30.0
12.0	99.7	99.3	98.7	98.0	97.1	96.0	94.7	93.3	91.6	89.7	87.6	85.3	82.6	79.7	76.5	72.8	68.7	64.1	58.8	52.7	45.3	36.9	22.2	22.2
12.5	99.7	99.2	98.7	97.9	96.9	95.8	94.5	93.0	91.2	89.3	87.1	84.6	81.8	78.7	75.3	71.4	67.1	62.1	56.4	49.7	41.4	30.3	8.9	8.9
13.0	99.7	99.2	98.6	97.8	96.8	95.6	94.3	92.7	90.9	88.8	86.5	83.9	81.0	77.8	74.1	70.0	65.4	60.1	53.9	46.5	37.0	23.2	12.8	12.8
13.5	99.6	99.2	98.5	97.7	96.7	95.5	94.0	92.4	90.5	88.3	85.9	83.2	80.2	76.8	72.9	68.6	63.7	58.0	51.2	43.0	32.1	18.8	12.8	12.8
14.0	99.6	99.2	98.5	97.6	96.6	95.3	93.8	92.1	90.1	87.9	85.4	82.5	79.3	75.8	71.7	67.1	61.9	55.8	48.4	39.2	26.2	12.8	12.8	12.8
14.5	99.6	99.1	98.4	97.5	96.4	95.1	93.6	91.8	89.7	87.4	84.8	81.8	78.5	74.7	70.5	65.6	60.0	53.4	45.4	35.0	21.4	18.8	12.8	12.8
15.0	99.6	99.1	98.4	97.5	96.3	94.9	93.3	91.5	89.4	87.4	84.2	81.1	77.6	73.7	69.2	64.1	58.1	51.0	42.2	30.2	18.8	12.8	12.8	12.8
15.5	99.6	99.1	98.3	97.4	96.2	94.8	93.1	91.2	89.0	86.5	83.6	80.4	76.8	72.6	67.9	62.5	56.2	48.5	38.7	24.5	18.8	12.8	12.8	12.8
16.0	99.6	99.0	98.3	97.3	96.1	94.6	92.9	90.9	88.6	86.0	83.0	79.7	75.9	71.6	66.6	60.9	54.1	45.8	34.9	16.9	18.8	12.8	12.8	12.8
16.5	99.6	99.0	98.2	97.2	95.9	94.4	92.6	90.6	88.2	85.5	82.4	79.0	75.0	70.5	65.3	59.2	52.0	42.9	30.6	18.8	12.8	12.8	12.8	12.8
17.0	99.5	99.0	98.2	97.1	95.8	94.2	92.4	90.3	87.8	85.0	81.8	78.2	74.1	69.4	63.9	57.5	49.7	39.9	25.5	18.8	12.8	12.8	12.8	12.8
17.5	99.5	98.9	98.1	97.0	95.7	94.1	92.2	90.0	87.4	84.5	81.2	77.5	73.2	68.2	62.5	55.7	47.4	36.5	19.1	18.8	12.8	12.8	12.8	12.8
18.0	99.5	98.9	98.1	96.9	95.6	93.9	91.9	89.7	87.1	84.1	80.6	76.7	72.3	67.1	61.1	53.9	44.9	32.8	8.9	18.8	12.8	12.8	12.8	12.8
18.5	99.5	98.9	98.0	96.9	95.4	93.7	91.7	89.4	86.7	83.6	80.0	76.0	71.3	65.9	59.6	52.0	42.3	28.7	18.8	12.8	12.8	12.8	12.8	12.8
19.0	99.5	98.8	97.9	96.8	95.3	93.5	91.5	89.1	86.3	83.1	79.4	75.2	70.4	64.7	58.1	50.0	39.5	23.8	18.8	12.8	12.8	12.8	12.8	12.8
19.5	99.5	98.8	97.8	96.7	95.2	93.4	91.2	88.7	85.9	82.6	78.7	74.4	69.4	63.5	56.5	47.9	36.5	17.6	7.2	18.8	12.8	12.8	12.8	12.8
20.0	99.5	98.8	97.8	96.6	95.1	93.2	91.0	88.4	85.5	82.1	78.2	73.6	68.4	62.3	54.9	45.7	33.2	7.2	18.8	12.8	12.8	12.8	12.8	12.8
20.5	99.5	98.8	97.8	96.5	94.9	93.0	90.8	88.1	85.1	81.6	77.5	72.9	67.4	61.0	53.3	43.5	29.6	18.8	12.8	12.8	12.8	12.8	12.8	12.8
21.0	99.4	98.7	97.7	96.4	94.8	92.8	90.5	87.8	84.7	81.1	76.9	72.1	66.4	59.7	51.6	41.1	25.4	18.8	12.8	12.8	12.8	12.8	12.8	12.8
21.5	99.4	98.7	97.7	96.3	94.7	92.7	90.3	87.5	84.3	80.6	76.2	71.2	65.4	58.4	49.8	38.5	20.3	18.8	12.8	12.8	12.8	12.8	12.8	12.8
22.0	99.4	98.7	97.6	96.2	94.5	92.5	90.0	87.2	83.9	80.0	75.6	70.4	64.3	57.0	48.0	35.7	13.5	18.8	12.8	12.8	12.8	12.8	12.8	12.8
22.5	99.4	98.6	97.6	96.2	94.4	92.3	89.8	86.9	83.5	79.5	74.9	69.6	63.3	55.6	46.0	32.7	18.8	12.8	12.8	12.8	12.8	12.8	12.8	12.8
23.0	99.4	98.6	97.5	96.1	94.3	92.1	89.6	86.6	83.1	79.0	74.3	68.7	62.2	54.2	44.0	29.5	18.8	12.8	12.8	12.8	12.8	12.8	12.8	12.8
23.5	99.4	98.6	97.5	96.0	94.2	91.9	89.3	86.2	82.7	78.5	73.6	67.9	61.1	52.7	42.0	25.7	18.8	12.8	12.8	12.8	12.8	12.8	12.8	12.8
24.0	99.4	98.5	97.4	95.9	94.0	91.8	89.1	85.9	82.2	77.9	72.9	67.0	60.0	51.2	39.7	21.4	18.8	12.8	12.8	12.8	12.8	12.8	12.8	12.8
24.5	99.3	98.5	97.3	95.8	93.9	91.6	88.8	85.6	81.8	77.4	72.3	66.2	59.8	49.7	37.4	15.8	18.8	12.8	12.8	12.8	12.8	12.8	12.8	12.8
25.0	99.3	98.5	97.3	95.7	93.8	91.4	88.6	85.3	81.4	76.9	71.6	65.3	57.6	48.1	34.9	6.6	18.8	12.8	12.8	12.8	12.8	12.8	12.8	12.8
25.5	99.3	98.5	97.2	95.6	93.6	91.2	88.3	85.0	81.0	76.3	70.9	64.4	56.4	46.4	32.2	18.8	12.8	12.8	12.8	12.8	12.8	12.8	12.8	12.8
26.0	99.3	98.4	97.2	95.5	93.5																			

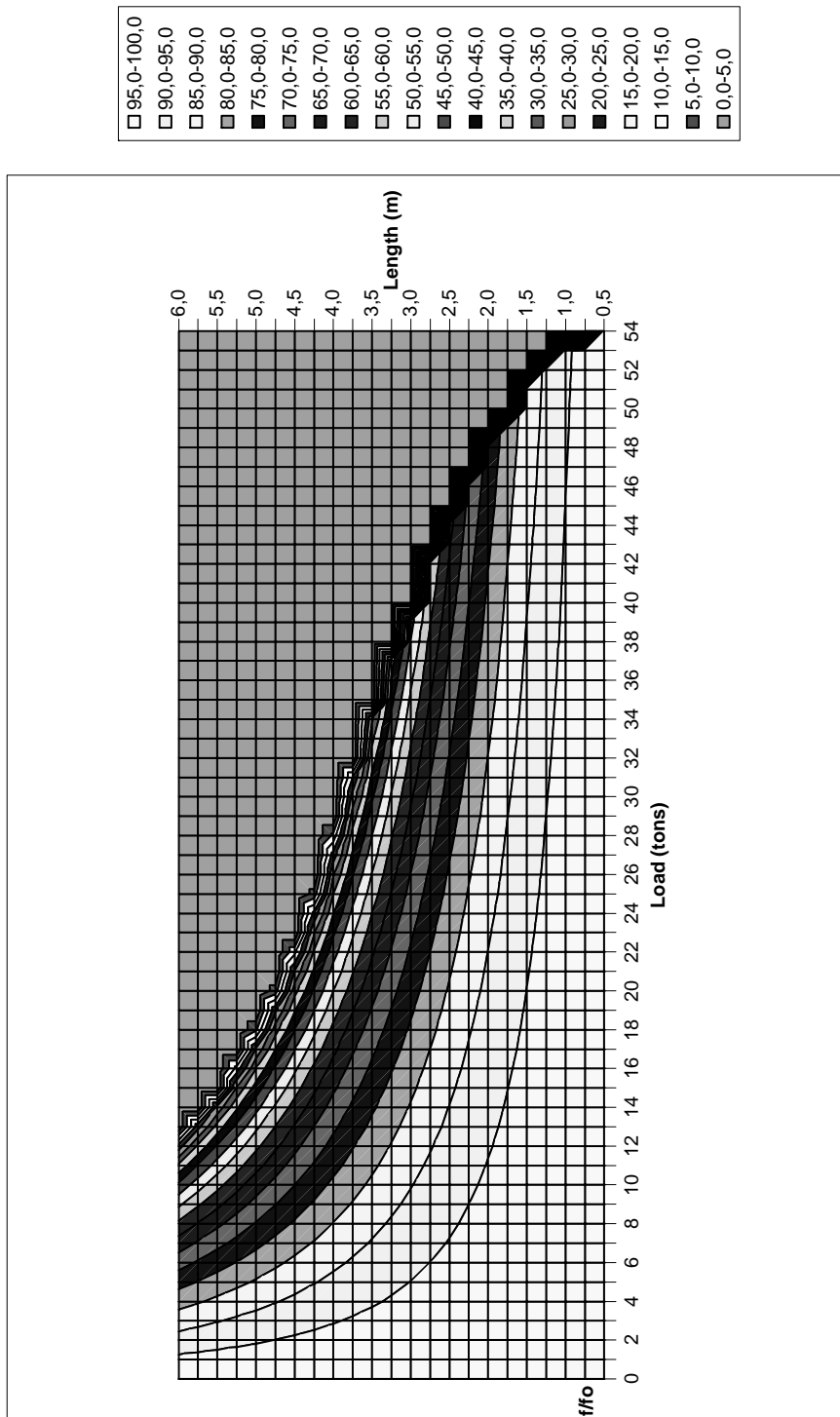


Figure A.5: Contour lines of the first vibration frequency ratios of the I160 steel column (in percentage) for certain lengths and loads

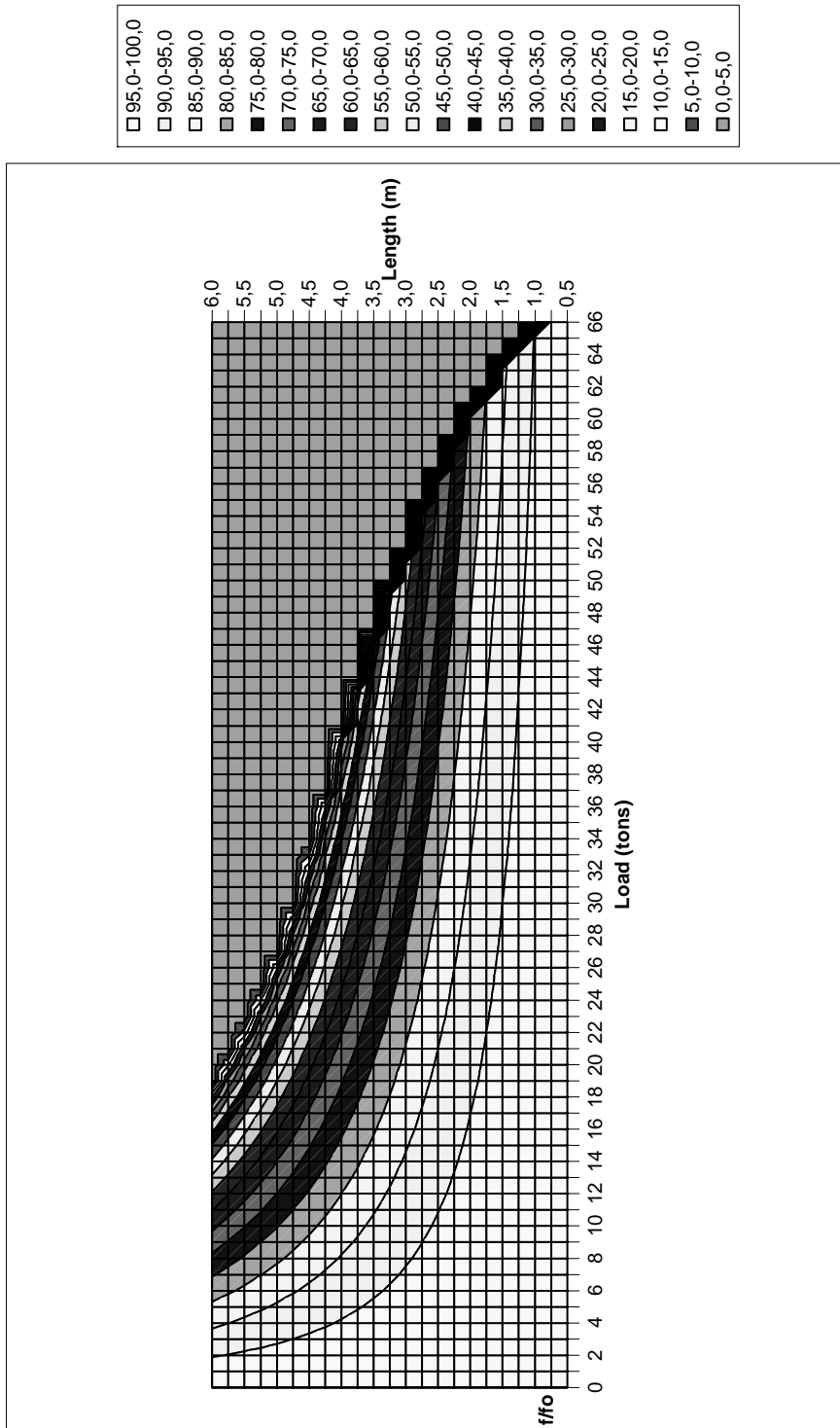


Figure A.6: Contour lines of the first vibration frequency ratios of the I180 steel column (in percentage) for certain lengths and loads

Table A.14. Fundamental frequency change in percentage versus axial load level for I200 steel column for different lengths for frequency change

f/f ₀ (%)	Length (m)																							
	0,50	0,75	1,00	1,25	1,50	1,75	2,00	2,25	2,50	2,75	3,00	3,25	3,50	3,75	4,00	4,25	4,50	4,75	5,00	5,25	5,50	5,75	6,00	
0	100,0	100,0	100,0	100,0	100,0	100,0	100,0	100,0	100,0	100,0	100,0	100,0	100,0	100,0	100,0	100,0	100,0	100,0	100,0	100,0	100,0	100,0	100,0	100,0
1	100,0	100,0	99,9	99,9	99,8	99,8	99,8	99,7	99,7	99,6	99,5	99,5	99,4	99,3	99,2	99,1	99,0	98,9	98,7	98,6	98,5	98,4	98,3	98,2
2	100,0	99,9	99,9	99,8	99,8	99,7	99,6	99,5	99,4	99,2	99,1	98,9	98,8	98,6	98,4	98,2	98,0	97,7	97,5	97,2	96,9	96,6	96,3	96,3
3	100,0	99,9	99,8	99,8	99,7	99,5	99,4	99,2	99,1	98,9	98,6	98,4	98,1	97,9	97,6	97,2	96,9	96,5	96,2	95,8	95,3	94,9	94,4	94,4
4	99,9	99,9	99,8	99,7	99,5	99,4	99,2	99,0	98,7	98,5	98,2	97,9	97,5	97,1	96,7	96,3	95,9	95,4	94,9	94,3	93,7	93,1	92,5	92,5
5	99,9	99,9	99,7	99,6	99,4	99,2	99,0	98,7	98,4	98,1	97,7	97,3	96,9	96,4	95,9	95,4	94,8	94,2	93,5	92,8	92,1	91,3	90,5	90,5
6	99,9	99,8	99,7	99,5	99,3	99,1	98,8	98,5	98,1	97,7	97,3	96,8	96,2	95,7	95,1	94,4	93,7	93,0	92,2	91,3	90,4	89,5	88,5	88,5
7	99,9	99,8	99,6	99,5	99,2	98,9	98,6	98,2	97,8	97,3	96,8	96,2	95,6	94,9	94,2	93,4	92,6	91,7	90,8	89,8	88,7	87,6	86,4	86,4
8	99,9	99,8	99,6	99,4	99,1	98,8	98,4	98,0	97,5	96,9	96,3	95,7	95,0	94,2	93,4	92,5	91,5	90,5	89,4	88,2	87,0	85,6	84,2	84,2
9	99,9	99,7	99,5	99,3	99,0	98,6	98,2	97,7	97,1	96,5	95,9	95,1	94,3	93,4	92,5	91,5	90,4	89,2	88,0	86,6	85,2	83,7	82,0	82,0
10	99,9	99,7	99,5	99,2	98,9	98,5	98,0	97,4	96,8	96,1	95,4	94,6	93,7	92,7	91,6	90,5	89,2	87,9	86,5	85,0	83,4	81,6	79,8	79,8
11	99,9	99,7	99,4	99,1	98,8	98,3	97,8	97,2	96,5	95,7	94,9	94,0	93,0	91,9	90,7	89,5	88,1	86,6	85,0	83,3	81,5	79,5	77,4	77,4
12	99,8	99,7	99,4	99,1	98,6	98,1	97,6	96,9	96,2	95,3	94,4	93,4	92,3	91,1	89,8	88,4	86,9	85,3	83,5	81,6	79,6	77,4	75,0	75,0
13	99,8	99,6	99,3	99,0	98,5	98,0	97,4	96,6	95,8	94,9	93,9	92,9	91,7	90,3	88,9	87,4	85,7	83,9	82,0	79,9	77,6	75,2	72,5	72,5
14	99,8	99,6	99,3	98,9	98,4	97,8	97,2	96,4	95,5	94,5	93,5	92,3	91,0	89,6	88,0	86,3	84,5	82,5	80,4	78,1	75,6	72,9	69,9	69,9
15	99,8	99,6	99,2	98,8	98,3	97,7	96,9	96,1	95,2	94,1	93,0	91,7	90,3	88,8	87,1	85,3	83,3	81,1	78,8	76,4	73,5	70,5	67,2	67,2
16	99,8	99,5	99,2	98,7	98,2	97,5	96,7	95,9	94,9	93,7	92,5	91,1	89,6	88,0	86,2	84,2	82,0	79,7	77,2	74,4	71,4	68,0	64,4	64,4
17	99,8	99,5	99,1	98,7	98,1	97,4	96,5	95,6	94,5	93,3	92,0	90,5	88,9	87,1	85,2	83,1	80,8	78,3	75,5	72,5	69,2	65,5	61,4	61,4
18	99,8	99,5	99,1	98,6	98,0	97,2	96,3	95,3	94,2	92,9	91,5	89,9	88,2	86,3	84,2	82,0	79,5	76,8	73,8	70,5	66,9	62,8	58,3	58,3
19	99,8	99,5	99,0	98,5	97,8	97,0	96,1	95,1	93,9	92,5	91,0	89,3	87,5	85,5	83,3	80,8	78,2	75,2	72,0	68,4	64,5	60,0	55,0	55,0
20	99,7	99,4	99,0	98,4	97,7	96,9	95,9	94,8	93,5	92,1	90,5	88,7	86,8	84,7	82,3	79,7	76,8	73,7	70,2	66,3	62,0	57,1	51,4	51,4
21	99,7	99,4	98,9	98,3	97,6	96,7	95,7	94,5	93,2	91,7	90,0	88,1	86,1	83,8	81,3	78,5	75,2	71,8	68,3	64,1	59,4	54,0	47,6	47,6
22	99,7	99,4	98,9	98,3	97,5	96,6	95,5	94,2	92,8	91,3	89,5	87,5	85,4	82,9	80,3	77,3	74,1	70,5	66,4	61,9	56,7	50,7	43,5	43,5
23	99,7	99,4	98,8	98,2	97,4	96,4	95,3	94,0	92,5	90,8	89,0	86,9	84,6	82,1	79,3	76,1	72,7	68,8	64,5	59,5	53,8	47,1	38,8	38,8
24	99,7	99,3	98,8	98,1	97,3	96,2	95,1	93,7	92,2	90,4	88,5	86,3	83,9	81,2	78,2	74,9	71,2	67,1	62,4	57,1	50,8	43,3	33,6	33,6
25	99,7	99,3	98,7	98,0	97,1	96,1	94,9	93,4	91,8	90,0	88,0	85,7	83,1	80,3	77,2	73,7	69,7	65,3	60,3	54,5	47,6	39,0	27,3	27,3
26	99,7	99,3	98,7	98,0	97,1	96,1	94,9	93,4	91,8	90,0	88,0	85,7	83,1	80,3	77,2	73,7	69,7	65,3	60,3	54,5	47,6	39,0	27,3	27,3
27	99,7	99,2	98,6	97,9	96,9	95,8	94,4	92,9	91,1	89,1	86,9	84,4	81,6	78,5	75,0	71,1	66,7	61,6	55,8	48,9	40,3	28,7	28,7	28,7
28	99,6	99,2	98,6	97,8	96,8	95,6	94,2	92,6	90,8	88,7	86,4	83,8	80,9	77,6	73,9	69,8	65,1	59,7	53,4	45,8	36,2	21,7	21,7	21,7
29	99,6	99,2	98,5	97,7	96,7	95,4	94,0	92,3	90,4	88,3	85,9	83,1	80,1	76,6	72,8	68,4	63,5	57,2	50,9	42,6	31,4	10,9	10,9	10,9
30	99,6	99,2	98,5	97,6	96,6	95,3	93,8	92,1	90,1	87,8	85,3	82,5	79,3	75,7	71,7	67,1	61,8	55,6	48,3	39,0	25,8	18,6	18,6	18,6
31	99,6	99,1	98,4	97,5	96,4	95,1	93,6	91,8	89,7	87,4	84,8	81,8	78,5	74,7	70,5	65,7	60,1	53,5	45,5	35,1	25,1	18,6	18,6	18,6
32	99,6	99,1	98,4	97,5	96,3	95,0	93,4	91,5	89,4	87,0	84,2	81,2	77,7	73,8	69,3	64,2	58,3	51,2	42,5	30,6	22,5	18,6	18,6	18,6
33	99,6	99,1	98,3	97,4	96,2	94,8	93,1	91,2	89,0	86,5	83,7	80,5	76,9	72,8	68,1	62,7	56,4	48,9	39,3	25,4	18,6	18,6	18,6	18,6
34	99,6	99,0	98,3	97,3	96,1	94,6	92,9	90,9	88,7	86,1	83,2	79,8	76,1	71,8	66,9	61,2	54,5	46,3	37,5	27,1	18,7	18,7	18,7	18,7
35	99,6	99,0	98,2	97,2	96,0	94,5	92,7	90,7	88,3	85,6	82,6	79,2	75,2	70,8	65,6	59,7	52,6	43,7	31,8	7,5	18,7	18,7	18,7	18,7
36	99,5	99,0	98,2	97,1	95,9	94,3	92,5	90,4	88,0	85,2	82,0	78,5	74,4	69,7	64,4	58,1	50,5	40,9	27,3	18,7	18,7	18,7	18,7	18,7
37	99,5	99,0	98,1	97,1	95,7	94,1	92,3	90,1	87,6	84,7	81,5	77,8	73,5	68,7	63,1	56,4	48,4	37,9	21,9	18,7	18,7	18,7	18,7	18,7
38	99,5	98,9	98,1	97,0	95,6	94,0	92,1	89,8	87,2	84,3	80,9	77,1	72,7	67,6	61,7	54,7	46,1	34,6	14,6	18,7	18,7	18,7	18,7	18,7
39	99,5	98,9	98,0	96,9	95,5	93,8	91,8	89,5	86,9	83,8	80,3	76,4	71,8	66,6	60,4	53,0	43,7	31,0	18,7	18,7	18,7	18,7	18,7	18,7
40	99,5	98,9	98,0	96,8	95,4	93,7	91,6	89,2	86,5	83,4	79,8	75,7	70,9	65,4	59,0	51,2	41,2	26,8	18,7	18,7	18,7	18,7	18,7	18,7
41	99,5	98,8	97,9	96,7	95,3	93,5	91,4	89,0	86,1	82,9	79,2	74,9	70,0	64,3	57,6	49,3	38,5	21,9	18,7	18,7	18,7	18,7	18,7	18,7
42	99,5	98,8	97,9	96,7	95,1	93,3	91,2	88,7	85,8	82,4	78,6	74,2	69,1	63,2	56,1	47,3	35,7	15,5	18,7	18,7	18,7	18,7	18,7	18,7
43	99,5	98,8	97,8	96,6	95,0	93,2	90,9	88,4	85,4	82,0	78,0	73,5	68,2	62,0	54,6	45,3	32,5	18,7	18,7	18,7	18,7	18,7	18,7	18,7
44	99,4	98,8	97,8	96,5	94,9	93,0	90,7	88,1	85,0	81,5	77,4	72,7	67,3	60,8	53,0	43,1	29,0	18,7	18,7	18,7	18,7	18,7	18,7	18,7
45	99,4	98,7	97,7	96,4	94,8	92,8	90,5	87,8	84,7	81,0	76,8	72,0	66,3	59,6	51,4	40,9	25,0	18,7	18,7	18,7	18,7	18,7	18,7	18,7
46	99,4	98,7	97,7	96,3	94,7	92,7	90,3	87,5	84,3	80,5	76,2	71,2	65,4	58,4	49,8	38,5	20,3	18,7	18,7	18,7	18,7	18,7	18,7	18,7
47	99,4	98,7	97,6	96,2	94,5	92,5	90,1	87,2	83,9	80,1	75,6	70,5	64,4	57,1	48,1	35,9	18,7	18,7	18,7	18,7	18,7	18,7	18,7	18,7
48	99,4	98,6	97,6	96,2	94,4	92,3	89,8	86,9	83,5	79,6	75,0	69,7	63,4	55,8	46,3	33,1	18,7	18,7	18,7	18,7	18,7	18,7	18,7	18,7
49	99,4	98,6	97,5	96,1	94,3	92,2	89,6	86,6	83,1	79,1	74,4	68,9	62,4	54,5	44,4	30,1	18,7	18,7	18,7	18,7	18,7	18,7	18,7	18,7
50	99,4	98,6	97,5	96,0	94,2	92,0	89,4	86,3	82,8	78,6	73,8	68,1	61,4	53,1	42,5	26,7	18,7	18,7	18,7	18,7	18,7	18,7	18,7	18,7
51	99,4	98,6	97,4	95,9	94,1	91,8	89,2	86,0	82,4	78,1	73,1	67,3	60,3	51,7	40,4	18,7	18,7	18,7	18,7	18,7	18,7	18,7	18,7	18,7
52	99,3	98,5	97,4	95,8	93,9	91,7	88,9	85,7	82,0	77,6	72,5	66,5	59,3	50,3	38,3	1								

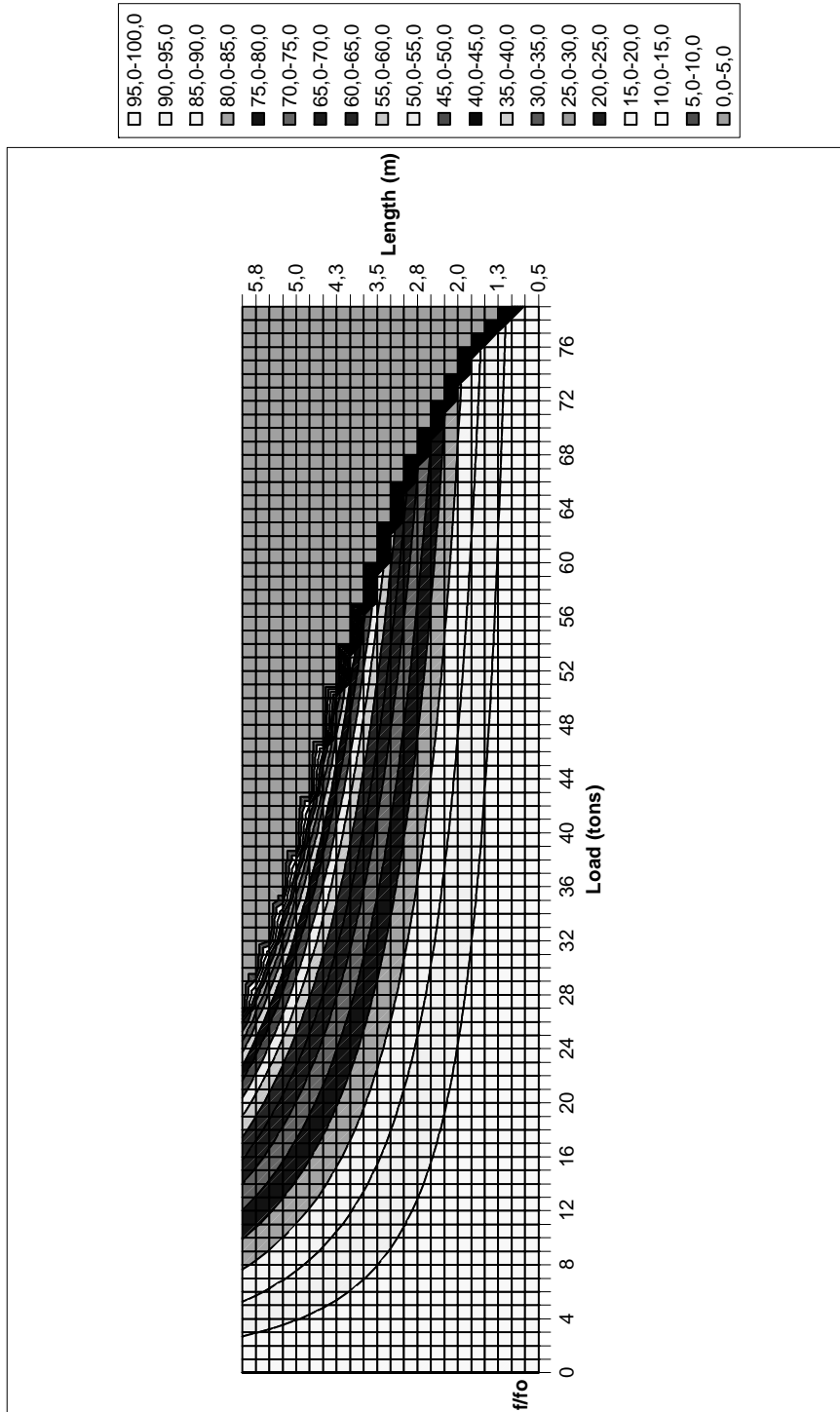


Figure A.7: Contour lines of the first vibration frequency ratios of the I200 steel column (in percentage) for certain lengths and loads

Table A.16. Fundamental frequency change in percentage versus axial load level for I220 steel column for different lengths for frequency change

f/f ₀ (%)	Length (m)																							
	0.50	0.75	1.00	1.25	1.50	1.75	2.00	2.25	2.50	2.75	3.00	3.25	3.50	3.75	4.00	4.25	4.50	4.75	5.00	5.25	5.50	5.75	6.00	
0	100.0	100.0	100.0	100.0	100.0	100.0	100.0	100.0	100.0	100.0	100.0	100.0	100.0	100.0	100.0	100.0	100.0	100.0	100.0	100.0	100.0	100.0	100.0	100.0
1	100.0	100.0	100.0	99.9	99.9	99.9	99.9	99.9	99.8	99.8	99.7	99.7	99.6	99.6	99.5	99.4	99.3	99.2	99.1	99.0	98.9	98.8	98.8	98.7
2	100.0	100.0	99.9	99.9	99.8	99.8	99.7	99.6	99.5	99.5	99.3	99.2	99.1	99.0	98.8	98.7	98.5	98.4	98.2	98.0	97.8	97.6	97.4	97.4
3	100.0	99.9	99.8	99.8	99.7	99.6	99.4	99.3	99.1	98.9	98.7	98.5	98.2	98.0	97.8	97.5	97.2	97.0	96.7	96.3	95.9	95.5	95.1	94.6
4	100.0	99.9	99.8	99.7	99.6	99.4	99.3	99.1	98.9	98.6	98.4	98.1	97.8	97.4	97.1	96.7	96.3	95.8	95.4	94.9	94.4	93.8	93.2	92.6
5	100.0	99.9	99.8	99.7	99.5	99.3	99.1	98.9	98.6	98.3	98.0	97.7	97.3	96.9	96.5	96.0	95.5	95.0	94.4	93.8	93.2	92.6	92.0	91.4
6	99.9	99.9	99.8	99.7	99.5	99.3	99.1	98.9	98.6	98.3	98.0	97.7	97.3	96.9	96.5	96.0	95.5	95.0	94.4	93.8	93.2	92.6	92.0	91.4
7	99.9	99.9	99.7	99.6	99.4	99.2	99.0	98.7	98.4	98.1	97.7	97.3	96.8	96.4	95.9	95.3	94.7	94.1	93.4	92.7	92.0	91.2	90.4	89.6
8	99.9	99.8	99.7	99.5	99.3	99.1	98.8	98.5	98.2	97.8	97.4	96.9	96.4	95.8	95.3	94.6	93.9	93.2	92.5	91.7	90.8	89.9	88.9	87.9
9	99.9	99.8	99.7	99.5	99.3	99.0	98.7	98.3	97.9	97.5	97.0	96.5	95.9	95.3	94.6	93.9	93.2	92.3	91.5	90.6	89.6	88.5	87.4	86.3
10	99.9	99.8	99.6	99.4	99.2	98.9	98.5	98.2	97.7	97.2	96.7	96.1	95.5	94.8	94.0	93.2	92.4	91.5	90.5	89.4	88.3	87.2	85.9	84.6
11	99.9	99.8	99.6	99.4	99.1	98.8	98.4	98.0	97.5	96.9	96.4	95.7	95.0	94.2	93.4	92.5	91.6	90.5	89.5	88.3	87.1	85.8	84.4	83.0
12	99.9	99.8	99.6	99.3	99.0	98.7	98.2	97.8	97.2	96.7	96.0	95.3	94.5	93.7	92.8	91.8	90.8	89.6	88.4	87.2	85.8	84.3	82.8	81.3
13	99.9	99.7	99.5	99.3	98.9	98.6	98.1	97.6	97.0	96.4	95.7	94.9	94.1	93.1	92.1	91.1	89.9	88.7	87.4	86.0	84.5	82.9	81.2	79.5
14	99.9	99.7	99.5	99.2	98.9	98.4	98.0	97.4	96.8	96.1	95.3	94.5	93.6	92.6	91.5	90.4	89.1	87.8	86.3	84.8	83.2	81.4	79.5	77.5
15	99.9	99.7	99.5	99.1	98.8	98.3	97.8	97.2	96.5	95.8	95.0	94.1	93.1	92.0	90.9	89.6	88.3	86.8	85.3	83.6	81.8	79.9	77.8	75.7
16	99.9	99.7	99.4	99.1	98.7	98.2	97.7	97.0	96.3	95.5	94.6	93.7	92.6	91.5	90.2	88.9	87.4	85.9	84.2	82.4	80.5	78.5	76.4	74.2
17	99.8	99.7	99.4	99.0	98.6	98.1	97.5	96.8	96.1	95.2	94.3	93.3	92.1	90.9	89.6	88.1	86.6	84.9	83.1	81.1	79.0	76.8	74.3	71.8
18	99.8	99.6	99.3	99.0	98.5	98.0	97.4	96.6	95.8	94.9	93.9	92.9	91.7	90.3	88.9	87.4	85.7	83.9	82.0	79.9	77.6	75.2	72.5	69.8
19	99.8	99.6	99.3	98.9	98.4	97.9	97.2	96.5	95.6	94.7	93.6	92.4	91.2	89.8	88.3	86.6	84.9	82.9	80.9	78.6	76.2	73.5	70.6	67.6
20	99.8	99.6	99.3	98.9	98.4	97.8	97.1	96.3	95.4	94.4	93.2	92.0	90.7	89.2	87.6	85.9	84.0	81.9	79.7	77.3	74.7	71.8	68.7	65.6
21	99.8	99.6	99.2	98.8	98.3	97.6	96.9	96.1	95.1	94.1	92.9	91.6	90.2	88.6	86.9	85.1	83.1	80.9	78.5	76.0	73.2	70.1	66.7	63.2
22	99.8	99.6	99.2	98.7	98.2	97.5	96.8	95.9	94.9	93.8	92.5	91.2	89.7	88.0	86.3	84.3	82.2	79.9	77.4	74.6	71.6	68.3	64.7	61.0
23	99.8	99.5	99.2	98.7	98.1	97.4	96.6	95.7	94.7	93.5	92.2	90.8	89.2	87.5	85.6	83.5	81.3	78.8	76.1	73.2	70.0	66.5	62.6	58.6
24	99.8	99.5	99.1	98.6	98.0	97.3	96.5	95.5	94.4	93.2	91.8	90.3	88.7	86.9	84.9	82.7	80.3	77.8	74.9	71.8	68.4	64.6	60.4	56.0
25	99.8	99.5	99.1	98.6	97.9	97.2	96.3	95.3	94.2	92.9	91.5	89.9	88.2	86.3	84.2	81.9	79.4	76.7	73.7	70.4	66.7	62.7	58.1	53.5
26	99.8	99.5	99.1	98.5	97.9	97.1	96.2	95.1	93.9	92.6	91.1	89.5	87.7	85.7	83.5	81.1	78.5	75.6	72.4	68.9	65.0	60.7	55.7	50.7
27	99.8	99.4	99.0	98.5	97.8	97.0	96.0	94.9	93.7	92.3	90.8	89.0	87.2	85.1	82.8	80.3	77.5	74.5	71.1	67.4	63.2	58.6	53.2	47.8
28	99.7	99.4	99.0	98.4	97.7	96.8	95.9	94.7	93.4	92.0	90.4	88.6	86.6	84.5	82.1	79.4	76.5	73.3	69.8	65.9	61.4	56.4	50.6	44.9
29	99.7	99.4	98.9	98.3	97.6	96.7	95.7	94.5	93.2	91.7	90.0	88.2	86.1	83.8	81.3	78.6	75.6	72.2	68.4	64.3	59.6	54.2	47.8	41.4
30	99.7	99.4	98.9	98.3	97.5	96.6	95.6	94.3	93.0	91.4	89.7	87.7	85.6	83.2	80.6	77.7	74.6	71.0	67.1	62.6	57.6	51.8	44.9	38.3
31	99.7	99.4	98.9	98.2	97.4	96.5	95.4	94.1	92.7	91.1	89.3	87.3	85.1	82.6	79.9	76.9	73.5	69.8	65.7	61.0	55.6	49.3	41.7	35.1
32	99.7	99.3	98.8	98.2	97.4	96.4	95.3	93.9	92.5	90.8	88.9	86.8	84.5	82.0	79.1	76.0	72.5	68.6	64.2	59.3	53.5	46.7	38.3	31.7
33	99.7	99.3	98.8	98.1	97.3	96.3	95.1	93.8	92.2	90.5	88.6	86.4	84.0	81.3	78.4	75.1	71.5	67.4	62.8	57.5	51.3	43.9	34.5	27.9
34	99.7	99.3	98.8	98.1	97.2	96.2	94.9	93.6	92.0	90.2	88.2	86.0	83.5	80.7	77.6	74.2	70.4	66.1	61.2	55.6	49.0	41.0	30.3	23.7
35	99.7	99.3	98.7	98.0	97.1	96.0	94.8	93.4	91.7	89.9	87.8	85.5	82.9	80.1	76.9	73.3	69.3	64.8	59.7	53.7	46.7	37.8	25.3	18.7
36	99.7	99.3	98.7	97.9	97.0	95.9	94.6	93.2	91.5	89.6	87.4	85.0	82.4	79.4	76.1	72.4	68.2	63.5	58.1	51.8	44.1	34.3	19.1	12.5
37	99.7	99.2	98.7	97.9	96.9	95.8	94.5	93.0	91.2	89.3	87.1	84.6	81.8	78.8	75.3	71.5	67.1	62.2	56.5	49.7	41.4	30.4	9.2	3.6
38	99.7	99.2	98.6	97.8	96.9	95.7	94.3	92.8	91.0	89.0	86.7	84.1	81.3	78.1	74.5	70.5	66.0	60.8	54.8	47.6	38.5	25.8	12.1	5.5
39	99.6	99.2	98.6	97.8	96.8	95.6	94.2	92.6	90.7	88.6	86.3	83.7	80.7	77.4	73.7	69.6	64.8	59.4	53.0	45.3	35.4	20.3	13.7	7.1
40	99.6	99.2	98.5	97.7	96.7	95.5	94.0	92.4	90.5	88.3	85.9	83.2	80.2	76.8	72.9	68.6	63.6	57.9	51.2	42.9	32.0	12.6	5.9	0.0
41	99.6	99.2	98.5	97.7	96.6	95.3	93.9	92.2	90.2	88.0	85.5	82.7	79.6	76.1	72.1	67.6	62.4	56.5	49.3	40.4	28.1	12.0	5.4	0.0
42	99.6	99.1	98.5	97.6	96.5	95.2	93.7	92.0	90.0	87.7	85.1	82.3	79.0	75.4	71.3	66.6	61.2	54.9	47.4	37.7	23.6	11.5	4.9	0.0
43	99.6	99.1	98.4	97.5	96.4	95.1	93.6	91.8	89.7	87.4	84.8	81.8	78.5	74.7	70.4	65.6	60.0	53.4	45.3	34.8	18.1	11.0	4.4	0.0
44	99.6	99.1	98.4	97.5	96.4	95.0	93.4	91.6	89.5	87.1	84.4	81.3	77.9	74.0	69.6	64.5	58.7	51.7	43.2	31.7	9.7	10.5	3.9	0.0
45	99.6	99.1	98.4	97.4	96.3	94.9	93.2	91.4	89.2	86.7	84.0	80.8	77.3	73.3	68.7	63.5	57.4	50.1	40.9	28.1	10.0	10.0	3.4	0.0
46	99.6	99.1	98.3	97.4	96.2	94.8	93.1	91.2	88.9	86.4	83.6	80.4	76.7	72.6	67.8	62.4	56.0	48.3	38.5	24.1	10.0	10.0	2.9	0.0
47	99.6	99.0	98.3	97.3	96.1	94.6	92.9	91.0	88.7	86.1	83.2	79.9	76.1	71.8	67.0	61.3	54.6	46.5	35.9	19.2	10.0	10.0	2.4	0.0
48	99.6	99.0	98.2	97.2	96.0	94.5	92.8	90.8	88.4	85.8	82.8	79.4	75.5	71.1	66.1	60.2	53.2	44.6	33.2	12.4	10.0	10.0	1.9	0.0
49	99.6	99.0	98.2	97.2	95.9	94.4	92.6	90.6	88.2	85.5	82.4	78.9	74.9	70.4	65.2	59.1	51.8	42.7	30.1	10.0	10.0	10.0	1.4	0.0
50	99.5	99.0	98.2	97.1	95.8	94.3	92.5	90.3	87.9	85.1	82.0	78.4	74.3	69.6	64.2	57.9	50.3	40.6	26.8	10.0	10.0	10.0	0.9	0.0
51	99.5	99.0	98.1	97.1	95.8	94.2	92.3	90.1	87.7	84.8	81.6	77.9	73.7	68.9	63.3	56.7	48.7	38.4	22.9	10.0	10.0	10.0	0.4	0.0
52	99.5	98.9	98.1	97.0	95.7	94.1	92.1	89.9	87.4	84.5	81.2	77.4	73.1	68.1	62.3	55.5	47.1	36.1						

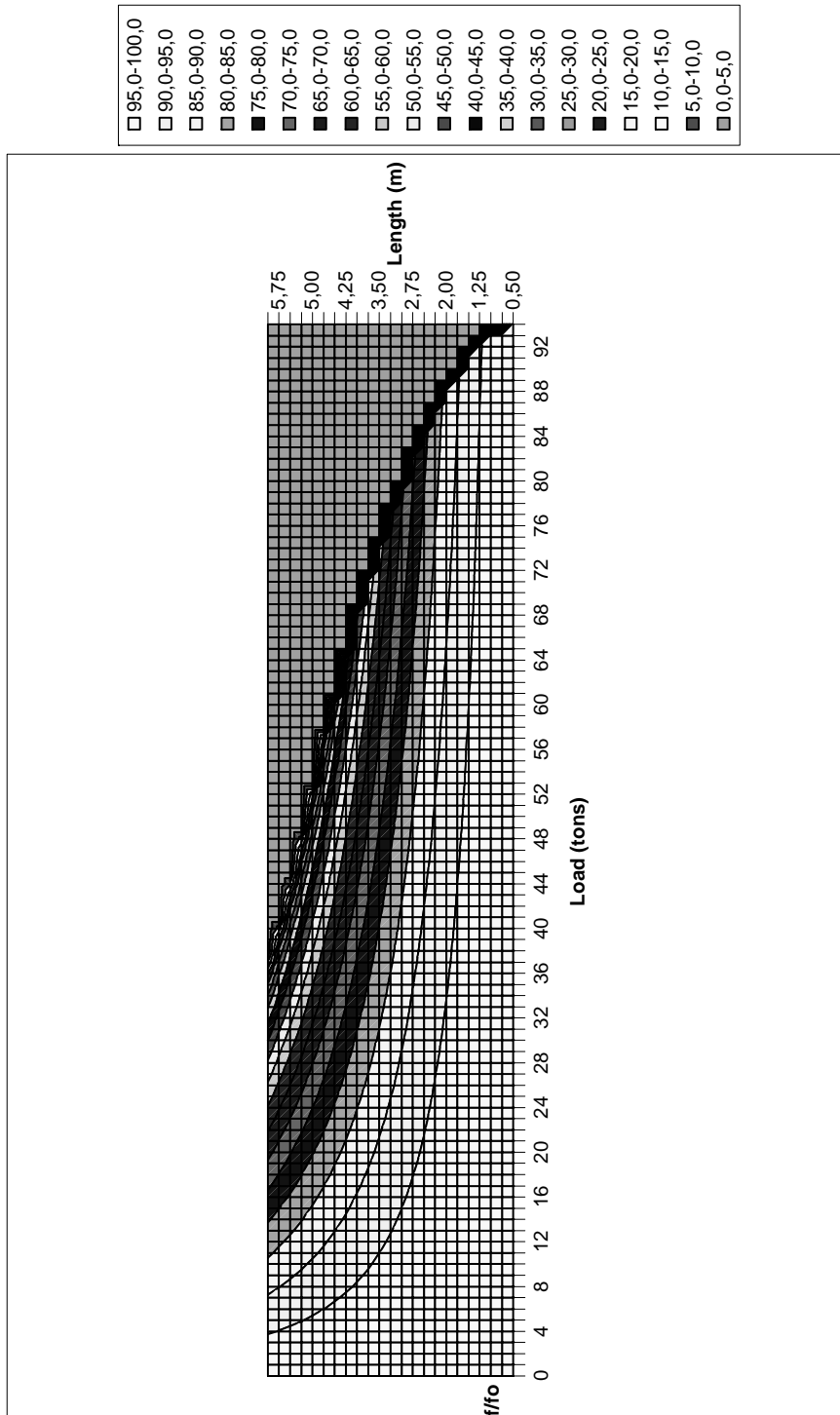


Figure A.8: Contour lines of the first vibration frequency ratios of the I220 steel column (in percentage) for certain lengths and loads

Table A.17. Fundamental frequency change in percentage versus axial load level for I240 steel column for different lengths for load level

		P _{cr} (tons)																																			
		110,2	109,7	109,0	108,0	106,9	105,5	103,9	102,1	100,2	98,0	95,6	92,9	90,1	87,1	83,8	80,4	76,7	72,9	68,8	64,5	60,0	55,3	50,8													
P (tons)	f/f ₀ (%)	Length (m)																																			
		0,50	0,75	1,00	1,25	1,50	1,75	2,00	2,25	2,50	2,75	3,00	3,25	3,50	3,75	4,00	4,25	4,50	4,75	5,00	5,25	5,50	5,75	6,00													
4																																					
6																							55,2	50,7													
8																							55,1	50,6													
10																						60,0	54,9	50,4													
12																						59,7	54,6	50,2													
14																						59,4	54,4	49,9													
16																						59,1	54,0	49,6													
18																					64,4	58,7	53,7	49,3													
20																					63,9	58,2	53,3	48,9													
22																					63,4	57,7	52,8	48,5													
24																					62,8	57,2	52,3	48,1													
26																				68,5	62,1	56,6	51,8	47,6													
28																				67,7	61,4	56,0	51,2	47,0													
30																				66,9	60,7	55,3	50,6	46,5													
32																				66,0	59,9	54,6	49,9	45,9													
34																			72,1	65,1	59,0	53,8	49,2	45,2													
36																			71,0	64,1	58,1	53,0	48,5	44,5													
38																			69,8	63,0	57,2	52,1	47,7	43,8													
40																		76,4	68,6	61,9	56,2	51,2	46,8	43,0													
42																		75,0	67,3	60,7	55,1	50,2	45,9	42,2													
44																		73,5	65,9	59,5	54,0	49,2	45,0	41,3													
46																		71,9	64,5	58,2	52,8	48,1	44,0	40,4													
48																	78,7	70,2	63,0	56,9	51,6	47,0	43,0	39,5													
50																	76,7	68,4	61,4	55,4	50,3	45,8	41,9	38,5													
52																	74,7	66,6	59,8	54,0	49,0	44,6	40,8	37,5													
54																81,9	72,6	64,7	58,1	52,4	47,6	43,3	39,7	36,4													
56																79,4	70,4	62,8	56,3	50,8	46,1	42,0	38,4	35,3													
58																76,9	68,1	60,7	54,5	49,2	44,6	40,7	37,2	34,2													
60															84,4	74,2	65,7	58,6	52,6	47,5	43,1	39,2	35,9	33,0													
62															81,3	71,4	63,3	56,4	50,6	45,7	41,5	37,8	34,6	31,7													
64															89,5	78,0	68,5	60,7	54,2	48,6	43,9	39,8	36,3	33,2	30,5												
66															85,7	74,6	65,6	58,1	51,8	46,5	42,0	38,1	34,7	31,7	29,1												
68															81,7	71,1	62,5	55,4	49,4	44,3	40,0	36,3	33,1	30,3	27,8												
70															77,5	67,5	59,4	52,6	46,9	42,1	38,0	34,5	31,4	28,7	26,4												
72															85,0	73,3	63,8	56,1	49,7	44,3	39,8	35,9	32,6	29,7	27,1	24,9											
74															93,8	79,9	68,9	60,0	52,7	46,7	41,7	37,4	33,8	30,6	27,9	25,5	23,4										
76															87,6	74,7	64,4	56,1	49,3	43,7	38,9	35,0	31,5	28,6	26,1	23,9	21,9										
78															96,8	81,3	69,3	59,7	52,0	45,7	40,5	36,1	32,4	29,3	26,5	24,2	22,1	20,3									
80															89,0	74,8	63,7	55,0	47,9	42,1	37,3	33,3	29,8	26,9	24,4	22,3	20,4	18,7									
82															98,1	81,1	68,1	58,1	50,1	43,6	38,3	34,0	30,3	27,2	24,5	22,3	20,3	18,5	17,0								
84															88,3	72,9	61,3	52,2	45,0	39,2	34,5	30,5	27,2	24,4	22,1	20,0	18,2	16,7	15,3								
86															96,5	78,1	64,6	54,3	46,2	39,9	34,7	30,5	27,0	24,1	21,6	19,5	17,7	16,1	14,8	13,6							
88															83,7	67,8	56,0	47,1	40,1	34,6	30,1	26,5	23,4	20,9	18,8	16,9	15,4	14,0	12,8	11,8							
90															89,3	70,5	57,1	47,2	39,7	33,8	29,1	25,4	22,3	19,8	17,6	15,8	14,3	13,0	11,8	10,8	9,9						
92															94,3	72,2	57,1	46,2	38,2	32,1	27,4	23,6	20,5	18,1	16,0	14,3	12,8	11,6	10,5	9,6	8,7	8,0					
94															97,4	71,6	54,8	43,3	35,1	29,0	24,3	20,7	17,9	15,6	13,7	12,1	10,8	9,7	8,8	8,0	7,2	6,6	6,1				
96															94,6	65,7	48,2	36,9	29,2	23,6	19,5	16,4	14,0	12,1	10,5	9,2	8,2	7,3	6,5	5,9	5,4	4,9	4,5	4,1			
98															74,7	47,8	33,2	24,4	18,7	14,8	12,0	9,9	8,3	7,1	6,1	5,3	4,7	4,1	3,7	3,3	3,0	2,7	2,5	2,3	2,1		
100	0,0	0,0	0,0	0,0	0,0	0,0	0,0	0,0	0,0	0,0	0,0	0,0	0,0	0,0	0,0	0,0	0,0	0,0	0,0	0,0	0,0	0,0	0,0	0,0	0,0	0,0	0,0	0,0	0,0	0,0	0,0	0,0	0,0	0,0	0,0	0,0	0,0

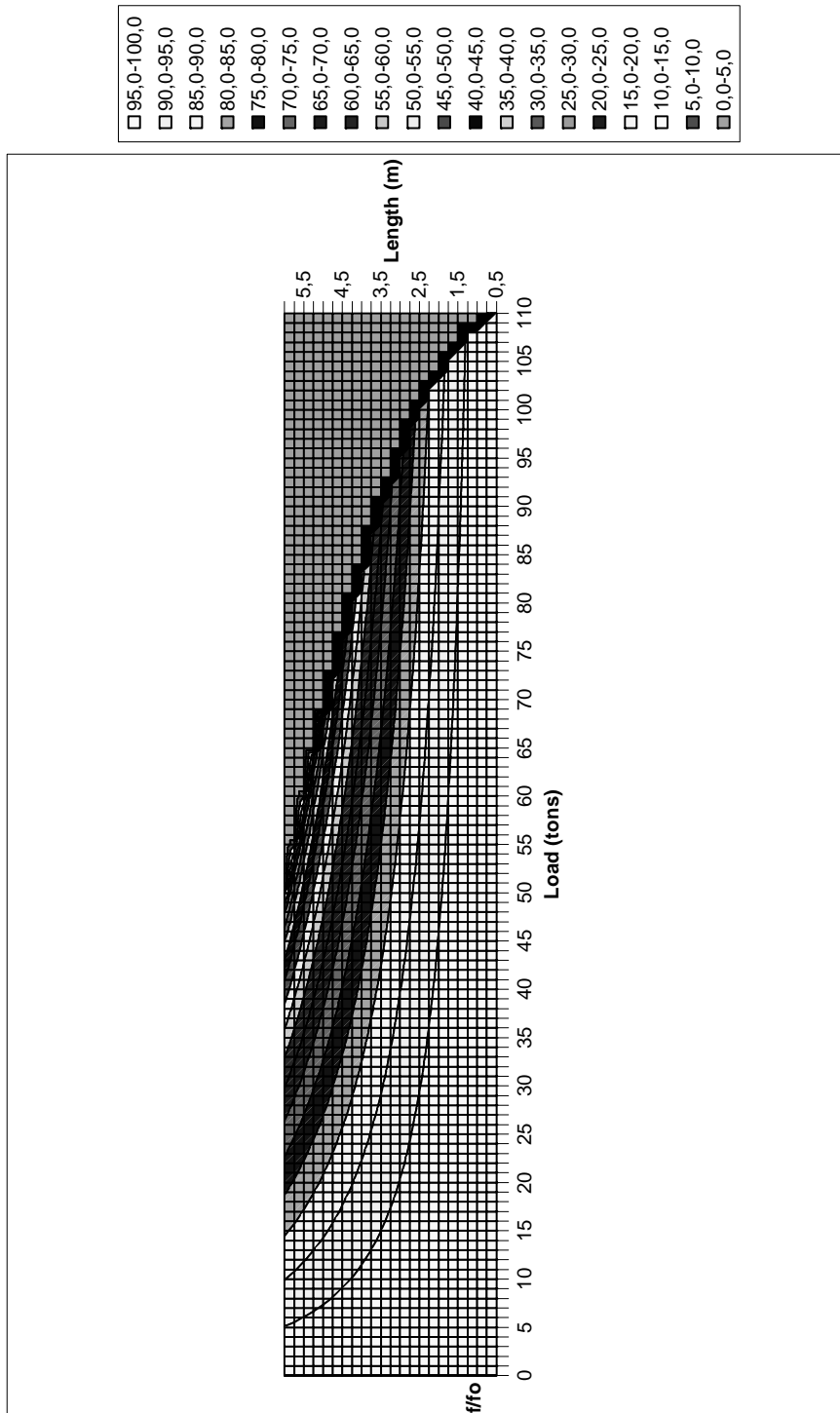


Figure A.9: Contour lines of the first vibration frequency ratios of the I240 steel column (in percentage) for certain lengths and loads

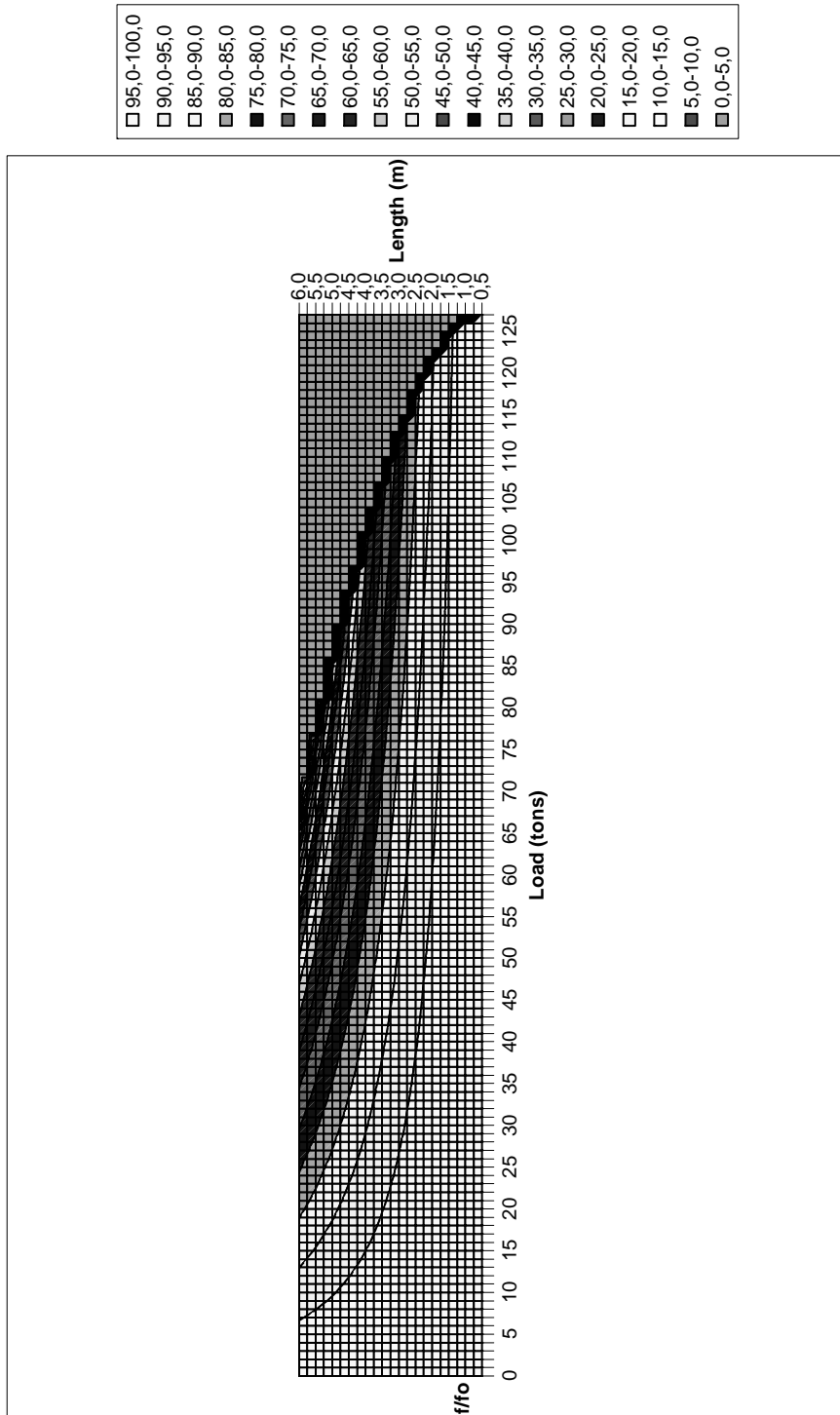


Figure A.10: Contour lines of the first vibration frequency ratios of the I260 steel column (in percentage) for certain lengths and loads

Table A.21. Fundamental frequency change in percentage versus axial load level for I280 steel column for different lengths for load level

P (tons)	P _{cr} (tons)																							
	145,9	145,4	144,6	143,6	142,4	140,9	139,2	137,4	135,2	132,9	130,3	127,6	124,6	121,3	117,9	114,2	110,3	106,2	101,9	97,3	92,6	87,6	82,3	
	Length (m)																							
	0,50	0,75	1,00	1,25	1,50	1,75	2,00	2,25	2,50	2,75	3,00	3,25	3,50	3,75	4,00	4,25	4,50	4,75	5,00	5,25	5,50	5,75	6,00	
4																								
6																								
8																								
10																								
12																								
14																								82,2
16																								81,8
18																								81,2
20																								80,6
22																								87,0
24																								79,9
26																								86,2
28																								79,2
30																								85,3
32																								78,3
34																								92,2
36																								84,4
38																								77,5
40																								91,1
42																								83,3
44																								76,5
46																								89,9
48																								82,2
50																								75,4
52																								97,2
54																								88,6
56																								81,1
58																								74,4
60																								95,7
62																								87,2
64																								79,8
66																								73,3
68																								94,2
70																								85,8
72																								78,5
74																								92,5
76																								84,3
78																								77,1
80																								70,8
82																								100,0
84																								90,7
86																								82,7
88																								75,6
90																								69,5
92																								98,0
94																								88,9
96																								81,0
98																								74,1
100	0,0	0,0	0,0	0,0	0,0	0,0	0,0	0,0	0,0	0,0	0,0	0,0	0,0	0,0	0,0	0,0	0,0	0,0	0,0	0,0	0,0	0,0	0,0	68,1

Table A.22. Fundamental frequency change in percentage versus axial load level for I280 steel column for different lengths for frequency change

f/f _o (%)	Length (m)																							
	0,50	0,75	1,00	1,25	1,50	1,75	2,00	2,25	2,50	2,75	3,00	3,25	3,50	3,75	4,00	4,25	4,50	4,75	5,00	5,25	5,50	5,75	6,00	
0	100,0	100,0	100,0	100,0	100,0	100,0	100,0	100,0	100,0	100,0	100,0	100,0	100,0	100,0	100,0	100,0	100,0	100,0	100,0	100,0	100,0	100,0	100,0	100,0
2	100,0	100,0	100,0	99,9	99,9	99,9	99,9	99,9	99,9	99,9	99,9	99,9	99,9	99,9	99,9	99,9	99,9	99,9	99,9	99,9	99,9	99,9	99,9	99,9
4	100,0	100,0	99,9	99,9	99,9	99,8	99,7	99,7	99,6	99,5	99,4	99,3	99,2	99,1	99,0	98,8	98,7	98,5	98,4	98,2	98,0	97,8	97,6	97,4
6	100,0	99,9	99,9	99,8	99,8	99,7	99,6	99,5	99,4	99,3	99,1	99,0	98,8	98,6	98,4	98,2	98,0	97,8	97,6	97,4	97,2	97,0	96,8	96,6
8	100,0	99,9	99,9	99,8	99,7	99,6	99,5	99,3	99,2	99,0	98,8	98,6	98,4	98,2	97,9	97,6	97,4	97,1	96,7	96,4	96,0	95,6	95,2	94,8
10	100,0	99,9	99,8	99,7	99,6	99,5	99,4	99,2	99,0	98,8	98,5	98,3	98,0	97,7	97,4	97,0	96,7	96,3	95,9	95,5	95,0	94,5	94,0	93,5
12	100,0	99,9	99,8	99,7	99,6	99,4	99,2	99,0	98,8	98,5	98,2	97,9	97,6	97,2	96,9	96,4	96,0	95,5	95,0	94,5	94,0	93,4	92,8	92,2
14	99,9	99,9	99,8	99,6	99,5	99,3	99,1	98,9	98,6	98,3	98,0	97,6	97,2	96,8	96,3	95,8	95,3	94,8	94,2	93,6	92,9	92,2	91,5	90,8
16	99,9	99,9	99,7	99,6	99,4	99,2	99,0	98,7	98,4	98,0	97,7	97,2	96,8	96,3	95,8	95,2	94,6	94,0	93,3	92,6	91,9	91,1	90,2	89,3
18	99,9	99,8	99,7	99,5	99,3	99,1	98,8	98,5	98,2	97,8	97,4	96,9	96,4	95,8	95,2	94,6	93,9	93,2	92,5	91,6	90,8	89,9	88,9	87,9
20	99,9	99,8	99,7	99,5	99,3	99,0	98,7	98,4	98,0	97,5	97,1	96,5	96,0	95,4	94,7	94,0	93,2	92,4	91,6	90,7	89,7	88,7	87,6	86,6
22	99,9	99,8	99,6	99,4	99,2	98,9	98,6	98,2	97,8	97,3	96,8	96,2	95,6	94,9	94,2	93,4	92,5	91,6	90,7	89,7	88,6	87,4	86,2	85,0
24	99,9	99,8	99,6	99,4	99,1	98,8	98,4	98,0	97,6	97,0	96,5	95,8	95,1	94,4	93,6	92,7	91,8	90,8	89,8	88,7	87,5	86,2	84,9	83,5
26	99,9	99,8	99,6	99,3	99,1	98,7	98,3	97,9	97,3	96,8	96,2	95,5	94,7	93,9	93,0	92,1	91,1	90,0	88,9	87,6	86,3	84,9	83,5	82,0
28	99,9	99,7	99,5	99,3	99,0	98,6	98,2	97,7	97,1	96,5	95,9	95,1	94,3	93,4	92,5	91,5	90,4	89,2	88,0	86,6	85,2	83,7	82,0	80,6
30	99,9	99,7	99,5	99,2	98,9	98,5	98,0	97,5	96,9	96,3	95,6	94,8	93,9	92,9	91,9	90,8	89,6	88,4	87,0	85,6	84,0	82,4	80,6	78,6
32	99,9	99,7	99,5	99,2	98,8	98,4	97,9	97,4	96,7	96,0	95,2	94,4	93,5	92,5	91,4	90,2	88,9	87,5	86,1	84,5	82,8	81,0	79,1	77,1
34	99,9	99,7	99,5	99,1	98,8	98,3	97,8	97,2	96,5	95,8	94,9	94,0	93,0	92,0	90,8	89,5	88,2	86,7	85,1	83,4	81,6	79,7	77,6	75,6
36	99,9	99,7	99,4	99,1	98,7	98,2	97,7	97,0	96,3	95,5	94,6	93,7	92,6	91,5	90,2	88,9	87,4	85,8	84,2	82,4	80,6	78,7	76,7	74,6
38	99,8	99,7	99,4	99,0	98,6	98,1	97,5	96,9	96,1	95,3	94,3	93,3	92,2	91,0	89,6	88,2	86,7	85,0	83,2	81,3	79,2	77,0	74,5	72,0
40	99,8	99,6	99,4	99,0	98,5	98,0	97,4	96,7	95,9	95,0	94,0	92,9	91,8	90,5	89,1	87,5	85,9	84,1	82,2	80,1	77,9	75,5	72,9	70,3
42	99,8	99,6	99,3	98,9	98,5	97,9	97,3	96,5	95,7	94,7	93,7	92,6	91,3	90,0	88,5	86,9	85,1	83,2	81,2	79,0	76,6	74,0	71,2	68,4
44	99,8	99,6	99,3	98,9	98,4	97,8	97,1	96,3	95,5	94,5	93,4	92,2	90,9	89,4	87,9	86,2	84,3	82,3	80,2	77,8	75,3	72,5	69,5	66,5
46	99,8	99,6	99,3	98,8	98,3	97,7	97,0	96,2	95,3	94,2	93,1	91,8	90,4	88,9	87,3	85,5	83,6	81,4	79,2	76,7	74,0	71,0	67,8	64,5
48	99,8	99,6	99,2	98,8	98,2	97,6	96,9	96,0	95,0	94,0	92,8	91,4	90,0	88,4	86,7	84,8	82,8	80,5	78,1	75,5	72,6	69,5	66,0	62,5
50	99,8	99,5	99,2	98,7	98,2	97,5	96,7	95,8	94,8	93,7	92,5	91,1	89,6	87,9	86,1	84,1	82,0	79,6	77,1	74,3	71,2	67,9	64,2	60,5
52	99,8	99,5	99,2	98,7	98,1	97,4	96,6	95,7	94,6	93,4	92,1	90,7	89,1	87,4	85,5	83,4	81,1	78,7	76,0	73,0	69,8	66,2	62,3	58,3
54	99,8	99,5	99,1	98,6	98,0	97,3	96,5	95,5	94,4	93,2	91,8	90,3	88,7	86,8	84,9	82,7	80,3	77,7	74,9	71,8	68,3	64,5	60,3	56,0
56	99,8	99,5	99,1	98,6	98,0	97,2	96,3	95,3	94,2	92,9	91,5	89,9	88,2	86,3	84,2	82,0	79,5	76,8	73,8	70,5	66,9	62,8	58,3	53,8
58	99,8	99,5	99,1	98,5	97,9	97,1	96,2	95,2	94,0	92,7	91,2	89,6	87,8	85,8	83,6	81,2	78,6	75,8	72,6	69,2	65,3	61,0	56,2	51,0
60	99,8	99,5	99,0	98,5	97,8	97,0	96,1	95,0	93,8	92,4	90,9	89,2	87,3	85,3	83,0	80,5	77,8	74,8	71,5	67,8	63,8	59,2	54,0	48,5
62	99,8	99,4	99,0	98,4	97,7	96,9	95,9	94,8	93,5	92,1	90,5	88,8	86,8	84,7	82,4	79,8	76,9	73,8	70,3	66,5	62,2	57,3	51,7	46,0
64	99,7	99,4	99,0	98,4	97,7	96,8	95,8	94,6	93,3	91,9	90,2	88,4	86,4	84,2	81,7	79,0	76,1	72,8	69,1	65,1	60,5	55,3	49,3	43,0
66	99,7	99,2	98,9	98,3	97,6	96,7	95,7	94,5	93,1	91,6	89,8	88,0	85,9	83,6	81,1	78,3	75,2	71,8	67,9	63,7	58,8	53,3	46,8	40,0
68	99,7	99,4	98,9	98,3	97,5	96,6	95,5	94,3	92,9	91,3	89,6	87,6	85,5	83,1	80,4	77,5	74,3	70,7	66,7	62,2	57,1	51,2	44,1	37,0
70	99,7	99,4	98,9	98,2	97,4	96,5	95,4	94,1	92,7	91,1	89,2	87,2	85,0	82,5	79,8	76,7	73,4	69,6	65,4	60,7	55,3	48,9	41,2	34,0
72	99,7	99,3	98,8	98,2	97,4	96,4	95,2	93,9	92,5	90,8	88,9	86,8	84,5	82,0	79,1	76,0	72,5	68,6	64,2	59,2	53,4	46,6	38,1	30,0
74	99,7	99,3	98,8	98,1	97,3	96,3	95,1	93,8	92,2	90,5	88,6	86,4	84,0	81,4	78,4	75,2	71,5	67,5	62,9	57,6	51,5	44,1	34,8	26,0
76	99,7	99,3	98,8	98,1	97,2	96,2	95,0	93,6	92,0	90,2	88,3	86,0	83,6	80,8	77,8	74,4	70,6	66,3	61,5	56,0	49,5	41,5	31,1	22,0
78	99,7	99,3	98,7	98,0	97,1	96,1	94,8	93,4	91,8	90,0	87,9	85,6	83,1	80,2	77,1	73,6	69,6	65,2	60,1	54,3	47,4	38,7	26,8	18,0
80	99,7	99,3	98,7	98,0	97,1	96,0	94,7	93,2	91,6	89,7	87,6	85,2	82,6	79,7	76,4	72,8	68,7	64,0	58,7	52,6	45,1	35,7	21,7	13,0
82	99,7	99,3	98,7	97,9	97,0	95,9	94,6	93,1	91,4	89,4	87,2	84,8	82,1	79,1	75,7	71,9	67,7	62,9	57,3	50,8	42,8	32,4	15,0	7,0
84	99,7	99,2	98,6	97,9	96,9	95,8	94,4	92,9	91,1	89,1	86,9	84,4	81,6	78,5	75,0	71,1	66,7	61,6	55,8	48,9	40,3	28,7	14,0	0,0
86	99,7	99,2	98,6	97,8	96,8	95,7	94,3	92,7	90,9	88,9	86,6	84,0	81,1	77,9	74,3	70,3	65,7	60,4	54,3	47,0	37,7	24,5	10,0	0,0
88	99,6	99,2	98,6	97,8	96,8	95,6	94,2	92,5	90,7	88,6	86,2	83,6	80,6	77,3	73,6	69,4	64,6	59,1	52,7	44,9	34,9	20,0	0,0	0,0
90	99,6	99,2	98,5	97,7	96,7	95,5	94,0	92,4	90,5	88,3	85,9	83,2	80,1	76,7	72,9	68,5	63,6	57,9	51,1	42,8	31,8	18,0	0,0	0,0
92	99,6	99,2	98,5	97,7	96,6	95,4	93,9	92,2	90,2	88,0	85,6	82,8	79,6	76,1	72,1	67,7	62,5	56,5	49,4	40,6	28,4	0,0	0,0	0,0
94	99,6	99,1	98,5	97,6	96,5	95,2	93,7	92,0	90,0	87,8	85,2	82,3	79,1	75,5	71,4	66,8	61,4	55,2	47,7	38,2	0,0	0,0	0,0	0,0
96	99,6	99,1	98,4	97,6	96,5	95,1	93,6	91,8	89,8	87,5	84,9	81,9	78,6	74,9	70,7	65,9	60,3	53,8	45,9	35,7	0,0	0,0	0,0	0,0
98	99,6	99,1	98,4	97,5	96,4	95,0	93,5	91,6	89,6	87,2	84,5	81,5	78,1	74,3	69,9	64,9	59,2	52,4	44,0	0,0	0,0	0,0	0,0	0,0
100	99,6	99,1	98,4	97,5	96,3	94,9	93,3	91,5	89,3	86,9	84,2	81,1	77,6	73,6	69,1	64,0	58,0	50,9	42,0	0,0	0,0	0,0	0,0	0,0
102	99,6	99,1	98,3	97,4	96,2	94,8	93,2	91,3	89,1	86,6	83,8	80,6	77,1	73,0	68,4	63,1	56,8	49,4	0,0	0,0	0,0	0,0	0,0	0,0
104	99,6	99,1	98,3	97,3	96,2	94,7	93,0	91,1	88,9	86,3	83,5	80,2	76,5	72,4	67,6	62,1	55,6	47,						

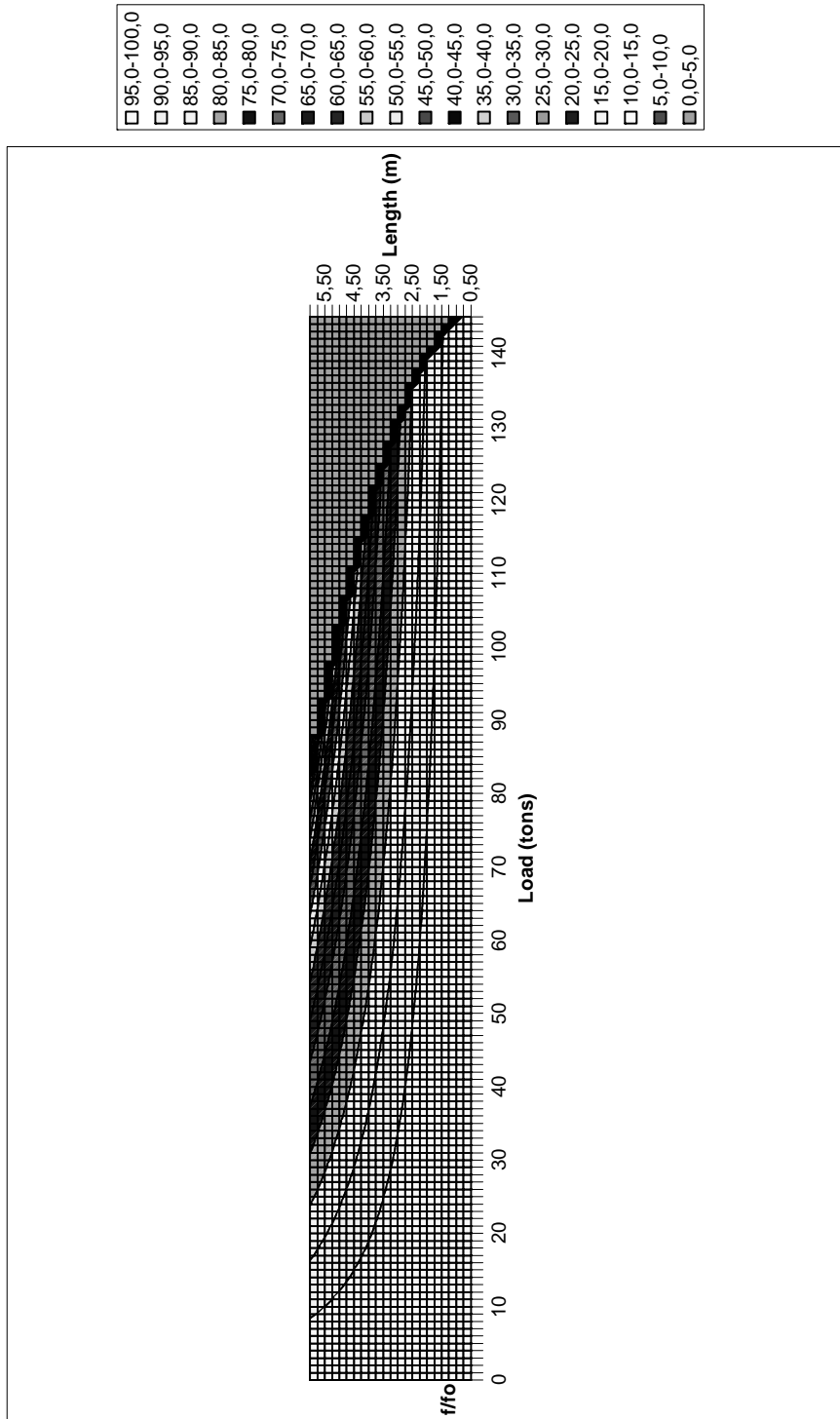


Figure A.11: Contour lines of the first vibration frequency ratios of the I280 steel column (in percentage) for certain lengths and loads

Table A.23. Fundamental frequency change in percentage versus axial load level for I300 steel column for different lengths for load level

		P _r (tons)																									
		165,1	164,5	163,7	162,7	161,4	159,9	158,2	156,3	154,1	151,7	149,0	146,1	143,0	139,7	136,2	132,4	128,3	124,1	119,6	114,9	110,0	104,8	99,4			
P (tons)	L (m)	Length (m)																									
		0,50	0,75	1,00	1,25	1,50	1,75	2,00	2,25	2,50	2,75	3,00	3,25	3,50	3,75	4,00	4,25	4,50	4,75	5,00	5,25	5,50	5,75	6,00			
4																											
6																											
8																											
10																											
12																											
14																											
16																											
18																											
20																											
22																										99,0	
24																										98,1	
26																										97,1	
28																										104,5	
30																										96,0	
32																										103,2	
34																										94,8	
36																										101,9	
38																										93,6	
40																										109,8	
42																										100,4	
44																										108,1	
46																										98,9	
48																										90,8	
50																										106,3	
52																										97,3	
54																										89,3	
56																										101,9	
58																										93,6	
60																										109,8	
62																										100,4	
64																										108,1	
66																										98,9	
68																										90,8	
70																										106,3	
72																										97,3	
74																										89,3	
76																										101,9	
78																										93,6	
80																										109,8	
82																										100,4	
84																										108,1	
86																										98,9	
88																										90,8	
90																										106,3	
92																										97,3	
94																										89,3	
96																										101,9	
98																										93,6	
100	0,0	0,0	0,0	0,0	0,0	0,0	0,0	0,0	0,0	0,0	0,0	0,0	0,0	0,0	0,0	0,0	0,0	0,0	0,0	0,0	0,0	0,0	0,0	0,0	0,0	0,0	

Table A.24. Fundamental frequency change in percentage versus axial load level for I300 steel column for different lengths for frequency change

Load (tons)	f/f ₀ (%)	Length (m)																						
		0.50	0.75	1.00	1.25	1.50	1.75	2.00	2.25	2.50	2.75	3.00	3.25	3.50	3.75	4.00	4.25	4.50	4.75	5.00	5.25	5.50	5.75	6.00
0	100.0	100.0	100.0	100.0	100.0	100.0	100.0	100.0	100.0	100.0	100.0	100.0	100.0	100.0	100.0	100.0	100.0	100.0	100.0	100.0	100.0	100.0	100.0	100.0
2	100.0	100.0	100.0	100.0	99.9	99.9	99.9	99.9	99.9	99.9	99.8	99.8	99.7	99.7	99.6	99.6	99.5	99.5	99.4	99.3	99.3	99.2	99.1	99.1
4	100.0	100.0	99.9	99.9	99.9	99.8	99.8	99.7	99.6	99.5	99.3	99.2	99.1	98.9	98.7	98.5	98.3	98.1	97.9	97.6	97.4	97.1	96.8	96.5
6	100.0	100.0	99.9	99.9	99.8	99.8	99.7	99.6	99.5	99.3	99.2	99.0	98.8	98.6	98.4	98.2	97.9	97.6	97.3	97.0	96.7	96.4	96.0	95.7
8	100.0	99.9	99.8	99.8	99.7	99.6	99.5	99.3	99.2	99.0	98.8	98.6	98.4	98.1	97.8	97.5	97.1	96.8	96.4	96.0	95.6	95.2	94.7	94.2
10	100.0	99.9	99.8	99.8	99.7	99.6	99.5	99.3	99.2	99.0	98.8	98.6	98.4	98.1	97.8	97.5	97.1	96.8	96.4	96.0	95.6	95.2	94.7	94.2
12	100.0	99.9	99.8	99.8	99.7	99.6	99.5	99.3	99.2	99.0	98.8	98.6	98.4	98.1	97.8	97.5	97.1	96.8	96.4	96.0	95.6	95.2	94.7	94.2
14	100.0	99.9	99.8	99.7	99.6	99.4	99.3	99.1	98.9	98.6	98.4	98.1	97.7	97.4	97.0	96.7	96.2	95.8	95.3	94.8	94.3	93.8	93.2	92.6
16	99.9	99.9	99.8	99.7	99.5	99.4	99.2	98.9	98.7	98.4	98.1	97.7	97.4	97.0	96.6	96.2	95.7	95.2	94.7	94.1	93.5	92.9	92.2	91.6
18	99.9	99.9	99.8	99.6	99.5	99.3	99.1	98.8	98.5	98.2	97.9	97.5	97.1	96.7	96.2	95.7	95.1	94.6	94.0	93.3	92.6	91.9	91.2	90.5
20	99.9	99.9	99.7	99.6	99.4	99.2	99.0	98.7	98.4	98.0	97.6	97.2	96.8	96.3	95.7	95.2	94.6	93.9	93.3	92.5	91.8	91.0	90.1	89.1
22	99.9	99.7	99.6	99.4	99.1	98.9	98.5	98.2	97.8	97.4	96.9	96.4	95.9	95.3	94.7	94.0	93.3	92.6	91.8	91.0	90.0	89.0	88.1	87.1
24	99.9	99.8	99.7	99.5	99.3	99.0	98.7	98.4	98.0	97.6	97.2	96.6	96.1	95.5	94.9	94.2	93.5	92.7	91.9	91.0	90.0	89.0	88.0	87.0
26	99.9	99.8	99.7	99.5	99.2	99.0	98.6	98.3	97.9	97.4	96.9	96.4	95.8	95.1	94.4	93.7	92.9	92.0	91.1	90.2	89.2	88.1	86.9	85.8
28	99.9	99.8	99.6	99.4	99.2	98.9	98.5	98.1	97.7	97.2	96.7	96.1	95.4	94.7	94.0	93.2	92.3	91.4	90.4	89.4	88.3	87.1	85.8	84.5
30	99.9	99.8	99.6	99.4	99.1	98.8	98.4	98.0	97.5	97.0	96.4	95.8	95.1	94.4	93.5	92.7	91.7	90.7	89.7	88.6	87.4	86.1	84.7	83.4
32	99.9	99.8	99.6	99.3	99.1	98.7	98.3	97.9	97.4	96.8	96.2	95.5	94.8	94.0	93.1	92.2	91.2	90.1	89.0	87.7	86.4	85.1	83.6	82.3
34	99.9	99.8	99.6	99.3	99.0	98.6	98.2	97.7	97.2	96.6	95.9	95.2	94.4	93.6	92.6	91.7	90.6	89.4	88.2	86.9	85.5	84.0	82.4	80.9
36	99.9	99.7	99.5	99.3	98.9	98.6	98.1	97.6	97.0	96.4	95.7	94.9	94.1	93.2	92.2	91.1	90.0	88.8	87.5	86.1	84.6	83.0	81.3	79.7
38	99.9	99.7	99.5	99.2	98.9	98.5	98.0	97.5	96.9	96.2	95.4	94.6	93.7	92.8	91.7	90.6	89.4	88.1	86.7	85.2	83.6	81.9	80.1	78.4
40	99.9	99.7	99.5	99.2	98.8	98.4	97.9	97.3	96.7	96.0	95.2	94.3	93.4	92.4	91.3	90.1	88.8	87.4	85.9	84.4	82.7	80.9	79.1	77.3
42	99.9	99.7	99.5	99.1	98.8	98.3	97.8	97.2	96.5	95.8	95.0	94.0	93.1	92.0	90.8	89.6	88.2	86.7	85.2	83.5	81.7	79.8	77.7	75.7
44	99.9	99.7	99.4	99.1	98.7	98.2	97.7	97.1	96.4	95.6	94.7	93.8	92.7	91.6	90.4	89.0	87.6	86.1	84.4	82.6	80.7	78.7	76.6	74.4
46	99.9	99.7	99.4	99.1	98.6	98.2	97.6	96.9	96.2	95.4	94.5	93.5	92.4	91.2	89.9	88.5	87.0	85.4	83.6	81.7	79.7	77.5	75.2	72.9
48	99.8	99.6	99.4	99.0	98.6	98.1	97.5	96.8	96.0	95.2	94.2	93.2	92.0	90.8	89.4	88.0	86.4	84.7	82.8	80.8	78.7	76.4	73.9	71.4
50	99.8	99.6	99.3	99.0	98.5	98.0	97.4	96.7	95.9	95.0	94.0	92.9	91.7	90.4	89.0	87.4	85.8	84.0	82.0	79.9	77.7	75.2	72.6	70.0
52	99.8	99.6	99.3	98.9	98.5	97.9	97.3	96.5	95.7	94.7	93.7	92.6	91.3	90.0	88.5	86.9	85.1	83.3	81.2	79.0	76.6	74.1	71.2	68.4
54	99.8	99.6	99.3	98.9	98.4	97.8	97.2	96.4	95.5	94.5	93.5	92.3	91.0	89.6	88.0	86.3	84.5	82.5	80.4	78.1	75.6	72.9	69.9	66.9
56	99.8	99.6	99.3	98.9	98.4	97.7	97.0	96.2	95.3	94.3	93.2	92.0	90.6	89.1	87.5	85.8	83.9	81.8	79.6	77.1	74.5	71.6	68.5	65.4
58	99.8	99.6	99.2	98.8	98.3	97.7	96.9	96.1	95.2	94.1	93.0	91.7	90.3	88.7	87.0	85.2	83.2	81.1	78.7	76.2	73.4	70.4	67.1	63.8
60	99.8	99.6	99.2	98.8	98.2	97.6	96.8	96.0	95.0	93.9	92.7	91.4	89.9	88.3	86.6	84.7	82.6	80.3	77.9	75.2	72.3	69.1	65.6	62.1
62	99.8	99.5	99.2	98.7	98.2	97.5	96.7	95.8	94.8	93.7	92.4	91.1	89.5	87.9	86.1	84.1	81.9	79.6	77.0	74.2	71.2	67.8	64.1	59.9
64	99.8	99.5	99.2	98.7	98.1	97.4	96.6	95.7	94.7	93.5	92.2	90.8	89.2	87.5	85.6	83.5	81.3	78.8	76.2	73.2	70.0	66.5	62.6	58.4
66	99.8	99.5	99.1	98.7	98.1	97.3	96.5	95.6	94.5	93.3	91.9	90.5	88.8	87.0	85.1	83.0	80.6	78.1	75.3	72.2	68.9	65.2	61.0	56.5
68	99.8	99.5	99.1	98.6	98.0	97.3	96.4	95.4	94.3	93.1	91.7	90.2	88.5	86.6	84.6	82.4	80.0	77.3	74.4	71.2	67.7	63.8	59.4	54.8
70	99.8	99.5	99.1	98.6	97.9	97.2	96.3	95.3	94.1	92.9	91.4	89.8	88.1	86.2	84.1	81.8	79.3	76.5	73.5	70.2	66.5	62.4	57.8	52.9
72	99.8	99.5	99.1	98.5	97.9	97.1	96.2	95.1	94.0	92.6	91.2	89.5	87.7	85.8	83.6	81.2	78.6	75.7	72.6	69.1	65.2	60.9	56.1	51.1
74	99.8	99.5	99.0	98.5	97.8	97.0	96.1	95.0	93.8	92.4	90.9	89.2	87.4	85.3	83.1	80.6	77.9	74.9	71.7	68.0	64.0	59.5	54.3	48.5
76	99.8	99.4	99.0	98.4	97.8	96.9	96.0	94.9	93.6	92.2	90.6	88.9	87.0	84.9	82.6	80.0	77.2	74.1	70.7	66.9	62.7	57.9	52.5	46.5
78	99.7	99.4	99.0	98.4	97.7	96.8	95.9	94.7	93.4	92.0	90.4	88.6	86.6	84.5	82.1	79.4	76.5	73.3	69.8	65.8	61.4	56.4	50.6	44.1
80	99.7	99.4	99.0	98.4	97.6	96.8	95.7	94.6	93.3	91.8	90.1	88.3	86.3	84.0	81.5	78.8	75.8	72.5	68.8	64.7	60.1	54.8	48.6	42.1
82	99.7	99.4	98.9	98.3	97.6	96.7	95.6	94.4	93.1	91.6	89.9	88.0	85.9	83.6	81.0	78.2	75.1	71.7	67.8	63.5	58.7	53.1	46.5	39.9
84	99.7	99.4	98.9	98.3	97.5	96.6	95.5	94.3	92.9	91.3	89.6	87.7	85.5	83.1	80.5	77.6	74.4	70.8	66.8	62.4	57.3	51.4	44.4	37.9
86	99.7	99.4	98.9	98.2	97.5	96.5	95.4	94.2	92.7	91.1	89.3	87.3	85.1	82.7	80.0	77.0	73.7	70.0	65.8	61.2	55.8	49.6	42.1	35.6
88	99.7	99.4	98.9	98.2	97.4	96.4	95.3	94.0	92.6	90.9	89.1	87.0	84.7	82.2	79.4	76.3	72.9	69.1	64.8	59.9	54.3	47.8	39.7	33.2
90	99.7	99.3	98.8	98.2	97.3	96.4	95.2	93.9	92.4	90.7	88.8	86.7	84.4	81.8	78.9	75.7	72.2	68.2	63.7	57.4	52.8	45.8	37.1	30.6
92	99.7	99.3	98.8	98.1	97.3	96.3	95.1	93.7	92.2	90.5	88.5	86.4	84.0	81.3	78.4	75.1	71.4	67.3	62.7	57.4	51.2	43.8	34.3	27.8
94	99.7	99.3	98.8	98.1	97.2	96.2	95.0	93.6	92.0	90.3	88.3	86.1	83.6	80.9	77.8	74.4	70.7	66.4	61.6	56.1	49.6	41.7	31.3	24.8
96	99.7	99.3	98.7	98.0	97.2	96.1	94.9	93.5	91.9	90.0	88.0	85.7	83.2	80.4	77.3	73.8	69.9	65.5	60.5	54.7	47.9	39.5	28.0	21.5
98	99.7	99.3	98.7	98.0	97.1	96.0	94.8	93.3	91.7	89.8	87.7	85.4	82.8	79.9	76.7	73.1	69.1	64.6	59.4	53.4	46.2	37.1	24.2	17.7
100	99.7	99.3	98.7	97.9	97.0	95.9	94.7	93.2	91.5	89.6	87.5	85.1	82.4	79.5	76.2	72.5	68.3	63.6	58.2	51.9	44.3	34.6	23.1	16.6
102	99.7	99.3	98.7	97.9	97.0	95.9	94.5	93.0	91.3	89.4	87.2	84.8	82.0	79.0	75.6	71.8	67.5	62.7	57.1	50.5	42.4	31.8	20.3	13.8
104	99.7	99.2	98.6	97.9	96.9	95.8	94.4	92.9	91.1	89.2	86.9	84.4												

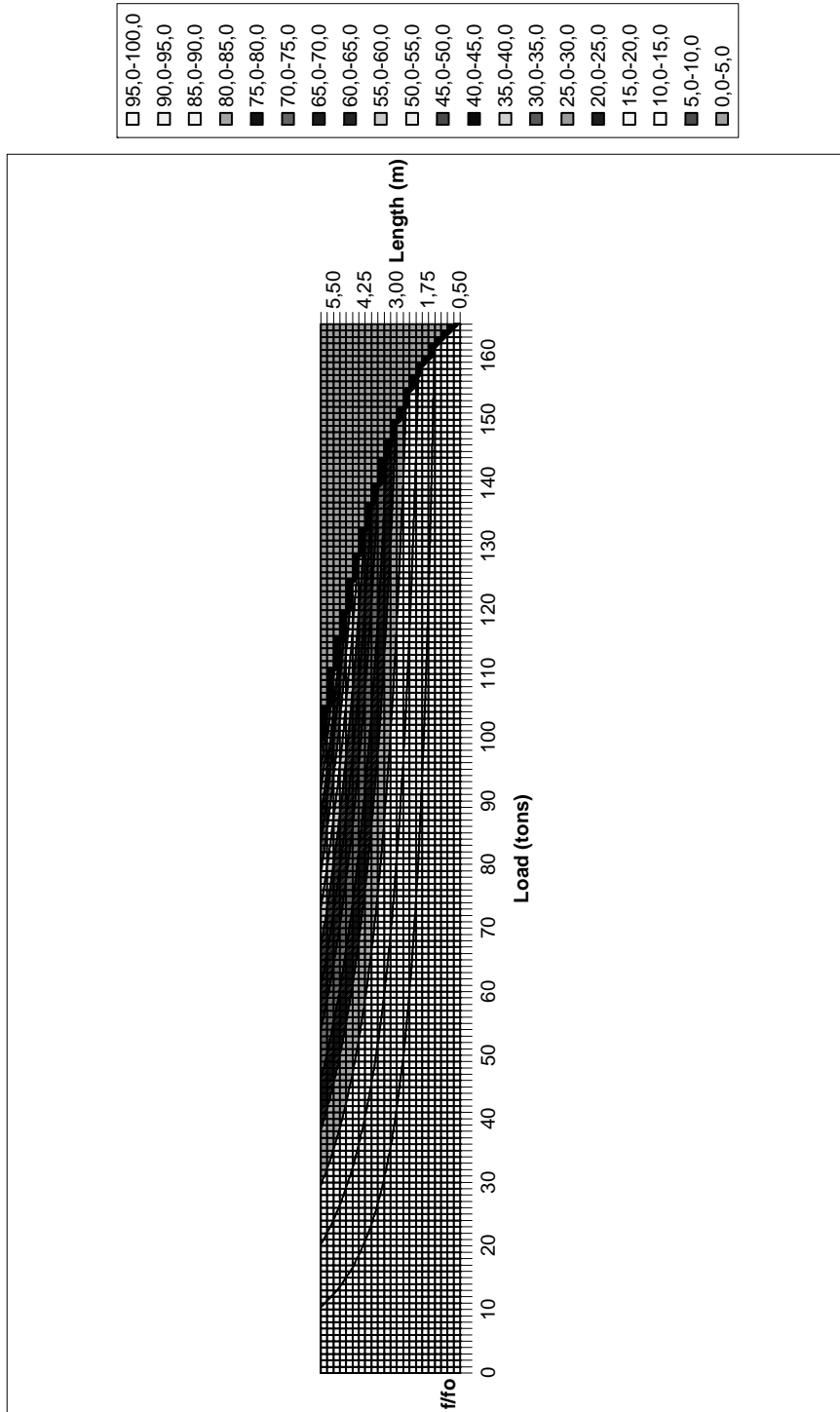


Figure A.12: Contour lines of the first vibration frequency ratios of the I300 steel column (in percentage) for certain lengths and loads

Table A.26. Fundamental frequency change in percentage versus axial load level for I320 steel column for different lengths for frequency change

Load (tons)	f/f ₀ (%)	Length (m)																						
		0.50	0.75	1.00	1.25	1.50	1.75	2.00	2.25	2.50	2.75	3.00	3.25	3.50	3.75	4.00	4.25	4.50	4.75	5.00	5.25	5.50	5.75	6.00
0	100.0	100.0	100.0	100.0	100.0	100.0	100.0	100.0	100.0	100.0	100.0	100.0	100.0	100.0	100.0	100.0	100.0	100.0	100.0	100.0	100.0	100.0	100.0	100.0
2	100.0	100.0	100.0	100.0	100.0	99.9	99.9	99.9	99.9	99.8	99.8	99.8	99.8	99.7	99.7	99.6	99.6	99.5	99.5	99.4	99.4	99.3	99.3	99.2
4	100.0	100.0	100.0	99.9	99.9	99.9	99.8	99.8	99.7	99.7	99.6	99.6	99.5	99.4	99.3	99.2	99.1	99.0	98.9	98.8	98.7	98.6	98.5	98.4
6	100.0	100.0	99.9	99.9	99.8	99.8	99.7	99.7	99.6	99.5	99.4	99.3	99.2	99.1	99.0	98.9	98.8	98.7	98.6	98.5	98.4	98.3	98.2	98.1
8	100.0	100.0	99.9	99.8	99.8	99.7	99.7	99.6	99.5	99.4	99.3	99.2	99.1	99.0	98.9	98.8	98.7	98.6	98.5	98.4	98.3	98.2	98.1	98.0
10	100.0	99.9	99.9	99.8	99.8	99.7	99.6	99.5	99.4	99.3	99.2	99.1	99.0	98.9	98.8	98.7	98.6	98.5	98.4	98.3	98.2	98.1	98.0	97.9
12	100.0	99.9	99.9	99.8	99.7	99.6	99.5	99.4	99.3	99.2	99.1	99.0	98.9	98.8	98.7	98.6	98.5	98.4	98.3	98.2	98.1	98.0	97.9	97.8
14	100.0	99.9	99.9	99.8	99.7	99.6	99.5	99.4	99.3	99.2	99.1	99.0	98.9	98.8	98.7	98.6	98.5	98.4	98.3	98.2	98.1	98.0	97.9	97.8
16	100.0	99.9	99.8	99.7	99.6	99.5	99.4	99.3	99.2	99.1	99.0	98.9	98.8	98.7	98.6	98.5	98.4	98.3	98.2	98.1	98.0	97.9	97.8	97.7
18	100.0	99.9	99.8	99.7	99.6	99.5	99.4	99.3	99.2	99.1	99.0	98.9	98.8	98.7	98.6	98.5	98.4	98.3	98.2	98.1	98.0	97.9	97.8	97.7
20	99.9	99.9	99.8	99.7	99.5	99.4	99.2	98.9	98.7	98.4	98.1	97.7	97.4	97.0	96.6	96.1	95.6	95.1	94.6	94.0	93.4	92.7	92.1	
22	99.9	99.9	99.8	99.6	99.5	99.3	99.1	98.8	98.5	98.2	97.9	97.5	97.1	96.7	96.2	95.7	95.2	94.6	94.0	93.4	92.7	92.0	91.2	
24	99.9	99.9	99.7	99.6	99.4	99.2	99.0	98.7	98.4	98.1	97.7	97.3	96.8	96.4	95.9	95.3	94.7	94.1	93.4	92.7	92.0	91.2	90.4	
26	99.9	99.8	99.7	99.6	99.4	99.2	98.9	98.6	98.3	97.9	97.5	97.1	96.6	96.1	95.5	94.9	94.3	93.6	92.9	92.1	91.3	90.4	89.5	
28	99.9	99.8	99.7	99.5	99.3	99.1	98.8	98.5	98.1	97.7	97.3	96.8	96.3	95.7	95.1	94.5	93.8	93.1	92.3	91.5	90.6	89.7	88.7	
30	99.9	99.8	99.7	99.5	99.3	99.0	98.7	98.4	98.0	97.6	97.1	96.6	96.0	95.4	94.8	94.1	93.4	92.6	91.7	90.8	89.9	88.9	87.8	
32	99.9	99.8	99.7	99.5	99.2	99.0	98.6	98.3	97.9	97.4	96.9	96.4	95.8	95.1	94.4	93.7	92.9	92.0	91.1	90.2	89.2	88.1	86.9	
34	99.9	99.8	99.6	99.4	99.2	98.9	98.6	98.2	97.7	97.2	96.7	96.1	95.5	94.8	94.1	93.3	92.4	91.5	90.5	89.5	88.4	87.3	86.0	
36	99.9	99.8	99.6	99.4	99.1	98.8	98.5	98.1	97.6	97.1	96.5	95.9	95.2	94.5	93.7	92.9	92.0	91.0	90.0	88.9	87.7	86.4	85.1	
38	99.9	99.8	99.6	99.4	99.1	98.8	98.4	97.9	97.5	96.9	96.3	95.7	95.0	94.2	93.3	92.5	91.5	90.5	89.4	88.2	87.0	85.6	84.2	
40	99.9	99.8	99.6	99.3	99.0	98.7	98.3	97.8	97.3	96.8	96.1	95.4	94.7	93.9	93.0	92.0	91.0	89.9	88.8	87.5	86.2	84.8	83.3	
42	99.9	99.8	99.6	99.3	99.0	98.6	98.2	97.7	97.2	96.6	95.9	95.2	94.4	93.5	92.6	91.6	90.5	89.4	88.2	86.9	85.5	84.0	82.4	
44	99.9	99.7	99.5	99.3	99.0	98.6	98.1	97.6	97.1	96.4	95.7	95.0	94.1	93.2	92.2	91.2	90.1	88.9	87.6	86.2	84.7	83.1	81.4	
46	99.9	99.7	99.5	99.2	98.9	98.5	98.0	97.5	96.9	96.3	95.5	94.7	93.9	92.9	91.9	90.8	89.6	88.3	86.9	85.5	83.9	82.3	80.5	
48	99.9	99.7	99.5	99.2	98.9	98.4	98.0	97.4	96.8	96.1	95.3	94.5	93.6	92.6	91.5	90.3	89.1	87.8	86.3	84.8	83.1	81.4	79.5	
50	99.9	99.7	99.5	99.2	98.8	98.4	97.9	97.3	96.6	95.9	95.1	94.3	93.3	92.3	91.1	89.9	88.6	87.2	85.7	84.1	82.4	80.5	78.5	
52	99.9	99.7	99.5	99.1	98.8	98.3	97.8	97.2	96.5	95.8	94.9	94.0	93.0	91.9	90.7	89.5	88.1	86.7	85.1	83.4	81.6	79.6	77.5	
54	99.9	99.7	99.4	99.1	98.7	98.2	97.7	97.1	96.4	95.6	94.7	93.8	92.7	91.6	90.4	89.1	87.6	86.1	84.4	82.7	80.8	78.7	76.5	
56	99.9	99.7	99.4	99.1	98.7	98.2	97.6	97.0	96.2	95.4	94.5	93.5	92.5	91.3	90.0	88.6	87.1	85.5	83.8	82.0	80.1	77.8	75.5	
58	99.9	99.7	99.4	99.0	98.6	98.1	97.5	96.8	96.1	95.3	94.3	93.3	92.2	91.0	89.6	88.2	86.6	85.0	83.2	81.2	79.1	76.8	74.5	
60	99.8	99.6	99.4	99.0	98.6	98.0	97.4	96.7	96.0	95.1	94.1	93.1	91.9	90.6	89.2	87.8	86.1	84.4	82.5	80.5	78.3	76.0	73.4	
62	99.8	99.6	99.3	99.0	98.5	98.0	97.3	96.6	95.8	94.9	93.9	92.8	91.6	90.3	88.9	87.3	85.6	83.8	81.9	79.8	77.5	75.0	72.3	
64	99.8	99.6	99.3	98.9	98.5	97.9	97.3	96.5	95.7	94.7	93.7	92.6	91.3	90.0	88.5	86.9	85.1	83.2	81.2	79.0	76.6	74.0	71.2	
66	99.8	99.6	99.3	98.9	98.4	97.8	97.2	96.4	95.5	94.6	93.5	92.3	91.0	89.6	88.1	86.4	84.6	82.7	80.5	78.3	75.8	73.1	70.1	
68	99.8	99.6	99.3	98.9	98.4	97.8	97.1	96.3	95.4	94.4	93.3	92.1	90.7	89.3	87.7	86.0	84.1	82.1	79.9	77.5	74.9	72.1	69.0	
70	99.8	99.6	99.3	98.8	98.3	97.7	97.0	96.2	95.3	94.2	93.1	91.8	90.5	89.0	87.3	85.5	83.6	81.5	79.2	76.7	74.0	71.1	67.9	
72	99.8	99.6	99.2	98.8	98.3	97.6	96.9	96.1	95.1	94.1	92.9	91.6	90.2	88.6	86.9	85.1	83.1	80.9	78.5	75.9	73.1	70.1	66.7	
74	99.8	99.6	99.2	98.8	98.2	97.6	96.8	96.0	95.0	93.9	92.7	91.3	89.9	88.3	86.5	84.6	82.5	80.3	77.8	75.2	72.2	69.0	65.5	
76	99.8	99.5	99.2	98.7	98.2	97.5	96.7	95.8	94.8	93.7	92.5	91.1	89.6	87.9	86.1	84.2	82.0	79.7	77.1	74.4	71.3	68.0	64.3	
78	99.8	99.5	99.2	98.7	98.1	97.4	96.6	95.7	94.7	93.6	92.3	90.9	89.3	87.6	85.7	83.7	81.5	79.1	76.4	73.6	70.4	66.9	63.1	
80	99.8	99.5	99.2	98.7	98.1	97.4	96.6	95.6	94.6	93.4	92.1	90.6	89.0	87.3	85.3	83.2	80.9	78.4	75.7	72.7	69.5	65.8	61.8	
82	99.8	99.5	99.1	98.6	98.0	97.3	96.5	95.5	94.4	93.2	91.9	90.4	88.7	86.9	84.9	82.8	80.4	77.8	75.0	71.9	68.6	64.7	60.5	
84	99.8	99.5	99.1	98.6	98.0	97.2	96.4	95.4	94.3	93.0	91.6	90.1	88.4	86.6	84.5	82.3	79.9	77.2	74.3	71.1	67.6	63.6	59.2	
86	99.8	99.5	99.1	98.6	97.9	97.2	96.3	95.3	94.1	92.9	91.4	89.9	88.1	86.2	84.1	81.8	79.3	76.6	73.5	70.2	66.5	62.5	57.9	
88	99.8	99.5	99.1	98.5	97.9	97.1	96.2	95.2	94.0	92.7	91.2	89.6	87.8	85.9	83.7	81.4	78.8	75.9	72.8	69.4	65.6	61.3	56.5	
90	99.8	99.5	99.0	98.5	97.8	97.0	96.1	95.1	93.9	92.5	91.0	89.4	87.5	85.5	83.3	80.9	78.2	75.3	72.1	68.5	64.5	60.1	55.1	
92	99.8	99.5	99.0	98.5	97.8	97.0	96.0	94.9	93.7	92.3	90.8	89.1	87.2	85.2	82.9	80.4	77.6	74.6	71.3	67.6	63.5	58.9	53.6	
94	99.8	99.4	99.0	98.4	97.7	96.9	95.9	94.8	93.6	92.2	90.6	88.9	86.9	84.8	82.5	79.9	77.1	74.0	70.5	66.7	62.5	57.6	52.1	
96	99.7	99.4	99.0	98.4	97.7	96.8	95.9	94.7	93.4	92.0	90.4	88.6	86.6	84.4	82.1	79.4	76.5	73.3	69.8	65.8	61.4	56.4	50.5	
98	99.7	99.4	99.0	98.4	97.6	96.8	95.8	94.6	93.3	91.8	90.2	88.3	86.3	84.1	81.6	78.9	75.9	72.6	69.0	64.9	60.3	55.1	48.9	
100	99.7	99.4	98.9	98.3	97.6	96.7	95.7	94.5	93.2	91.6	90.0	88.1	86.0	83.7	81.2	78.4	75.4	72.0	68.2	64.0	59.2	53.7	47.3	
102	99.7	99.4	98.9	98.3	97.5	96.6	95.6	94.4	93.0	91.5	89.7	87.8	85.7	83.4	80.8	77.9	74.8	71.3	67.4	63.0	58.1	52.3	45.6	
104	99.7	99.4	98.9	98.3	97.5	96.6	95.5	94.3	92.9	91.3	89.5	87.6	85.4	83.0	80.4	77.4	74.2	70.6	66.6	62.1	56.9	50.9	43.8	
106	99.7	99.4	98.9	98.2	97.4	96.5	95.4	94.2	92.7	91.1	89.3	87.3	85.1	82.6	79.9	76.9	73.6	69.9	65.8	61.1	55.7	49.5	41.9	
108	99.7	99.4	98.9	98.2	97.4																			

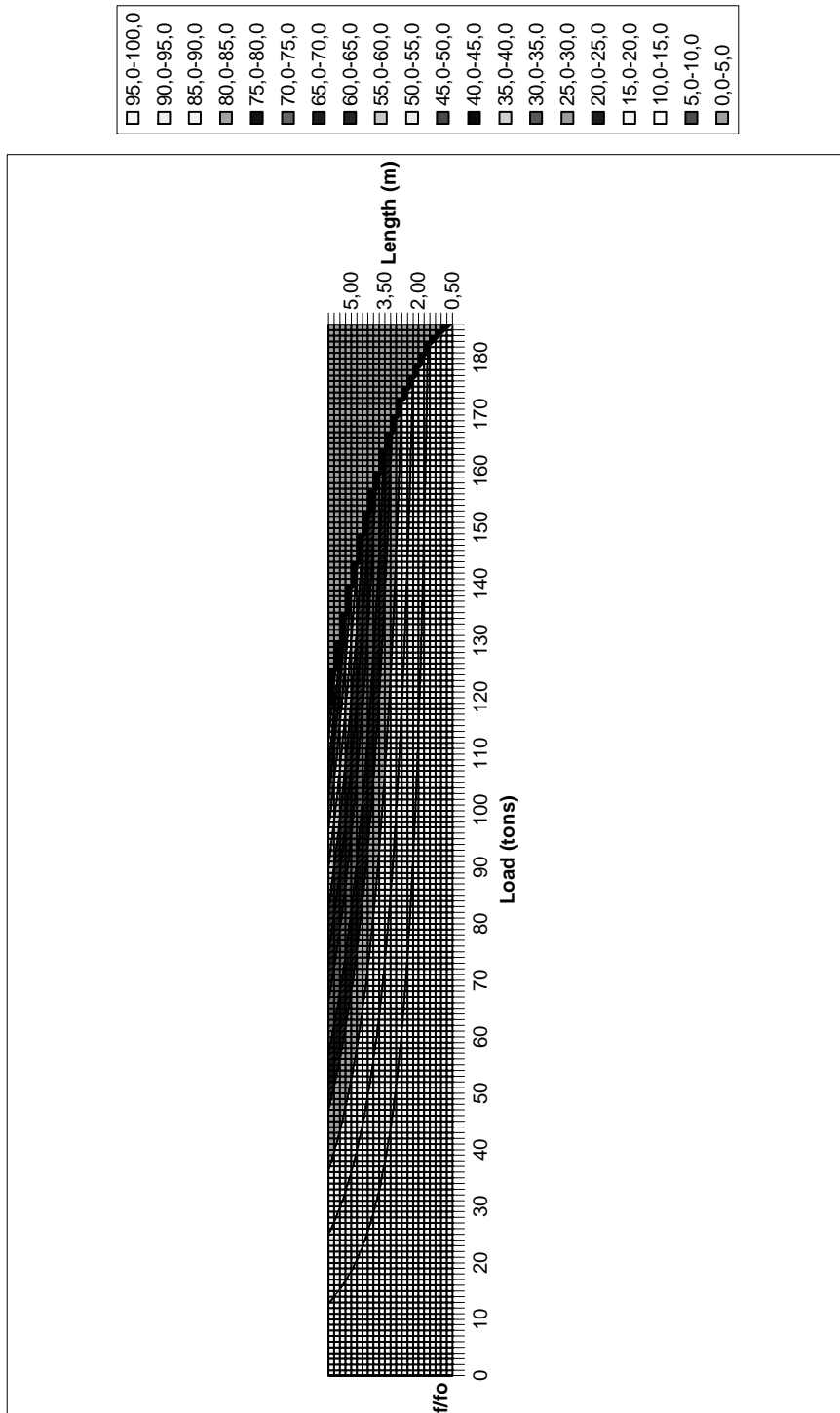


Figure A.13: Contour lines of the first vibration frequency ratios of the I320 steel column (in percentage) for certain lengths and loads

Table A.27. Fundamental frequency change in percentage versus axial load level for I340 steel column for different lengths for load level

		P _r (tons)																						
		207,6	207,0	206,1	205,0	203,7	202,1	200,3	198,2	195,9	193,3	190,5	187,5	184,2	180,7	176,9	172,9	168,7	164,2	159,5	154,5	149,3	143,8	138,1
P (tons)	f/f ₀ (%)	Length (m)																						
		0,50	0,75	1,00	1,25	1,50	1,75	2,00	2,25	2,50	2,75	3,00	3,25	3,50	3,75	4,00	4,25	4,50	4,75	5,00	5,25	5,50	5,75	6,00
4																								
6																								
8																								
10																								
12																								
14																								
16																								
18																								
20																								
22																								
24																								
26																								
28																								
30																								
32																								
34																								137,8
36																								135,7
38																								133,5
40																								142,8
42																								140,1
44																								137,2
46																								146,7
48																								143,3
50																								153,4
52																								149,3
54																								145,1
56																								155,1
58																								150,0
60																								160,4
62																								154,5
64																								165,2
66																								158,0
68																								168,9
70																								160,4
72																								171,1
74																								160,9
76																								171,0
78																								182,2
80																								167,6
82																								177,1
84																								186,9
86																								165,5
88																								170,8
90																								174,2
92																								174,0
94																								167,1
96																								200,3
98																								145,8
100	0,0	0,0	0,0	0,0	0,0	0,0	0,0	0,0	0,0	0,0	0,0	0,0	0,0	0,0	0,0	0,0	0,0	0,0	0,0	0,0	0,0	0,0	0,0	0,0

Table A.28. Fundamental frequency change in percentage versus axial load level for I340 steel column for different lengths for frequency change

f _{ff} (%)	Length (m)																							
	0.50	0.75	1.00	1.25	1.50	1.75	2.00	2.25	2.50	2.75	3.00	3.25	3.50	3.75	4.00	4.25	4.50	4.75	5.00	5.25	5.50	5.75	6.00	
0.0	100.0	100.0	100.0	100.0	100.0	100.0	100.0	100.0	100.0	100.0	100.0	100.0	100.0	100.0	100.0	100.0	100.0	100.0	100.0	100.0	100.0	100.0	100.0	100.0
2.5	100.0	100.0	100.0	100.0	100.0	99.9	99.9	99.9	99.9	99.9	99.9	99.8	99.8	99.7	99.7	99.6	99.6	99.5	99.5	99.5	99.4	99.3	99.3	99.2
5.0	100.0	100.0	100.0	99.9	99.9	99.9	99.8	99.7	99.7	99.6	99.5	99.4	99.3	99.2	99.1	99.0	98.8	98.7	98.5	98.4	98.2	98.0	97.8	97.6
7.5	100.0	100.0	99.9	99.9	99.9	99.8	99.7	99.7	99.6	99.5	99.4	99.3	99.2	99.1	99.0	98.8	98.7	98.5	98.2	98.0	97.7	97.5	97.2	97.0
10.0	100.0	100.0	99.9	99.9	99.8	99.7	99.7	99.6	99.5	99.3	99.2	99.1	99.0	98.9	98.8	98.6	98.4	98.2	98.0	97.8	97.6	97.3	97.1	96.8
12.5	100.0	99.9	99.9	99.8	99.8	99.7	99.6	99.4	99.3	99.2	99.0	98.8	98.7	98.5	98.2	98.0	97.8	97.5	97.2	97.0	96.7	96.5	96.3	96.0
15.0	100.0	99.9	99.9	99.8	99.7	99.6	99.5	99.3	99.2	99.0	98.8	98.6	98.4	98.1	97.9	97.6	97.3	97.0	96.7	96.5	96.2	96.0	95.6	95.2
17.5	100.0	99.9	99.8	99.8	99.7	99.5	99.4	99.2	99.0	98.8	98.6	98.4	98.1	97.8	97.5	97.2	96.9	96.5	96.1	95.7	95.3	94.8	94.4	94.0
20.0	100.0	99.9	99.8	99.7	99.6	99.5	99.3	99.1	98.9	98.7	98.4	98.1	97.8	97.5	97.2	96.8	96.4	96.0	95.6	95.1	94.6	94.1	93.5	92.9
22.5	100.0	99.9	99.8	99.7	99.6	99.4	99.2	99.0	98.8	98.5	98.2	97.9	97.6	97.2	96.8	96.4	96.0	95.5	95.0	94.4	93.9	93.3	92.7	92.1
25.0	99.9	99.9	99.8	99.7	99.5	99.3	99.1	98.9	98.6	98.3	98.0	97.7	97.3	96.9	96.5	96.0	95.5	95.0	94.4	93.8	93.2	92.5	91.8	91.0
27.5	99.9	99.9	99.8	99.6	99.5	99.3	99.0	98.8	98.5	98.2	97.8	97.4	97.0	96.6	96.1	95.6	95.0	94.4	93.8	93.2	92.5	91.7	91.0	90.1
30.0	99.9	99.9	99.7	99.6	99.4	99.2	99.0	98.7	98.4	98.0	97.6	97.2	96.8	96.3	95.7	95.2	94.6	93.9	93.2	92.5	91.7	91.0	90.1	89.2
32.5	99.9	99.8	99.7	99.6	99.4	99.1	98.9	98.6	98.2	97.8	97.4	97.0	96.5	95.9	95.4	94.8	94.1	93.4	92.7	91.9	91.0	90.1	89.2	88.3
35.0	99.9	99.8	99.7	99.5	99.3	99.1	98.8	98.4	98.1	97.7	97.2	96.7	96.2	95.6	95.0	94.3	93.6	92.9	92.1	91.2	90.3	89.3	88.3	87.4
37.5	99.9	99.8	99.7	99.5	99.3	99.0	98.7	98.3	97.9	97.5	97.0	96.5	95.9	95.3	94.6	93.9	93.2	92.3	91.5	90.5	89.5	88.5	87.4	86.5
40.0	99.9	99.8	99.7	99.5	99.2	98.9	98.6	98.2	97.8	97.3	96.8	96.3	95.6	95.0	94.3	93.5	92.7	91.8	90.9	89.9	88.8	87.7	86.5	85.5
42.5	99.9	99.8	99.6	99.4	99.2	98.9	98.5	98.1	97.7	97.2	96.6	96.0	95.4	94.7	93.9	93.1	92.2	91.3	90.3	89.2	88.1	86.9	85.6	84.4
45.0	99.9	99.7	99.6	99.4	99.1	98.8	98.4	98.0	97.5	97.0	96.4	95.8	95.1	94.3	93.5	92.6	91.7	90.7	89.6	88.5	87.3	86.0	84.7	83.4
47.5	99.9	99.8	99.6	99.4	99.1	98.7	98.3	97.9	97.4	96.8	96.2	95.5	94.8	94.0	93.1	92.2	91.2	90.2	89.0	87.8	86.5	85.2	83.7	82.4
50.0	99.9	99.8	99.6	99.3	99.0	98.7	98.2	97.8	97.2	96.7	96.0	95.3	94.5	93.7	92.8	91.8	90.7	89.6	88.4	87.1	85.8	84.3	82.8	81.3
52.5	99.9	99.7	99.5	99.3	99.0	98.6	98.2	97.7	97.1	96.5	95.8	95.1	94.2	93.3	92.4	91.4	90.3	89.1	87.8	86.4	85.0	83.4	81.8	80.2
55.0	99.9	99.7	99.5	99.3	98.9	98.5	98.1	97.5	97.0	96.3	95.6	94.8	93.9	93.0	92.0	90.9	89.8	88.5	87.2	85.7	84.2	82.6	80.9	79.2
57.5	99.9	99.7	99.5	99.2	98.9	98.5	98.0	97.4	96.8	96.1	95.4	94.6	93.7	92.7	91.6	90.5	89.3	87.9	86.5	85.0	83.4	81.7	79.8	77.9
60.0	99.9	99.7	99.5	99.2	98.8	98.4	97.9	97.3	96.7	96.0	95.2	94.3	93.4	92.4	91.2	90.0	88.8	87.4	85.9	84.3	82.6	80.8	78.8	76.8
62.5	99.9	99.7	99.5	99.1	98.8	98.3	97.8	97.2	96.5	95.8	95.0	94.1	93.1	92.0	90.9	89.6	88.3	86.8	85.2	83.6	81.9	79.7	77.5	75.2
65.0	99.9	99.7	99.4	99.1	98.7	98.3	97.7	97.1	96.4	95.6	94.8	93.8	92.8	91.7	90.5	89.2	87.8	86.2	84.6	82.8	81.0	78.9	76.8	74.6
67.5	99.9	99.7	99.4	99.1	98.7	98.2	97.6	97.0	96.3	95.5	94.6	93.6	92.5	91.3	90.1	88.7	87.2	85.7	83.9	82.1	80.1	78.0	75.7	73.4
70.0	99.8	99.7	99.4	99.0	98.6	98.1	97.5	96.9	96.1	95.3	94.4	93.3	92.2	91.0	89.7	88.3	86.7	85.1	83.3	81.4	79.3	77.1	74.6	72.1
72.5	99.8	99.6	99.4	99.0	98.6	98.1	97.4	96.8	96.0	95.1	94.1	93.1	91.9	90.7	89.3	87.8	86.2	84.5	82.6	80.6	78.4	76.1	73.6	71.1
75.0	99.8	99.6	99.3	99.0	98.5	98.0	97.4	96.6	95.8	94.9	93.9	92.8	91.6	90.3	88.9	87.4	85.7	83.9	81.9	79.8	77.6	75.1	72.5	70.0
77.5	99.8	99.6	99.3	98.9	98.5	97.9	97.3	96.5	95.7	94.8	93.7	92.6	91.3	90.0	88.5	86.9	85.2	83.3	81.3	79.1	76.7	74.1	71.3	68.5
80.0	99.8	99.6	99.3	98.9	98.4	97.8	97.2	96.4	95.6	94.6	93.5	92.3	91.1	89.6	88.1	86.5	84.7	82.7	80.6	78.3	75.8	73.1	70.2	67.3
82.5	99.8	99.6	99.3	98.9	98.4	97.8	97.1	96.3	95.4	94.4	93.3	92.1	90.8	89.3	87.7	86.0	84.1	82.1	79.9	77.5	74.9	72.1	69.1	66.1
85.0	99.8	99.6	99.3	98.8	98.3	97.7	97.0	96.2	95.3	94.2	93.1	91.8	90.5	89.0	87.3	85.5	83.6	81.5	79.2	76.7	74.0	71.1	67.9	64.7
87.5	99.8	99.6	99.2	98.8	98.3	97.6	96.9	96.1	95.1	94.1	92.9	91.6	90.2	88.6	86.9	85.1	83.1	80.9	78.5	75.9	73.1	70.0	66.7	63.4
90.0	99.8	99.6	99.2	98.8	98.2	97.6	96.8	96.0	95.0	93.9	92.7	91.3	89.9	88.3	86.5	84.6	82.5	80.3	77.8	75.1	72.2	69.0	65.5	62.0
92.5	99.8	99.5	99.2	98.7	98.2	97.5	96.7	95.8	94.8	93.7	92.5	91.1	89.6	87.9	86.1	84.1	82.0	79.6	77.1	74.3	71.2	67.9	64.2	60.5
95.0	99.8	99.5	99.2	98.7	98.1	97.4	96.6	95.7	94.7	93.5	92.2	90.8	89.3	87.6	85.7	83.6	81.4	79.0	76.4	73.5	70.3	66.8	62.9	58.9
97.5	99.8	99.5	99.1	98.7	98.1	97.4	96.5	95.6	94.5	93.4	92.0	90.6	89.0	87.2	85.3	83.2	80.9	78.4	75.6	72.6	69.3	65.7	61.6	57.3
100.0	99.8	99.5	99.1	98.6	98.0	97.3	96.5	95.5	94.4	93.2	91.8	90.3	88.7	86.8	84.9	82.7	80.3	77.7	74.9	71.8	68.3	64.5	60.3	56.0
102.5	99.8	99.5	99.1	98.6	98.0	97.2	96.4	95.4	94.3	93.0	91.6	90.1	88.4	86.5	84.4	82.2	79.8	77.1	74.1	70.9	67.3	63.4	58.9	54.4
105.0	99.8	99.5	99.1	98.6	97.9	97.2	96.3	95.3	94.1	92.8	91.4	89.8	88.1	86.1	84.0	81.7	79.2	76.4	73.4	70.0	66.3	62.2	57.5	52.8
107.5	99.8	99.5	99.1	98.5	97.9	97.1	96.2	95.1	94.0	92.6	91.2	89.5	87.7	85.8	83.6	81.2	78.6	75.8	72.6	69.1	65.3	61.0	56.1	51.2
110.0	99.8	99.5	99.0	98.5	97.8	97.0	96.1	95.0	93.8	92.5	91.0	89.3	87.4	85.4	83.2	80.7	78.0	75.1	71.8	68.2	64.2	59.7	54.6	49.5
112.5	99.8	99.4	99.0	98.5	97.8	97.0	96.0	94.9	93.7	92.3	90.7	89.0	87.1	85.0	82.8	80.2	77.5	74.4	71.1	67.3	63.2	58.5	53.1	47.8
115.0	99.8	99.4	99.0	98.4	97.7	96.9	95.9	94.8	93.5	92.1	90.5	88.8	86.8	84.7	82.3	79.7	76.9	73.7	70.3	66.4	62.1	57.2	51.6	46.1
117.5	99.7	99.4	99.0	98.4	97.7	96.8	95.8	94.7	93.4	91.9	90.3	88.5	86.5	84.3	81.9	79.2	76.3	73.1	69.5	65.5	61.0	55.9	50.0	44.1
120.0	99.7	99.4	99.0	98.4	97.6	96.8	95.7	94.6	93.2	91.7	90.1	88.2	86.2	83.9	81.5	78.7	75.7	72.4	68.7	64.5	59.9	54.5	48.3	42.4
122.5	99.7	99.4	98.9	98.3	97.6	96.7	95.6	94.4	93.1	91.6	89.9	88.0	85.9	83.6	81.0	78.2	75.1	71.7	67.8	63.5	58.7	53.1	46.6	40.7
125.0	99.7	99.4	98.9	98.3	97.5	96.6	95.6	94.3	92.9	91.4	89.6	87.7	85.6	83.2	80.6	77.7	74.5	71.0	67.0	62.6	57.5	51.7	44.8	38.9
127.5	99.7	99.4	98.9	98.3	97.5	96.5	95.5	94.2	92.8	91.2	89.4	87.4	85.3	82.8	80.1	77.2	73.9	70.3	66.2	61.6	56.3	50.2	42.9	37.0
130.0																								

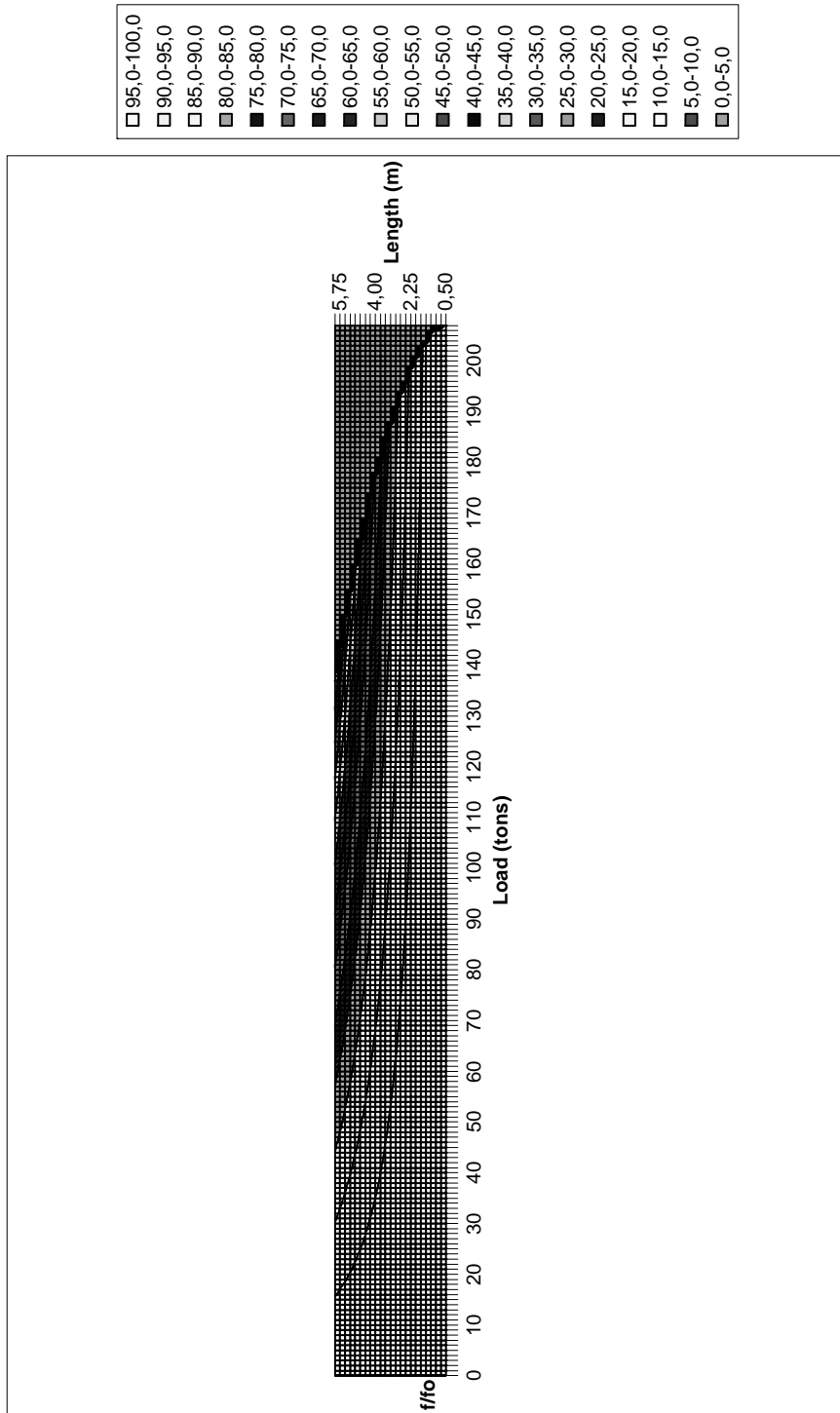


Figure A.14: Contour lines of the first vibration frequency ratios of the I340 steel column (in percentage) for certain lengths and loads

Table A.30. Fundamental frequency change in percentage versus axial load level for I360 steel column for different lengths for frequency change

Load (tons)	f/f ₀ (%)	Length (m)																							
		0.50	0.75	1.00	1.25	1.50	1.75	2.00	2.25	2.50	2.75	3.00	3.25	3.50	3.75	4.00	4.25	4.50	4.75	5.00	5.25	5.50	5.75	6.00	
0.0	100.0	100.0	100.0	100.0	100.0	100.0	100.0	100.0	100.0	100.0	100.0	100.0	100.0	100.0	100.0	100.0	100.0	100.0	100.0	100.0	100.0	100.0	100.0	100.0	
2.5	100.0	100.0	100.0	100.0	100.0	99.9	99.9	99.9	99.9	99.9	99.8	99.8	99.8	99.7	99.7	99.6	99.6	99.6	99.6	99.6	99.6	99.5	99.5	99.4	99.4
5.0	100.0	100.0	100.0	99.9	99.9	99.9	99.9	99.8	99.8	99.7	99.7	99.6	99.6	99.5	99.4	99.4	99.3	99.2	99.1	99.0	98.9	98.8	98.8	98.7	98.7
7.5	100.0	100.0	99.9	99.9	99.8	99.8	99.7	99.6	99.5	99.4	99.3	99.2	99.1	99.0	98.9	98.8	98.7	98.6	98.5	98.4	98.3	98.2	98.1	98.0	97.9
10.0	100.0	100.0	99.9	99.9	99.8	99.8	99.7	99.6	99.5	99.4	99.3	99.2	99.1	99.0	98.9	98.8	98.7	98.6	98.5	98.4	98.3	98.2	98.1	98.0	97.9
12.5	100.0	99.9	99.9	99.8	99.8	99.7	99.6	99.5	99.4	99.3	99.2	99.1	99.0	98.9	98.8	98.7	98.6	98.5	98.4	98.3	98.2	98.1	98.0	97.9	97.8
15.0	100.0	99.9	99.9	99.8	99.8	99.7	99.6	99.5	99.4	99.3	99.2	99.1	99.0	98.9	98.8	98.7	98.6	98.5	98.4	98.3	98.2	98.1	98.0	97.9	97.8
17.5	100.0	99.9	99.9	99.8	99.7	99.6	99.5	99.4	99.3	99.2	99.1	99.0	98.9	98.8	98.7	98.6	98.5	98.4	98.3	98.2	98.1	98.0	97.9	97.8	97.7
20.0	100.0	99.9	99.9	99.8	99.7	99.6	99.4	99.3	99.1	98.9	98.7	98.5	98.2	98.0	97.7	97.4	97.1	96.7	96.4	96.0	95.5	95.0	94.5	93.9	93.2
22.5	100.0	99.9	99.8	99.7	99.6	99.5	99.4	99.2	99.0	98.8	98.5	98.3	98.0	97.7	97.4	97.0	96.7	96.3	95.9	95.5	95.0	94.5	94.0	93.4	92.7
25.0	100.0	99.9	99.8	99.7	99.6	99.5	99.3	99.1	98.9	98.6	98.4	98.1	97.8	97.4	97.1	96.7	96.3	95.9	95.4	94.9	94.4	93.9	93.2	92.6	91.9
27.5	100.0	99.9	99.8	99.7	99.6	99.4	99.2	99.0	98.8	98.5	98.2	97.9	97.6	97.2	96.8	96.4	95.9	95.4	94.9	94.4	93.9	93.3	92.6	92.0	91.3
30.0	99.9	99.9	99.8	99.7	99.5	99.3	99.1	98.9	98.6	98.4	98.0	97.7	97.3	96.9	96.5	96.0	95.5	95.0	94.5	94.0	93.5	93.0	92.3	91.7	91.0
32.5	99.9	99.9	99.8	99.6	99.5	99.3	99.1	98.8	98.5	98.2	97.9	97.5	97.1	96.7	96.2	95.7	95.2	94.6	94.0	93.3	92.7	92.0	91.3	90.7	90.0
35.0	99.9	99.9	99.8	99.6	99.4	99.2	99.0	98.7	98.4	98.1	97.7	97.3	96.9	96.4	95.9	95.4	94.8	94.2	93.5	92.8	92.1	91.3	90.6	90.0	89.3
37.5	99.9	99.8	99.7	99.6	99.4	99.2	98.9	98.6	98.3	97.9	97.6	97.1	96.7	96.1	95.6	95.0	94.4	93.7	93.0	92.3	91.5	90.7	90.0	89.3	88.6
40.0	99.9	99.8	99.7	99.6	99.4	99.1	98.8	98.5	98.2	97.8	97.4	96.9	96.4	95.9	95.3	94.7	94.0	93.3	92.6	91.7	90.9	90.2	89.5	88.8	88.1
42.5	99.9	99.8	99.7	99.5	99.3	99.1	98.8	98.4	98.1	97.7	97.2	96.7	96.2	95.6	95.0	94.3	93.6	92.9	92.1	91.2	90.3	89.5	88.8	88.1	87.4
45.0	99.9	99.8	99.7	99.5	99.3	99.0	98.7	98.4	98.0	97.5	97.1	96.5	96.0	95.4	94.7	94.0	93.2	92.4	91.6	90.6	89.7	88.9	88.2	87.5	86.8
47.5	99.9	99.8	99.7	99.5	99.2	99.0	98.6	98.3	97.9	97.4	96.9	96.3	95.7	95.1	94.4	93.6	92.8	92.0	91.1	90.1	89.1	88.0	87.0	86.0	85.0
50.0	99.9	99.8	99.6	99.4	99.2	98.9	98.6	98.2	97.7	97.3	96.7	96.1	95.5	94.8	94.1	93.3	92.4	91.5	90.6	89.5	88.5	87.3	86.3	85.3	84.3
52.5	99.9	99.8	99.6	99.4	99.2	98.8	98.5	98.1	97.6	97.1	96.6	95.9	95.3	94.6	93.8	92.9	92.0	91.1	90.1	89.0	87.9	86.8	85.7	84.6	83.5
55.0	99.9	99.8	99.6	99.4	99.1	98.8	98.4	98.0	97.5	97.0	96.4	95.7	95.0	94.3	93.5	92.6	91.7	90.6	89.6	88.4	87.2	86.0	84.8	83.6	82.4
57.5	99.9	99.8	99.6	99.4	99.1	98.7	98.3	97.9	97.4	96.8	96.2	95.5	94.8	94.0	93.2	92.2	91.3	90.2	89.1	87.9	86.6	85.4	84.2	83.0	81.8
60.0	99.9	99.8	99.6	99.3	99.0	98.7	98.3	97.8	97.3	96.7	96.1	95.3	94.6	93.8	92.9	91.9	90.9	89.7	88.6	87.3	86.0	84.7	83.4	82.1	80.8
62.5	99.9	99.7	99.6	99.3	99.0	98.6	98.2	97.7	97.2	96.6	95.9	95.1	94.3	93.5	92.5	91.5	90.4	89.3	88.0	86.7	85.4	84.1	82.8	81.5	80.2
65.0	99.9	99.7	99.5	99.3	98.9	98.6	98.1	97.6	97.0	96.4	95.7	94.9	94.1	93.2	92.2	91.2	90.0	88.8	87.5	86.2	84.9	83.6	82.3	81.0	79.7
67.5	99.9	99.7	99.5	99.2	98.9	98.5	98.0	97.5	96.9	96.3	95.5	94.7	93.9	92.9	91.9	90.8	89.6	88.4	87.0	85.6	84.0	82.3	80.6	78.9	77.2
70.0	99.9	99.7	99.5	99.2	98.9	98.5	98.0	97.4	96.8	96.1	95.4	94.5	93.6	92.7	91.6	90.5	89.2	87.9	86.5	85.0	83.3	81.6	79.9	78.2	76.5
72.5	99.9	99.7	99.5	99.2	98.8	98.4	97.9	97.3	96.7	96.0	95.2	94.3	93.4	92.4	91.3	90.1	88.8	87.4	86.0	84.4	82.7	81.0	79.3	77.6	75.9
75.0	99.9	99.7	99.5	99.2	98.8	98.3	97.8	97.2	96.6	95.8	95.0	94.1	93.2	92.1	91.0	89.7	88.4	87.0	85.4	83.8	82.0	80.3	78.6	76.9	75.2
77.5	99.9	99.7	99.4	99.1	98.7	98.3	97.8	97.1	96.5	95.7	94.9	93.9	92.9	91.8	90.7	89.4	88.0	86.5	84.9	83.2	81.3	79.4	77.5	75.6	73.7
80.0	99.9	99.7	99.4	99.1	98.7	98.2	97.7	97.1	96.4	95.6	94.7	93.7	92.7	91.6	90.3	89.0	87.6	86.0	84.4	82.6	80.7	78.8	76.9	75.0	73.1
82.5	99.9	99.7	99.4	99.1	98.7	98.2	97.6	97.0	96.2	95.4	94.5	93.5	92.5	91.3	90.0	88.6	87.1	85.5	83.8	82.0	80.1	78.2	76.3	74.4	72.5
85.0	99.8	99.7	99.4	99.0	98.6	98.1	97.5	96.9	96.1	95.3	94.4	93.3	92.2	91.0	89.7	88.3	86.7	85.1	83.3	81.4	79.3	77.3	75.3	73.3	71.3
87.5	99.8	99.6	99.4	99.0	98.6	98.1	97.5	96.8	96.0	95.1	94.2	93.1	92.0	90.7	89.4	87.9	86.3	84.6	82.7	80.7	78.6	76.5	74.4	72.3	70.2
90.0	99.8	99.6	99.4	99.0	98.5	98.0	97.4	96.7	95.9	95.0	94.0	92.9	91.7	90.4	89.0	87.5	85.9	84.1	82.2	80.1	77.9	75.7	73.5	71.3	69.1
92.5	99.8	99.6	99.3	99.0	98.5	98.0	97.3	96.6	95.8	94.9	93.8	92.7	91.5	90.2	88.7	87.1	85.4	83.6	81.6	79.5	77.2	74.9	72.6	70.3	68.0
95.0	99.8	99.6	99.3	98.9	98.5	97.9	97.2	96.5	95.6	94.7	93.7	92.5	91.3	89.9	88.4	86.8	85.0	83.1	81.1	78.8	76.4	73.9	71.4	68.9	66.4
97.5	99.8	99.6	99.3	98.9	98.4	97.8	97.2	96.4	95.5	94.6	93.5	92.3	91.0	89.6	88.1	86.4	84.6	82.6	80.5	78.2	75.7	73.1	70.5	67.9	65.3
100.0	99.8	99.6	99.3	98.9	98.4	97.8	97.1	96.3	95.4	94.4	93.3	92.1	90.8	89.3	87.7	86.0	84.1	82.1	79.9	77.6	75.0	72.3	69.6	66.9	64.2
102.5	99.8	99.6	99.3	98.8	98.3	97.7	97.0	96.2	95.3	94.3	93.1	91.9	90.5	89.0	87.4	85.6	83.7	81.6	79.4	76.9	74.2	71.4	68.6	65.8	63.0
105.0	99.8	99.6	99.2	98.8	98.3	97.7	96.9	96.1	95.2	94.1	93.0	91.7	90.3	88.7	87.1	85.2	83.3	81.1	78.8	76.2	73.5	70.6	67.7	64.8	61.9
107.5	99.8	99.6	99.2	98.8	98.3	97.6	96.9	96.0	95.1	94.0	92.8	91.5	90.0	88.5	86.7	84.9	82.8	80.6	78.2	75.6	72.8	69.9	67.0	64.1	61.2
110.0	99.8	99.6	99.2	98.8	98.2	97.6	96.8	95.9	94.9	93.8	92.6	91.3	89.8	88.2	86.4	84.5	82.4	80.1	77.6	74.9	71.9	68.7	65.5	62.3	59.1
112.5	99.8	99.5	99.2	98.7	98.2	97.5	96.7	95.8	94.8	93.7	92.4	91.1	89.5	87.9	86.1	84.1	81.9	79.6	77.0	74.2	71.2	67.8	64.4	61.0	57.6
115.0	99.8	99.5	99.2	98.7	98.1	97.4	96.6	95.7	94.7	93.6	92.3	90.9	89.3	87.6	85.7	83.7	81.5	79.1	76.4	73.5	70.4	66.9	63.4	59.9	56.4
117.5	99.8	99.5	99.2	98.7	98.1	97.4	96.6	95.6	94.6	93.4	92.1	90.6	89.0	87.3	85.4	83.3	81.0	78.5	75.8	72.8	69.6	66.0	62.4	58.8	55.2
120.0	99.8	99.5	99.1	98.6	98.0	97.3	96.5	95.5	94.5	93.3	91.9	90.4	88.8	87.0	85.0	82.9	80.6	78.0	75.2	72.2	68.8	65.1	61.4	57.7	54.0
122.5	99.8	99.5	99.1	98.6	98.0	97.3	96.4	95.5	94.3	93.1	91.7	90.2	88.5	86.7	84.7	82.5	80.1	77.5	74.6	71.4	68.0	64.1	59.8	55.5	51.2
125.0	99.8																								

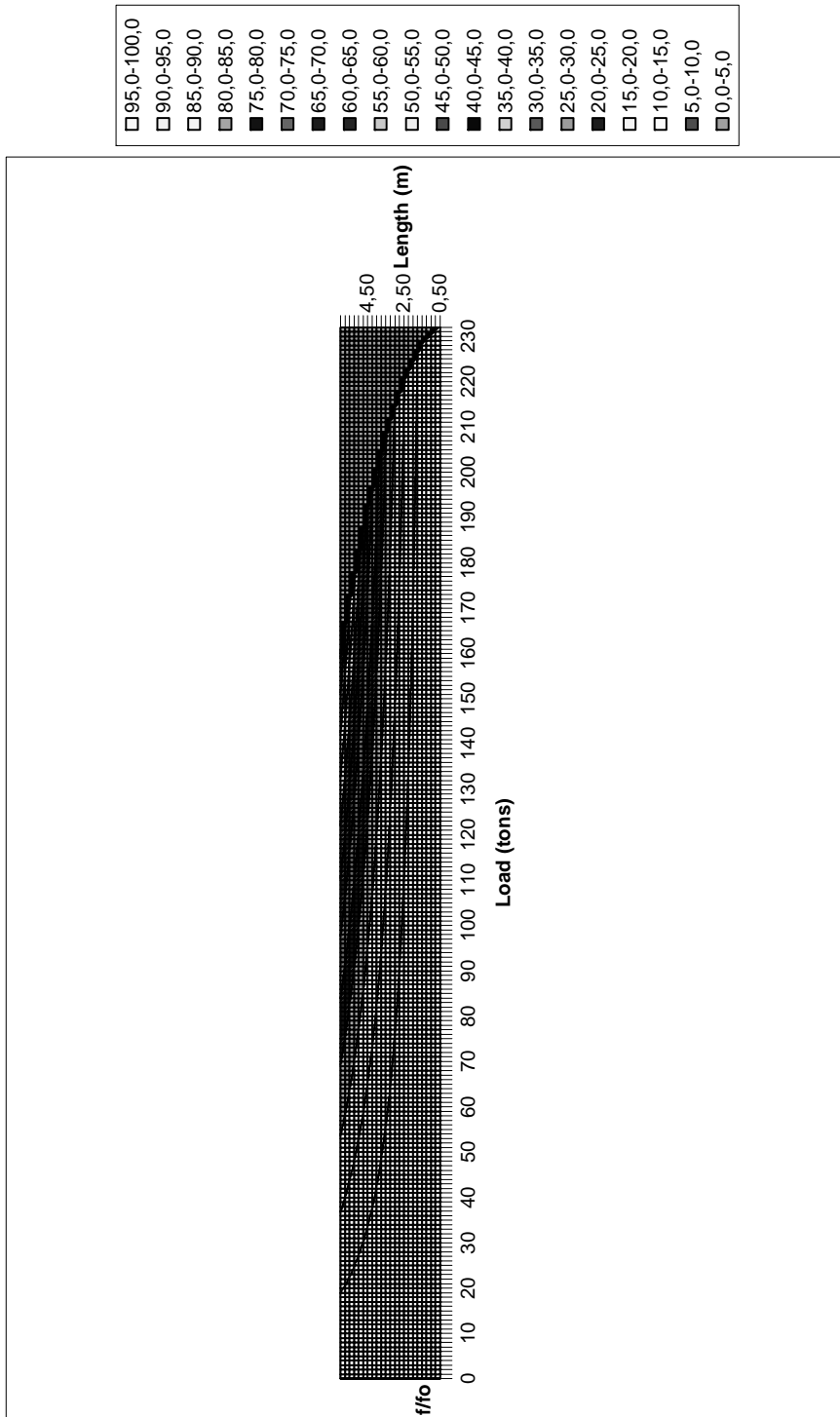


Figure A.15: Contour lines of the first vibration frequency ratios of the I360 steel column (in percentage) for certain lengths and loads

Table A.31. Fundamental frequency change in percentage versus axial load level for I380 steel column for different lengths for load level

		P _r (tons)																						
		256,3	255,6	254,7	253,6	252,1	250,5	248,6	246,4	243,9	241,3	238,3	235,1	231,7	228,0	224,0	219,8	215,3	210,6	205,6	200,4	194,9	189,1	183,1
P (tons)	L (m)	Length (m)																						
		0,50	0,75	1,00	1,25	1,50	1,75	2,00	2,25	2,50	2,75	3,00	3,25	3,50	3,75	4,00	4,25	4,50	4,75	5,00	5,25	5,50	5,75	6,00
4																								
6																								
8																								
10																								
12																								
14																								
16																								
18																								
20																								
22																								
24																								
26																								
28																								
30																								
32																								
34																								
36																								
38																								
40																								
42																								
44																								182,3
46																								178,3
48																								174,2
50																								185,0 169,9
52																								180,0 165,4
54																								191,2 174,9 160,7
56																								185,4 169,6 155,8
58																								196,9 179,4 164,1 150,7
60																								190,0 173,1 158,4 145,5
62																								201,6 182,9 166,6 152,5 140,0
64																								193,5 175,5 159,9 146,3 134,4
66																								205,2 185,2 167,9 153,0 140,0 128,6
68																								195,6 176,5 160,1 145,9 133,5 122,6
70																								206,9 185,7 167,6 152,0 138,5 126,7 116,4
72																								219,2 195,5 175,5 158,4 143,7 130,9 119,8 110,0
74																								206,1 183,9 165,0 148,9 135,1 123,1 112,6 103,4
76																								217,4 192,6 171,8 154,2 139,2 126,2 115,0 105,2 96,6
78																								201,8 178,7 159,4 143,1 129,1 117,1 106,7 97,6 89,7
80																								211,2 185,7 164,5 146,7 131,7 118,8 107,8 98,2 89,8 82,5
82																								220,9 192,4 169,1 149,8 133,6 119,9 108,2 98,2 89,4 81,8 75,2
84																								230,4 198,7 173,1 152,1 134,7 120,2 107,9 97,3 88,3 80,5 73,6 67,6
86																								204,0 175,9 153,2 134,7 119,3 106,4 95,5 86,2 78,2 71,2 65,2 59,9
88																								207,6 176,9 152,5 132,9 116,8 103,4 92,3 82,8 74,7 67,8 61,8 56,5 51,9
90																								208,3 175,0 149,1 128,6 112,0 98,4 87,2 77,8 69,8 63,0 57,1 52,1 47,6 43,8
92																								203,9 168,5 141,6 120,7 104,0 90,6 79,7 70,6 62,9 56,5 51,0 46,2 42,1 38,6 35,4
94																								241,7 191,0 154,7 127,8 107,4 91,5 78,9 68,8 60,4 53,5 47,7 42,9 38,7 35,1 32,0 29,2 26,9
96																								212,8 163,0 128,8 104,3 86,2 72,4 61,7 53,2 46,4 40,7 36,1 32,2 28,9 26,1 23,6 21,5 19,7 18,1
98																								210,9 146,5 107,6 82,4 65,1 52,7 43,6 36,6 31,2 26,9 23,4 20,6 18,2 16,3 14,6 13,2 12,0 10,9 10,0 9,2
100	0,0	0,0	0,0	0,0	0,0	0,0	0,0	0,0	0,0	0,0	0,0	0,0	0,0	0,0	0,0	0,0	0,0	0,0	0,0	0,0	0,0	0,0	0,0	0,0

Table A.32. Fundamental frequency change in percentage versus axial load level for I380 steel column for different lengths for frequency change

Load (tons)	f/f ₀ (%)	Length (m)																						
		0.50	0.75	1.00	1.25	1.50	1.75	2.00	2.25	2.50	2.75	3.00	3.25	3.50	3.75	4.00	4.25	4.50	4.75	5.00	5.25	5.50	5.75	6.00
0	100.0	100.0	100.0	100.0	100.0	100.0	100.0	100.0	100.0	100.0	100.0	100.0	100.0	100.0	100.0	100.0	100.0	100.0	100.0	100.0	100.0	100.0	100.0	100.0
3	100.0	100.0	100.0	100.0	100.0	99.9	99.9	99.9	99.9	99.9	99.9	99.9	99.9	99.9	99.9	99.9	99.9	99.9	99.9	99.9	99.9	99.9	99.9	99.9
6	100.0	100.0	100.0	99.9	99.9	99.9	99.9	99.9	99.8	99.8	99.7	99.7	99.6	99.6	99.5	99.4	99.3	99.2	99.1	99.0	98.9	98.8	98.8	98.7
9	100.0	100.0	99.9	99.9	99.9	99.8	99.8	99.7	99.6	99.5	99.4	99.3	99.2	99.1	99.0	98.8	98.7	98.5	98.4	98.2	98.0	97.8	97.6	97.4
12	100.0	100.0	99.9	99.9	99.8	99.8	99.7	99.6	99.5	99.4	99.3	99.2	99.1	99.0	98.8	98.7	98.5	98.4	98.2	98.0	97.8	97.6	97.4	
15	100.0	99.9	99.9	99.9	99.8	99.7	99.6	99.5	99.4	99.3	99.2	99.0	98.9	98.7	98.5	98.4	98.2	97.9	97.7	97.5	97.2	97.0	96.7	
18	100.0	99.9	99.9	99.8	99.8	99.7	99.6	99.5	99.3	99.2	99.0	98.9	98.7	98.5	98.3	98.0	97.8	97.5	97.3	97.0	96.7	96.4	96.0	
21	100.0	99.9	99.9	99.8	99.7	99.6	99.5	99.4	99.2	99.0	98.9	98.7	98.4	98.2	98.0	97.7	97.4	97.1	96.8	96.5	96.1	95.7	95.3	
24	100.0	99.9	99.8	99.8	99.7	99.6	99.4	99.3	99.1	98.9	98.7	98.5	98.2	98.0	97.7	97.4	97.0	96.7	96.3	95.9	95.4	95.0	94.7	
27	100.0	99.9	99.8	99.7	99.6	99.5	99.3	99.2	99.0	98.8	98.5	98.3	98.0	97.7	97.4	97.0	96.7	96.3	95.9	95.4	95.0	94.5	94.0	
30	100.0	99.9	99.8	99.7	99.6	99.4	99.3	99.1	98.9	98.6	98.4	98.1	97.8	97.4	97.1	96.7	96.3	95.8	95.4	94.9	94.4	93.8	93.3	
33	100.0	99.9	99.8	99.7	99.6	99.4	99.2	99.0	98.8	98.5	98.2	97.9	97.5	97.2	96.8	96.3	95.9	95.4	94.9	94.4	93.8	93.2	92.6	
36	99.9	99.9	99.8	99.7	99.5	99.3	99.1	98.9	98.6	98.4	98.0	97.7	97.3	96.9	96.5	96.0	95.5	95.0	94.4	93.8	93.2	92.6	91.9	
39	99.9	99.8	99.8	99.6	99.5	99.3	99.1	98.8	98.5	98.2	97.9	97.5	97.1	96.6	96.2	95.7	95.1	94.6	94.0	93.3	92.6	91.9	91.1	
42	99.9	99.8	99.7	99.6	99.4	99.2	99.0	98.7	98.4	98.1	97.7	97.3	96.9	96.4	95.9	95.3	94.7	94.1	93.5	92.8	92.0	91.2	90.4	
45	99.9	99.8	99.7	99.6	99.4	99.2	98.9	98.6	98.3	97.9	97.5	97.1	96.6	96.1	95.6	95.0	94.4	93.7	93.0	92.2	91.4	90.6	89.7	
48	99.9	99.8	99.7	99.5	99.3	99.1	98.8	98.5	98.2	97.8	97.4	96.9	96.4	95.9	95.3	94.6	94.0	93.3	92.5	91.7	90.8	89.9	89.0	
51	99.9	99.8	99.7	99.5	99.3	99.1	98.8	98.4	98.1	97.7	97.2	96.7	96.2	95.6	95.0	94.3	93.6	92.8	92.0	91.1	90.2	89.2	88.2	
54	99.9	99.8	99.7	99.5	99.3	99.0	98.7	98.3	98.0	97.5	97.0	96.5	95.9	95.3	94.7	93.9	93.2	92.4	91.5	90.6	89.6	88.6	87.5	
57	99.9	99.8	99.7	99.5	99.2	98.9	98.6	98.3	97.8	97.4	96.9	96.3	95.7	95.1	94.4	93.6	92.8	91.9	91.0	90.0	89.0	87.9	86.7	
60	99.9	99.8	99.6	99.4	99.2	98.9	98.5	98.2	97.7	97.2	96.7	96.1	95.5	94.8	94.0	93.2	92.4	91.5	90.5	89.5	88.4	87.2	86.0	
63	99.9	99.8	99.6	99.4	99.1	98.8	98.5	98.1	97.6	97.1	96.5	95.9	95.2	94.5	93.7	92.9	92.0	91.0	90.0	88.9	87.7	86.5	85.2	
66	99.9	99.8	99.6	99.4	99.1	98.8	98.4	98.0	97.5	97.0	96.4	95.7	95.0	94.2	93.4	92.5	91.6	90.6	89.5	88.3	87.1	85.8	84.4	
69	99.9	99.8	99.6	99.4	99.1	98.7	98.3	97.9	97.4	96.8	96.2	95.5	94.8	94.0	93.1	92.2	91.2	90.1	89.0	87.8	86.5	85.1	83.6	
72	99.9	99.8	99.6	99.3	99.0	98.7	98.3	97.8	97.3	96.7	96.0	95.3	94.5	93.7	92.8	91.8	90.8	89.7	88.5	87.2	85.8	84.4	82.8	
75	99.9	99.7	99.5	99.3	99.0	98.6	98.2	97.7	97.1	96.5	95.9	95.1	94.3	93.4	92.5	91.5	90.4	89.2	88.0	86.6	85.2	83.7	82.0	
78	99.9	99.7	99.5	99.3	98.9	98.6	98.1	97.6	97.0	96.4	95.7	94.9	94.1	93.2	92.2	91.1	90.0	88.7	87.4	86.0	84.5	82.9	81.2	
81	99.9	99.7	99.5	99.2	98.9	98.5	98.0	97.5	96.9	96.2	95.5	94.7	93.8	92.9	91.9	90.8	89.6	88.3	86.9	85.4	83.9	82.2	80.4	
84	99.9	99.7	99.5	99.2	98.9	98.4	98.0	97.4	96.8	96.1	95.3	94.5	93.6	92.6	91.5	90.4	89.1	87.8	86.4	84.9	83.2	81.5	79.6	
87	99.9	99.7	99.5	99.2	98.8	98.4	97.9	97.3	96.7	96.0	95.2	94.3	93.4	92.3	91.2	90.0	88.7	87.3	85.9	84.3	82.5	80.7	78.8	
90	99.9	99.7	99.5	99.2	98.8	98.3	97.8	97.2	96.6	95.8	95.0	94.1	93.1	92.1	90.9	89.7	88.3	86.9	85.3	83.7	81.9	80.0	77.9	
93	99.9	99.7	99.4	99.1	98.7	98.3	97.7	97.1	96.4	95.7	94.8	93.9	92.9	91.8	90.6	89.3	87.9	86.4	84.8	83.1	81.2	79.2	77.1	
96	99.9	99.7	99.4	99.1	98.7	98.2	97.7	97.0	96.3	95.5	94.7	93.7	92.6	91.5	90.3	88.9	87.5	85.9	84.2	82.4	80.5	78.4	76.2	
99	99.9	99.7	99.4	99.1	98.7	98.2	97.6	96.9	96.2	95.4	94.5	93.5	92.4	91.2	89.9	88.6	87.1	85.4	83.7	81.8	79.7	77.5	75.3	
102	99.8	99.7	99.4	99.0	98.6	98.1	97.5	96.8	96.1	95.2	94.3	93.3	92.2	90.9	89.6	88.2	86.6	85.0	83.2	81.2	79.1	76.9	74.4	
105	99.8	99.6	99.4	99.0	98.6	98.0	97.4	96.8	96.0	95.1	94.1	93.1	91.9	90.7	89.3	87.8	86.2	84.5	82.6	80.6	78.4	76.1	73.5	
108	99.8	99.6	99.3	99.0	98.5	98.0	97.4	96.7	95.9	95.0	94.0	92.9	91.7	90.4	89.0	87.4	85.8	84.0	82.0	80.0	77.7	75.3	72.6	
111	99.8	99.6	99.3	99.0	98.5	97.9	97.3	96.6	95.7	94.8	93.8	92.7	91.4	90.1	88.6	87.1	85.3	83.5	81.5	79.3	77.0	74.4	71.7	
114	99.8	99.6	99.3	98.9	98.4	97.9	97.2	96.5	95.6	94.7	93.6	92.5	91.2	89.8	88.3	86.7	84.9	83.0	80.9	78.7	76.2	73.6	70.8	
117	99.8	99.6	99.3	98.9	98.4	97.8	97.1	96.4	95.5	94.5	93.4	92.3	91.0	89.5	88.0	86.3	84.5	82.5	80.3	78.0	75.5	72.8	69.8	
120	99.8	99.6	99.3	98.9	98.4	97.8	97.1	96.3	95.4	94.4	93.3	92.0	90.7	89.2	87.6	85.9	84.0	82.0	79.8	77.4	74.8	71.9	68.8	
123	99.8	99.6	99.3	98.8	98.3	97.7	97.0	96.2	95.3	94.2	93.1	91.8	90.5	89.0	87.3	85.5	83.6	81.5	79.2	76.7	74.0	71.1	67.9	
126	99.8	99.6	99.2	98.8	98.3	97.7	96.9	96.1	95.1	94.1	92.9	91.6	90.2	88.7	87.0	85.1	83.1	81.0	78.6	76.1	73.3	70.2	66.9	
129	99.8	99.6	99.2	98.8	98.2	97.6	96.8	96.0	95.0	93.9	92.7	91.4	90.0	88.4	86.6	84.7	82.7	80.5	78.0	75.4	72.5	69.3	65.9	
132	99.8	99.6	99.2	98.8	98.2	97.5	96.8	95.9	94.9	93.8	92.6	91.2	89.7	88.1	86.3	84.4	82.2	79.9	77.4	74.7	71.7	68.4	64.8	
135	99.8	99.5	99.2	98.7	98.2	97.5	96.7	95.8	94.8	93.7	92.4	91.0	89.5	87.8	86.0	84.0	81.8	79.4	76.8	74.0	70.9	67.5	63.8	
138	99.8	99.5	99.2	98.7	98.1	97.4	96.6	95.7	94.7	93.5	92.2	90.8	89.2	87.5	85.6	83.6	81.3	78.9	76.2	73.3	70.1	66.6	62.7	
141	99.8	99.5	99.1	98.7	98.1	97.4	96.5	95.6	94.5	93.4	92.0	90.6	89.0	87.2	85.3	83.2	80.9	78.4	75.6	72.6	69.3	65.7	61.6	
144	99.8	99.5	99.1	98.6	98.0	97.3	96.5	95.5	94.4	93.2	91.9	90.4	88.7	86.9	84.9	82.8	80.4	77.8	75.0	71.9	68.5	64.7	60.5	
147	99.8	99.5	99.1	98.6	98.0	97.3	96.4	95.4	94.3	93.1	91.7	90.2	88.5	86.6	84.6	82.4	80.0	77.3	74.4	71.2	67.7	63.8	59.4	
150	99.8	99.5	99.1	98.6	98.0	97.2	96.3	95.3	94.2	92.9	91.5	89.9	88.2	86.3	84.2	82.0	79.5	76.8	73.8	70.5	66.9	62.8	58.3	
153	99.8	99.5	99.1	98.6	97.9	97.1	96.2	95.2	94.1	92.8	91.3	89.7	88.0	86.0	83.9	81.6	79.0	76.2	73.1	69.8	66.0	61.8	57.1	
156	99.8	99.5	99.1	98.5	97.9	97.1	96.2	95.1	93.9	92.6	91.1	89.5	87.7	85.7	83.5	81.2	78.5	75.7	72.5	69.0	65.1	60.8	55.9	
159	99.8	99.5	99.0	98.5	97.8	97.0	96.1	95.0	93.8	92.5	91.0	89.3	87.5	85.4	83.2	80.8	78.1	75.1	71.9	68.3	64.3	59.8	54.7	
162	99.8	99.5	99.0	98.5	97.8	97.0	96.0	94.9	93.															

Table A.34. Fundamental frequency change in percentage versus axial load level for I400 steel column for different lengths for frequency change

ff _o (%)	Length (m)																								
	0.50	0.75	1.00	1.25	1.50	1.75	2.00	2.25	2.50	2.75	3.00	3.25	3.50	3.75	4.00	4.25	4.50	4.75	5.00	5.25	5.50	5.75	6.00		
0	100.0	100.0	100.0	100.0	100.0	100.0	100.0	100.0	100.0	100.0	100.0	100.0	100.0	100.0	100.0	100.0	100.0	100.0	100.0	100.0	100.0	100.0	100.0	100.0	
4	100.0	100.0	100.0	100.0	100.0	99.9	99.9	99.9	99.9	99.8	99.8	99.8	99.7	99.7	99.6	99.6	99.5	99.5	99.4	99.4	99.3	99.3	99.2	99.2	99.3
8	100.0	100.0	100.0	99.9	99.9	99.9	99.8	99.8	99.7	99.7	99.6	99.6	99.5	99.5	99.4	99.4	99.3	99.3	99.2	99.1	99.0	98.9	98.8	98.7	98.5
12	100.0	100.0	99.9	99.9	99.8	99.8	99.7	99.7	99.6	99.5	99.5	99.4	99.3	99.1	99.0	98.9	98.8	98.6	98.5	98.3	98.1	98.0	97.8	97.8	97.8
16	100.0	100.0	99.9	99.9	99.8	99.8	99.7	99.6	99.5	99.4	99.3	99.1	99.0	98.9	98.7	98.5	98.4	98.2	98.0	97.7	97.5	97.3	97.3	97.0	97.0
20	100.0	99.9	99.9	99.8	99.8	99.7	99.6	99.5	99.4	99.2	99.1	98.9	98.8	98.6	98.4	98.2	97.9	97.7	97.4	97.2	96.9	96.6	96.3	96.3	96.3
24	100.0	99.9	99.9	99.8	99.7	99.6	99.5	99.4	99.2	99.1	98.9	98.7	98.5	98.3	98.0	97.8	97.5	97.2	96.9	96.6	96.3	96.0	95.7	95.5	95.5
28	100.0	99.9	99.9	99.8	99.7	99.6	99.4	99.3	99.1	98.9	98.7	98.5	98.3	98.0	97.7	97.4	97.1	96.8	96.4	96.0	95.6	95.2	94.8	94.8	94.8
32	100.0	99.9	99.8	99.7	99.6	99.5	99.4	99.2	99.0	98.8	98.5	98.3	98.0	97.7	97.4	97.0	96.7	96.3	95.9	95.4	95.0	94.5	94.0	94.0	94.0
36	100.0	99.9	99.8	99.7	99.6	99.4	99.3	99.1	98.9	98.6	98.4	98.1	97.7	97.4	97.0	96.7	96.2	95.8	95.3	94.8	94.3	93.8	93.3	93.3	93.2
40	99.9	99.9	99.8	99.7	99.5	99.4	99.2	99.0	98.7	98.5	98.2	97.8	97.5	97.1	96.7	96.3	95.8	95.3	94.8	94.3	93.7	93.1	92.4	92.4	92.4
44	99.9	99.8	99.8	99.7	99.5	99.3	99.1	98.9	98.6	98.3	98.0	97.6	97.2	96.8	96.4	95.9	95.4	94.8	94.3	93.7	93.0	92.3	91.6	91.6	91.6
48	99.9	99.9	99.8	99.6	99.5	99.3	99.0	98.8	98.5	98.1	97.8	97.4	97.0	96.5	96.0	95.5	95.0	94.4	93.7	93.1	92.4	91.6	90.8	90.8	90.8
52	99.9	99.9	99.7	99.6	99.4	99.2	98.9	98.7	98.3	98.0	97.6	97.2	96.7	96.2	95.7	95.1	94.5	93.9	93.2	92.5	91.7	90.9	90.1	90.1	90.1
56	99.9	99.8	99.7	99.6	99.4	99.1	98.9	98.6	98.2	97.8	97.4	97.0	96.5	95.9	95.4	94.7	94.1	93.4	92.6	91.9	91.0	90.1	89.2	89.2	89.2
60	99.9	99.8	99.7	99.5	99.3	99.1	98.8	98.5	98.1	97.7	97.2	96.7	96.2	95.6	95.0	94.4	93.6	92.9	92.1	91.2	90.3	89.4	88.4	88.4	88.4
64	99.9	99.8	99.7	99.5	99.3	99.0	98.7	98.4	98.0	97.5	97.0	96.5	96.0	95.3	94.7	94.0	93.2	92.4	91.5	90.6	89.6	88.6	87.6	87.6	87.6
68	99.9	99.8	99.7	99.5	99.2	98.9	98.6	98.2	97.8	97.4	96.9	96.3	95.7	95.0	94.3	93.6	92.8	91.9	91.0	90.0	89.0	88.0	87.0	87.0	87.0
72	99.9	99.8	99.6	99.4	99.2	98.9	98.5	98.1	97.7	97.2	96.7	96.1	95.4	94.7	94.0	93.2	92.3	91.4	90.4	89.4	88.4	87.4	86.4	86.4	86.4
76	99.9	99.8	99.6	99.4	99.1	98.8	98.5	98.0	97.6	97.1	96.5	95.9	95.2	94.4	93.6	92.8	91.9	90.9	89.9	88.7	87.6	86.6	85.6	85.6	85.6
80	99.9	99.8	99.6	99.4	99.1	98.8	98.4	97.9	97.4	96.9	96.3	95.6	94.9	94.1	93.3	92.4	91.4	90.4	89.3	88.1	86.8	85.5	84.5	84.5	84.5
84	99.9	99.8	99.6	99.3	99.0	98.7	98.3	97.8	97.3	96.7	96.1	95.4	94.7	93.8	92.9	92.0	91.0	89.9	88.7	87.3	85.8	84.2	82.5	81.6	81.6
88	99.9	99.7	99.6	99.3	99.0	98.6	98.2	97.7	97.2	96.6	95.9	95.2	94.4	93.5	92.6	91.6	90.5	89.4	88.1	86.8	85.4	83.9	82.3	81.4	81.4
92	99.9	99.7	99.5	99.3	98.9	98.6	98.1	97.6	97.1	96.4	95.7	95.0	94.1	93.2	92.2	91.2	90.1	88.8	87.4	86.2	84.6	82.8	80.9	79.9	79.9
96	99.9	99.7	99.5	99.2	98.9	98.5	98.0	97.5	96.9	96.3	95.5	94.7	93.9	92.9	91.9	90.8	89.6	88.3	87.0	85.5	83.9	82.3	80.5	79.5	79.5
100	99.9	99.7	99.5	99.2	98.9	98.4	98.0	97.4	96.8	96.1	95.3	94.5	93.6	92.6	91.5	90.4	89.1	87.8	86.4	84.8	83.2	81.5	79.6	79.6	79.6
104	99.9	99.7	99.5	99.2	98.8	98.4	97.9	97.3	96.7	95.9	95.1	94.3	93.3	92.3	91.2	90.0	88.7	87.3	85.8	84.2	82.5	80.6	78.6	78.6	78.6
108	99.9	99.7	99.5	99.1	98.8	98.3	97.8	97.2	96.5	95.8	95.0	94.1	93.1	92.0	90.8	89.6	88.2	86.8	85.2	83.5	81.7	79.8	77.7	77.7	77.7
112	99.9	99.7	99.4	99.1	98.7	98.3	97.7	97.1	96.4	95.6	94.8	93.8	92.8	91.7	90.5	89.2	87.7	86.2	84.6	82.8	80.9	78.9	76.7	76.7	76.7
116	99.9	99.7	99.4	99.1	98.7	98.2	97.6	97.0	96.3	95.5	94.6	93.6	92.5	91.4	90.1	88.7	87.3	85.7	84.0	82.1	80.2	78.0	75.8	75.8	75.8
120	99.8	99.7	99.4	99.0	98.6	98.1	97.5	96.9	96.1	95.3	94.4	93.4	92.3	91.0	89.7	88.3	86.8	85.1	83.4	81.4	79.4	77.2	74.8	74.8	74.8
124	99.8	99.6	99.4	99.0	98.6	98.1	97.5	96.8	96.0	95.1	94.2	93.1	92.0	90.7	89.4	87.9	86.3	84.6	82.7	80.7	78.6	76.3	73.8	73.8	73.8
128	99.8	99.6	99.4	99.0	98.5	98.0	97.4	96.7	95.9	95.0	94.0	92.9	91.7	90.4	89.0	87.5	85.8	84.0	82.1	80.0	77.8	75.4	72.7	72.7	72.7
132	99.8	99.6	99.3	99.0	98.5	97.9	97.3	96.6	95.7	94.8	93.8	92.7	91.4	90.1	88.6	87.1	85.3	83.5	81.5	79.3	77.0	74.5	71.7	71.7	71.7
136	99.8	99.6	99.3	98.9	98.4	97.9	97.2	96.5	95.6	94.7	93.6	92.4	91.2	89.8	88.3	86.6	84.9	82.9	80.9	78.6	76.2	73.5	70.7	70.7	70.7
140	99.8	99.6	99.3	98.9	98.4	97.8	97.1	96.4	95.5	94.5	93.4	92.2	90.9	89.5	87.9	86.2	84.4	82.4	80.2	77.9	75.3	72.6	69.6	69.6	69.6
144	99.8	99.6	99.3	98.9	98.4	97.7	97.0	96.2	95.3	94.3	93.2	92.0	90.6	89.1	87.5	85.8	83.9	81.8	79.6	77.1	74.5	71.6	68.5	68.5	68.5
148	99.8	99.6	99.3	98.8	98.3	97.7	97.0	96.1	95.2	94.2	93.0	91.7	90.3	88.8	87.2	85.3	83.4	81.2	78.9	76.4	73.7	70.7	67.4	67.4	67.4
152	99.8	99.6	99.2	98.8	98.3	97.6	96.9	96.0	95.1	94.0	92.8	91.5	90.1	88.5	86.8	84.9	82.9	80.7	78.3	75.7	72.8	69.7	66.3	66.3	66.3
156	99.8	99.6	99.2	98.8	98.2	97.6	96.8	95.9	94.9	93.8	92.6	91.3	89.8	88.2	86.4	84.5	82.4	80.1	77.6	74.9	71.9	68.7	65.1	65.1	65.1
160	99.8	99.5	99.2	98.7	98.2	97.5	96.7	95.8	94.8	93.7	92.4	91.0	89.5	87.8	86.0	84.0	81.9	79.5	76.9	74.1	71.1	67.7	64.0	64.0	64.0
164	99.8	99.5	99.2	98.7	98.1	97.4	96.6	95.7	94.7	93.5	92.2	90.8	89.2	87.5	85.6	83.6	81.4	78.9	76.3	73.4	70.2	66.7	62.8	62.8	62.8
168	99.8	99.5	99.1	98.7	98.1	97.4	96.5	95.6	94.5	93.3	92.0	90.6	89.0	87.2	85.3	83.1	80.8	78.3	75.6	72.6	69.3	65.6	61.6	61.6	61.6
172	99.8	99.5	99.1	98.6	98.0	97.3	96.5	95.5	94.4	93.2	91.8	90.3	88.7	86.9	84.9	82.7	80.3	77.7	74.9	71.8	68.4	64.6	60.3	60.3	60.3
176	99.8	99.5	99.1	98.6	98.0	97.2	96.4	95.4	94.3	93.0	91.6	90.1	88.4	86.5	84.5	82.3	79.8	77.1	74.2	71.0	67.4	63.5	59.1	59.1	59.1
180	99.8	99.5	99.1	98.6	97.9	97.2	96.3	95.3	94.1	92.9	91.4	89.8	88.1	86.2	84.1	81.8	79.3	76.5	73.5	70.2	66.5	62.4	57.8	57.8	57.8
184	99.8	99.5	99.1	98.5	97.9	97.1	96.2	95.2	94.0	92.7	91.2	89.6	87.8	85.9	83.7	81.3	78.8	75.9	72.8	69.4	65.5	61.3	56.5	56.5	56.5
188	99.8	99.5	99.0	98.5	97.8	97.0	96.1	95.1	93.9	92.5	91.0	89.4	87.5	85.5	83.3	80.9	78.2	75.3	72.1	68.5	64.6	60.1	55.1	55.1	55.1
192	99.8	99.5	99.0	98.5	97.8	97.0	96.0	95.0	93.7	92.4	90.8	89.1	87.2	85.2	82.9	80.4	77.7	74.7	71.4	67.7	63.6	59.0	53.7	53.7	53.7
196	99.8	99.4	99.0	98.4	97.7	96.9	96.0	94.8	93.6	92.2	90.6	88.9	87.0	84.8	82.5	80.0	77.1	74.1	70.6	66.8	62.6	57.8	52.3	52.3	52.3
200	99.7	99.4	99.0	98.4	97.7	96.9	95.9	94.7	93.5	92.0	90.4	88.6													

Table A.36. Fundamental frequency change in percentage versus axial load level for I425 steel column for different lengths for frequency change

f/f ₀ (%)	Length (m)																								
	0.50	0.75	1.00	1.25	1.50	1.75	2.00	2.25	2.50	2.75	3.00	3.25	3.50	3.75	4.00	4.25	4.50	4.75	5.00	5.25	5.50	5.75	6.00		
0	100.0	100.0	100.0	100.0	100.0	100.0	100.0	100.0	100.0	100.0	100.0	100.0	100.0	100.0	100.0	100.0	100.0	100.0	100.0	100.0	100.0	100.0	100.0	100.0	
4	100.0	100.0	100.0	100.0	100.0	100.0	99.9	99.9	99.9	99.9	99.9	99.9	99.8	99.8	99.7	99.7	99.6	99.6	99.6	99.6	99.5	99.5	99.5	99.4	99.4
8	100.0	100.0	100.0	99.9	99.9	99.9	99.8	99.8	99.8	99.8	99.7	99.7	99.6	99.6	99.5	99.5	99.4	99.4	99.3	99.3	99.2	99.1	99.0	98.9	98.8
12	100.0	100.0	100.0	99.9	99.9	99.9	99.8	99.8	99.7	99.6	99.6	99.5	99.4	99.3	99.2	99.1	99.0	98.9	98.8	98.6	98.6	98.5	98.4	98.2	98.2
16	100.0	100.0	99.9	99.9	99.9	99.8	99.7	99.7	99.6	99.5	99.4	99.3	99.2	99.1	99.0	98.8	98.7	98.5	98.4	98.2	98.2	98.0	97.8	97.6	97.6
20	100.0	100.0	99.9	99.8	99.8	99.7	99.6	99.5	99.4	99.3	99.1	99.0	98.8	98.7	98.5	98.3	98.1	97.9	97.7	97.5	97.3	97.0	96.7	96.4	96.4
24	100.0	99.9	99.9	99.8	99.8	99.7	99.6	99.5	99.4	99.3	99.1	99.0	98.8	98.6	98.4	98.2	98.0	97.8	97.5	97.3	97.0	96.7	96.4	96.2	96.2
28	100.0	99.9	99.9	99.8	99.7	99.7	99.5	99.4	99.3	99.1	99.0	98.8	98.6	98.4	98.2	97.9	97.7	97.4	97.1	96.8	96.5	96.2	95.9	95.6	95.6
32	100.0	99.9	99.9	99.8	99.7	99.6	99.5	99.3	99.2	99.0	98.8	98.6	98.4	98.2	97.9	97.6	97.3	97.0	96.7	96.3	96.0	95.6	95.3	95.0	95.0
36	100.0	99.9	99.9	99.8	99.7	99.6	99.4	99.3	99.1	98.9	98.7	98.4	98.2	97.9	97.6	97.3	97.0	96.6	96.3	95.9	95.5	95.1	94.7	94.4	94.4
40	100.0	99.9	99.8	99.7	99.6	99.5	99.3	99.2	99.0	98.8	98.5	98.3	98.0	97.7	97.4	97.0	96.6	96.3	95.8	95.4	94.9	94.4	93.9	93.5	93.5
44	100.0	99.9	99.8	99.7	99.6	99.5	99.3	99.1	98.9	98.6	98.4	98.1	97.8	97.4	97.1	96.7	96.3	95.9	95.4	94.9	94.4	93.9	93.4	93.0	93.0
48	100.0	99.9	99.8	99.7	99.6	99.4	99.2	99.0	98.8	98.5	98.2	97.9	97.6	97.2	96.8	96.4	96.0	95.5	95.0	94.5	94.0	93.5	93.0	92.5	92.5
52	99.9	99.9	99.8	99.7	99.5	99.4	99.2	98.9	98.7	98.4	98.1	97.7	97.4	97.0	96.6	96.1	95.6	95.1	94.6	94.0	93.4	92.7	92.1	91.5	91.5
56	99.9	99.9	99.8	99.6	99.5	99.3	99.1	98.8	98.6	98.3	97.9	97.6	97.2	96.7	96.3	95.8	95.3	94.7	94.1	93.5	92.8	92.1	91.5	90.9	90.9
60	99.9	99.9	99.8	99.6	99.4	99.3	99.0	98.8	98.5	98.1	97.8	97.4	97.0	96.5	96.0	95.5	94.9	94.3	93.7	93.0	92.3	91.5	90.8	90.2	90.2
64	99.9	99.9	99.7	99.6	99.4	99.2	99.0	98.7	98.4	98.0	97.6	97.2	96.8	96.3	95.7	95.2	94.6	93.9	93.2	92.5	91.5	90.6	89.6	89.0	89.0
68	99.9	99.8	99.7	99.6	99.4	99.1	98.9	98.6	98.3	97.9	97.5	97.0	96.5	96.0	95.5	94.9	94.2	93.5	92.8	92.0	91.2	90.1	89.4	88.7	88.7
72	99.9	99.8	99.7	99.5	99.3	99.1	98.8	98.5	98.2	97.8	97.3	96.9	96.3	95.8	95.2	94.6	93.9	93.1	92.4	91.5	90.7	89.8	88.8	88.8	88.8
76	99.9	99.8	99.7	99.5	99.3	99.0	98.8	98.4	98.0	97.6	97.2	96.7	96.1	95.5	94.9	94.2	93.5	92.7	91.9	91.0	90.1	89.0	88.1	87.1	87.1
80	99.9	99.8	99.7	99.5	99.3	99.0	98.7	98.3	97.9	97.5	97.0	96.5	95.9	95.3	94.6	93.9	93.2	92.3	91.5	90.6	89.6	88.5	87.5	86.5	86.5
84	99.9	99.8	99.7	99.5	99.2	98.9	98.6	98.3	97.8	97.4	96.9	96.3	95.7	95.1	94.4	93.6	92.8	91.9	91.0	90.1	89.0	87.9	86.8	85.8	85.8
88	99.9	99.8	99.6	99.4	99.2	98.9	98.6	98.2	97.7	97.3	96.7	96.1	95.5	94.8	94.1	93.3	92.4	91.5	90.6	89.5	88.5	87.3	86.3	85.3	85.3
92	99.9	99.8	99.6	99.4	99.2	98.8	98.5	98.1	97.6	97.1	96.6	96.0	95.3	94.6	93.8	93.0	92.1	91.1	90.1	89.0	87.9	86.7	85.7	84.7	84.7
96	99.9	99.8	99.6	99.4	99.1	98.8	98.4	98.0	97.5	97.0	96.4	95.8	95.1	94.3	93.5	92.7	91.7	90.7	89.5	88.5	87.3	86.3	85.2	84.2	84.2
100	99.9	99.8	99.6	99.4	99.1	98.7	98.4	97.9	97.4	96.9	96.3	95.6	94.9	94.1	93.2	92.3	91.4	90.3	89.2	88.0	86.7	85.4	84.0	82.6	82.6
104	99.9	99.8	99.6	99.3	99.0	98.7	98.3	97.8	97.3	96.7	96.1	95.4	94.7	93.8	93.0	92.0	91.0	89.9	88.7	87.5	86.2	84.8	83.3	81.8	81.8
108	99.9	99.8	99.6	99.3	99.0	98.6	98.2	97.8	97.2	96.6	96.0	95.2	94.5	93.6	92.7	91.7	90.6	89.5	88.3	87.0	85.6	84.1	82.5	81.0	81.0
112	99.9	99.7	99.5	99.3	99.0	98.6	98.2	97.7	97.1	96.5	95.8	95.1	94.2	93.4	92.4	91.4	90.3	89.1	87.8	86.5	85.0	83.5	81.9	80.4	80.4
116	99.9	99.7	99.5	99.3	98.9	98.5	98.1	97.6	97.0	96.4	95.7	94.9	94.0	93.1	92.1	91.0	89.9	88.7	87.3	85.9	84.4	82.8	81.1	79.6	79.6
120	99.9	99.7	99.5	99.2	98.9	98.5	98.0	97.5	96.9	96.2	95.5	94.7	93.8	92.9	91.8	90.7	89.5	88.2	86.9	85.4	83.8	82.1	80.3	78.6	78.6
124	99.9	99.7	99.5	99.2	98.9	98.4	98.0	97.4	96.8	96.1	95.3	94.5	93.6	92.6	91.5	90.4	89.2	87.8	86.4	84.9	83.2	81.5	79.6	77.9	77.9
128	99.9	99.7	99.5	99.2	98.8	98.4	97.9	97.3	96.7	96.0	95.2	94.3	93.4	92.4	91.3	90.1	88.8	87.4	85.9	84.3	82.6	80.8	78.9	77.1	77.1
132	99.9	99.7	99.5	99.2	98.8	98.3	97.8	97.2	96.6	95.8	95.0	94.1	93.2	92.1	91.0	89.7	88.4	87.0	85.4	83.8	82.0	80.1	78.1	76.3	76.3
136	99.9	99.7	99.4	99.1	98.7	98.3	97.8	97.2	96.5	95.7	94.9	94.0	93.0	91.9	90.7	89.4	88.0	86.5	84.9	83.2	81.4	79.4	77.3	75.5	75.5
140	99.9	99.7	99.4	99.1	98.7	98.2	97.7	97.1	96.4	95.6	94.7	93.8	92.7	91.6	90.4	89.1	87.6	86.1	84.5	82.7	80.8	78.7	76.5	74.7	74.7
144	99.9	99.7	99.4	99.1	98.7	98.2	97.6	97.0	96.3	95.5	94.6	93.6	92.5	91.4	90.1	88.7	87.3	85.7	84.0	82.1	80.2	78.0	75.8	74.0	74.0
148	99.8	99.7	99.4	99.1	98.6	98.1	97.6	96.9	96.2	95.3	94.4	93.4	92.3	91.1	89.8	88.4	86.9	85.2	83.5	81.6	79.5	77.3	75.0	73.2	73.2
152	99.8	99.7	99.4	99.0	98.6	98.1	97.5	96.8	96.1	95.2	94.3	93.2	92.1	90.9	89.5	88.1	86.5	84.8	83.0	81.0	78.9	76.6	74.1	72.3	72.3
156	99.8	99.6	99.4	99.0	98.6	98.0	97.4	96.7	95.9	95.1	94.1	93.0	91.9	90.6	89.2	87.7	86.1	84.4	82.5	80.5	78.3	75.9	73.3	71.5	71.5
160	99.8	99.6	99.3	99.0	98.5	98.0	97.4	96.6	95.8	94.9	93.9	92.9	91.7	90.3	88.9	87.4	85.7	83.9	82.0	79.9	77.6	75.2	72.5	70.7	70.7
164	99.8	99.6	99.3	99.0	98.5	97.9	97.3	96.6	95.7	94.8	93.8	92.7	91.4	90.1	88.6	87.0	85.3	83.5	81.5	79.3	77.0	74.4	71.7	69.9	69.9
168	99.8	99.6	99.3	98.9	98.5	97.9	97.2	96.5	95.6	94.7	93.6	92.5	91.2	89.8	88.3	86.7	84.9	83.0	81.0	78.7	76.3	73.7	70.8	69.0	69.0
172	99.8	99.6	99.3	98.9	98.4	97.8	97.2	96.4	95.5	94.6	93.5	92.3	91.0	89.6	88.0	86.4	84.5	82.6	80.5	78.1	75.6	72.9	70.0	68.2	68.2
176	99.8	99.6	99.3	98.9	98.4	97.8	97.1	96.3	95.4	94.4	93.3	92.1	90.8	89.3	87.7	86.0	84.1	82.1	79.9	77.5	75.0	72.2	69.1	67.3	67.3
180	99.8	99.6	99.3	98.8	98.3	97.7	97.0	96.2	95.3	94.3	93.2	91.9	90.6	89.1	87.4	85.7	83.8	81.7	79.4	77.0	74.3	71.4	68.2	66.4	66.4
184	99.8	99.6	99.2	98.8	98.3	97.7	97.0	96.1	95.2	94.2	93.0	91.7	90.3	88.8	87.1	85.3	83.4	81.2	78.9	76.4	73.6	70.6	67.3	65.5	65.5
188	99.8	99.6	99.2	98.8	98.3	97.6	96.9	96.0	95.1	94.0	92.8	91.5	90.1	88.5	86.8	85.0	82.9	80.7	78.4	75.8	72.9	69.8	66.4	64.6	64.6
192	99.8	99.6	99.2	98.8	98.2	97.6	96.8	96.0	95.0	93.9	92.7	91.3	89.9	88.3	86.5	84.6	82.5	80.3	77.8	75.2	72.2	69.0	65.5	63.7	63.7
196	99.8	99.6	99.2	98.7	98.2	97.5	96.8	95.9	94.9	93.8	92.5	91.2	89.7	88.0	86.2	84.3	82.1	79.8	77.3	74.5	71.5	68.2	64.6	62.8	62.8
200	99.8	99.5	99.2	98.7	98.2	97.5	96.7	95.8	94.8	93.6	92.4														

Table A.37. Fundamental frequency change in percentage versus axial load level for I450 steel column for different lengths for load level

P (tons)	P _{cr} (tons)																						
	352,2	351,5	350,6	349,3	347,8	346,1	344,0	341,7	339,1	336,2	333,1	329,7	326,0	322,1	317,9	313,4	308,6	303,6	298,3	292,7	286,9	280,7	274,3
f _{fo} (%)	Length (m)																						
	0,50	0,75	1,00	1,25	1,50	1,75	2,00	2,25	2,50	2,75	3,00	3,25	3,50	3,75	4,00	4,25	4,50	4,75	5,00	5,25	5,50	5,75	6,00
4																							
6																							
8																							
10																							
12																							
14																							
16																							
18																							
20																							
22																							
24																							
26																							
28																							
30																							
32																							
34																							
36																							
38																							
40																							
42																							
44																							
46																							
48																							
50																							
52																							
54																							
56																							
58																							267,4
60																							258,1
62																							270,5
64																						283,8	259,7
66																						271,5	248,4
68																						284,1	258,8
70																						297,4	269,7
72																						281,1	254,9
74																						292,8	264,2
76																						304,9	273,6
78																						282,9	253,9
80																						291,8	260,3
82																						300,0	265,8
84																						307,1	269,9
86																						312,1	271,9
88																						313,9	270,6
90																						310,5	264,6
92																						299,1	251,3
94																						338,9	274,5
96																						289,2	228,5
98																						259,9	190,9
100	0,0	0,0	0,0	0,0	0,0	0,0	0,0	0,0	0,0	0,0	0,0	0,0	0,0	0,0	0,0	0,0	0,0	0,0	0,0	0,0	0,0	0,0	0,0

Table A.38. Fundamental frequency change in percentage versus axial load level for I450 steel column for different lengths for frequency change

f/f ₀ (%)	Length (m)																						
	0.50	0.75	1.00	1.25	1.50	1.75	2.00	2.25	2.50	2.75	3.00	3.25	3.50	3.75	4.00	4.25	4.50	4.75	5.00	5.25	5.50	5.75	6.00
0	100.0	100.0	100.0	100.0	100.0	100.0	100.0	100.0	100.0	100.0	100.0	100.0	100.0	100.0	100.0	100.0	100.0	100.0	100.0	100.0	100.0	100.0	100.0
4	100.0	100.0	100.0	100.0	100.0	100.0	100.0	100.0	100.0	100.0	100.0	100.0	100.0	100.0	100.0	100.0	100.0	100.0	100.0	100.0	100.0	100.0	100.0
8	100.0	100.0	100.0	100.0	99.9	99.9	99.9	99.9	99.9	99.8	99.8	99.7	99.7	99.6	99.6	99.5	99.5	99.4	99.3	99.3	99.2	99.1	99.0
12	100.0	100.0	100.0	100.0	99.9	99.9	99.8	99.8	99.7	99.6	99.6	99.5	99.4	99.3	99.1	99.0	98.8	98.7	98.5	98.3	98.1	97.9	97.7
16	100.0	100.0	99.9	99.9	99.9	99.8	99.8	99.7	99.7	99.6	99.5	99.4	99.3	99.1	99.0	98.9	98.8	98.6	98.5	98.3	98.1	97.9	97.7
20	100.0	100.0	99.9	99.9	99.8	99.8	99.7	99.7	99.6	99.5	99.4	99.3	99.2	99.0	98.9	98.8	98.6	98.5	98.3	98.1	97.9	97.7	97.5
24	100.0	100.0	99.9	99.9	99.8	99.8	99.7	99.6	99.5	99.4	99.3	99.1	99.0	98.9	98.7	98.5	98.3	98.1	97.9	97.7	97.5	97.3	97.0
28	100.0	99.9	99.9	99.9	99.8	99.7	99.6	99.5	99.4	99.3	99.1	99.0	98.8	98.7	98.5	98.3	98.1	97.8	97.6	97.4	97.1	96.8	96.5
32	100.0	99.9	99.9	99.8	99.7	99.6	99.5	99.3	99.2	99.0	98.8	98.7	98.5	98.3	98.0	97.8	97.5	97.3	97.0	96.7	96.4	96.1	95.8
36	100.0	99.9	99.9	99.8	99.7	99.6	99.5	99.4	99.2	99.1	98.9	98.7	98.5	98.3	98.0	97.8	97.5	97.2	96.9	96.6	96.2	95.9	95.5
40	100.0	99.9	99.9	99.8	99.7	99.6	99.5	99.3	99.2	99.0	98.8	98.6	98.3	98.1	97.8	97.5	97.2	96.9	96.6	96.2	95.8	95.4	95.0
44	100.0	99.9	99.9	99.8	99.7	99.5	99.4	99.2	99.1	98.9	98.7	98.4	98.2	97.9	97.6	97.3	96.9	96.6	96.2	95.8	95.4	94.9	94.5
48	100.0	99.9	99.8	99.7	99.6	99.5	99.3	99.2	99.0	98.8	98.5	98.3	98.0	97.7	97.4	97.0	96.7	96.3	95.8	95.4	94.9	94.5	94.0
52	100.0	99.9	99.8	99.7	99.6	99.5	99.3	99.1	98.9	98.7	98.4	98.1	97.8	97.5	97.1	96.8	96.4	95.9	95.5	95.0	94.5	94.0	93.4
56	100.0	99.9	99.8	99.7	99.6	99.4	99.2	99.0	98.8	98.6	98.3	98.0	97.6	97.3	96.9	96.5	96.1	95.6	95.1	94.6	94.1	93.5	92.9
60	99.9	99.9	99.8	99.7	99.5	99.4	99.2	99.0	98.7	98.5	98.2	97.8	97.5	97.1	96.7	96.3	95.8	95.3	94.8	94.2	93.6	93.0	92.4
64	99.9	99.9	99.8	99.7	99.5	99.3	99.1	98.9	98.6	98.3	98.0	97.7	97.3	96.9	96.5	96.0	95.5	95.0	94.4	93.8	93.2	92.5	91.8
68	99.9	99.8	99.8	99.6	99.5	99.3	99.1	98.8	98.6	98.2	97.9	97.5	97.1	96.7	96.2	95.7	95.2	94.7	94.1	93.4	92.8	92.0	91.3
72	99.9	99.9	99.8	99.6	99.5	99.3	99.0	98.8	98.5	98.1	97.8	97.4	97.0	96.5	96.0	95.5	94.9	94.3	93.7	93.0	92.3	91.6	90.8
76	99.9	99.9	99.7	99.6	99.4	99.2	99.0	98.7	98.4	98.0	97.7	97.2	96.8	96.3	95.8	95.2	94.6	94.0	93.3	92.6	91.9	91.1	90.2
80	99.9	99.8	99.7	99.6	99.4	99.2	98.9	98.6	98.3	97.9	97.5	97.1	96.6	96.1	95.6	95.0	94.3	93.7	93.0	92.2	91.4	90.6	89.7
84	99.9	99.8	99.7	99.6	99.4	99.1	98.9	98.6	98.2	97.8	97.4	96.9	96.5	95.9	95.3	94.7	94.1	93.3	92.6	91.8	91.0	90.1	89.1
88	99.9	99.8	99.7	99.5	99.3	99.1	98.8	98.5	98.1	97.7	97.3	96.8	96.3	95.7	95.1	94.5	93.8	93.0	92.2	91.4	90.5	89.6	88.6
92	99.9	99.8	99.7	99.5	99.3	99.0	98.7	98.4	98.0	97.6	97.2	96.7	96.1	95.5	94.9	94.2	93.5	92.7	91.9	91.0	90.1	89.1	88.0
96	99.9	99.8	99.7	99.5	99.3	99.0	98.7	98.3	97.9	97.5	97.0	96.5	95.9	95.3	94.6	93.9	93.2	92.4	91.5	90.6	89.6	88.5	87.5
100	99.9	99.8	99.7	99.5	99.2	99.0	98.6	98.3	97.9	97.4	96.9	96.4	95.8	95.1	94.4	93.7	92.9	92.0	91.1	90.1	89.1	88.0	86.9
104	99.9	99.8	99.6	99.4	99.2	98.9	98.6	98.2	97.8	97.3	96.8	96.2	95.6	94.9	94.2	93.4	92.6	91.7	90.8	89.7	88.7	87.5	86.3
108	99.9	99.8	99.6	99.4	99.2	98.9	98.5	98.1	97.7	97.2	96.7	96.1	95.4	94.7	94.0	93.1	92.3	91.3	90.4	89.3	88.2	87.0	85.7
112	99.9	99.8	99.6	99.4	99.1	98.8	98.5	98.1	97.6	97.1	96.5	95.9	95.2	94.5	93.7	92.9	92.0	91.0	90.0	88.9	87.7	86.5	85.2
116	99.9	99.8	99.6	99.4	99.1	98.8	98.4	98.0	97.5	97.0	96.4	95.8	95.1	94.3	93.5	92.6	91.7	90.7	89.6	88.5	87.2	86.0	84.6
120	99.9	99.8	99.6	99.4	99.1	98.7	98.4	97.9	97.4	96.9	96.3	95.6	94.9	94.1	93.3	92.3	91.4	90.3	89.2	88.0	86.8	85.4	84.0
124	99.9	99.8	99.6	99.3	99.1	98.7	98.3	97.9	97.3	96.8	96.1	95.5	94.7	93.9	93.0	92.1	91.1	90.0	88.8	87.6	86.3	84.9	83.4
128	99.9	99.8	99.6	99.3	99.0	98.7	98.3	97.8	97.3	96.7	96.0	95.3	94.5	93.7	92.8	91.8	90.8	89.6	88.4	87.2	85.8	84.4	82.8
132	99.9	99.7	99.6	99.3	99.0	98.6	98.2	97.7	97.2	96.6	95.9	95.2	94.4	93.5	92.6	91.5	90.5	89.3	88.1	86.7	85.3	83.8	82.2
136	99.9	99.7	99.5	99.3	99.0	98.6	98.1	97.6	97.1	96.5	95.8	95.0	94.2	93.3	92.3	91.3	90.2	89.0	87.7	86.3	84.8	83.3	81.6
140	99.9	99.7	99.5	99.3	98.9	98.5	98.1	97.6	97.0	96.3	95.6	94.9	94.0	93.1	92.1	91.0	89.8	88.6	87.3	85.9	84.3	82.7	81.0
144	99.9	99.7	99.5	99.2	98.9	98.5	98.0	97.5	96.9	96.2	95.5	94.7	93.8	92.9	91.8	90.7	89.5	88.3	86.9	85.4	83.8	82.2	80.4
148	99.9	99.7	99.5	99.2	98.9	98.5	98.0	97.4	96.8	96.1	95.4	94.5	93.6	92.7	91.6	90.5	89.2	87.9	86.5	85.0	83.3	81.6	79.8
152	99.9	99.7	99.5	99.2	98.8	98.4	97.9	97.4	96.7	96.0	95.2	94.4	93.5	92.5	91.4	90.2	88.9	87.6	86.1	84.5	82.8	81.1	79.1
156	99.9	99.7	99.5	99.2	98.8	98.4	97.9	97.3	96.6	95.9	95.1	94.2	93.3	92.3	91.1	89.9	88.6	87.2	85.7	84.1	82.3	80.5	78.5
160	99.9	99.7	99.5	99.2	98.8	98.3	97.8	97.2	96.6	95.8	95.0	94.1	93.1	92.0	90.9	89.6	88.3	86.8	85.3	83.6	81.8	79.9	77.9
164	99.9	99.7	99.4	99.1	98.7	98.3	97.8	97.1	96.5	95.7	94.9	93.9	92.9	91.8	90.6	89.4	88.0	86.5	84.9	83.2	81.3	79.3	77.2
168	99.9	99.7	99.4	99.1	98.7	98.2	97.7	97.1	96.4	95.6	94.7	93.8	92.8	91.6	90.4	89.1	87.7	86.1	84.5	82.7	80.8	78.8	76.6
172	99.9	99.7	99.4	99.1	98.7	98.2	97.6	97.0	96.3	95.5	94.6	93.6	92.6	91.4	90.2	88.8	87.3	85.8	84.1	82.3	80.3	78.2	75.9
176	99.9	99.7	99.4	99.1	98.7	98.2	97.6	96.9	96.2	95.4	94.5	93.5	92.4	91.2	89.9	88.5	87.0	85.4	83.7	81.8	79.8	77.6	75.3
180	99.8	99.7	99.4	99.0	98.6	98.1	97.5	96.9	96.1	95.3	94.3	93.3	92.2	91.0	89.7	88.2	86.7	85.0	83.3	81.3	79.2	77.0	74.6
184	99.8	99.6	99.4	99.0	98.6	98.1	97.5	96.8	96.0	95.2	94.2	93.2	92.0	90.8	89.4	88.0	86.4	84.7	82.8	80.9	78.7	76.4	73.9
188	99.8	99.6	99.4	99.0	98.6	98.0	97.4	96.7	95.9	95.1	94.1	93.0	91.8	90.6	89.2	87.7	86.1	84.3	82.4	80.4	78.2	75.8	73.2
192	99.8	99.6	99.3	99.0	98.5	98.0	97.4	96.7	95.8	94.9	94.0	92.9	91.7	90.4	88.9	87.4	85.7	83.9	82.0	79.9	77.6	75.2	72.5
196	99.8	99.6	99.3	99.0	98.5	97.9	97.3	96.6	95.8	94.8	93.8	92.7	91.5	90.1	88.7	87.1	85.4	83.6	81.6	79.4	77.1	74.6	71.9
200	99.8	99.6	99.3	98.9	98.5	97.9	97.3	96.5	95.7	94.7	93.7	92.6	91.3	89.9	88.4	86.8	85.1	83.2	81.1	78.9	76.6	74.0	71.2
204	99.8	99.6	99.3	98.9	98.4	97.9	97.2	96.4	95.6	94.6	93.6	92.4	91.1	89.7	88.2	86.5	84.8	82.8	80.7	78.5	76.0	73.3	70.4
208	99.8	99.6	99.3	98.9	98.4	97.8	97.1	96.4	95.5	94.5	93.4	92.2	90.9	89.5	88.0	86.3	84.4	82.5	80.3	78.0	75.5	72.7	69.7
212	99.8	99.6	99.3	98.9	98.4	97.8	97.1	96.3	95.4	94.4	93.3	92.1	90.7	89.3	87.7	86.0	84.1	82.1	79.9	77.5	74.9	72.1	69.0
216	99.8	99.6	99.3	98.9	98.3	97.7	97.0	96.2	95.3	94.3													

Table A.40. Fundamental frequency change in percentage versus axial load level for I475 steel column for different lengths for frequency change

Freq. (Hz)	Length (m)																							
	0,50	0,75	1,00	1,25	1,50	1,75	2,00	2,25	2,50	2,75	3,00	3,25	3,50	3,75	4,00	4,25	4,50	4,75	5,00	5,25	5,50	5,75	6,00	
0	100,0	100,0	100,0	100,0	100,0	100,0	100,0	100,0	100,0	100,0	100,0	100,0	100,0	100,0	100,0	100,0	100,0	100,0	100,0	100,0	100,0	100,0	100,0	100,0
5	100,0	100,0	100,0	100,0	100,0	100,0	99,9	99,9	99,9	99,9	99,9	99,9	99,9	99,9	99,9	99,9	99,9	99,9	99,9	99,9	99,9	99,9	99,9	99,9
10	100,0	100,0	100,0	100,0	100,0	99,9	99,9	99,9	99,9	99,9	99,9	99,9	99,9	99,9	99,9	99,9	99,9	99,9	99,9	99,9	99,9	99,9	99,9	99,9
15	100,0	100,0	100,0	99,9	99,9	99,9	99,8	99,8	99,7	99,7	99,6	99,6	99,5	99,4	99,3	99,2	99,1	99,0	98,9	98,8	98,7	98,6	98,5	98,4
20	100,0	100,0	99,9	99,9	99,9	99,8	99,8	99,7	99,6	99,6	99,5	99,4	99,3	99,2	99,1	99,0	98,9	98,7	98,6	98,4	98,3	98,1	98,0	97,9
25	100,0	100,0	99,9	99,9	99,8	99,8	99,7	99,6	99,6	99,5	99,4	99,3	99,1	99,0	98,9	98,7	98,6	98,4	98,2	98,0	97,9	97,7	97,4	97,2
30	100,0	100,0	99,9	99,8	99,8	99,7	99,7	99,6	99,5	99,4	99,2	99,1	99,0	98,8	98,6	98,5	98,3	98,1	97,9	97,7	97,4	97,2	96,9	96,7
35	100,0	99,9	99,9	99,8	99,8	99,7	99,6	99,5	99,4	99,3	99,1	99,0	98,8	98,6	98,4	98,2	98,0	97,8	97,5	97,3	97,0	96,7	96,4	96,2
40	100,0	99,9	99,9	99,8	99,7	99,7	99,6	99,4	99,3	99,1	99,0	98,8	98,6	98,4	98,2	98,0	97,7	97,4	97,2	96,9	96,5	96,2	95,9	95,7
45	100,0	99,9	99,9	99,8	99,7	99,6	99,5	99,4	99,2	99,1	98,9	98,7	98,4	98,2	98,0	97,7	97,4	97,1	96,8	96,5	96,1	95,7	95,3	95,0
50	100,0	99,9	99,9	99,8	99,7	99,6	99,4	99,3	99,1	98,9	98,7	98,5	98,3	98,0	97,7	97,4	97,1	96,8	96,4	96,1	95,7	95,2	94,8	94,3
55	100,0	99,9	99,8	99,8	99,7	99,6	99,5	99,4	99,2	99,0	98,8	98,6	98,4	98,1	97,8	97,5	97,2	96,8	96,5	96,1	95,7	95,2	94,8	94,3
60	100,0	99,9	99,8	99,7	99,6	99,5	99,3	99,1	98,9	98,7	98,5	98,2	97,9	97,6	97,3	96,9	96,5	96,1	95,7	95,2	94,8	94,3	93,7	93,2
65	100,0	99,9	99,8	99,7	99,6	99,4	99,3	99,1	98,9	98,6	98,3	98,1	97,7	97,4	97,0	96,7	96,2	95,8	95,3	94,8	94,3	93,8	93,2	92,6
70	100,0	99,9	99,8	99,7	99,6	99,4	99,2	99,0	98,8	98,5	98,2	97,9	97,6	97,2	96,8	96,4	95,9	95,5	95,0	94,4	93,9	93,3	92,6	92,0
75	99,9	99,9	99,8	99,7	99,5	99,4	99,2	98,9	98,7	98,4	98,1	97,8	97,4	97,0	96,6	96,1	95,6	95,1	94,6	94,0	93,4	92,8	92,1	91,5
80	99,9	99,9	99,8	99,6	99,5	99,3	99,1	98,9	98,6	98,3	98,0	97,6	97,2	96,8	96,3	95,9	95,3	94,8	94,2	93,6	93,0	92,3	91,5	90,8
85	99,9	99,9	99,8	99,6	99,5	99,3	99,0	98,8	98,5	98,2	97,8	97,5	97,0	96,6	96,1	95,6	95,0	94,4	93,8	93,2	92,5	91,8	91,0	90,2
90	99,9	99,9	99,7	99,6	99,4	99,2	99,0	98,7	98,4	98,1	97,7	97,3	96,9	96,4	95,9	95,3	94,7	94,1	93,5	92,8	92,0	91,2	90,4	89,6
95	99,9	99,9	99,7	99,6	99,4	99,2	98,9	98,6	98,3	98,0	97,6	97,1	96,7	96,2	95,6	95,1	94,4	93,8	93,1	92,3	91,6	90,7	89,9	89,1
100	99,9	99,8	99,7	99,6	99,4	99,1	98,9	98,6	98,2	97,9	97,4	97,0	96,5	96,0	95,4	94,8	94,1	93,4	92,7	91,9	91,1	90,2	89,3	88,5
105	99,9	99,8	99,7	99,5	99,3	99,1	98,8	98,5	98,1	97,7	97,3	96,8	96,3	95,8	95,2	94,5	93,8	93,1	92,3	91,5	90,6	89,7	88,7	87,8
110	99,9	99,8	99,7	99,5	99,3	99,1	98,8	98,4	98,1	97,6	97,2	96,7	96,1	95,6	94,9	94,3	93,5	92,8	91,9	91,1	90,2	89,2	88,1	87,1
115	99,9	99,8	99,7	99,5	99,3	99,0	98,7	98,4	98,0	97,5	97,1	96,5	96,0	95,4	94,7	94,0	93,2	92,4	91,6	90,6	89,7	88,7	87,6	86,6
120	99,9	99,8	99,7	99,5	99,2	99,0	98,6	98,3	97,9	97,4	96,9	96,3	95,6	94,9	94,1	93,3	92,3	91,2	90,2	89,2	88,2	87,1	86,0	84,9
125	99,9	99,8	99,6	99,5	99,2	98,9	98,6	98,2	97,8	97,3	96,8	96,2	95,6	94,9	94,2	93,4	92,6	91,7	90,8	89,8	88,7	87,6	86,4	85,3
130	99,9	99,8	99,6	99,4	99,2	98,9	98,5	98,1	97,7	97,2	96,7	96,1	95,4	94,7	94,0	93,2	92,3	91,4	90,4	89,3	88,2	87,1	85,8	84,6
135	99,9	99,8	99,6	99,4	99,1	98,8	98,5	98,1	97,6	97,1	96,5	95,9	95,2	94,5	93,7	92,9	92,0	91,0	90,0	88,9	87,7	86,5	85,2	84,0
140	99,9	99,8	99,6	99,4	99,1	98,8	98,4	98,0	97,5	97,0	96,4	95,8	95,1	94,3	93,5	92,6	91,7	90,7	89,6	88,5	87,3	86,0	84,6	83,2
145	99,9	99,8	99,6	99,4	99,1	98,7	98,4	97,9	97,4	96,9	96,3	95,6	94,9	94,1	93,3	92,3	91,4	90,3	89,2	88,0	86,8	85,4	84,0	82,6
150	99,9	99,8	99,6	99,3	99,1	98,7	98,3	97,8	97,3	96,8	96,1	95,4	94,7	93,9	93,0	92,1	91,1	90,0	88,8	87,6	86,3	84,9	83,4	81,9
155	99,9	99,8	99,6	99,3	99,0	98,7	98,2	97,8	97,2	96,7	96,0	95,3	94,5	93,7	92,8	91,8	90,7	89,6	88,4	87,1	85,8	84,3	82,8	81,3
160	99,9	99,7	99,6	99,3	99,0	98,6	98,2	97,7	97,2	96,5	95,9	95,1	94,3	93,5	92,5	91,5	90,4	89,3	88,0	86,7	85,3	83,8	82,1	80,4
165	99,9	99,7	99,5	99,3	99,0	98,6	98,1	97,6	97,1	96,4	95,7	95,0	94,2	93,3	92,3	91,2	90,1	88,9	87,6	86,2	84,8	83,2	81,5	79,8
170	99,9	99,7	99,5	99,3	98,9	98,5	98,1	97,6	97,0	96,3	95,6	94,8	94,0	93,0	92,0	91,0	89,8	88,5	87,2	85,8	84,3	82,6	80,9	79,2
175	99,9	99,7	99,5	99,2	98,9	98,5	98,0	97,5	96,9	96,2	95,5	94,7	93,8	92,8	91,8	90,7	89,5	88,2	86,8	85,3	83,7	82,0	80,2	78,4
180	99,9	99,7	99,5	99,2	98,9	98,4	98,0	97,4	96,8	96,1	95,3	94,5	93,6	92,6	91,5	90,4	89,2	87,8	86,4	84,9	83,2	81,5	79,6	77,6
185	99,9	99,7	99,5	99,2	98,8	98,4	97,9	97,3	96,7	96,0	95,2	94,4	93,4	92,4	91,3	90,1	88,8	87,5	86,0	84,4	82,7	80,9	78,9	76,9
190	99,9	99,7	99,5	99,2	98,8	98,4	97,8	97,3	96,6	95,9	95,1	94,2	93,2	92,2	91,1	89,8	88,5	87,1	85,6	83,9	82,2	80,3	78,3	76,3
195	99,9	99,7	99,5	99,1	98,8	98,3	97,8	97,2	96,5	95,8	94,9	94,0	93,0	92,0	90,8	89,5	88,2	86,7	85,1	83,5	81,7	79,7	77,6	75,6
200	99,9	99,7	99,4	99,1	98,7	98,3	97,7	97,1	96,4	95,7	94,8	93,9	92,9	91,8	90,6	89,3	87,9	86,3	84,7	83,0	81,1	79,1	77,0	75,0
205	99,9	99,7	99,4	99,1	98,7	98,2	97,7	97,0	96,3	95,6	94,7	93,7	92,7	91,5	90,3	89,0	87,5	86,0	84,3	82,5	80,6	78,5	76,3	74,1
210	99,9	99,7	99,4	99,1	98,7	98,2	97,6	97,0	96,2	95,4	94,5	93,6	92,5	91,3	90,1	88,7	87,2	85,6	83,9	82,0	80,1	77,9	75,6	73,4
215	99,8	99,7	99,4	99,1	98,6	98,1	97,6	96,9	96,2	95,3	94,4	93,4	92,3	91,1	89,8	88,4	86,9	85,2	83,5	81,6	79,5	77,3	74,9	72,5
220	99,8	99,7	99,4	99,0	98,6	98,1	97,5	96,8	96,1	95,2	94,3	93,2	92,1	90,9	89,5	88,1	86,5	84,9	83,0	81,1	79,0	76,7	74,2	71,7
225	99,8	99,6	99,4	99,0	98,6	98,0	97,4	96,8	96,0	95,1	94,1	93,1	91,9	90,7	89,3	87,8	86,2	84,5	82,6	80,6	78,4	76,1	73,5	70,9
230	99,8	99,6	99,4	99,0	98,5	98,0	97,4	96,7	95,9	95,0	94,0	92,9	91,7	90,4	89,0	87,5	85,9	84,1	82,2	80,1	77,9	75,4	72,8	70,2
235	99,8	99,6	99,3	99,0	98,5	98,0	97,3	96,6	95,8	94,9	93,9	92,8	91,5	90,2	88,8	87,2	85,5	83,7	81,7	79,6	77,3	74,8	72,1	69,4
240	99,8	99,6	99,3	98,9	98,5	97,9	97,3	96,5	95,7	94,8	93,7	92,6	91,4	90,0	88,5	86,9	85,2	83,3	81,3	79,1	76,7	74,2	71,4	68,6
245	99,8	99,6	99,3	98,9	98,4	97,9	97,2	96,5	95,6	94,7	93,6	92,4	91,2	89,8	88,3	86,6	84,9	82,9	80,9	78,6	76,2	73,5	70,7	67,9
250	99,8	99,6	99,3	98,9	98,4	97,8	97,2	96,4	95,5	94,5	93,5	92,3	91,0	89,6	88,0	86,3	84,5	82,6	80,4	78,1	75,6	72,9	69,9	66,9
255	99,8	99,6	99,3	98,9	98,4	97,8	97,1	96,3	95,4	94,4	93,3	92,1	90,8	89,3	87,8	86,0	84,2	82,2	80,0	77,6	75,0	72,2	69,2	66,2
260	99,8	99,6	99,3	98,9	98,3	97,7	97,0	96,2	95,3															

Table A.42. Fundamental frequency change in percentage versus axial load level for I500 steel column for different lengths for frequency change

f/c _o (%)	Length (m)																							
	0.50	0.75	1.00	1.25	1.50	1.75	2.00	2.25	2.50	2.75	3.00	3.25	3.50	3.75	4.00	4.25	4.50	4.75	5.00	5.25	5.50	5.75	6.00	
0	100.0	100.0	100.0	100.0	100.0	100.0	100.0	100.0	100.0	100.0	100.0	100.0	100.0	100.0	100.0	100.0	100.0	100.0	100.0	100.0	100.0	100.0	100.0	
5	100.0	100.0	100.0	100.0	99.9	99.9	99.9	99.9	99.9	99.9	99.9	99.9	99.9	99.9	99.8	99.8	99.8	99.8	99.7	99.7	99.7	99.7	99.6	99.6
10	100.0	100.0	100.0	100.0	99.9	99.9	99.9	99.9	99.9	99.8	99.8	99.7	99.7	99.6	99.6	99.5	99.5	99.4	99.3	99.2	99.1	99.0	98.9	98.7
15	100.0	100.0	100.0	99.9	99.9	99.9	99.9	99.8	99.8	99.7	99.7	99.6	99.6	99.5	99.4	99.4	99.3	99.2	99.1	99.0	98.9	98.8	98.7	98.3
20	100.0	100.0	99.9	99.9	99.9	99.8	99.8	99.7	99.6	99.6	99.5	99.4	99.3	99.1	99.0	98.8	98.7	98.5	98.3	98.1	97.9	97.7	97.5	97.0
25	100.0	100.0	99.9	99.9	99.8	99.7	99.6	99.5	99.4	99.3	99.1	99.0	98.8	98.7	98.5	98.3	98.1	97.8	97.6	97.3	97.0	96.7	96.4	95.9
30	100.0	100.0	99.9	99.9	99.8	99.7	99.6	99.5	99.4	99.2	99.0	98.8	98.6	98.4	98.1	97.8	97.6	97.2	96.8	96.3	95.8	95.2	94.5	93.8
35	100.0	100.0	99.9	99.9	99.8	99.7	99.6	99.5	99.4	99.2	99.0	98.8	98.6	98.3	98.0	97.7	97.3	96.9	96.5	96.1	95.6	94.9	94.2	93.5
40	100.0	99.9	99.9	99.8	99.8	99.7	99.6	99.5	99.4	99.2	99.0	98.8	98.6	98.3	98.0	97.7	97.3	96.9	96.5	96.1	95.6	94.9	94.2	93.5
45	100.0	99.9	99.9	99.8	99.8	99.7	99.6	99.5	99.4	99.2	99.0	98.8	98.6	98.3	98.0	97.7	97.3	96.9	96.5	96.1	95.6	94.9	94.2	93.5
50	100.0	99.9	99.9	99.8	99.7	99.6	99.5	99.4	99.3	99.1	98.9	98.7	98.5	98.3	98.1	97.8	97.6	97.3	97.0	96.7	96.3	95.8	95.2	94.5
55	100.0	99.9	99.9	99.8	99.7	99.6	99.5	99.4	99.3	99.1	98.9	98.7	98.5	98.3	98.1	97.8	97.6	97.3	97.0	96.7	96.3	95.8	95.2	94.5
60	100.0	99.9	99.9	99.8	99.7	99.6	99.5	99.4	99.3	99.1	98.9	98.7	98.5	98.3	98.1	97.8	97.6	97.3	97.0	96.7	96.3	95.8	95.2	94.5
65	100.0	99.9	99.8	99.8	99.7	99.6	99.5	99.4	99.2	99.0	98.8	98.6	98.4	98.1	97.8	97.5	97.2	96.8	96.5	96.1	95.7	95.2	94.5	93.8
70	100.0	99.9	99.8	99.7	99.6	99.5	99.3	99.2	99.0	98.7	98.5	98.2	98.0	97.6	97.3	97.0	96.6	96.2	95.8	95.3	94.9	94.4	93.8	93.2
75	100.0	99.9	99.8	99.7	99.6	99.5	99.3	99.1	98.9	98.7	98.4	98.1	97.8	97.5	97.1	96.7	96.3	95.9	95.5	95.0	94.5	94.0	93.4	92.8
80	100.0	99.9	99.8	99.7	99.6	99.4	99.2	99.0	98.8	98.6	98.3	98.0	97.7	97.3	96.9	96.5	96.1	95.6	95.2	94.6	94.1	93.5	92.9	92.3
85	99.9	99.9	99.8	99.7	99.5	99.4	99.2	99.0	98.7	98.5	98.2	97.9	97.5	97.1	96.7	96.3	95.8	95.4	94.8	94.3	93.7	93.1	92.5	91.9
90	99.9	99.9	99.8	99.7	99.5	99.3	99.1	98.9	98.7	98.4	98.1	97.7	97.4	97.0	96.5	96.1	95.6	95.1	94.5	94.0	93.4	92.8	92.2	91.6
95	99.9	99.9	99.8	99.6	99.5	99.3	99.1	98.9	98.6	98.3	98.0	97.6	97.2	96.8	96.3	95.9	95.3	94.8	94.2	93.6	93.0	92.4	91.8	91.2
100	99.9	99.9	99.8	99.6	99.5	99.3	99.1	98.8	98.5	98.2	97.9	97.5	97.1	96.6	96.1	95.6	95.1	94.5	93.9	93.2	92.6	92.0	91.4	90.8
105	99.9	99.9	99.8	99.6	99.4	99.2	99.0	98.7	98.4	98.1	97.7	97.3	96.9	96.4	95.9	95.4	94.8	94.2	93.6	92.9	92.2	91.6	91.0	90.4
110	99.9	99.9	99.7	99.6	99.4	99.2	99.0	98.7	98.4	98.0	97.6	97.2	96.8	96.3	95.7	95.2	94.6	93.9	93.3	92.5	91.8	91.0	90.1	89.6
115	99.9	99.8	99.7	99.6	99.4	99.2	98.9	98.6	98.3	97.9	97.5	97.1	96.6	96.1	95.5	95.0	94.3	93.7	92.9	92.2	91.4	90.5	89.6	88.7
120	99.9	99.8	99.7	99.6	99.4	99.1	98.9	98.6	98.2	97.8	97.4	97.0	96.5	95.9	95.4	94.7	94.1	93.4	92.6	91.8	91.0	90.1	89.2	88.3
125	99.9	99.8	99.7	99.5	99.3	99.1	98.8	98.5	98.1	97.7	97.3	96.8	96.3	95.8	95.2	94.5	93.8	93.1	92.3	91.5	90.6	89.7	88.7	87.7
130	99.9	99.8	99.7	99.5	99.3	99.1	98.8	98.4	98.1	97.6	97.2	96.7	96.2	95.6	95.0	94.3	93.6	92.8	92.0	91.1	90.2	89.2	88.2	87.2
135	99.9	99.8	99.7	99.5	99.3	99.0	98.7	98.4	98.0	97.6	97.1	96.6	96.0	95.4	94.8	94.1	93.3	92.5	91.7	90.8	89.8	88.8	87.7	86.7
140	99.9	99.8	99.7	99.5	99.3	99.0	98.7	98.3	97.9	97.5	97.0	96.4	95.9	95.2	94.6	93.8	93.0	92.2	91.3	90.4	89.4	88.3	87.2	86.2
145	99.9	99.8	99.7	99.5	99.2	98.9	98.6	98.3	97.8	97.4	96.9	96.3	95.7	95.1	94.4	93.6	92.8	91.9	91.0	90.0	89.0	87.9	86.7	85.7
150	99.9	99.8	99.6	99.4	99.2	98.9	98.6	98.2	97.8	97.3	96.8	96.2	95.6	94.9	94.1	93.4	92.5	91.6	90.7	89.7	88.6	87.4	86.2	85.2
155	99.9	99.8	99.6	99.4	99.2	98.9	98.5	98.1	97.7	97.2	96.6	96.0	95.4	94.7	93.9	93.1	92.3	91.3	90.3	89.3	88.2	87.0	85.7	84.5
160	99.9	99.8	99.6	99.4	99.1	98.8	98.5	98.1	97.6	97.1	96.5	95.9	95.3	94.5	93.7	92.9	92.0	91.0	90.0	88.9	87.8	86.5	85.2	84.0
165	99.9	99.8	99.6	99.4	99.1	98.8	98.4	98.0	97.5	97.0	96.4	95.8	95.1	94.4	93.5	92.7	91.7	90.7	89.7	88.6	87.3	86.1	84.7	83.4
170	99.9	99.8	99.6	99.4	99.1	98.8	98.4	97.9	97.5	96.9	96.3	95.7	94.9	94.2	93.3	92.4	91.5	90.5	89.4	88.2	86.9	85.6	84.2	82.9
175	99.9	99.8	99.6	99.4	99.1	98.7	98.3	97.9	97.4	96.8	96.2	95.5	94.8	94.0	93.1	92.2	91.2	90.2	89.0	87.8	86.5	85.1	83.7	82.3
180	99.9	99.8	99.6	99.3	99.0	98.7	98.3	97.8	97.3	96.7	96.1	95.3	94.5	94.6	93.8	92.9	92.0	91.0	89.9	88.7	87.4	86.1	84.7	83.2
185	99.9	99.8	99.6	99.3	99.0	98.7	98.2	97.8	97.2	96.6	96.0	95.3	94.5	93.6	92.7	91.7	90.7	89.6	88.3	87.1	85.7	84.2	82.6	81.1
190	99.9	99.7	99.6	99.3	99.0	98.6	98.2	97.7	97.2	96.5	95.9	95.1	94.3	93.5	92.5	91.5	90.4	89.3	88.0	86.7	85.3	83.7	82.1	80.5
195	99.9	99.7	99.5	99.3	99.0	98.6	98.1	97.6	97.1	96.5	95.8	95.0	94.2	93.3	92.3	91.3	90.2	89.0	87.7	86.3	84.8	83.3	81.6	80.0
200	99.9	99.7	99.5	99.3	98.9	98.5	98.1	97.6	97.0	96.4	95.6	94.9	94.0	93.1	92.1	91.0	89.9	88.6	87.3	85.9	84.4	82.8	81.1	79.5
205	99.9	99.7	99.5	99.2	98.9	98.5	98.0	97.5	96.9	96.3	95.5	94.7	93.9	92.9	91.9	90.8	89.6	88.3	87.0	85.5	84.0	82.3	80.5	78.7
210	99.9	99.7	99.5	99.2	98.9	98.5	98.0	97.5	96.8	96.2	95.4	94.6	93.7	92.7	91.7	90.6	89.3	88.0	86.6	85.1	83.5	81.8	80.0	78.2
215	99.9	99.7	99.5	99.2	98.9	98.4	97.9	97.4	96.8	96.1	95.3	94.5	93.6	92.6	91.5	90.3	89.1	87.7	86.3	84.8	83.1	81.3	79.4	77.4
220	99.9	99.7	99.5	99.2	98.8	98.4	97.9	97.3	96.7	96.0	95.2	94.3	93.4	92.4	91.3	90.1	88.8	87.4	85.9	84.4	82.7	80.8	78.9	76.9
225	99.9	99.7	99.5	99.2	98.8	98.4	97.9	97.3	96.6	95.9	95.1	94.2	93.2	92.2	91.1	89.8	88.5	87.1	85.6	84.0	82.2	80.4	78.3	76.3
230	99.9	99.7	99.5	99.1	98.8	98.3	97.8	97.2	96.5	95.8	95.0	94.1	93.1	92.0	90.9	89.6	88.3	86.8	85.2	83.6	81.8	79.9	77.8	75.7
235	99.9	99.7	99.4	99.1	98.7	98.3	97.8	97.1	96.5	95.7	94.9	93.9	92.9	91.8	90.7	89.4	88.0	86.5	84.9	83.2	81.3	79.4	77.2	75.1
240	99.9	99.7	99.4	99.1	98.7	98.2	97.7	97.1	96.4	95.6	94.8	93.8	92.8	91.7	90.4	89.1	87.7	86.2	84.5	82.8	80.9	78.9	76.7	74.5
245	99.9	99.7	99.4	99.1	98.7	98.2	97.7	97.0	96.3	95.5	94.6	93.7	92.6	91.5	90.2	88.9	87.4	85.9	84.2	82.4	80.4	78.3	76.1	73.9
250	99.9	99.7	99.4	99.1	98.7	98.2	97.6	97.0	96.3	95.5	94.5	93.5	92.5	91.3	90.0	88.6	87.2	85.6	83.8	82.0	80.0	77.8	75.5	73.2
255	99.8	99.7	99.4	99.1	98.6	98.1	97.6	96.9	96.2	95.3	94.4	93.4	92.3	91.1	89.8	88.4	86.9	85.2	83.5	81.6	79.5	77.3	74.9	72.5
260	99.8	99.7	99.4	99.0	98.6	98.1	97.5	96.8	96.1															

Table A.44. Fundamental frequency change in percentage versus axial load level for I550 steel column for different lengths for frequency change

Load (tons)	f _{ff} (%)	Length (m)																						
		0.50	0.75	1.00	1.25	1.50	1.75	2.00	2.25	2.50	2.75	3.00	3.25	3.50	3.75	4.00	4.25	4.50	4.75	5.00	5.25	5.50	5.75	6.00
0	100.0	100.0	100.0	100.0	100.0	100.0	100.0	100.0	100.0	100.0	100.0	100.0	100.0	100.0	100.0	100.0	100.0	100.0	100.0	100.0	100.0	100.0	100.0	100.0
6	100.0	100.0	100.0	100.0	100.0	100.0	100.0	100.0	100.0	100.0	100.0	100.0	100.0	100.0	100.0	100.0	100.0	100.0	100.0	100.0	100.0	100.0	100.0	100.0
12	100.0	100.0	100.0	100.0	100.0	100.0	99.9	99.9	99.9	99.9	99.8	99.8	99.8	99.8	99.7	99.7	99.6	99.6	99.5	99.5	99.4	99.4	99.3	99.3
18	100.0	100.0	100.0	100.0	100.0	99.9	99.9	99.9	99.9	99.8	99.8	99.8	99.7	99.7	99.6	99.6	99.5	99.5	99.4	99.3	99.2	99.2	99.1	99.0
24	100.0	100.0	100.0	100.0	99.9	99.9	99.9	99.8	99.8	99.8	99.7	99.7	99.6	99.6	99.5	99.4	99.3	99.2	99.1	99.0	98.9	98.8	98.7	98.6
30	100.0	100.0	99.9	99.9	99.9	99.8	99.8	99.7	99.7	99.6	99.5	99.5	99.4	99.3	99.2	99.1	99.0	98.9	98.8	98.7	98.6	98.5	98.3	98.2
36	100.0	100.0	99.9	99.9	99.9	99.8	99.8	99.7	99.6	99.5	99.5	99.4	99.3	99.1	99.0	98.9	98.8	98.7	98.6	98.5	98.4	98.2	98.0	97.8
42	100.0	100.0	99.9	99.9	99.8	99.8	99.7	99.6	99.6	99.5	99.4	99.3	99.1	99.0	98.9	98.7	98.6	98.4	98.2	98.0	97.8	97.6	97.4	97.1
48	100.0	100.0	99.9	99.9	99.8	99.8	99.7	99.6	99.5	99.4	99.3	99.1	99.0	98.9	98.7	98.5	98.4	98.2	98.0	97.8	97.5	97.2	97.0	96.7
54	100.0	99.9	99.9	99.9	99.8	99.7	99.6	99.5	99.4	99.3	99.2	99.0	98.9	98.7	98.5	98.3	98.1	97.9	97.7	97.5	97.2	97.0	96.7	96.4
60	100.0	99.9	99.9	99.8	99.8	99.7	99.6	99.5	99.4	99.2	99.1	98.9	98.8	98.6	98.4	98.2	97.9	97.7	97.4	97.2	96.9	96.6	96.3	95.9
66	100.0	99.9	99.9	99.8	99.8	99.7	99.6	99.4	99.3	99.2	99.0	98.8	98.6	98.4	98.2	98.0	97.7	97.5	97.2	96.9	96.6	96.3	95.9	95.5
72	100.0	99.9	99.9	99.8	99.7	99.6	99.5	99.4	99.2	99.1	98.9	98.7	98.5	98.3	98.0	97.8	97.5	97.2	96.9	96.6	96.3	95.9	95.5	95.1
78	100.0	99.9	99.9	99.8	99.7	99.6	99.5	99.3	99.2	99.0	98.8	98.6	98.4	98.1	97.9	97.6	97.3	97.0	96.7	96.3	96.0	95.6	95.2	94.8
84	100.0	99.9	99.9	99.8	99.7	99.6	99.4	99.3	99.1	98.9	98.7	98.5	98.3	98.0	97.7	97.4	97.1	96.8	96.4	96.0	95.6	95.2	94.8	94.4
90	100.0	99.9	99.8	99.8	99.7	99.5	99.4	99.2	99.1	98.9	98.6	98.4	98.1	97.9	97.6	97.2	96.9	96.5	96.1	95.7	95.3	94.9	94.4	94.0
96	100.0	99.9	99.8	99.7	99.6	99.5	99.4	99.2	99.0	98.8	98.5	98.3	98.0	97.7	97.4	97.0	96.7	96.3	95.9	95.5	95.0	94.5	94.0	93.6
102	100.0	99.9	99.8	99.7	99.6	99.5	99.3	99.1	98.9	98.7	98.4	98.2	97.9	97.6	97.2	96.9	96.5	96.1	95.6	95.2	94.7	94.2	93.6	93.0
108	100.0	99.9	99.8	99.7	99.6	99.4	99.3	99.1	98.9	98.6	98.4	98.1	97.8	97.4	97.1	96.7	96.3	95.8	95.4	94.9	94.3	93.8	93.2	92.6
114	100.0	99.9	99.8	99.7	99.6	99.4	99.2	99.0	98.8	98.5	98.3	98.0	97.6	97.3	96.9	96.5	96.0	95.6	95.1	94.6	94.0	93.4	92.8	92.2
120	99.9	99.9	99.8	99.7	99.5	99.4	99.2	99.0	98.7	98.5	98.2	97.8	97.5	97.1	96.7	96.3	95.8	95.3	94.8	94.3	93.7	93.1	92.4	91.8
126	99.9	99.9	99.8	99.7	99.5	99.4	99.2	98.9	98.7	98.4	98.1	97.7	97.4	97.0	96.6	96.1	95.6	95.1	94.6	94.0	93.4	92.7	92.0	91.4
132	99.9	99.9	99.8	99.7	99.5	99.3	99.1	98.9	98.6	98.3	98.0	97.6	97.2	96.8	96.4	95.9	95.4	94.9	94.3	93.7	93.0	92.4	91.7	91.0
138	99.9	99.9	99.8	99.6	99.5	99.3	99.1	98.8	98.5	98.2	97.9	97.5	97.1	96.7	96.2	95.7	95.2	94.6	94.0	93.3	92.7	92.0	91.3	90.6
144	99.9	99.9	99.8	99.6	99.5	99.3	99.0	98.8	98.5	98.2	97.8	97.4	97.0	96.5	96.1	95.5	95.0	94.4	93.7	93.1	92.4	91.6	90.9	90.2
150	99.9	99.9	99.8	99.6	99.4	99.2	99.0	98.7	98.4	98.1	97.7	97.3	96.9	96.4	95.9	95.3	94.8	94.1	93.5	92.8	92.0	91.3	90.6	89.9
156	99.9	99.9	99.7	99.6	99.4	99.2	98.9	98.7	98.4	98.0	97.6	97.2	96.7	96.2	95.7	95.1	94.5	93.9	93.2	92.5	91.7	90.9	90.2	89.5
162	99.9	99.8	99.7	99.6	99.4	99.2	98.9	98.6	98.3	97.9	97.5	97.1	96.6	96.1	95.5	95.0	94.3	93.7	92.9	92.2	91.4	90.5	89.6	88.9
168	99.9	99.8	99.7	99.6	99.4	99.1	98.9	98.6	98.2	97.8	97.4	97.0	96.5	95.9	95.4	94.8	94.1	93.4	92.7	91.9	91.0	90.2	89.2	88.2
174	99.9	99.8	99.7	99.5	99.3	99.1	98.8	98.5	98.2	97.8	97.3	96.9	96.4	95.8	95.2	94.6	93.9	93.2	92.4	91.6	90.7	89.8	88.8	87.8
180	99.9	99.8	99.7	99.5	99.3	99.1	98.8	98.5	98.1	97.7	97.2	96.8	96.2	95.7	95.0	94.4	93.7	92.9	92.1	91.3	90.4	89.4	88.4	87.4
186	99.9	99.8	99.7	99.5	99.3	99.0	98.7	98.4	98.0	97.6	97.1	96.6	96.1	95.5	94.9	94.2	93.4	92.7	91.8	91.0	90.0	89.0	88.0	87.0
192	99.9	99.8	99.7	99.5	99.3	99.0	98.7	98.4	98.0	97.5	97.1	96.5	96.0	95.4	94.7	94.0	93.2	92.4	91.6	90.6	89.7	88.7	87.6	86.6
198	99.9	99.8	99.7	99.5	99.2	99.0	98.7	98.3	97.9	97.5	97.0	96.4	95.8	95.2	94.5	93.8	93.0	92.2	91.3	90.3	89.3	88.3	87.1	86.0
204	99.9	99.8	99.7	99.5	99.2	98.9	98.6	98.3	97.8	97.4	96.9	96.3	95.7	95.1	94.4	93.6	92.8	91.9	91.0	90.0	89.0	87.9	86.7	85.6
210	99.9	99.8	99.6	99.4	99.2	98.9	98.6	98.2	97.8	97.3	96.8	96.2	95.6	94.9	94.2	93.4	92.6	91.7	90.7	89.7	88.6	87.5	86.3	85.2
216	99.9	99.8	99.6	99.4	99.2	98.9	98.5	98.1	97.7	97.2	96.7	96.1	95.4	94.8	94.0	93.2	92.3	91.4	90.4	89.4	88.3	87.1	85.9	84.7
222	99.9	99.8	99.6	99.4	99.2	98.9	98.5	98.1	97.6	97.1	96.6	96.0	95.3	94.6	93.8	93.0	92.1	91.2	90.2	89.1	87.9	86.7	85.4	84.2
228	99.9	99.8	99.6	99.4	99.1	98.8	98.5	98.0	97.6	97.1	96.5	95.9	95.2	94.5	93.7	92.8	91.9	90.9	89.9	88.8	87.6	86.3	85.0	83.7
234	99.9	99.8	99.6	99.4	99.1	98.8	98.4	98.0	97.5	97.0	96.4	95.8	95.1	94.3	93.5	92.6	91.7	90.7	89.6	88.5	87.2	86.0	84.6	83.3
240	99.9	99.8	99.6	99.4	99.1	98.8	98.4	97.9	97.4	96.9	96.3	95.6	94.9	94.2	93.3	92.4	91.5	90.4	89.3	88.1	86.9	85.6	84.1	82.6
246	99.9	99.8	99.6	99.4	99.1	98.7	98.3	97.9	97.4	96.8	96.2	95.5	94.8	94.0	93.1	92.2	91.2	90.2	89.0	87.8	86.5	85.2	83.7	82.2
252	99.9	99.8	99.6	99.3	99.0	98.7	98.3	97.8	97.3	96.7	96.1	95.4	94.7	93.9	93.0	92.0	91.0	89.9	88.7	87.5	86.2	84.8	83.3	81.8
258	99.9	99.8	99.6	99.3	99.0	98.7	98.3	97.8	97.3	96.7	96.0	95.3	94.5	93.7	92.8	91.8	90.8	89.7	88.5	87.2	85.8	84.4	82.8	81.3
264	99.9	99.8	99.6	99.3	99.0	98.6	98.2	97.7	97.2	96.6	95.9	95.2	94.4	93.5	92.6	91.6	90.5	89.4	88.2	86.9	85.5	84.0	82.4	80.8
270	99.9	99.7	99.5	99.3	99.0	98.6	98.2	97.7	97.1	96.5	95.8	95.1	94.3	93.4	92.4	91.4	90.3	89.1	87.9	86.5	85.1	83.6	81.9	80.3
276	99.9	99.7	99.5	99.3	99.0	98.6	98.1	97.6	97.1	96.4	95.7	95.0	94.1	93.2	92.3	91.2	90.1	88.9	87.6	86.2	84.7	83.2	81.5	79.9
282	99.9	99.7	99.5	99.3	98.9	98.5	98.1	97.6	97.0	96.4	95.6	94.9	94.0	93.1	92.1	91.0	89.9	88.6	87.3	85.8	84.4	82.7	81.0	79.4
288	99.9	99.7	99.5	99.2	98.9	98.5	98.0	97.5	96.9	96.3	95.5	94.7	93.9	92.9	91.9	90.8	89.6	88.4	87.0	85.6	84.0	82.3	80.6	78.9
294	99.9	99.7	99.5	99.2	98.9	98.5	98.0	97.5	96.9	96.2	95.4	94.6	93.7	92.8	91.7	90.6	89.4	88.1	86.7	85.2	83.6	81.9	80.1	78.4
300	99.9	99.7	99.5	99.2	98.9	98.4	98.0	97.4	96.8	96.1	95.4	94.5	93.6	92.6	91.6	90.4	89.2	87.8	86.4	84.9	83.3	81.5	79.6	77.8
306	99.9	99.7	99.5	99.2	98.8	98.4	97.9	97.4	96.7	96.0	95.3	94.4	93.5	92.5	91.4	90.2	88.9	87.6	86.1	84.6	82.9	81.1	79.2	77.4
312	99.9	99.7	99.5																					

APPENDIX B

TICO ULTRASONIC INSTRUMENT

Figures are given in order to describe “TICO Ultrasonic Instrument”.



Figure B.1: TICO ultrasonic instrument

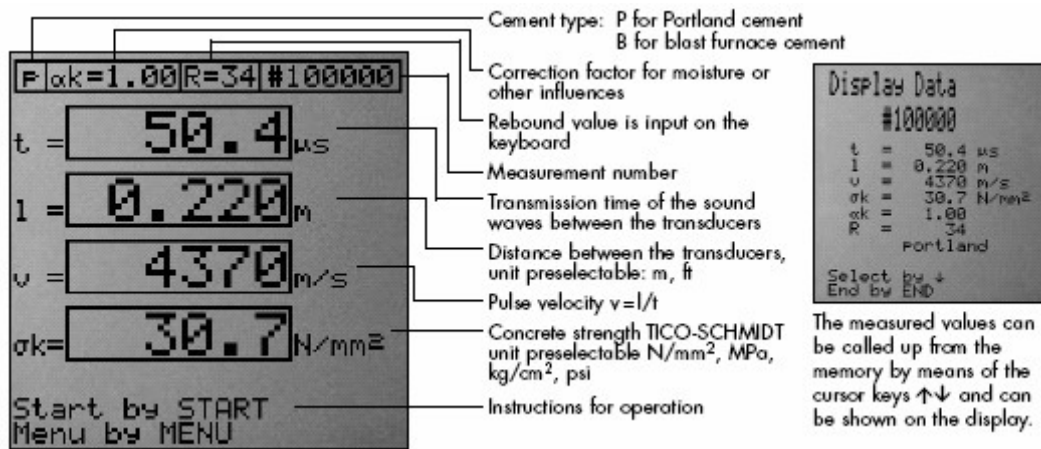


Figure B.2: TICO display unit



Figure B.3: Application of TICO



Figure B.4: Another application of TICCO



Figure B.5: The package of TICCO

TICCO Package:

- Display unit with memory for 250 measured values, 128 X 128 graphic LCD.
- RS 232 C interface.
- Integrated software for transmission of the measured values to PC.
- Measuring Range: ~15 bis to 6553.5 μ sec.
- Resolution: 0.1 μ sec.
- Voltage Pulse: 600 V.

- Pulse Rate: 3/s.
- Impedance at Input: 1 k Ω .
- Temperature Range: -10 to +60 °C
- Battery operation with 6 LR 6 batteries, 1.5 V, for 30 hours.
- 54 kHz transducers, cable, calibration rod, coupling paste, carrying strap, operating instructions and carrying case 325 x 295 x 105 mm.
- Total Weight: 3 kg.
- Accessories: Transducers with other frequencies.

Price of the TICO: [25]

= 6 045 * 0.95 * 1.18 = 6 777 Switzerland Frank

~ 7.3 billion Turkish Lira (TL) (12.02.2004)